

University of Windsor

Scholarship at UWindor

Electronic Theses and Dissertations

Theses, Dissertations, and Major Papers

2023

Sediment Microbial Community Diversity and Function in Response to Legacy and Prevailing Pollutants in Southern Ontario Watersheds

Nicolas Falk
University of Windsor

Follow this and additional works at: <https://scholar.uwindsor.ca/etd>



Part of the [Environmental Chemistry Commons](#), and the [Environmental Sciences Commons](#)

Recommended Citation

Falk, Nicolas, "Sediment Microbial Community Diversity and Function in Response to Legacy and Prevailing Pollutants in Southern Ontario Watersheds" (2023). *Electronic Theses and Dissertations*. 8973. <https://scholar.uwindsor.ca/etd/8973>

This online database contains the full-text of PhD dissertations and Masters' theses of University of Windsor students from 1954 forward. These documents are made available for personal study and research purposes only, in accordance with the Canadian Copyright Act and the Creative Commons license—CC BY-NC-ND (Attribution, Non-Commercial, No Derivative Works). Under this license, works must always be attributed to the copyright holder (original author), cannot be used for any commercial purposes, and may not be altered. Any other use would require the permission of the copyright holder. Students may inquire about withdrawing their dissertation and/or thesis from this database. For additional inquiries, please contact the repository administrator via email (scholarship@uwindsor.ca) or by telephone at 519-253-3000ext. 3208.

**Sediment Microbial Community Diversity and Function in Response to Legacy and
Prevailing Pollutants in Southern Ontario Watersheds**

By

Nicholas Falk

A Dissertation
Submitted to the Faculty of Graduate Studies
Through the Faculty of Science
And in support of the Great Lakes Institute for Environmental Research
In Partial Fulfillment of the Requirements for
The Degree of Doctor of Philosophy
At the University of Windsor

Windsor, Ontario, Canada

2023

© 2023 Nicholas Falk

**Sediment Microbial Community Diversity and Function in Response to Legacy and
Prevailing Pollutants in Southern Ontario Watersheds**

By

Nicholas Falk

APPROVED BY:

M. Dittrich

University of Toronto Scarborough

N. Biswas

Department of Civil and Environmental Engineering

I.G. Droppo

Great Lakes Institute for Environmental Research

S. Mundle

Great Lakes Institute for Environmental Research

C. Weisener, Co-Advisor

Great Lakes Institute for Environmental Research

K.G. Drouillard, Co-Advisor

Great Lakes Institute for Environmental Research

December 9, 2022

DECLARATION OF CO-AUTHORSHIP / PREVIOUS PUBLICATION

I. Co-Authorship

I hereby declare that this thesis incorporates material that is result of joint research, as follows:

Chapter 2 of the thesis was co-authored with T. Reid, A. Skoyles, A. Grgicak-Mannion, K. Drouillard and C.G.Weisener, under the supervision of both K. Drouillard and C.G.Weisener. In all cases, the key ideas, primary contributions, data analysis, interpretation, and writing were performed by the author, and the contribution of co-authors was primarily through the provision of grant funding alongside experimental design and field work aid. All co-authors also provided feedback for the purpose of editing and refining the manuscript.

Chapter 3 of the thesis was co-authored with I.G. Droppo, K. Drouillard, and C.G.Weisener under the supervision of both K. Drouillard and C.G.Weisener. In all cases, the key ideas, primary contributions, data analysis, interpretation, and writing were performed by the author, and the contribution of co-authors was primarily through the provision of grant funding alongside experimental design and field work aid. All co-authors also provided feedback for the purpose of editing and refining the manuscript.

I am aware of the University of Windsor Senate Policy on Authorship and I certify that I have properly acknowledged the contribution of other researchers to my thesis, and have obtained written permission from each of the co-author(s) to include the above material(s) in my thesis.

I certify that, with the above qualification, this thesis, and the research to which it refers, is the product of my own work.

II. Previous Publication

This thesis includes 2 original papers that have been previously published/submitted to journals for publication, as follows:

Thesis Chapter	Publication title/full citation	Publication status*
Chapter [2]	Falk, N., Reid, T., Skoyles, A., Grgicak-Mannion, A., Drouillard, K., Weisener, C.G., 2019. Microbial metatranscriptomic investigations across contaminant gradients of the Detroit River. <i>Sci. Total Environ.</i> 690, 121–131. https://doi.org/10.1016/j.scitotenv.2019.06.451	Published
Chapter [3]	Falk, N., Droppo, I.G., Drouillard, K.G., Weisener, C.G., 2022. Integrating microbial DNA community analyses into time - integrated suspended sediment sampling methods. <i>J. Soils Sediments.</i> https://doi.org/10.1007/s11368-022-03293-x	Published

I certify that I have obtained a written permission from the copyright owner(s) to include the above published material(s) in my thesis. I certify that the above material describes work completed during my registration as a graduate student at the University of Windsor.

III. General

I declare that, to the best of my knowledge, my thesis does not infringe upon anyone's copyright nor violate any proprietary rights and that any ideas, techniques, quotations, or any other material from the work of other people included in my thesis, published or otherwise, are fully acknowledged in accordance with the standard referencing practices. Furthermore, to the extent that I have included copyrighted material that surpasses the bounds of fair dealing within the meaning of the Canada Copyright Act, I certify that I have obtained a written permission from the copyright owner(s) to include such material(s) in my thesis.

I declare that this is a true copy of my thesis, including any final revisions, as approved by my thesis committee and the Graduate Studies office, and that this thesis has not been submitted for a higher degree to any other University or Institution.

ABSTRACT

Managing and mitigating point and non-point contamination to freshwater resources depends on reliable and sensitive monitoring of ecosystem health. Microorganisms in surface waters and sediments respond rapidly to anthropogenic disturbances, making them valuable bioindicators of human-induced landscape change. However, there lacks a baseline understanding of microbial community composition and function in industrially and agriculturally impacted regions of the Great Lakes. Without a reference state of microbial diversity and activity, future investigations seeking to integrate microorganisms into ecosystem assessments will lack context. Using genomic tools and measurements of chemical and nutrient contaminants, this thesis provides case studies of microbial community responses to persistent non-point stressors in lower Great Lakes watersheds.

In the first study, Detroit River bed sediments collected over a gradient of chemical contamination were analyzed for microbial gene expression via RNA-seq metatranscriptomics. Results showed that microbial communities exploit unique anabolic and catabolic pathways to derive and store energy from industrial organic contaminants, including nitrate reduction, beta-oxidation, and gluconeogenesis, while simultaneously recruiting stress-response and gene transfer mechanisms to cope with xenobiotic pressures. These observations prove that microbial function, as measured by RNA, is sensitive to legacy-contamination in freshwater sediments.

The following studies of this thesis focused on agricultural-impacted headwaters of Southern Ontario, with an emphasis on bed and suspended sediment microbial community responses to fertilizer practice. In an initial study, suspended sediment was collected and assessed for its potential as a carrier and indicator of riverine microbial taxa within Big Creek, Essex County. Results showed that time-integrated sampling using passive Phillips Tube (PT) samplers provided reliable and consistent collection of the suspended phases microbial community based on DNA-metabarcoding. However, it was observed that sampler precision was greatest during higher flow periods, and that deployment times exceeding two weeks resulted in dissolved oxygen depletion within the sampler apparatus, leading to shifts of the microbial community in-situ. These results show that passive

sampling of suspended sediment can be supplementary to bed sediment microbiological investigations, so long as timeframes of collection are considered.

In the next study, Big Creek and two additional sites, Nissouri Creek and the Saugeen River, were assessed for Phosphorus (P) and Nitrogen (N) impacts and bed sediment microbial community response as a function of watershed-wide fertilizer practice. Big Creek, characterized by chemical fertilizer, showed historical and current day P concentrations in exceedance of guidelines, with suspended sediment identified as the primary carrier and release vector of internal P. Nissouri Creek, characterized by a manure-chemical fertilizer mix, showed greater N concentrations, with bed sediments being vulnerable to redox-driven internal P release. The Saugeen River was confirmed as an appropriate reference system that exhibited low nutrient concentrations and low internal P-release risk. Big Creek supported a more varied microbial community, while Nissouri Creek and the Saugeen River shared more similarities, despite their overarching nutrient differences. No sets of microbial taxa were found to be reliable indicators of sediment P-release across all sites, however, several genera showed high differential abundance during a notable P-source event during spring sampling at Nissouri Creek.

The final study applied microbial DNA and RNA-seq methods to bed sediments of Big Creek, Nissouri Creek, and the Saugeen River to associate function with community composition, and to strengthen evidence that metatranscriptomics can co-align with trends in anthropogenic non-point pollution stress. Results showed differences in N, P, and Sulfur (S) metabolism pathways, indicating that fertilizer practice can alter sediment microbial community biogeochemical cycling. Further, DNA and RNA-based amplicon sequencing of bed and suspended sediments, as well as surface water phase microbial communities revealed that RNA-based communities were lower in alpha diversity and represented a subset of the total DNA-based community across river substrates, with surface water showing a high proportion of non-active taxa inferred to be of allochthons origin.

This thesis work lays a foundation for pairing microbial genomics with assessments of industrial and agricultural non-point pollution to assess bottom-up ecosystem functioning in lower Great Lakes watersheds.

DEDICATION

This work is dedicated to Gary Malloy. If everyone could have a mentor and friend like you, the world would be a wiser, more understanding, and funnier place.

ACKNOWLEDGEMENTS

I would like to thank my advisory committee for their help in planning, implementing, and publishing this body of research. Particularly, my co-supervisors Drs. Chris Weisener and Ken Douillard and program reader Dr. Ian Droppo, who helped in arrangements for funding, sampling logistics, data processing, and data analysis. They have supported me both as a scientist and an individual, and I could not have navigated this PhD without their guidance.

I also thank Dr. Scott Mundle for his contributions to widening the scope of the project and for serving as a program reader, and Dan Heath for his role in project management. I also thank Dr. Nihar Biswas for serving as the outside program reader and as a voice of encouragement in the lab and on the track, and Dr. Maria Dittrich for lending her time as external thesis advisor.

To my family, I'm forever grateful for your love and support. Thanks to my parents for instilling curiosity, kindness, and discipline in my life, and to my brother for being my longest and closest friend. To my four grandparents, who I'm lucky enough to know and love, thank you for all you have done in getting me to where I am today, and for being influential in shaping the happiness and fulfillment of all your grandchildren.

This research would not have been possible without the support of the students at the Great Lakes Institute for Environmental Research. To former lab members Zach DiLoreto, Sara Butler, Adam Skoyles, Sabari Prakasan Mullapulli Raveendran, Ryan Boudens, Danielle Gleason, and Tom Reid, I thank you for helping in my work and making my foray into graduate school a joyful one. To Drs. Danielle and Tom, especially, thank you for being great role models in the Weisener lab and for all GLIER students. Thanks to graduate students Chelsea Salter, Emily Varga, Alicia DiCarlo, Savannah Knorr, Yu-Ting Chen, Tilak Patel, Nadia Tarakki, Matt Day, and Chelsea Crundwell for their help, encouragement, and above all, friendship through my degree. I am lucky to have been surrounded by so many wonderful graduate students through my years at GLIER.

Many undergraduate students and research assistants shared in the work and the laughs. Thank you to Lauren Goddard, Princess Vergara, Cameron Myshok, Katie Crundwell, Bryce Ducharme, Zachary Hilbert, Luke Mawhinney and Sean Leng.

A big thanks goes out to all the staff at GLIER and in the School of the Environment. Sharon Lackie, J.C. Barrette, Shelby Mackie, Nargis Ismail, Jon Leblanc, and Meagan Beaton have all been so helpful and kind in sharing their technical expertise. I'm eternally grateful for your contributions to the successful production of data for my research. To Christine Weisener, Marg Mayer, Kendra Thompson-Kumar, and Nia Khuong, thank you for advising myself and all graduate students through our degrees. An especially big thank you and hug to Mary Lou Scratch for all you do at GLIER for students and staff alike.

Finally, a heap of gratitude to all my friends, teammates, and coaches who I've had the privilege to get to know through athletics. My time as a member of the varsity cross country and track and field teams at the University of Windsor taught me more in the ways of persistence and dedication than any single degree ever could. To Dennis Fairall, Gary Malloy, Anna Patterson, and Brett Lumley, thank you for your commitment and passion towards the athletics community.

TABLE OF CONTENTS

DECLARATION OF CO-AUTHORSHIP / PREVIOUS PUBLICATION	iii
ABSTRACT.....	v
DEDICATION	vii
ACKNOWLEDGEMENTS	viii
LIST OF TABLES	xiv
LIST OF FIGURES	xv
LIST OF APPENDICES	xix
CHAPTER 1: INTRODUCTION	1
1.1 The Anthropocene.....	1
1.2 Great Lakes Significance	2
1.3 Point and Non-Point Pollution to the Lower Great Lakes	3
1.3.1 Metals and Persistent Organic Pollutants (POPs)	4
1.3.2 Suspended Sediment	4
1.3.3 Nutrients.....	5
1.4 Phosphorus.....	6
1.4.1 Phosphorus in the Global Context	6
1.4.2 Phosphorus and the Great Lakes	8
1.4.3 Phosphorus Cycling in Lotic Systems	9
1.4.4 Internal P Loading.....	10
1.5 Bioindicators	10
1.6 Microbial Community Ecology	11
1.6.1 A (Very) Brief History of Microbiology.....	11
1.6.2 Microbial Control on Ecosystem Processes in Freshwater Systems.....	12
1.7 Thesis Objectives	13
References.....	16
CHAPTER 2: MICROBIAL METATRANSCRIPTOMIC INVESTIGATIONS ACROSS CONTAMINANT GRADIENTS OF THE DETROIT RIVER	29
2.1 Introduction.....	30
2.2 Methods	32
2.2.1 Site Characteristics and Sediment Sampling Locations.....	32
2.2.2 Sediment Contaminant Chemistry Profiles.....	33
2.2.3 RNA Extraction and Functional and Taxonomic Annotation.....	34

2.3 Results.....	35
2.3.1 Interpolated Site Chemistry	35
2.3.2 Metals.....	35
2.3.3 Organic Contaminants	36
2.3.4 Microbial Diversity and Taxonomy.....	37
2.3.5 Differential Gene Expression Across Sites.....	37
2.4 Discussion.....	38
2.4.1 Overview.....	38
2.4.2 Energy and Metabolic Pathways Associated with Differences in Detroit River Sediments.....	39
2.4.3 Microbial Stress Response and Adaptive Strategies in Contaminated Sediments.....	42
2.5 Conclusion	43
Figures and Tables	45
References.....	54
CHAPTER 3: INTEGRATING MICROBIAL DNA COMMUNITY ANALYSES INTO TIME- INTEGRATED SUSPENDED SEDIMENT SAMPLING METHODS	60
3.1 Introduction.....	61
3.2 Methods	62
3.2.1 Site and Sampling Information	62
3.2.2 Water and Bed Sediment Sampling	63
3.2.3 Suspended Sediment Sampling by Time-Integrated Passive Samplers	63
3.2.4 DNA Extraction	64
3.2.5 Microbial Community Taxonomy and Diversity Metrics.....	65
3.2.6 In-Situ DO measurements from PT Samplers.....	66
3.3 Results.....	66
3.3.1 Seasonal Water Quality Parameters.....	66
3.3.2 Microbial Community Diversity in Bed and Suspended Sediments.....	67
3.3.3 Microbial Community Analysis.....	68
3.4 Discussion.....	69
3.4.1 Precision and Replicability of Microbial SSP in Phillips Tube Samplers	69
3.4.2 Microbial Characteristics of Bed and Suspended Sediments.....	70
3.4.2.1 Alpha and Beta Diversity.....	70
3.4.2.2 Microbial Biomarkers of Bed and Suspended Sediments.....	71
3.4.3 Precipitation, Redox, and Microbial Effects on Phillips Tube Samplers.....	73

3.5 Conclusions.....	74
Figures and Tables	77
References.....	86
CHAPTER 4: BIOGEOCHEMICAL MECHANISMS ASSOCIATED WITH IN-SITU SEDIMENT P RELEASE IN SOUTHERN ONTARIO HEADWATERS.....	95
4.1 Introduction.....	96
4.2 Methods	98
4.2.1 Site Selection and Watershed Characteristics	98
4.2.2 Point Sampling of Bed Sediment and Surface Water	98
4.2.3 Suspended Sediment Collection	99
4.2.4 Physico-Chemical Analyses of Water and Sediment.....	99
4.2.4.1 Select Water Chemistry	99
4.2.4.2 Sediment Phosphorus Equilibrium.....	100
4.2.4.3 In-situ Sediment Redox.....	101
4.2.5 Bed Sediment Microbial Community Analysis	101
4.2.6 Historical Watershed and Climate Data.....	102
4.2.7 Data Analysis.....	102
4.3 Results.....	102
4.3.1 Legacy TN and TP Concentrations	102
4.3.2 Bed and Suspended Sediment Buffering Capacity by EPC ₀	102
4.3.3 Site Physico-chemical Water Quality Variable Correlations.....	104
4.3.4 Vertical Microsensor Redox and DO Profiling.....	104
4.3.5 Temporal and Spatial Bed Sediment Microbial Community Analysis.....	104
4.4 Discussion.....	105
4.4.1 Legacy Nutrient Trends	105
4.4.2 Headwater Bed Sediment P Buffering	106
4.4.2.1 Non-point P from Suspended Sediment at Big Creek.....	106
4.4.2.2 Non-point P at Nissouri Creek from Bed Sediments	108
4.4.5 Microbial Community Effects	110
4.5 Conclusions.....	111
Figures And Tables.....	113
References.....	121
CHAPTER 5: MICROBIAL COMMUNITY-DRIVEN NUTRIENT TRANSFORMATIONS IN SOUTHERN ONTARIO TRIBUTARY SEDIMENTS; AN RNA-DNA APPROACH.....	127

5.1 Introduction.....	128
5.2 Methods	129
5.2.1 Site Overview.....	129
5.2.2 Surface Water and Bed Sediment Sampling	130
5.2.3 Time-Integrated Suspended Sediment Collection.....	130
5.2.4 Microbial Sampling and Preservation.....	131
5.2.5 DNA and rDNA Metabarcoding for Microbial Community Analysis.....	131
5.2.5.1 Extraction and Sequencing.....	131
5.2.5.2 Microbial Community Profiling	132
5.2.5.3 Active, Neutral, and Non-Active Taxa Classification	132
5.2.5.4 Additional Microbial Community Analysis and Statistics.....	133
5.2.6 mRNA Sequencing and Metatranscriptomics of Bed Sediments	133
5.3 Results.....	134
5.3.2 DNA and rDNA Microbial Community Comparisons	134
5.3.3 Active Microbial Community Investigations.....	135
5.3.4 Metatranscriptomics Overview	136
5.3.5 Spatial and Temporal Expression in N, P, and S Metabolism in Bed Sediments	137
5.3.5.1 Summer Metatranscriptomic Profiling.....	137
5.3.5.2 Fall Metatranscriptomic Profiling.....	137
5.4 Discussion.....	139
5.4.1 Microbial Diversity Across Source Material and DNA/RNA	139
5.4.2 Significantly Active Taxa across Season and Sites.....	141
5.4.3 Metatranscriptomic Analysis of Sediment Microbial Gene Expression	141
5.4.3.1 Overview.....	141
5.4.3.2 Big Creek	142
5.4.3.3 Nissouri Creek	143
5.4.3.4 Saugeen River	144
5.4.3.5 Land-Use Implications.....	145
5.5 Conclusions.....	146
Figures And Tables.....	149
References.....	160
CHAPTER 6: DISSERTATION CONCLUSIONS, DISCUSSION AND FUTURE DIRECTIONS.....	167

6.1 Chapter Summaries and Significance	168
6.1.1 Data Chapter 2	168
6.1.2 Data Chapter 3	170
6.1.3 Data Chapter 4	172
6.1.4 Data Chapter 5	177
6.2 Conclusions.....	181
References.....	183
APPENDICES	186
VITA AUCTORIS	222

LIST OF TABLES

CHAPTER 2	46
Table 1: Mean concentrations of total organic and metal contaminants across sediment designations. Concentrations stated in $\mu\text{g g}^{-1}$ dry weight, except for TOC which is stated as a percentage (\pm standard error)	46
CHAPTER 3	77
Table 1: Big Creek Water Quality Parameters from grab samples and time-integrated suspended sediment samplers (\pm standard deviation).....	78
CHAPTER 4	113
Table 1: Significant Sediment and Water Quality Variable Correlations	113
CHAPTER 5	149
Table 1: Seasonal Water Quality Parameters for Big Creek, Nissouri Creek, and the Saugeen River.....	150

LIST OF FIGURES

CHAPTER 2	45
Figure 1: Sediment sampling locations from the present study and their contaminant designation in the lower Detroit River. Inset map shows the location of the Detroit River within the Lower Great Lakes (Circles C=Cold, Squares I=Intermediate, Triangles H=HOT, X= previous sediment sampling locations from 1999 and 2009 surveys from which contaminant designations were derived)	47
Figure 2: PC1 and PC2 scores of sediment samples based on total interpolated concentrations of metals and organic contaminants. Circles = COLD sites, squares = INT sites, triangles = HOT sites	48
Figure 3: RNA-based microbial taxonomy %abundances at a) phylum resolution and b) class-genus resolution across contaminant regions.....	49
Figure 4: Non-metric multidimensional scaling (stress = 0.103) of all 13 sediment samples for total metatranscriptomic profiles based on COG abundance count matrix. Circles = COLD sites, squares = INT sites, triangles = HOT sites	50
Figure 5: Summed Log2Fold change values across COG Functional Categories for low (COLD, n=5) and high (HOT, n=5) contaminated sediments. Negative values represent COLD sediments and positive values represent HOT sediments. Broad highlighted boxes represent; [M] – [Z] Cellular Processes and Signalling, [B] – [X] Information Storage and Processing, [C] – [Q] Metabolism	51
Figure 6: Average relative abundance of select genes across COLD and HOT sediments. Asterisks denote differential expression ($p < 0.05$) between COLD and HOT. napA: periplasmic nitrate reductase, mcr: methylcoenzyme M reductase, dsrAB: dissimilatory sulfite reductase alpha and beta subunit, nifD/H: Nitrogenase molybdenum-iron protein, alpha and beta chains. Aromatic degradation genes; Ubid: 3-polyprenyl-4hydroxybenzoate decarboxylase, HgdB: benzoyl-CoA reductase/2-hydroxyglutaryl-CoA dehydratase subunit, YciV: predicted metal-dependent phosphoesterase, FcbT: TRAP-type mannitol/chloroaromatic compound transport system, Yoal: aromatic ring hydroxylase, LigB: aromatic ring-opening dioxygenase, catalytic subunit, DodA: aromatic ring-cleaving dioxygenase, Paal: acyl-coenzyme A thioesterase PaaI, contains HGG motif. ACCS: Acyl-CoA synthetase, PepCK: phosphoenolpyruvate carboxykinase, PhaC: poly 3hydroxyalkanoate synthetase, Lpd: pyruvate/2-oxoglutarate dehydrogenase complex, Trp: transposases	52
Figure 7: Proposed carbon transformation pathways in legacy contaminated sediments of the Detroit River. Transcripts shown are involved in N-reduction, beta-oxidation, methanogenesis, polyester synthesis, and gluconeogenesis exhibited differential expression ($p > 0.05$) in HOT sediments compared to less contaminated environments as quantified through DESeq2	53
CHAPTER 3	77

Figure 1: A) Big Creek subsite sampling locations, downstream (S1) to upstream (S5). B) Location of Big Creek in Essex County, Ontario, Canada. C) Replicate suspended sediment samplers being submerged at S1	79
Figure 2: Big Creek physicochemical time series data. A) 2018 max daily air temperature (line) and precipitation (bars) during the 86-day sampling period from April to July. Sampling timepoints are denoted by dashed lines. B) 2021 deployment max daily air temperature, precipitation, and stream temperature and dissolved oxygen (DO) with Sampler DO. Recorded Sampler temperature was identical to Stream temperature	80
Figure 3: PCoA with Bray-Curtis distances of feature-level microbial community composition across samples. Labelled by Source and Month. Closed and open symbols represent bed and suspended phase microbial samples, respectively	81
Figure 4: Microbial phylum distribution across months and sediment source displayed as % abundance	82
Figure 5: LEfSe biomarker analysis identifying significantly different phyla between suspended and bed sediments over all sampling timepoints. A default log linear discriminant analysis (LDA) score of ± 2 was used as the default cut-off for differential expression with a false detection rate-adjusted p-value cut-off of 0.05. Suspended and bed sediment phyla are arbitrarily designated with positive (+) and negative (-) LDA scores, respectively	83
Figure 6: Distribution of the number of differentially expressed genera (n=271) across months and sediment source as determined through LEfSe. AM = April-May, MJ = May-June, JJ = June-July	84
Figure 7: LEfSe biomarker analysis identifying the top 50 significantly different genera between sediment source and month. A default log linear discriminant analysis (LDA) score of ± 2 was used as the default cut-off for differential expression with a false detection rate-adjusted p-value cut-off of 0.05. Suspended and bed sediment phyla are arbitrarily designated with positive (+) and negative (-) LDA scores, respectively. AM = April-May, MJ = May-June, JJ = June-July	85
CHAPTER 4	113
Figure 1: Total Nitrogen (TN), Total Phosphorus (TP), and TN:TP for Big Creek, Nissouri Creek, and the Saugeen River. Falk et al., data represents the range of values collected as part of this study, with Provincial Water Quality Monitoring Network (PWQMN) data representing values obtained for 2000 – 2020 from the open data catalogue from the Ministry of Environment, Conservation and Parks (MECP) (https://data.ontario.ca/dataset/provincial-stream-water-quality-monitoring-network)	115
Figure 2: Box plot annual distributions of surface water soluble reactive phosphorus (SRP) and bed sediment zero equilibrium phosphorus concentrations (EPC0) for Big Creek, Nissouri Creek, and the Saugeen River sampling sites	116
Figure 3: Seasonal point sampling characteristics for Big Creek, Nissouri Creek, and the Saugeen River for 2018 through 2020. Stacked bars represent the total interval precipitation (mm) with top sections specifying the seven-day precipitation amount preceding sampling. Dashed lines separate sampling years: Nissouri Creek and the Saugeen River were not sampled in 2018. EPC0 measured as mg L ⁻¹ SRP	117

Figure 4: Mid Spring 2019 vertical microsensor profiles for dissolved oxygen (DO) and oxidation-reduction potential (ORP). Horizontal dashed lines represent the location of the sediment water interface (SWI). Inset bar graph shows average DO and ORP depletion rates with depth, and average minimum (Min) recorded ORP across all measurements for Big Creek (BC), Nissouri Creek (NC), and the Saugeen River (SR).....	118
Figure 5: PCoA with Bray-Curtis distances of genus-level microbial community composition across samples. A) Samples labelled by site and timepoint with 95% confidence ellipses. BC = Big Creek, NC = Nissouri Creek, SR = Saugeen River. B) Samples labelled by the cumulative sum scaled abundance of the ammonia oxidizing archaea (AOA) <i>Candidatus Nitrosocosmicus</i>	119
Figure 6: Nissouri Creek 2019 concentrations of ammonium, nitrate, and nitrite.....	120
CHAPTER 5	149
Figure 1: Microbial community Shannon (H) alpha diversity distribution for substrate (bed sediment, suspended sediments, surface water) and nucleic acid type (DNA, RNA) across samples.....	151
Figure 2: NMDS ordination of microbial community samples across substrate (bed sediment, suspended sediments, surface water) and nucleic acid type (DNA, RNA). Ellipses represent 95% confidence intervals for DNA and RNA-based samples.....	152
Figure 3: Mantel tests between DNA and RNA microbial community Bray Curtis distances for bed sediments, suspended sediments, and surface water samples. R value represents the Spearman correlation between distance matrices	153
Figure 4: Abundances of active, neutral, and non-active microbial genera across sample groups	154
Figure 5a: Summer shared and unique active microbial genera for Big Creek, Nissouri Creek, and Saugeen River bed sediments, ordered by LEfSe LDA score. LDA scores represent the effect size of the genera abundance, with higher LDA scores indicating a stronger association with the site	155
Figure 5b: Fall shared and unique active microbial genera for Big Creek, Nissouri Creek, and Saugeen River bed sediments, ordered by LEfSe LDA score. LDA scores represent the effect size of the genera abundance, with higher LDA scores indicating a stronger association with the site	156
Figure 6: Relative expression heatmap of primary microbial functional categories across river sites and seasons. High expression (red) indicates greater than average abundance with low expression (blue) indicating lower than average abundance across samples.....	157
Figure 7a: Summer differentially expressed genes within primary Phosphorus, Nitrogen, and Sulfur Metabolism across big Creek (BC) Nissouri Creek (NC) and Saugeen River (SR) bed sediments. Secondary metabolic pathways are denoted by brackets within phosphorus and sulfur metabolism. Nitrogen secondary pathways of denitrification, dissimilatory nitrate reduction to ammonia (DNRA), nitrosative stress, N-fixation, and Ammonia Assimilation/Oxidation are denoted within the N-cycling pathway diagram. High expression (red) indicates greater than	

average abundance with low expression (blue) indicating lower than average abundance across samples.....	158
Figure 7b: Fall differentially expressed genes within primary Phosphorus, Nitrogen, and Sulfur Metabolism across big Creek (BC) Nissouri Creek (NC) and Saugeen River (SR) bed sediments	159

LIST OF APPENDICES

Appendix A (Chapter 2).....	186
Appendix B (Chapter 3).....	199
Appendix C (Chapter 4).....	210
Appendix D (Chapter 5).....	218

CHAPTER 1 INTRODUCTION

1.1 The Anthropocene

You wouldn't want to be in the Jornada del Muerto desert of New Mexico on July 16, 1945. At 5:29 a.m. local time, the first successful nuclear test was performed. Over the next half century, over 2000 more detonations would occur. Beyond palpable technological and social change, nuclear fallout resulted in a definitive and persistent chemostratigraphic change in deposits across the planet; that of radionuclide signatures. In particular, the accumulation of radioactive Strontium, Cesium, Carbon, and Plutonium, some of which existed in negligible quantities in any one place before human intervention. This detectable alteration in soils, sediments, and ice cores across the planet marks the beginning of the atomic age and, pending scientific consensus from the International Commission on Stratigraphy, may serve as the official geologic boundary of the newest proposed epoch on the planet, the Anthropocene (Lewis and Maslin, 2015; Zalasiewicz et al., 2015).

Unlike preceding epochs, such as the Holocene and Pleistocene, the Anthropocene is not defined by ice sheet retreats or advances, but represents the nexus of societal, industrial, economic, and above all, human influences that are altering natural systems. The effects of the Anthropocene are vast and complex but are rooted in detriments to earth's biogeochemical cycles due to deforestation, greenhouse gas emissions, ozone-depleting substances, biodiversity loss, and water quality impairments (Díaz et al., 2020; Foley et al., 2005; WHO, 2015). Though these effects are widespread across world biomes, some landscapes are more vulnerable than others and are in vital need of research, management, and conservation. The Laurentian Great Lakes of North America fall into this category. Home to over 40 million people (including 40% of the Canadian population), the Great Lakes region is under sustained pressure from the multiple and combining stressors that come along with human habitation. These include, but are not limited to, freshwater withdrawal, invasive species, emerging chemicals and pollutants, nuisance algal blooms, and climate change, all compounded by an accelerating population (Hartig et al., 2020; Smith et al., 2019). If not properly combatted, these threats spell an unpredictable future for one of the world's greatest freshwater resources.

1.2 Great Lakes Significance

The Great Lakes and their watersheds hold high economic, cultural, and ecological significance. For over 200 years the lakes have served as an integral part of the modern Great Lakes-St. Lawrence Seaway System; a bi-national transportation route that now moves more than 160 million metric tons of commodities per year (Martin Associates, 2018). This system is estimated to support 56 million jobs and a Gross Domestic Product (GDP) of US \$5 - 6 trillion, including \$15.9 billion in Ontario and Québec (McKindles et al., 2020). The region supports one of the world's most valuable freshwater fisheries, with commercial and sport angling activities contributing over \$800 million per year to Ontario's economy (MECP, 2012). The Lakes provide over 80% of the drinking water for Ontario residents and generate an equal proportion of the province's electricity via hydroelectric power. Recreational opportunities afforded by the aesthetics of the Great Lakes, including boating, camping, and hiking lure millions of tourists every year. Over 4700 shipwrecks provide some of the best freshwater diving attractions in the world. The infamous sinking of the Edmund Fitzgerald, cemented into folk history by the Gordon Lightfoot ballad, brings to light the cultural significance of the Great Lakes to both indigenous groups and colonizers. Indigenous Peoples have maintained an ecological and spiritual relationship with the region for millennia, well before European settlement. Fishing, farming, hunting, and trading within the Great Lakes region are deeply instilled in the cultures of First Nations groups, though it is understood through traditional knowledge that these practices must be performed in a sustainable fashion. For example, the Walpole Island First Nation people of the St. Clair River delta, an area that is home to 12% of Canada's at-risk species, have been able to live off the region's rich biodiversity and natural services while simultaneously engaging in preservation initiatives (Beckford et al., 2010). Elsewhere, Anishinaabe culture maintains a strong bond between women and water, both understood to be givers of life. This spiritual transcendence of clean water stewardship beyond political or environmental gains has manifested in the Mother Earth Water Walks, where women journey around the Great Lakes raising awareness for the responsible and sustainable use of fresh water and its bond with humanity (MECP, 2012; "Mother Earth Water Walks", n.d.). Further, many reviews of governance and management of the Great Lakes basin highlight First Nations

and Métis groups as vital stakeholders and stewards of biodiversity, whose Traditional and Ecological Knowledge (TEK) benefit decision-making processes and enhance educational outreach (Jetoo et al., 2015). Overlapping with the economic and cultural value of the Great Lakes are the ecological benefits of the region. The basin holds roughly one fifth of the worlds accessible fresh water and is a habitat for over 4000 species of plants, fish, and wildlife, many of which are endemic to the region (MECP, 2012). Wetlands sustain biodiversity and mitigate erosion and flooding, while also serving as sinks for anthropogenic contaminants (Campbell et al., 2015; Krantzberg and De Boer, 2008). Coastal wetlands have been estimate to have an annual value of USD \$69 billion (Horton et al., 2019). Beaches serve as refuges for endangered species and as shoreline barriers. Natural regions, both forested and coastal, act to assimilate carbon and recycle nutrients vital for the maintenance of biogeochemical cycles (Dila and Biddanda, 2015). Beyond the water bodies themselves, the network of rivers and streams that comprise the Great Lakes watersheds provide terrestrial drainage and are vectors for sediment and macronutrient transport, as well as spawning locations for fish (Gomi et al., 2002; Hosen et al., 2014). Multiple studies have concluded that investments in preserving and promoting the ecosystem services of the Great Lakes results in an increased economic/monetary return (Hartig and Krantzberg, 2022). Yet despite the understood value of the Great Lakes region, pressures from population and economic growth in both Canada and the USA often conflict with water security and conservation, resulting in unchanging or deteriorating statuses of beaches, fish consumption, species habitat, toxic chemicals, and nutrient and algae concentrations. This is especially true in the Huron-Erie Corridor (HEC); the southern bottleneck of the Great Lakes comprising of the St. Clair River, Lake St. Clair, Detroit River, and the Lake Erie Western Basin. Persistent discharges of anthropogenic contaminants and nutrients are a direct result of industrial development and agriculture in the region. The natural retention for contaminants and buffering capacity for macronutrients (nitrogen and phosphorous) are potentially being exceeded in these regions due to point and non-point pollution sources that have been continuous for the better part of a century.

1.3 Point and Non-point Pollution to the Lower Great Lakes

1.3.1 Metals and Persistent Organic Pollutants (POPs)

The accelerating growth of industry and agriculture in the lower great Lakes through the 20th century resulted in chronic supplies of exogenous materials to the waters, including high loads of complex synthetic chemicals, metals, nutrients, salts, and total suspended solids (TSS) (Chapra et al., 2009; EPA, 2022). Industrial sites and complexes that utilize the waterways for processing and transportation of raw materials within the HEC continue to be common point sources of pollution. The boom of the automotive industry in southern Michigan was a major driver of increased production, manifesting in a wave of manufacturing in the region that, despite economic prosperity, yielded both surface water and atmospheric deposition of chemicals. For example, the Ford Rouge River industrial complex, located in the Rouge River catchment that flows into the Detroit River, employed over 90,000 workers at its peak in the early 1930's and sprawled over 5 km². Sediments of the Rouge and Detroit river in the vicinity have been shown to be enriched in both harmful inorganic and organic constituents, with exceeded guidelines for Cr, Cu, Fe, Ni, Pb, Zn, and total PCBs (Murray et al., 1999). Indeed, much of the American shoreline of the Detroit River is characterized by abnormal levels of metals and complex organic contaminants, from both historical and current-day industrial and municipal sources (Hamdy and Post, 1985; Szalinska et al., 2007). Dissolved constituents may be flushed and diluted into Lake Erie via the high flow rate of the Detroit River, however, riverine bed sediments are often sinks for these persistent organic pollutants (POPs) and metals, due to both the common proximity of industrial point sources to shorelines and the affinity of benthic particles for contaminant attachment. Thus, sediment-centered surveys and rehabilitation have been the focus of many studies within the HEC (Hartig et al., 2020).

1.3.2 Suspended Sediment

Like many forms of pollution, suspended sediment is not inherently disruptive to ecosystems. On the contrary, suspended sediment is a natural and essential component of all fluvial environments, and shapes riverine environments from headwaters to deltas. The characteristics that make suspended sediment undesirable are often related to and/or cause by anthropogenic features, such as agricultural and urban development that increase erosion, sediment export, and turbidity, or dams/reservoirs that disrupt

sediment transport. Increases in suspended sediment loads can alter the physical environment of fish and disrupt their migration, feeding, and spawning, with analogous effects on primary and secondary producers, but mostly affecting photosynthesis-efficiency and grazing/predation, respectively (Newcombe and Macdonald, 1991). Although the term suspended sediment (sometimes synonymous with “fine suspended sediment”) usually encompasses the spectrum of grain sizes from sand (50-2000 μm) to silt (2-50 μm) to clay (0-2 μm), it is primarily the silt and clay-sized fractions that are of concern with respect to chemical and biological contaminant transport (Spencer et al., 2021). This is because of the cohesiveness of these finer fractions, which lends to the ability of these particles to aggregate into flocs, composed of a complex mixture of organic (biological + non-biological) and inorganic (i.e., mineral particles) material as well as water-filled pore space (Droppo, 2001). This cohesiveness, as well as the high adsorption capacity due to the large surface area to volume ratio of fine particles, makes fine-grained suspended sediments vectors for transport of pollutants including heavy metals (Hudson-Edwards et al., 1999), organic contaminants (Yunker et al., 2002), nutrients (Sharpley et al., 2007), and pathogens (Droppo et al., 2009). Further, the presence of microorganisms with flocs contributes to their cohesive characteristics, as bacterial extracellular polymeric substances (EPS) (a primary component of biofilms) aids in particle binding (Chen et al., 2017). The ubiquity of microbial communities associated with fine suspended sediment permits microorganisms to be used in sediment source identification using novel genomic tools (VanMensel et al., 2022). This approach is advantageous, as microbial source tracking can be performed independently of floc structure.

1.3.3 Nutrients

In addition to complex synthetic chemicals and suspended matter, excess nutrient loads to Great Lakes watersheds have been an enduring matter, resulting in ecological and aesthetic impairments to the region. For decades, intensive agricultural and concomitant application of fertilizers have been altering macronutrient transport and processing through watersheds and within the lakes themselves. Visible declines in Lake Erie through the 1960s and 1970s lead to legislative framework to confront water quality impairments and prompted additional research into the dynamics of primary production

within freshwater systems (Wilson et al., 2019). Pioneering bioassay research into nutrient limitations concluded that nitrogen and phosphorus played greater roles in primary production than inorganic carbon supplies, with many laboratory and whole-lake experiments further suggesting that phosphorous alone was the silver bullet for phytoplankton blooms (Hutchinson 1977, Lewis and Wurtsbaugh, 2008; Schindler, 1974). The conclusions for P-limitation are bolstered by the fact that inorganic carbon and nitrogen may be supplied through photosynthesis and nitrogen fixation, respectively, whereas phosphorus cycling lacks a significant atmospheric vector, and that P concentrations showed strong correlations with chlorophyll-*a* (a proxy for algal biomass) in many early studies (Dillon and Rigler, 1974, Sakamoto 1966, Schindler 1977, Vollenweider 1976). These studies set the paradigm of P-limitation that persists today, though research continues to unravel the complexities associated with N, P, and additional macro and micronutrient co-limitation. As experimentation preceded through the 20th century, variables including agricultural practice, meteorological conditions (i.e., wind, temperature, precipitation), micronutrients, and lake circulation have been shown to be important in regulating primary production (Bowes et al., 2016; Dodds and Smith, 2016; Giles et al., 2016). However, as these factors are either difficult or impossible to control, particularly in the face of climate change, management strategies continue to focus on point and not-point phosphorus sources to improve water quality. Many studies have cited significant results from models that predict loads of total and dissolved phosphorous from the outlets to Lake Erie and Lake St. Clair (Bocaniov et al., 2019; Maccoux et al., 2016; Scavia et al., 2019), however P-dynamics upstream and in headwater catchments of Southern Ontario are less understood.

1.4 Phosphorus

1.4.1 Phosphorus in the Global Context

Like many findings of the time, the discovery of P in 1669 by the alchemist Hennig Brandt was rather serendipitous. In the pursuit of compounds that could convert base metals into gold, Brandt accidentally purified ammonium sodium hydrogen phosphate, $(\text{NH}_4)\text{NaHPO}_4$ from urine. The compound, which easily oxidized while giving off brilliant light, was named *phosphorus mirabilis*, from the Ancient Greek name for the luminous planet Venus. Although P was later extracted from bone and guano, it

has since found grand commercial use as fertilizers when extracted from phosphate rock, as P is an essential macronutrient for all life. Through the agricultural revolution of the 20th century, highlighted by technological advancements in crop varieties, equipment, farming techniques (i.e. planting, harvesting, irrigation), and chemical fertilizers, mineral fertilizer production has increased nearly 4 fold (da Silva, 2019; Sharpley et al., 2018). This increase has led, as Sharpley et al., put it, to the conundrum of P deficiency and excess, where reserves of mineral P are gradually depleted and soluble P exports to watersheds from fertilizer amendments are amplified.

Many reviews and meta-analyses have focused on quantifying P export loads to marine and freshwater systems. Baseline, natural inputs of P to freshwater on global scale have been estimated by Yuan et al., to be $6.5 \pm 1.5 \text{ Tg P yr}^{-1}$ through synthesis of coupled nutrient retention models and estimates of global soil P content and erosion rates (Yuan et al., 2018). In addition, the authors suggest a total of $10.4 \pm 5.7 \text{ Tg P}$ is lost from cropland to freshwater systems per year, implying that agricultural alterations to land use can increase the baseline P inputs globally by 60%. Liu et al., estimate a similar loss of P from the world's cropland at $10.5 \text{ Tg P yr}^{-1}$ (10.5 million metric tons), while others have calculated greater loads of soil P loss from agriculture in the range of 14.9 to 26.4 Tg P yr^{-1} (totals of both inorganic and organic P) (Liu et al., 2008; Quinton et al., 2010). However, there are clear differences in estimates of total point and non-point sources of P to the world's inland waters. For example, Mekonnen et al., model loads of 1.5 Tg P yr^{-1} , with Liu et al., estimating between $2.7 \pm 0.5 \text{ kg P ha}^{-1} \text{ yr}^{-1}$ and $3.6 \pm 0.7 \text{ kg P ha}^{-1} \text{ yr}^{-1}$ depending on future climate scenarios (Liu et al., 2020; Mekonnen and Hoekstra, 2018). The latter two estimates amount to 1.9 and 2.5 Tg P yr^{-1} , respectively, when taking into account global crop area (Erenstein et al., 2021; Terzić et al., 2018). Larger estimates of P inputs into streams from various human activities are as high as 9 Tg P yr^{-1} , and models of P loads into all aquatic systems range from 12-21 Tg P yr^{-1} (Beusen et al., 2016; Tiessen et al., 2011). Although global-scale nutrient delivery modelling is complex and outputs can vary by orders of magnitude, there is agreement in several overarching outcomes; P losses from agriculture account for a major proportion of diffuse sources, P loads and eutrophication are increasing worldwide, and there is a growing decrease of P-use efficiency (PUE), meaning the proportion of P taken up by crops is decreasing relative to

that lost from various physical/chemical processes in soils (Biswas Chowdhury and Zhang, 2021; Yuan et al., 2018). The consequences of these scenarios are increased mobilization of P from the terrestrial to the aquatic landscape, and a higher reliance on chemical and organic fertilizers.

1.4.2 Phosphorus and the Great Lakes

Like global P modelling efforts, estimates of total P loads to the Great Lakes are problematic due to the vastness of the basin and the multiple and combining point and non-point sources of P. Thus, nutrient inputs by lake or by region/area of concern are often performed as they are more accurate and more relevant to regional load reduction targets. However, some approximations have been made for past and recent total P loadings to the Great lakes, including a summed 27,340 metric tonnes per annum (MTA) by Dolan and Chapra (0.02734 Tg P y⁻¹) and a U.S.-only load estimate of 11,549 MTA (0.011549 Tg P y⁻¹) and 13,220 MTA (0.01322 Tg P y⁻¹) for 2002 and 1983-1985, respectively (Dolan and Chapra, 2012; Robertson and Saad, 2011). Curbing P loads to the lower Great Lakes has been the subject of many remedial action plans (RAPs) over the latter 20th and early 21st century, driven by policy momentum through the 1960's to 1980's including the Canada Water Act (1970), the U.S. National Environmental Policy Act (1970), the U.S. Clean Water Act (1972), and the Canada-U.S. Great Lakes Water Quality Agreement (GLWQA) (1972) (Hartig et al., 2020). The GLWQA, which has had revisions in 1978, 1987, and 2012, is particularly central to the reductions of point-source P to Lake Erie that were achieved throughout its formation. For example, as a result of meeting a reduced loading target of 11,000 MTA in 1981, phytoplankton biomass decreased 52-89% across the Lake Erie basins (Wilson et al., 2019), central basin hypoxia declined (Scavia et al., 2014), and open lake total P concentrations and P loads decreased by the end of the 1980's (Dolan, 1993; Joosse and Baker, 2011; Scavia et al., 2014). Further, evidence of rehabilitation in communities of fish and benthic invertebrates surfaced post-GLWQA (Ludsin et al., 2001; Scavia et al., 2014). These improvements are largely attributed to P load reduction programs targeted at industrial and municipal point sources, as well as P contents of detergents (Baker et al., 2014). However, there is scientific consensus that trends in eutrophication have been reversing in Lake Erie over the last two decades, particularly in the shallower western basin,

culminating in harmful algal blooms (HABs) that have in some cases shut down municipal drinking water supplies (Chaffin et al., 2021; Steffen et al., 2017; Watson et al., 2016). In fact, since 2011, 5 of the worst blooms on record have occurred. Although there is high inter-annual variability in P loadings to the lower Great Lakes, including Lake Erie and the Huron-Erie Corridor, there is some evidence that TP loads have maintained in the last decade, but the percentage of TP comprised of SRP has increased (Daloğlu et al., 2012; Richards et al., 2010; Scavia et al., 2014). This trend may be more evident in U.S. watersheds compared to Canadian counterparts, however, as other studies point to decreasing or unchanging TP and SRP concentrations in southern Ontario watersheds (although some of these results do not include winter loads) (Raney and Eimers, 2014; Stammel et al., 2017). When taking into account winter loads, studies often suggest increasing nutrient export from single, high flow events, due to warmer winter air temperatures and increased rainfall and freeze-thaw days (Daloğlu et al., 2012; Nelligan et al., 2021). Despite these spatial/temporal discrepancies across studies, there is agreement that across HEC catchments, non-point agriculture P, particularly the more immediately bioavailable SRP, is highly correlated with eutrophication events and the extent of algal blooms (Dodds and Smith, 2016; Jarvie et al., 2017, 2005; Jenny et al., 2020; Joosse and Baker, 2011; Lam et al., 2016; McDowell et al., 2017).

1.4.3 Phosphorus Cycling in Lotic Systems

As the majority of P entering the lower Great Lakes is transported through the networks of rivers, streams, and drains that connect the terrestrial and lacustrine systems, in-stream P cycling is important to understand. For example, recent models have shown that the amount of P as fertilizer applied in Ontario is less than what enters the lower Great Lakes from its primary tributaries (Van Staden et al., 2021). Thus, there is a large amount of P predicted to be retained in soils and sediments. As PUE is also decreasing worldwide (i.e., P fertilizer is still required to obtain desired yields), P must be transported and stored more in lotic networks than in soils. The concept of this internal lotic reservoir of P is not new (Schindler, 1974; Stone and Droppo, 1994; Vollenweider, 1975) nor is the quantification of P-adsorption/desorption to soils and sediments using isotherms (Froelich, 1988; Taylor and Kunishi, 1971). Many studies have used P-isotherms, particularly the Equilibrium Phosphorus Concentration at zero net sorption

(EPC₀) assay to label sediments as either potential sources or sinks of bioavailable P in relation to the water column (Simpson et al., 2021), however the site-specific context of this sink/source designation and the factors that alleviate or exasperate sediment P release are still highly debated, including the dependence of current day P-flux on past states of nutrient loading (i.e., hysteresis effects).

1.4.4 Internal P Loading

The current paradigm of internal P loading is that two primary factors control to the movement of P between the sediment water interface (SWI): 1) Physical diffusion gradients caused by increased or decreased P in the water column that may be externally influenced, and 2) Redox changes in sediments that contribute to P-desorption from P-bearing mineral phases. Both factors have multiple sub-factors that can contribute to the process. For example, a physical diffusion gradient may develop after a rainfall event dilutes P concentrations in the water column relative to the sediment, leading to P flux out of the sediment, or increased primary production in the water column may consume P, leading to the same outcome. Redox changes in sediments may result from increased dissolved oxygen (DO) depletion from eutrophication, and/or from microbial metabolism in sediments consuming alternative terminal electron acceptors (TEAs) such as NO₃⁻, Mn, or Fe, which has been shown to increase P desorption. These factors have been confirmed to correlate with increased sediment P-flux in laboratory studies and investigation near the SWI (Giles et al., 2016; Parsons et al., 2017), however there is a lack of understanding of the role that microbes play in redox-influenced P-source scenarios. The ability to quantify the specific microbial guilds and genes that are associated with P-loading events can aid in understanding the biotic mechanisms associated with internal nutrient fluxes and identify species that can be used as early warning indicators of sediment redox shifts.

1.5 Bioindicators

Following perturbations to freshwaters from multiple and combining anthropogenic stressors, there have been efforts to quantify the effects on ecosystem components beyond just physical-chemical parameters (Dafforn et al., 2012; Norris and Thoms, 1999). Early studies in ecotoxicology, for example, focused on the detriments to

various organisms in Great Lakes watersheds. The health of individual and populations of invertebrates (Cook and Johnson, 1974), fish (Lucas et al., 1970), and birds (Giesy et al., 1994; Peakall and Fox, 2007; Stalling et al., 1985) are consistently found to correlate with abnormal concentrations of pesticides, chemicals, and metals. Ecosystem approaches that integrate interrelationships across food webs pioneered by Vallentyne (a student of George Evelyn Hutchinson) and others, have come to similar conclusions, generating interest in understanding multi-stressor and multi-species testing at the community or guild level in the field and the lab (Karr, 1987; Vallentyne and Beeton, 1988). However, biomonitoring programs have traditionally been limited to the macrofauna and their morphological traits and/or alterations. Though informative, these biological methods are often time and resource intensive, and fail to match the scale of data collected and compiled through physical and chemical investigations. It was not until the late 20th century when research began to incorporate microorganisms into the ecosystem approach, reinforced by revolutions in microbial techniques.

1.6 Microbial Community Ecology

1.6.1 A (Very) Brief History of Microbiology

A detailed and thorough history of microbiology is beyond the scope of this thesis, however, there are several keystone moments in the past of the field that contribute to our abilities to study and understand microbial communities today and their influences on environmental processes. The first detailed accounting of microbes was performed by Dutch scientist Antonie van Leeuwenhoek in the late 1600's, whose improved lenses made the miniscule observations possible. Microorganisms and their connection to infection and illness dominated ideas over the next two centuries, such as the pioneering work by Edward Jenner, Agostino Bassi, Ignaz Semmelweis, and Heinrich Anton de Bary, to name a few. The following “Golden Age of Microbiology” (roughly 1850 -1910) included seminal findings by Louis Pasteur, Robert Koch, and Hans Christian Gram, who brought scientific rigor into the study of microbiology. However, it was the Ukrainian scientist Sergei N. Winogradski (1 September 1856 – 25 February 1953) who began to unveil the undeniable role of microbial communities on biogeochemical cycling in non-living host environments, and who would lay the foundation for the concepts of chemoautotrophy (Dworkin, 2012). Fundamental to these

ideas is that assemblages of microbes contribute to the subsurface transformations of macronutrients (N, P, S, C) and that specific functional guilds of prokaryotes possess protein-coding genes that make these transformations possible. Investigations of the diversity and function of these genes exploded in the late 20th century with the advent of culture-free genomic techniques. Notably, Woese and colleagues who posited that 16S ribosomal RNA could be used as a phylogenetic marker, positioning bacteria into their own branch in the tree of life, and Norman Pace and colleagues, who used the technique to sequence bacterial communities in the environment without culturing, a giant leap forward in exploring microbial assemblages in their natural habitats (Pace, 1997; Woese et al., 1990).

1.6.2 Microbial Control on Ecosystem Processes in Freshwater Systems

Microorganisms and their populations at the SWI in freshwater environments play vital roles in ecosystem functioning; they are the primary regulators of organic matter degradation, they mediate nutrient availability to higher trophic levels, and they exert control over pH and redox gradients from stream/lake beds to the hyporheic zone (Abram, 2015; Beattie et al., 2020; Cabral et al., 2016; Fasching et al., 2020). Just as the macrofauna exhibit measurable responses to anthropogenic stress, microbial communities too are altered in their compositional diversity and function, metrics that are now quantifiable through advances in sequencing technologies. Improvements in both high-throughput DNA sequencers and downstream bioinformatic analysis pipelines have shown success in using microbial genomic data to inform about baseline ecosystem functions (Birrer et al., 2017), which often show correlation with traditional abiotic/biotic indexes such as sediment chemistry report cards and macroinvertebrate surveys (Horton et al., 2019). The advantage of using microbial information as proxies for in-situ ecosystem health is that microorganisms are often early responders to environmental changes, making them valuable early warning indicators of stress (Simonin et al., 2019; Yang et al., 2019). The caveat is that the capricious nature of microbes in dynamic environments such as surface waters and stream beds may make them unreliable as gauges of long-term trends; thus study design, site location, and the application of parallel lab-based studies are important if microbial communities are to be integrated into environmental assessments. Worldwide, this type of work is gradually being refined in both

quality and quantity, however studies targeting areas of concern in the lower Great Lakes are lacking.

1.7 Thesis Objectives

The primary goal of this dissertation work will be to improve the understanding of microbial activity and diversity as a result of human-induced landscape changes in several study systems of the lower Great Lakes region and coupling this information with relevant abiotic chemical stressors and stressor signals that are understood to impair the systems. Specifically, this work seeks to link microbial diversity and function at the sediment-water interface to gradients of anthropogenic stressors caused by 1) industrial pollutants and heavy metals, and 2) nutrients from agriculture. The work will have its foundation in field work campaigns that will collect sediment and water samples from the study sites with appropriate spatial and temporal designs, followed by in-lab chemical and microbiological characterizations.

In data Chapter 2, the microbial response to legacy contamination in Detroit River bed sediments is assessed. Pollution from polycyclic aromatic hydrocarbons (PAHs), polychlorinated biphenyls (PCBs), and metals, is well characterized through the Detroit River, thus regions of low and high contaminant concentrations can be tested for patterns in microbial diversity and gene expression via metatranscriptomics. Using this well-defined contaminant gradient, microbial community structure and function can be more robustly related to the influences of sediment pollution. The overarching null hypotheses are as follows:

H2.1: Microbial community diversity is not different in low vs. high contaminant sediment regions in the lower Detroit River.

H2.2: Microbial expression of PAH-degrading genes is not different in low vs. high contaminant regions.

In data Chapter 3, suspended and bed sediment phase microbial communities were assessed seasonally in an agriculturally impacted river in Southern Ontario (Big Creek). The primary objectives were to test the precision and replicability between individual suspended sediment samplers (with respect to the accumulated microbial

communities), compare suspended and bed sediment phase microbial diversity and composition, and to investigate any potential redox shifts inside the samplers. The overarching null hypotheses are as follows:

H3.1: Microbial community composition is not different between individual suspended sediment samplers along the river segment.

H3.2: Suspended and bed sediment phase microbial communities do not differ in their composition.

H3.3: The oxidation-reduction potential inside the suspended sediment sampler is not different from that in the stream environment.

In data Chapter 4, three watercourses differing in watershed-wide trends of fertilizer application type (Big Creek by inorganic/chemical fertilizer, Nissouri Creek by organic/manure fertilizer, and the Saugeen River as a forested reference site) were investigated for internal P loading risk via the EPC₀ assay. Site visits through the growing seasons of 2018-2020 investigated the site-specific variables that correlated with high EPC₀ values, including N and P concentrations, precipitation, temperature, in-situ sediment redox, and bed sediment microbial community composition. The overarching null hypotheses are as follows:

H4.1: Big Creek, Nissouri Creek, and the Saugeen River show no difference in past and present total N and total P concentrations.

H4.2: Bed and suspended sediments are primarily sinks of P with no difference in EPC₀ values across sites and seasons.

H4.3: Bed sediment microbial community composition is not different between sites and not affected by internal P loading risk.

In Chapter 5, the three watercourses (Big Creek, Nissouri Creek, and Saugeen River) are further investigated for seasonal changes in microbial community composition in the three primary lotic substrates: surface waters, suspended sediments, and bed sediments, using both RNA and DNA-based metabarcoding. In addition, total microbial

gene function is assessed in bed sediments via metatranscriptomics. The overarching null hypotheses are as follows:

H5.1: Alpha diversity within a site is not different between substrate type (i.e., surface waters, suspended sediments, and bed sediments) or between the nucleic acid extraction method (i.e., RNA vs. DNA).

H5.2: Alpha diversity between DNA metabarcoding and RNA metabarcoding samples is not different across all samples.

H5.3: Abundance of N, P, and S-metabolism genes are not different between sites and seasons.

References

- Abram, F., 2015. Systems-based approaches to unravel multi-species microbial community functioning. *Comput. Struct. Biotechnol. J.* 13, 24–32.
<https://doi.org/10.1016/j.csbj.2014.11.009>
- Baker, D.B., Confesor, R., Ewing, D.E., Johnson, L.T., Kramer, J.W., Merryfield, B.J., 2014. Phosphorus loading to Lake Erie from the Maumee, Sandusky and Cuyahoga rivers: The importance of bioavailability. *J. Great Lakes Res.* 40, 502–517.
<https://doi.org/10.1016/J.JGLR.2014.05.001>
- Beattie, R.E., Bandla, A., Swarup, S., Hristova, K.R., 2020. Freshwater Sediment Microbial Communities Are Not Resilient to Disturbance From Agricultural Land Runoff. *Front. Microbiol.* 11, 1–14. <https://doi.org/10.3389/fmicb.2020.539921>
- Beckford, C., Jacobs, C., Williams, N., Nahdee, R., 2010. Aboriginal environmental wisdom, stewardship, and sustainability: Lessons from the Walpole island first nations, Ontario, Canada. *J. Environ. Educ.* 41, 239–248.
<https://doi.org/10.1080/00958961003676314>
- Beusen, A.H.W., Bouwman, A.F., Van Beek, L.P.H., Mogollón, J.M., Middelburg, J.J., 2016. Global riverine N and P transport to ocean increased during the 20th century despite increased retention along the aquatic continuum. *Biogeosciences* 13, 2441–2451. <https://doi.org/10.5194/bg-13-2441-2016>
- Birrer, S.C., Dafforn, K.A., Johnston, E.L., 2017. Microbial Community Responses to Contaminants and the Use of Molecular Techniques, in: *Microbial Ecotoxicology*. Springer International Publishing, Cham, pp. 165–183. https://doi.org/10.1007/978-3-319-61795-4_8
- Biswas Chowdhury, R., Zhang, X., 2021. Phosphorus use efficiency in agricultural systems: A comprehensive assessment through the review of national scale substance flow analyses. *Ecol. Indic.* 121, 107172.
<https://doi.org/10.1016/j.ecolind.2020.107172>

- Bocaniov, S.A., Van Cappellen, P., Scavia, D., 2019. On the Role of a Large Shallow Lake (Lake St. Clair, USA-Canada) in Modulating Phosphorus Loads to Lake Erie. *Water Resour. Res.* 55, 10548–10564. <https://doi.org/10.1029/2019WR025019>
- Bowes, M.J., Loewenthal, M., Read, D.S., Hutchins, M.G., Prudhomme, C., Armstrong, L.K., Harman, S.A., Wickham, H.D., Gozzard, E., Carvalho, L., 2016. Identifying multiple stressor controls on phytoplankton dynamics in the River Thames (UK) using high-frequency water quality data. *Sci. Total Environ.* 569–570, 1489–1499. <https://doi.org/10.1016/j.scitotenv.2016.06.239>
- Cabral, L., Júnior, G.V.L., Pereira de Sousa, S.T., Dias, A.C.F., Lira Cadete, L., Andreote, F.D., Hess, M., de Oliveira, V.M., 2016. Anthropogenic impact on mangrove sediments triggers differential responses in the heavy metals and antibiotic resistomes of microbial communities. *Environ. Pollut.* 216, 460–469. <https://doi.org/10.1016/j.envpol.2016.05.078>
- Campbell, M., Cooper, M.J., Friedman, K., Anderson, W.P., 2015. The economy as a driver of change in the Great Lakes-St. Lawrence River basin. *J. Great Lakes Res.* 41, 69–83. <https://doi.org/10.1016/j.jglr.2014.11.016>
- Chaffin, J.D., Bratton, J.F., Verhamme, E.M., Bair, H.B., Beecher, A.A., Binding, C.E., Birbeck, J.A., Bridgeman, T.B., Chang, X., Crossman, J., Currie, W.J.S., Davis, T.W., Dick, G.J., Drouillard, K.G., Errera, R.M., Frenken, T., MacIsaac, H.J., McClure, A., McKay, R.M., Reitz, L.A., Domingo, J.W.S., Stanislawczyk, K., Stumpf, R.P., Swan, Z.D., Snyder, B.K., Westrick, J.A., Xue, P., Yancey, C.E., Zastepa, A., Zhou, X., 2021. The Lake Erie HABs Grab: A binational collaboration to characterize the western basin cyanobacterial harmful algal blooms at an unprecedented high-resolution spatial scale. *Harmful Algae* 108, 102080. <https://doi.org/10.1016/j.hal.2021.102080>
- Chapra, S.C., Dove, A., Rockwell, D.C., 2009. Great Lakes chloride trends: Long-term mass balance and loading analysis. *J. Great Lakes Res.* 35, 272–284. <https://doi.org/10.1016/j.jglr.2008.11.013>

- Chen, X.D., Zhang, C.K., Zhou, Z., Gong, Z., Zhou, J.J., Tao, J.F., Paterson, D.M., Feng, Q., 2017. Stabilizing Effects of Bacterial Biofilms: EPS Penetration and Redistribution of Bed Stability Down the Sediment Profile. *J. Geophys. Res. Biogeosciences* 122, 3113–3125. <https://doi.org/10.1002/2017JG004050>
- Cook, D.G., Johnson, M.G., 1974. Benthic macroinvertebrates of the St. Lawrence Great Lakes. *J. Fish. Res. Board Canada* 31, 763–782.
- da Silva, J.G., 2019. From Fome Zero to Zero Hunger, From Fome Zero to Zero Hunger. <https://doi.org/10.18356/d3dc1fea-en>
- Dafforn, K.A., Simpson, S.L., Kelaher, B.P., Clark, G.F., Komyakova, V., Wong, C.K.C., Johnston, E.L., 2012. The challenge of choosing environmental indicators of anthropogenic impacts in estuaries. *Environ. Pollut.* 163, 207–217. <https://doi.org/10.1016/j.envpol.2011.12.029>
- Daloğlu, I., Cho, K.H., Scavia, D., 2012. Evaluating causes of trends in long-term dissolved reactive phosphorus loads to lake erie. *Environ. Sci. Technol.* 46, 10660–10666. <https://doi.org/10.1021/es302315d>
- Díaz, S., Settele, J., Brondízio, E., Ngo, T.H., Guèze, M., Agard, J., 2020. Summary for policymakers of the global assessment report on biodiversity and ecosystem services of the Intergovernmental Science-Policy Platform on Biodiversity and Ecosystem Services.
- Dila, D.K., Biddanda, B.A., 2015. From land to lake: Contrasting microbial processes across a Great Lakes gradient of organic carbon and inorganic nutrient inventories. *J. Great Lakes Res.* 41, 75–85. <https://doi.org/10.1016/j.jglr.2015.04.014>
- Dillon, P.J., Rigler, F.H., 1974. The phosphorus-chlorophyll relationship in lakes 19.
- Dodds, W.K., Smith, V.H., 2016. Nitrogen, phosphorus, and eutrophication in streams. *Int. Waters* 6, 155–164. <https://doi.org/10.5268/TW-6.2.909>
- Dolan, D.M., 1993. Point Source Loadings of Phosphorus to Lake Erie: 1986–1990. *J. Great Lakes Res.* 19, 212–223. [https://doi.org/10.1016/S0380-1330\(93\)71212-5](https://doi.org/10.1016/S0380-1330(93)71212-5)

- Dolan, D.M., Chapra, S.C., 2012. Great Lakes total phosphorus revisited: 1. Loading analysis and update (1994-2008). *J. Great Lakes Res.* 38, 730–740.
<https://doi.org/10.1016/j.jglr.2012.10.001>
- Droppo, I.G., 2001. Rethinking what constitutes suspended sediment. *Hydrol. Process.* 15, 1551–1564. <https://doi.org/10.1002/hyp.228>
- Droppo, I.G., Liss, S.N., Williams, D., Nelson, T., Jaskot, C., Trapp, B., 2009. Dynamic existence of waterborne pathogens within river sediment compartments. Implications for water quality regulatory affairs. *Environ. Sci. Technol.* 43, 1737–1743. <https://doi.org/10.1021/es802321w>
- Dworkin, M., 2012. Sergei Winogradsky: A founder of modern microbiology and the first microbial ecologist. *FEMS Microbiol. Rev.* 36, 364–379.
<https://doi.org/10.1111/j.1574-6976.2011.00299.x>
- EPA, 2022. State of the Great Lakes 2022 Report.
- Erenstein, O., Chamberlin, J., Sonder, K., 2021. Estimating the global number and distribution of maize and wheat farms. *Glob. Food Sec.* 30, 100558.
<https://doi.org/10.1016/j.gfs.2021.100558>
- Fasching, C., Akotoye, C., Bižić, M., Fonvielle, J., Ionescu, D., Mathavarajah, S., Zoccarato, L., Walsh, D.A., Grossart, H.P., Xenopoulos, M.A., 2020. Linking stream microbial community functional genes to dissolved organic matter and inorganic nutrients. *Limnol. Oceanogr.* 65, S71–S87.
<https://doi.org/10.1002/lno.11356>
- Foley, J.A., DeFries, R., Asner, G.P., Barford, C., Bonan, G., Carpenter, S.R., Chapin, F.S., Coe, M.T., Daily, G.C., Gibbs, H.K., Helkowski, J.H., Holloway, T., Howard, E.A., Kucharik, C.J., Monfreda, C., Patz, J.A., Prentice, I.C., Ramankutty, N., Snyder, P.K., 2005. Global consequences of land use. *Science* (80-.). 309, 570–574.
<https://doi.org/10.1126/science.1111772>
- Froelich, P.N., 1988. Kinetic control of dissolved phosphate in natural rivers and

- estuaries: A primer on the phosphate buffer mechanism. *Limnol. Oceanogr.* 33, 649–668. <https://doi.org/10.4319/lo.1988.33.4part2.0649>
- Giesy, J.P., Ludwig, J.P., Tillitt, D.E., 1994. Deformities in birds of the great lakes region : Assigning casualty. *Environ. Sci. Technol.* 28. <https://doi.org/10.1021/es00052a720>
- Giles, C.D., Isles, P.D.F., Manley, T., Xu, Y., Druschel, G.K., Schroth, A.W., 2016. The mobility of phosphorus, iron, and manganese through the sediment–water continuum of a shallow eutrophic freshwater lake under stratified and mixed water-column conditions. *Biogeochemistry* 127, 15–34. <https://doi.org/10.1007/s10533-015-0144-x>
- Gomi, T., Sidle, R.C., Richardson, J.S., 2002. Understanding processes and downstream linkages of headwater systems. *Bioscience* 52, 905–916. [https://doi.org/10.1641/0006-3568\(2002\)052\[0905:UPADLO\]2.0.CO;2](https://doi.org/10.1641/0006-3568(2002)052[0905:UPADLO]2.0.CO;2)
- Hamdy, Y., Post, L., 1985. Distribution of Mercury, Trace Organics, and Other Heavy Metals in Detroit River Sediments. *J. Great Lakes Res.* 11, 353–365. [https://doi.org/10.1016/S0380-1330\(85\)71779-0](https://doi.org/10.1016/S0380-1330(85)71779-0)
- Hartig, J.H., Krantzberg, G., 2022. Reflections on social and organizational dimensions of Great Lakes remediation , restoration , and revitalization. *J. Great Lakes Res.* 8–10. <https://doi.org/10.1016/j.jglr.2022.08.003>
- Hartig, J.H., Krantzberg, G., Alsip, P., 2020. Thirty-five years of restoring Great Lakes Areas of Concern: Gradual progress, hopeful future. *J. Great Lakes Res.* 46, 429–442. <https://doi.org/10.1016/j.jglr.2020.04.004>
- Horton, D.J., Theis, K.R., Uzarski, D.G., Learman, D.R., 2019. Microbial community structure and microbial networks correspond to nutrient gradients within coastal wetlands of the Laurentian Great Lakes. *FEMS Microbiol. Ecol.* 95, 1–17. <https://doi.org/10.1093/femsec/fiz033>
- Hosen, J.D., Mcdonough, O.T., Febria, C.M., Palmer, M.A., 2014. Dissolved Organic

- Matter Quality and Bioavailability Changes Across an Urbanization Gradient in Headwater Streams - Environmental Science & Technology (ACS Publications).
- Hudson-Edwards, K.A., Macklin, M.G., Taylor, M.P., 1999. 2000 years of sediment-borne heavy metal storage in the Yorkshire Ouse basin, NE England, UK. *Hydrol. Process.* 13, 1087–1102. [https://doi.org/10.1002/\(SICI\)1099-1085\(199905\)13:7<1087::AID-HYP791>3.0.CO;2-T](https://doi.org/10.1002/(SICI)1099-1085(199905)13:7<1087::AID-HYP791>3.0.CO;2-T)
- Jarvie, H.P., Johnson, L.T., Sharpley, A.N., Smith, D.R., Baker, D.B., Bruulsema, T.W., Confesor, R., 2017. Increased Soluble Phosphorus Loads to Lake Erie: Unintended Consequences of Conservation Practices? *J. Environ. Qual.* 46, 123. <https://doi.org/10.2134/jeq2016.07.0248>
- Jarvie, H.P., Jurgens, M.D., Williams, R.J., Neal, C., Davies, J.J.L., Barrett, C., White, J., 2005. Role of river bed sediments as sources and sinks of phosphorus across two major eutrophic UK river basins : the Hampshire Avon and Herefordshire Wye. *J. Hydrol.* 304, 51–74. <https://doi.org/10.1016/j.jhydrol.2004.10.002>
- Jenny, J.P., Anneville, O., Arnaud, F., Baulaz, Y., Bouffard, D., Domaizon, I., Bocaniov, S.A., Chèvre, N., Dittrich, M., Dorioz, J.M., Dunlop, E.S., Dur, G., Guillard, J., Guinaldo, T., Jacquet, S., Jamoneau, A., Jawed, Z., Jeppesen, E., Krantzberg, G., Lenters, J., Leoni, B., Meybeck, M., Nava, V., Nöges, T., Nöges, P., Patelli, M., Pebbles, V., Perga, M.E., Rasconi, S., Ruetz, C.R., Rudstam, L., Salmaso, N., Sapna, S., Straile, D., Tammeorg, O., Twiss, M.R., Uzarski, D.G., Ventelä, A.M., Vincent, W.F., Wilhelm, S.W., Wängberg, S.Å., Weyhenmeyer, G.A., 2020. Scientists' Warning to Humanity: Rapid degradation of the world's large lakes. *J. Great Lakes Res.* <https://doi.org/10.1016/j.jglr.2020.05.006>
- Jetoo, S., Thorn, A., Friedman, K., Gosman, S., Krantzberg, G., 2015. Governance and geopolitics as drivers of change in the Great Lakes-St. Lawrence basin. *J. Great Lakes Res.* 41, 108–118. <https://doi.org/10.1016/j.jglr.2014.11.011>
- Joosse, P.J., Baker, D.B., 2011. Context for re-evaluating agricultural source phosphorus loadings to the Great Lakes. *Can. J. Soil Sci.* 91, 317–327.

<https://doi.org/10.4141/cjss10005>

- Karr, J.R., 1987. Biological monitoring and environmental assessment: a conceptual framework. *Environ. Manage.* 11, 249–256. <https://doi.org/10.1007/BF01867203>
- Krantzberg, G., De Boer, C., 2008. A valuation of ecological services in the Laurentian Great Lakes Basin with an emphasis on Canada. *J. / Am. Water Work. Assoc.* 100, 100–111. <https://doi.org/10.1002/j.1551-8833.2008.tb09657.x>
- Lam, W. V., Macrae, M.L., English, M.C., O’Halloran, I.P., Wang, Y.T., 2016. Effects of tillage practices on phosphorus transport in tile drain effluent under sandy loam agricultural soils in Ontario, Canada. *J. Great Lakes Res.* 42, 1260–1270. <https://doi.org/10.1016/j.jglr.2015.12.015>
- Lewis, S.L., Maslin, M.A., 2015. Defining the Anthropocene. *Nature* 519, 171–180. <https://doi.org/10.1038/nature14258>
- Lewis, W.M., Wurtsbaugh, W.A., 2008. Control of lacustrine phytoplankton by nutrients: Erosion of the phosphorus paradigm. *Int. Rev. Hydrobiol.* 93, 446–465. <https://doi.org/10.1002/iroh.200811065>
- Liu, W., Ciais, P., Liu, X., Yang, H., Hoekstra, A.Y., Tang, Q., Wang, X., Li, X., Cheng, L., 2020. Global Phosphorus Losses from Croplands under Future Precipitation Scenarios. *Environ. Sci. Technol.* 54, 14761–14771. <https://doi.org/10.1021/acs.est.0c03978>
- Liu, Y., Villalba, G., Ayres, R.U., Schroder, H., 2008. Global phosphorus flows and environmental impacts from a consumption perspective. *J. Ind. Ecol.* 12, 229–247. <https://doi.org/10.1111/j.1530-9290.2008.00025.x>
- Lucas, F., Encrncron, N., Dia, P., Lakes, G., Arbor, A., 1970. Concentrations Hnxnv of Trace Elernents in Great Lakes Fishes. *J. Fish. Reserach Board Canada* 27, 677–684.
- Ludsin, S.A., Kershner, M.W., Blocksom, K.A., Knight, R.L., Stein, R.A., 2001. *Life After Death in Lake Erie : Nutrient Controls Drive Fish Species Richness , Rehabilitation* Published by : Wiley on behalf of the Ecological Society of America

Stable URL : <http://www.jstor.org/stable/3061113> REFERENCES Linked
references are available. *Ecol. Appl.* 11, 731–746.

Maccoux, M.J., Dove, A., Backus, S.M., Dolan, D.M., 2016. Total and soluble reactive phosphorus loadings to Lake Erie: A detailed accounting by year, basin, country, and tributary. *J. Great Lakes Res.* 42, 1151–1165.
<https://doi.org/10.1016/j.jglr.2016.08.005>

Martin Associates, 2018. Economic impacts of maritime shipping in the Great Lakes - St. Lawrence Region.

McDowell, R.W., Elkin, K.R., Kleinman, P.J.A., 2017. Temperature and Nitrogen Effects on Phosphorus Uptake by Agricultural Stream-Bed Sediments. *J. Environ. Qual.* 46, 295–301. <https://doi.org/10.2134/jeq2016.09.0352>

McKindles, K., Thijs, F., McKay, R.M.L., Bullerjahn, G.S., 2020. Binational Efforts Addressing Cyanobacterial Harmful Algal Blooms in the Great Lakes. *Handb. Environ. Chem.* 5, 1–12. <https://doi.org/10.1007/698>

MECP, 2012. Ontario's Great Lakes Strategy PIBS 9198e.

Mekonnen, M.M., Hoekstra, A.Y., 2018. Global Anthropogenic Phosphorus Loads to Freshwater and Associated Grey Water Footprints and Water Pollution Levels: A High-Resolution Global Study. *Water Resour. Res.* 54, 345–358.
<https://doi.org/10.1002/2017WR020448>

Murray, K.S., Cauvet, D., Lybeer, M., Thomas, J.C., 1999. Particle size and chemical control of heavy metals in bed sediment from the Rouge River, southeast Michigan. *Environ. Sci. Technol.* 33, 987–992. <https://doi.org/10.1021/es9807946>

Nelligan, C., Sorichetti, R.J., Yousif, M., Thomas, J.L., Wellen, C.C., Parsons, C.T., Mohamed, M.N., 2021. Then and now: Revisiting nutrient export in agricultural watersheds within southern Ontario's lower Great Lakes basin. *J. Great Lakes Res.*
<https://doi.org/10.1016/j.jglr.2021.08.010>

Newcombe, C.P., Macdonald, D.D., 1991. Effects of Suspended Sediments on Aquatic

- Ecosystems. North Am. J. Fish. Manag. 11, 72–82. [https://doi.org/10.1577/1548-8675\(1991\)011<0072:eossoa>2.3.co;2](https://doi.org/10.1577/1548-8675(1991)011<0072:eossoa>2.3.co;2)
- Norris, R.H., Thoms, M.C., 1999. What is river health? Freshw. Biol. 41, 197–209. <https://doi.org/10.1046/j.1365-2427.1999.00425.x>
- Pace, N.R., 1997. A molecular view of microbial diversity and the biosphere. Science (80-.). 276, 734–740. <https://doi.org/10.1126/science.276.5313.734>
- Parsons, C.T., Rezanezhad, F., O’Connell, D.W., Van Cappellen, P., 2017. Sediment phosphorus speciation and mobility under dynamic redox conditions. Biogeosciences 14, 3585–3602. <https://doi.org/10.5194/bg-14-3585-2017>
- Peakall, D.B., Fox, G.A., 2007. Toxicological Investigations of Pollutant-Related Effects in Great Lakes Gulls. Environ. Health Perspect. 71, 187. <https://doi.org/10.2307/3430425>
- Quinton, J.N., Govers, G., Van Oost, K., Bardgett, R.D., 2010. The impact of agricultural soil erosion on biogeochemical cycling. Nat. Geosci. 3, 311–314. <https://doi.org/10.1038/ngeo838>
- Raney, S.M., Eimers, M.C., 2014. Unexpected declines in stream phosphorus concentrations across southern Ontario. Can. J. Fish. Aquat. Sci. 71, 337–342. <https://doi.org/10.1139/cjfas-2013-0300>
- Richards, R.P., Baker, D.B., Crumrine, J.P., Stearns, A.M., 2010. Unusually large loads in 2007 from the Maumee and Sandusky Rivers, tributaries to Lake Erie. J. Soil Water Conserv. 65, 450–462. <https://doi.org/10.2489/jswc.65.6.450>
- Robertson, D.M., Saad, D.A., 2011. Nutrient Inputs to the Laurentian Great Lakes by Source and Watershed Estimated Using SPARROW Watershed Models. J. Am. Water Resour. Assoc. 47, 1011–1033. <https://doi.org/10.1111/j.1752-1688.2011.00574.x>
- Scavia, D., Allan, J.D., Arend, K.K., Bartell, S., Beletsky, D., Bosch, N.S., Brandt, S.B., Briland, R.D., Dalo, I., Depinto, J. V, Dolan, D.M., Anne, M., Farmer, T.M., Goto,

- D., Han, H., Höök, T.O., Knight, R., Ludsin, S.A., Mason, D., Michalak, A.M., Richards, R.P., Roberts, J.J., Rucinski, D.K., Rutherford, E., Schwab, D.J., Sesterhenn, T.M., Zhang, H., Zhou, Y., Erie, L., 2014. Assessing and addressing the re-eutrophication of Lake Erie : Central basin hypoxia 40, 226–246.
<https://doi.org/10.1016/j.jglr.2014.02.004>
- Scavia, D., Bocaniov, S.A., Dagnew, A., Long, C., Wang, Y.C., 2019. St. Clair-Detroit River system: Phosphorus mass balance and implications for Lake Erie load reduction, monitoring, and climate change. *J. Great Lakes Res.* 45, 40–49.
<https://doi.org/10.1016/j.jglr.2018.11.008>
- Schindler, D.W., 1974. Eutrophication and recovery in experimental lakes: Implications for lake management. *Science* (80-.). 184, 897–899.
<https://doi.org/10.1126/science.184.4139.897>
- Sharpley, A., Jarvie, H., Flaten, D., Kleinman, P., 2018. Celebrating the 350th Anniversary of Phosphorus Discovery: A Conundrum of Deficiency and Excess. *J. Environ. Qual.* 47, 774. <https://doi.org/10.2134/jeq2018.05.0170>
- Sharpley, A.N., Krogstad, T., Kleinman, P.J.A., Haggard, B.E., Shigaki, F., Saporito, L.S., 2007. Managing natural processes in drainage ditches for nonpoint source phosphorus control. *J. Soil Water Conserv.* 64, 197–206.
- Simonin, M., Voss, K.A., Hassett, B.A., Rocca, J.D., Wang, S.Y., Bier, R.L., Violin, C.R., Wright, J.P., Bernhardt, E.S., 2019. In search of microbial indicator taxa: shifts in stream bacterial communities along an urbanization gradient. *Environ. Microbiol.* 21, 3653–3668. <https://doi.org/10.1111/1462-2920.14694>
- Simpson, Z.P., McDowell, R.W., Condrón, L.M., McDaniel, M.D., Jarvie, H.P., Abell, J.M., 2021. Sediment phosphorus buffering in streams at baseflow: A meta-analysis. *J. Environ. Qual.* 50, 287–311. <https://doi.org/10.1002/jeq2.20202>
- Smith, S.D.P., Bunnell, D.B., Burton, G.A., Ciborowski, J.J.H., Davidson, A.D., Dickinson, C.E., Eaton, L.A., Esselman, P.C., Evans, M.A., Kashian, D.R., Manning, N.F., McIntyre, P.B., Nalepa, T.F., Pérez-Fuentetaja, A., Steinman, A.D.,

- Uzarski, D.G., Allan, J.D., 2019. Evidence for interactions among environmental stressors in the Laurentian Great Lakes. *Ecol. Indic.* 101, 203–211. <https://doi.org/10.1016/j.ecolind.2019.01.010>
- Spencer, K.L., Wheatland, J.A.T., Bushby, A.J., Carr, S.J., Droppo, I.G., Manning, A.J., 2021. A structure–function based approach to floc hierarchy and evidence for the non-fractal nature of natural sediment flocs. *Sci. Rep.* 11, 1–10. <https://doi.org/10.1038/s41598-021-93302-9>
- Stalling, D.L., Norstrom, R.J., Smith, L.M., Simon, M., 1985. Patterns of PCDD, PCDF, and PCB contamination in Great Lakes fish and birds and their characterization by principal components analysis. *Chemosphere* 14, 627–643.
- Stammler, K.L., Taylor, W.D., Mohamed, M.N., 2017. Long-term decline in stream total phosphorus concentrations : A pervasive pattern in all watershed types in Ontario. *J. Great Lakes Res.* 43, 930–937. <https://doi.org/10.1016/j.jglr.2017.07.005>
- Steffen, M.M., Davis, T.W., McKay, R.M.L., Bullerjahn, G.S., Krausfeldt, L.E., Stough, J.M.A., Neitzey, M.L., Gilbert, N.E., Boyer, G.L., Johengen, T.H., Gossiaux, D.C., Burtner, A.M., Palladino, D., Rowe, M.D., Dick, G.J., Meyer, K.A., Levy, S., Boone, B.E., Stumpf, R.P., Wynne, T.T., Zimba, P. V., Gutierrez, D., Wilhelm, S.W., 2017. Ecophysiological Examination of the Lake Erie Microcystis Bloom in 2014: Linkages between Biology and the Water Supply Shutdown of Toledo, OH. *Environ. Sci. Technol.* 51, 6745–6755. <https://doi.org/10.1021/acs.est.7b00856>
- Stone, M., Droppo, I.G., 1994. In-channel surficial fine-grained sediment laminae. Part II: Chemical characteristics and implications for contaminant transport in fluvial systems. *Hydrol. Process.* 8, 113–124. <https://doi.org/10.1002/HYP.3360080203>
- Szalinska, E., Haffner, G.D., Drouillard, K.G., 2007. Metals in the sediments of the Huron-Erie Corridor in North America : Factors regulating metal distribution and mobilization 217–236. <https://doi.org/10.1111/j.1440-1770.2007.00339.x>
- Taylor, A.W., Kunishi, H.M., 1971. Phosphate Equilibria on Stream Sediment and Soil in a Watershed Draining an Agricultural Region. *J. Agric. Food Chem.* 19, 827–831.

<https://doi.org/10.1021/jf60177a061>

- Terzić, D., Popović, V., Tatić, M., Vasileva, V., Đekić, V., Ugrenović, V., Popović, S., Avdić, P., 2018. Soybean Area, Yield and Production in World. XXII Eco-Conference 2018 Ecol. Mov. Novi Sad 135–145.
- Tiessen, H., Ballester, M.V., Salcedo, I., 2011. Phosphorus and Global Change. Phosphorus in Action. Springer, Berlin, Heidelb. 26, 459–471.
<https://doi.org/10.1007/978-3-642-15271-9>
- Vallentyne, J.R., Beeton, A.M., 1988. The ‘Ecosystem’ approach to managing human uses and abuses of natural resources in the great lakes basin. Environ. Conserv. 15, 58–62. <https://doi.org/10.1017/S0376892900028460>
- Van Staden, T.L., Van Meter, K.J., Basu, N.B., Parsons, C.T., Akbarzadeh, Z., Van Cappellen, P., 2021. Agricultural phosphorus surplus trajectories for Ontario, Canada (1961–2016), and erosional export risk. Sci. Total Environ. 151717.
<https://doi.org/10.1016/j.scitotenv.2021.151717>
- VanMensel, D., Droppo, I.G., Weisener, C.G., 2022. Identifying chemolithotrophic and pathogenic-related gene expression within suspended sediment flocs in freshwater environments: A metatranscriptomic assessment. Sci. Total Environ. 807, 150996.
<https://doi.org/10.1016/j.scitotenv.2021.150996>
- Vollenweider, R.A., 1975. Input-output models - With special reference to the phosphorus loading concept in limnology. Schweizerische Zeitschrift für Hydrol. 37, 53–84. <https://doi.org/10.1007/BF02505178>
- Watson, S.B., Miller, C., Arhonditsis, G., Boyer, G.L., Carmichael, W., Charlton, M.N., Confesor, R., Depew, D.C., Ludsin, S.A., Matisoff, G., Mcelmurry, S.P., Ho, T.O., Murray, M.W., Richards, R.P., Rao, Y.R., Steffen, M.M., Wilhelm, S.W., 2016. The re-eutrophication of Lake Erie : Harmful algal blooms and hypoxia. Harmful Algae 56, 44–66. <https://doi.org/10.1016/j.hal.2016.04.010>
- WHO, 2015. Health in 2015: from MDGs, millennium development goals to SDGs,

- sustainable development goals. <https://doi.org/10.1017/S1744552306002023>
- Wilson, R.S., Beetstra, M.A., Reutter, J.M., Hesse, G., Fussell, K.M.D.V., Johnson, L.T., King, K.W., LaBarge, G.A., Martin, J.F., Winslow, C., 2019. Commentary: Achieving phosphorus reduction targets for Lake Erie. *J. Great Lakes Res.* 45, 4–11. <https://doi.org/10.1016/j.jglr.2018.11.004>
- Woese, C.R., Kandler, O., Wheelis, M.L., 1990. Towards a natural system of organisms: proposal for the domains Archaea, Bacteria, and Eucarya. *Proc. Natl. Acad. Sci.* 87, 4576–4579. <https://doi.org/10.1073/pnas.87.12.4576>
- Yang, Y., Li, S., Gao, Y., Chen, Y., Zhan, A., 2019. Environment-driven geographical distribution of bacterial communities and identification of indicator taxa in Songhua River. *Ecol. Indic.* 101, 62–70. <https://doi.org/10.1016/j.ecolind.2018.12.047>
- Yuan, Z., Jiang, S., Sheng, H., Liu, Xin, Hua, H., Liu, Xuewei, Zhang, Y., 2018. Human Perturbation of the Global Phosphorus Cycle: Changes and Consequences. *Environ. Sci. Technol.* 52, 2438–2450. <https://doi.org/10.1021/acs.est.7b03910>
- Yunker, M.B., Macdonald, R.W., Vingarzan, R., Mitchell, H., Goyette, D., Sylvestre, S., 2002. PAHs in the Fraser River basin: a critical appraisal of PAH ratios as indicators of PAH source and composition. *Org. Geochem.* 33, 489–515.
- Zalasiewicz, J., Waters, C.N., Williams, M., Barnosky, A.D., Cearreta, A., Crutzen, P., Ellis, E., Ellis, M.A., Fairchild, I.J., Grinevald, J., Haff, P.K., Hajdas, I., Leinfelder, R., McNeill, J., Odada, E.O., Poirier, C., Richter, D., Steffen, W., Summerhayes, C., Syvitski, J.P.M., Vidas, D., Waple, M., Wing, S.L., Wolfe, A.P., An, Z., Oreskes, N., 2015. When did the Anthropocene begin? A mid-twentieth century boundary level is stratigraphically optimal. *Quat. Int.* 383, 196–203. <https://doi.org/10.1016/j.quaint.2014.11.045>

CHAPTER 2: MICROBIAL METATRANSCRIPTOMIC INVESTIGATIONS ACROSS CONTAMINANT GRADIENTS OF THE DETROIT RIVER

2.1 Introduction

Current insights into the activities of microorganisms in subsurface environments is lending increasing value to their roles as degraders of exogenous, anthropogenically-sourced contaminants. Their ubiquitous nature (conservative estimates of 10^6 unique taxa per gram of soil) and vast enzymatic flexibility enable them to effectively convert matter, including organic pollutants and metals, into simpler, less hazardous forms (Abramowicz, 1990; Birrer et al., 2017; Díaz, 2004; Lynch and Neufeld, 2015). This ecological service, which extends to the breakdown of polycyclic aromatic hydrocarbons (PAHs), polychlorinated biphenyls (PCBs), and other organochloride residues is imperative to ecosystem health, and is vital where high-molecular weight carbon compounds accumulate in the environment (Antwis et al., 2017). Lacustrine and riverine bed sediments are often sinks for persistent organic pollutants (POPs) and metals, owing to the common proximity of industrial point sources to water bodies and the affinity for contaminant attachment to inorganic and organic benthic particulates. As microbes are pervasive and functionally diverse in sediments, they serve as vital buffers against the detrimental effects of POPs and metals on all higher trophic levels, and serve simultaneously as primary bioindicators of compromised freshwater ecosystems (Gibbons et al., 2014; Lozupone and Knight, 2007).

Past studies have gained an understanding of microbial response to POPs primarily through laboratory experiments that augment sediments and/or soils with high concentrations of individual or mixtures of pollutants. This approach often elicits a relatively rapid change within the enriched microbial community, consisting of shifts in composition (Korlević et al., 2015; Widenfalk et al., 2008) aromatic-cleavage gene expression (Sawulski et al., 2014; Sotsky et al., 1994), and associated reductions in primary contaminant concentrations. These studies are vital for understanding the initial mechanisms that microbes deploy to biodegrade pollutants. However, they are limited in their scope to understand nutrient and energy flow within legacy perturbed settings and the associated state of microbial community function, where contaminant congeners are transformed over time from high molecular weight organics into versatile cellular substrates such as acetyl-CoA and succinyl-CoA (Fuchs et al., 2011). Furthermore, observations are often constrained to assays based on pre-selected genes, and sometimes only cultivatable species. To be able to assess how natural microbial assemblages respond

to contaminant stress over varying spatial scales, real-world reference sites and higher throughput molecular tools are necessary. Meta-omic investigations are helping bridge this gap by providing genomic information on in situ microbial functioning in a variety of contaminated environments without a priori knowledge of microbial assemblages (Birrner et al., 2017; Maphosa et al., 2010; Weisener and Reid, 2017). While microbial genomic potential can be reconstructed via metagenomic analysis of environmentally-extracted DNA, metatranscriptomics can shed light on the transcribed products of DNA, providing a wealth of information on total messenger RNA (mRNA) output; a proxy for gene expression. As microorganisms are coupled to many biogeochemical cycles in the environment, metatranscriptomic studies of anthropogenically-affected sediments are valuable in many facets; 1) understanding significant responses of the biosphere to perturbations, 2) assessing if and how microbial communities are functioning to moderate the effects of legacy contamination in aquatic systems, and 3) exploring microbial diversity as a function of human-induced landscape changes. Additionally, biodegradation gene pathways in anoxic settings, including fresh water sediments, are much less understood than those rich in oxygen. This is a significant distinction, as redox conditions exert immense control over microbial behaviour, and by extension, contaminant fate (Díaz, 2004; Ghosal et al., 2016). By surveying these environments, our understanding of gene expression in anoxic settings can be broadened and integrated into organic contaminant degradation paradigms as well as ecotoxicological monitoring.

The Detroit River bordering the United States (state of Michigan) and Canada (province of Ontario) represents an ideal location for microbial omic investigations with regards to anthropogenic contaminants. The river has a complex history of industrialization, urbanization and agricultural land use, and is designated a binational Area of Concern (AOC) in the Laurentian Great Lakes. Comprehensive sediment surveys and modelling have delineated the river into discrete contaminant regions based on concentrations of polycyclic aromatic hydrocarbons (PAHs), polychlorinated biphenyls (PCBs), and metals (Drouillard et al., 2006; Szalinska et al., 2013). Building on this work, we have performed total mRNA extractions and metatranscriptomic analysis on sediments sampled across a gradient of established polluted sections to investigate correlations between contaminant levels and microbial gene transcription profiles and diversity.

2.2 Methods

2.2.1 Site Characteristics and Sediment Sampling Locations

The Detroit River is a connecting waterway of the lower Laurentian Great Lakes of North America, flowing southward from Lake St. Clair to Lake Erie with an average flow of $5240 \text{ m}^3 \text{ s}^{-1}$. It borders Michigan (United States) to the west and Ontario (Canada) to the east, flowing through several large population centres including Detroit, USA (pop. 673,104) and Windsor, Canada (pop. 217,188) (Statistics Canada, 2017; U.S. Census Bureau, 2017). The lower reach of the river, comprising the most southern 23 km of the total 51 km of the river length, was sampled for this study, which comprises both industrialized and more pristine regions. The lower reach has gently sloping banks and contains two large islands which divide the river into several channels. Dredged shipping channels have a max depth of 15 m, with non-dredged sections having an average depth of 3 m. Thirteen sampling points were selected within the lower reach based on two previous sediment surveys of metals, PCBs, PAHs, and other organochloride residues performed in 1999 and 2009 which measured 90 sites in the region (Drouillard et al., 2006; Szalinska et al., 2006). The 13 points were categorized as one of three contaminant divisions termed COLD (C), INT (I), and HOT (H) based on previously assigned low, intermediate, and high weighted averages of contaminants, respectively. Five sites were designated COLD, three INT, and five HOT (Fig 1). Figure 1 also designates the sediment sampling sites from the 1999 and 2009 surveys. COLD sites were located on the Canadian side of the river, with HOT sites located primarily in industrialized areas on the American side. Previous temporal analysis of the sampling sites has shown stable decadal level of contaminants (Szalinska et al., 2013); thus, we have adopted an a priori experimental design to test the hypothesis that contaminated locations of the river (HOT sites) have altered microbial function compared to non-contaminated reference regions (COLD sites). Sediment sampling for microbial metatranscriptomic analysis was performed over two days in October 2016. A grab sampler was used to collect bed sediments at each location, from which duplicate 5 g subsamples were removed with sterile utensils and flash frozen in liquid nitrogen and stored at -80 degrees Celsius until nucleic acid extraction.

2.2.2 Sediment Contaminant Chemistry Profiles

As the 13 sites selected for this study were not all identical to previous sampling locations, contaminant profiles were spatially interpolated from the datasets obtained in 1999 and 2009 based on previous methods (Szalinska et al., 2013). In brief, the Hot Spot Analysis tool within ArcGIS was first used to assign clusters of previous sampling locations to high, intermediate, and low chemical concentration regions relative to river wide sediment concentrations for each given chemical based on a Getis-Ord G_i^* statistic. Once these clusters were determined, polygon areas were manually assigned around equivalent G_i^* values to map the contaminant gradients (i.e. low, int, high) of the lower reach of the river. It was then determined which contaminant zone the 13 new sampling locations from this study fell into, after which chemical concentrations profiles were constructed for each of the new sites using inverse distance weighted (IDW) interpolation from the previous dataset concentrations. The analysis included concentrations ($\mu\text{g g}^{-1}$ dry weight) of 10 metals (As, Cd, Cr, Cu, Fe, Hg, Mn, Ni, Pb, Zn), 23 PAHs, 193 PCB congeners, and several other organochloride pesticides (OGCs) based on geospatial weighted averages of the nearest neighbouring sampling locations.

For statistical analysis of contaminants within and between sites, individual metal and summed PAH, PCB, and organochloride pesticide concentrations were initially subjected to principle component analysis (PCA) to reduce the dimensionality of the dataset and to generate values free of inter-chemical correlations (Olsen et al., 2012). Loadings of the correlation coefficients of each contaminant on significant axes (eigenvalue ≥ 1) were generated and noted for strong correlations (values > 0.8). Analysis of Variance (ANOVA) using Tukey's pairwise comparisons was then performed on the PCA scores for the axis relevant to the contaminant or contaminant group to deduce differences between sites. Similarity percentage (SIMPER) analysis was used to assess how variables contributed to differences between groups of samples. Organic contaminant concentrations were normalized for organic matter content by dividing by the TOC% for comparisons between designations. Site chemistry was also measured against provincial sediment quality metrics including Lowest Effect Level (LEL), Severe Effect Level (SEL), and Background Concentrations for relevant metals and contaminants (Fletcher et al., 2008).

2.2.3 RNA Extraction and Functional and Taxonomic Annotation

A total RNA extraction was performed on all sediment samples using the PowerSoil Total RNA Isolation Kit (MoBio Laboratories Inc. Carlsbad, CA, USA, Cat No:12866-25) per the manufacturers instructions. RNA purity was tested on an Agilent 2100 Bioanalyzer using designated minimum quality parameters as detailed previously (Falk et al., 2018). The higher quality sample from each site was sent to the McGill University and Genome Quebec Innovation Centre (<http://www.genomequebec.com/en/home.html>) for bacterial rRNA depletion using a Ribo-Zero rRNA removal kit, cDNA reverse transcription, and shotgun sequencing of resultant mRNA on an Illumina HiSeq 2000. The 13 samples had an average of 22 million reads outputted in FASTQ file format (Table S1).

Sequence analysis for microbial function and taxonomy was performed through the open-source MetaTrans pipeline (Martinez et al., 2016). In brief, all reads were first quality control-checked and filtered through the report-tool FASTQC (Andrews, 2010, available at <http://www.bioinformatics.babraham.ac.uk/projects/fastqc>) and the Kraken Pipeline (Davis et al., 2013), respectively. Filtering for recovery of quality reads removed regions with Phred score < 10 and reads < 30bp. Reads were then sorted into either rRNA/tRNA or non-rRNA/tRNA (i.e. potential mRNA) through SortMeRNA using multiple rRNA databases (Kopylova et al., 2012). Functional annotation of potential mRNA proceeded with joining of paired-end reads using a minimum overlap of 8 bp and a maximum difference of 10% (Erik Aronesty, 2011: <http://code.google.com/p/ea-utils>), putative gene prediction through FragGeneScan (Rho et al., 2010), and gene clustering with 90% overlap at 95% identity using CD-HIT. Reads were then mapped to the COG database (Clusters of Orthologous Groups) for functional assignment, generating a functional profile for each sample. For taxonomic annotation, rRNA/tRNA reads were joined using the same methods as the mRNA and then clustered and mapped using UCLUST and SOAP2 against the 16S rRNA Greengenes database, respectively (Edgar, 2010; McDonald et al., 2012)

For all 13 samples, the *DESeq2* package (Love et al., 2014) was used to normalize read count data generated from the annotation step for quantitative comparison and statistical analysis of gene expression across samples and among the designated sampling groups (COLD, INT, HOT). Normalized read counts were averaged across contaminant

regions, with base means compared for each individual COG, expressed as Log2Fold change. Pairwise comparisons generated p-values to identify statistically significant differences ($p < 0.05$) in COG functional genes between sites.

α -diversity metrics, permutational multivariate analysis of variance, (PERMANOVA), and non-metric multidimensional scaling (NMDS) were performed in Past3 statistical software for microbial community and total transcriptomic profile comparisons across samples and contaminant divisions.

2.3 Results

2.3.1 Interpolated Site Chemistry

Three regions (e.g. COLD, INT (intermediate) and HOT) were compared for a range of representative sediment contaminants that included concentrations of metals, total PAHs, total PCBs, and several other organochloride pesticides (total OGCs) to assess the accuracy of the a priori site selections based on previous sediment surveys. Principle component analysis (PCA) displayed separation of the sampling sites and regions when plotted on the two axes that explained the most variation (Fig. 2). The loadings table generated from the PCA displays the correlation coefficients of each contaminant on these axes and denotes those which exhibit strong correlations (Table S2). ANOVA test on site scores for PC1 showed a significant difference between COLD and HOT sites ($p = 0.0002$) and INT and HOT sites ($p = 0.0004$) but no difference between COLD and INT sites (Tukey's Q). No significant differences were observed for sampling site scores for PC2. Thus, only contaminants with strong correlations to PC1 (Total PAH, Total PCB, Cd, Cr, Cu, Fe, Hg, Ni, Pb, Zn, TOC%) exhibited a statistically significant difference from the HOT sites to the COLD and INT. SIMPER analysis revealed that Fe concentrations contributed strongly to the dissimilarity between sites (97.0%), followed by Zn (1.3%), Mn (0.9%) and Total PAHs (0.2%) (Table S3). Contaminant concentration data is summarized in Table 1. Descriptive results of metal and organic contaminant data follow in sections 3.2 and 3.3.

2.3.2 Metals

Of the ten selected metals of concern, 4 metals within the COLD sites (As, Cd, Cu, Ni), 5 metals in the INT sites (As, Cd, Cu, Hg, Ni), and 7 metals in the HOT sites (Cd, Cr,

Cu, Fe, Hg, Ni, Zn) were interpolated to exceed the LEL as outlined by Provincial Sediment Quality Guidelines. No metals in any region exceeded the SEL. Eight metals (Cd, Cu, Cr, Fe, Hg, Ni, Pb, and Zn) showed significantly higher concentrations in the HOT sediments over both the COLD and INT sediments based on ANOVA tests of PC1 scores. COLD and INT sites showed no significant difference in metal concentrations. Within HOT sites, Zn and Hg showed specifically high exceedances of background concentrations based on pre-colonial sediment horizons.

2.3.3 Organic Contaminants

Fourteen individual PAHs exceeded LEL concentrations in the HOT sites, with 7 and 6 exceeding LEL in the COLD and INT, respectively. COLD, INT, and HOT all exceeded the LEL for total PAHs (4.0, 4.3, and 14.0 $\mu\text{g g}^{-1}$ dry wt., respectively). HOT sites were significantly different from both COLD and INT in terms of total PAHs, showing over 3 times higher concentrations. No difference was observed between COLD and INT sites. When normalized for TOC%, HOT sites also showed a significantly higher concentration of total PAHs over COLD and INT. No sites exceeded the SEL for individual or total PAHs.

193 PCB congeners were analyzed and summed across the COLD, INT, and HOT divisions. All divisions were predicted to exceed the LEL for total PCBs of 0.07 $\mu\text{g g}^{-1}$ dry wt., with COLD and INT sites at 0.16 and the HOT at 0.51. No regions exceeded the SEL for total PCBs. Both raw dry wt. values and dry wt. normalized to TOC% values modelled the HOT sites having a significantly higher concentration of total PCBs over the COLD and INT, with COLD and INT sites showing no difference. COLD, INT, and HOT regions all exhibited exceedances of the background concentration for total PCBs (background concentration = 0.02 $\mu\text{g g}^{-1}$ dry wt.). For the OGCs analyzed, only Hexachlorobenzene (HCB) exceeded the LEL in INT and HOT sites, with Dichlorodiphenyldichloroethylene (DDE) and Aldrin exceeding only in the HOT, with all 3 compounds showing high exceedance of background concentrations. No significant differences were observed for total OGC concentrations across sites.

2.3.4 Microbial Diversity and Taxonomy

Significant decreases in α -diversity between COLD to HOT sites were observed from the Simpson and Berger-Parker indices, suggesting a condition of taxa dominance correlating with the HOT sediments. Two-way PERMANOVA test based on total RNA extraction as an indicator of active taxa, sites showed an increase of archaea over bacteria, with archaea comprising 62%, 77%, and 75% of the whole community in COLD, INT, and HOT sites, respectively (Fig 3a). Abundant phyla across the three regions included Euryarchaeota (47%, 55%, 68%), Proteobacteria (18%, 9%, 8%), and Crenarchaeota (11%, 20%, 8%), with Bacteroidetes, Parvarchaeota, Acidobacteria, and Chloroflexi also exhibiting high abundances. Fig. 3b shows microbial groups comprising the top 80% of the community across divisions as annotated at the highest taxonomic division from class to genus through MetaTrans. The acetocalstic archaeon, *Methanosaeta*, was the most prominent genus across all regions comprising 17%, 27%, and 39% of the community across COLD, INT, and HOT sites, respectively. Methane-cycling archaea, including *Candidatus* of the *Methanoregulaceae*, as well as known ammonia-oxidizers including *Nitrosopumilus* and those of the orders *pGrfC26* and *Ellin6067* were also dominant in sediments at one or more regions.

2.3.5 Differential Gene Expression Across Sites

Non-metric multidimensional scaling (NMDS) applied to the COG abundance count matrix revealed separation between sediment sites and between COLD, INT, and HOT regions (Fig. 4). Two of the three INT sites showed similarity, grouping between the COLD and HOT clusters, with COLD and HOT divisions exhibiting a clear separation. The cluster of HOT sediment sites represents sampling in more industrialized regions of the Detroit River. Due to the separation of COLD and HOT sites based on transcript NMDS and interpolated contaminant concentrations, further differential gene expression analysis is focused on these two divisions.

Analysis of RNA-seq data through *DESeq2* of the MetaTrans pipeline resulted in 207 out of 19576 COGs showing significant differential expression between the COLD and HOT regions (1.06% of total transcriptome), with 45 and 162 showing increased transcription in the COLD and HOT, respectively. Fig. 5 summarizes these differences in

broad COG functional categories across the two regions quantified by summed Log₂Fold changes, with - values representing higher expression across COLD sites and + values representing higher expression across the HOT. COLD site sediments had lower magnitude Log₂Fold values across COG functional categories than HOT sites, except for genes within “[J] Translation, ribosomal structure and biogenesis”, “[B] Chromatin structure and dynamics”, “[Z] Cytoskeleton”, and “[M] Cell wall/membrane/envelope biogenesis”. HOT sites exhibited greater Log₂Fold changes across the remaining functional categories, with high values in “[X] Phage-derived proteins, transposases and other mobilome components”, “[C] Energy production and conversion”, “[T] Signal transduction mechanisms”, “[I] Lipid transport and metabolism”, and “[P] Inorganic ion transport and metabolism”.

The 162 transcripts that showed up-expression in the HOT sediments comprised groups of genes involved primarily in stress response, β -oxidation pathways, polyester synthesis, gluconeogenesis, and methanogenesis. All differentially expressed COGs are summarized with Log₂Fold and p-values in Table S4. Specific COGs associated with aromatic degradation were detected in relatively small abundances and showed no differential expression between COLD and HOT regions (Fig. 6). Although not differentially expressed across regions, genes involved in dissimilatory nitrate reduction to ammonia (DNRA), denitrification, and annamox exhibited relatively high expression in all sediments. Of the 45 up-expressed transcripts within the COLD sediments only 21 were annotated to the COG database (Table S4). Literature searches of these genes exhibited no trends with regards to specific degradation pathways and were assumed to be representative of natural conditions. Thus, further discussion is focused on genes expressed in the HOT sediments which are theorized to be driven primarily by higher contaminant concentrations.

2.4 Discussion

2.4.1 Overview

Interpolative modelling of sediment chemistry based on previously published surveys showed that sites categorized to be in highly contaminated regions (i.e. those labelled as HOT) had significantly higher concentrations of most metals, total PAHs, and

total PCBs than those designated COLD or INT. This provides support that the selected sites do differ in their degree of sediment contamination, and agrees with independent studies that have performed similar surveys in the Detroit River (Furlong et al., 1988; Metcalfe et al., 2000). From PCA, this separation was most evident between the sites designated COLD and HOT, with HOT sites being primarily located in and around the industrialized Trenton Channel on the U.S. side of the river. Further, the regions in question have shown unchanging contaminant concentrations (Szalinska et al., 2013). Thus, we believe it sufficient to hypothesize that variations in observed microbial diversity and function across sites are driven primarily by pollutants. RNA-based taxonomy revealed several patterns associated with the degree of sediment contamination. α -diversity metrics were altered significantly from the COLD to HOT zones, suggesting that the sediment microbial community may be perturbed from anthropogenic pollution. This pattern has been observed in situ in multiple environments, including streams, soils, and ocean and fresh water sediments (Korlević et al., 2015; Sawulski et al., 2014; Zeglin, 2015). It should be noted that microbial diversity is not always negatively correlated with anthropogenic stressors, especially where other environmental factors, such as pH, salinity, moisture, and grain size are variable (Wang et al., 2018). Sediments of the lower Detroit River have been shown to be relatively consistent in physical characteristics (Szalinska et al., 2013), thus it is believed that legacy pollutants are a driver of microbial community shifts. It should also be noted that microbial diversity decreases cannot be interpreted as having negative ecosystem consequences without parallel taxonomic and functional investigations. Thus, we analyzed both community structure as well as microbial gene expression through shotgun metatranscriptomics from the Detroit River sediments to assess carbon and energy cycling pertinent to contaminant fate.

2.4.2 Energy and Metabolic Pathways Associated with Differences in Detroit River Sediments

The relative abundance of Archaea expanded from COLD to INT to HOT regions, resulting primarily from an increase in *Methanosaeta*, an acetoclastic, cytochrome-utilizing methanogen. Functional gene analysis also showed a significant expression of the methyl-coenzyme M reductase, alpha subunit (*mcr*) gene as well as multiple cytochrome units within the HOT sites. This is evidence that methanogens, including *Methanosaeta*,

are more active within these contaminated sediments governed by low-energy carbon transformations of intermediate compounds, possibly originating from anoxic hydrocarbon degradation (Gieg et al., 2014). Interestingly, this metabolic niche has been explored within research of the Deepwater Horizon oil spill, where separate studies, together, elude to a temporal shift towards a methanogenic community 1 year after hydrocarbon exposure (Liu et al., 2013; Mason et al., 2014). Further, studies within natural hydrocarbon deposits also show an active CH₄-utilizing community, suggesting that the life methanogenic is thermodynamically favoured where high molecular weight organics, such as POPs, are abundant, and desirable electron donors (O₂, NO₃, SO₄) are rapidly depleted (Michas et al., 2017; Reid et al., 2018). The increase in *mcr* abundance from the COLD to HOT sediments supports this concept, however nitrogen-metabolizing genes were still present, and in the case of specific transcripts such as the periplasmic nitrate reductase *napA*, higher expression than *mcr* was observed (Fig. 6). The abundance of N-reduction genes observed may seem counterintuitive considering past observations of very low total nitrogen (TN) values and high C:N ratios in Detroit River sediments (Szalinska et al., 2011). However, recent isotopic data from the river sediments shows evidence of high microbial nitrate metabolism, suggesting a high N-turnover rate to explain low TN rather than low inputs (Colborne et al., 2019), and that high C values may be in part due to the abundance of POPs. It is likely that this denitrification, as well as dissimilatory nitrate reduction to ammonia (DNRA) play a role in primary PAH degradation, with methanogens acting syntrophically to metabolize by-products (i.e. acetate and carbon dioxide) in lower pathway processes. This microbial cooperation has been documented in omic studies previously and is likely a pervasive process in hydrocarbon-rich sediments (Scott et al., 2014). Since nitrate reduction is carried out by a diverse polyphyletic group of bacteria, no single genus is a reliable sign of this process in the environment (Smith et al., 2007). The presence of differentially expressed N-reduction transcripts lends more powerful evidence of these processes occurring in the stressed Detroit River sediments than taxonomic identification alone. The abundant ammonia oxidizing groups *pGrfC26* and *Ellin6067*, as well as the genus *Nitrosopumilus* could be involved in metabolizing DNRA-derived ammonia back to nitrate, cycling nitrogen within the system. This loop may be necessary to supply reducible nitrate to the sediments, as N₂ fixing genes (*nifD/H*) that can provide usable N were found

to be in low abundance across samples and assumed to be negligible from other studies. In this case, the source of initial N to the river sediments is presumed to be from waste water treatment plants (WWTPs) along the river corridor (Colborne et al., 2019).

Nitrate reduction and methanogenesis appear to be primary processes in contaminant transformations in the Detroit River sediments. Further exploration of differentially expressed genes revealed concomitant pathways responsible for carbon catabolism (Fig. 7). In HOT sediments, “[I] Lipid transport and metabolism” was one of the dominant functional categories (7.3 Summed Log2Fold Change), which included genes responsible for beta oxidation-like pathways. It has been observed that after multi-ringed hydrocarbons are broken down to single-ring by-products, such as benzoyl-CoA, beta-oxidation processes serve to liberate carbon into key cellular currencies, such as acetyl-CoA and succinyl-CoA (Díaz, 2004; Fuchs et al., 2011). Acyl-CoA synthetase (*ACCS*), enoyl-CoA hydratase (*CaiD*), propionyl-CoA carboxylase (*PccA*), and methylmalonyl-CoA mutase (*Sbm*) catalyse these reactions and produce substrates necessary for the tricarboxylic acid (TCA) cycle, all of which showed significantly increased expression in the HOT sediments of the Detroit River. In parallel, COGs identified as the pyruvate/2-oxoglutarate dehydrogenase complex (*Lpd*) and aconitase B (*AcnB*) of the TCA cycle exhibited increased expression, providing evidence of links between beta-oxidation and energy generation through acetyl-CoA oxidation. Two interesting consequential pathways were also identified based on differentially expressed genes. In HOT sediments, polyester synthesis and gluconeogenesis transcripts were highly abundant and linked to TCA cycle substrates by key differentially expressed genes, including poly 3-hydroxyalkanoate synthetase (*PhaC*) and phosphoenolpyruvate carboxykinase (*PepCK*). *PhaC* synthesises water insoluble polyesters, potentially from diverse/toxic carbon compounds while under stress conditions, while *PepCK* acts as a junction between the TCA cycle and glucose production via transformation of oxaloacetate (Cheng and Charles, 2016; Kessler et al., 2001; Kim and Lenz, 2001). Carbon accumulated in the form of polyesters and glucose is less toxic than in complex, anthropogenically-derived hydrocarbons. Thus, the abundance of these genes in HOT sediments suggests that the natural microbial assemblages may be facilitating pollutant-derived carbon sequestration; a beneficial ecosystem service. Furthermore, bacterial polyesters in the form of polyhydroxyalkanoates are key in the

manufacturing of bioplastics, and knowledge of their associated genes in contaminated environments may aid in optimizing production in lab and industrial-scale operations (Chen and Jiang, 2017). However, this study along with others show that industrial Detroit River sediments contain proportionately higher concentrations of large PAHs (> 2 rings), and lower concentrations of small ones (< 2 rings) (Fig. S1), indicating that the sediment biota may be more adept to metabolize the latter. The lower solubility of more complex PAHs is also a contributing factor and can limit bioavailability. Regardless, it is understood that heavy-weight POPs are more resistant to microbial degradation, and that their persistence in Detroit River sediments is an ongoing concern.

2.4.3 Microbial Stress Response and Adaptive Strategies in Contaminated Sediments

The above energy pathways described in the HOT sediments suggest that the microbial community is expressing genes that can effectively convert organic contaminants into accessible carbon compounds, and eventually methane, through activation of specific energy pathways. However, microbial ecological research often suggests that these contaminants and metals simultaneously impose pressures on the community, and that trade offs in cellular functions exist (Schimel et al., 2007). The significant decrease in α -diversity measured from RNA-based taxonomy is one sign of increased stress in HOT site sediments. Further, the COG functional categories “[M] Cell wall/membrane/envelope biogenesis” and “[J] Translation, Ribosomal structure and biogenesis” showed significantly decreased levels in the HOT compared to the COLD sites (Fig. 5), and may be evidence of interference on DNA, and by extension, cell replication. Several stress-related genes involved in DNA modifications were also differentially expressed in the HOT sediments over the COLD (Table S4). Thus, although microbial pathways were observed that can liberate energy in the form of accessible carbon compounds, the microbial communities exposed to higher contamination may be simultaneously jeopardized, and growth and reproduction mechanisms may be inhibited in exchange for transcription of stress related, and PAH and PCB processing genes. The effects of metals, mainly Fe, Zn, and Mn, may be the most significant on the microbial communities as expressed through SIMPER analysis of COLD vs. HOT sediments, aligning with parallel research of anthropogenic stressors (Zeglin, 2015). On this note, an interesting observation of this research was the prominence of transcripts of the COG functional category “[X] Phage-

derived proteins, transposases and other mobilome components” in the HOT sediments, which showed the highest differential expression between COLD and HOT sites (10.6 Summed Log2Fold Change). This category was driven by expression of transposable elements; jumping genes that contribute to lateral gene transfer and confer adaption within and between microbial cells. Multiple studies have proposed that these genes are powerful drivers of adaption in chemically stressed environments, especially where metals are present (Birrer et al., 2017; Díaz, 2004; Gibbons et al., 2014; Hemme et al., 2010). Here we provide statistically significant metatranscriptomic evidence of these transcripts in legacy polluted Detroit River sediments. The strong evidence of transposable elements may explain why a less diverse community, as observed in HOT sediments, is able to thrive amongst organic contaminants; adaptations acquired through lateral transfer provide a bolstered and diverse genetic arsenal. Interestingly, transposase-driven metabolic versatility has been cited in studies of acetoclastic methanogen genomes, which aligns with the dominance of the acetate-fermenting *Methanosaeta* in the HOT sediments of the Detroit River in this study (Deppenmeier et al., 2002). Further metagenomic investigations of contaminated environments is required to reveal how the genomic potential of these organisms contribute to the proliferation of transposons-related transcripts.

2.5 Conclusions

Quantitative and holistic gene expression tools such as metatranscriptomics are powerful in leveraging microbial activities in compromised aquatic environments. By sampling sediments within both naturalized and more contaminated regions of the Detroit River, key differences in carbon utilization and transformation pathways were observed, as well as transcripts involved in stress response and adaption. Statistically significant differential expressed gene profiles as quantified by Log2Fold Change revealed nitrate reduction and methanogenesis to be important microbial processes and the ends of the biodegradation spectrum for sediments modelled to have high concentrations of persistent organic pollutants. Further, beta oxidation, gluconeogenesis, and polyester synthesis showed high expression where PAHs, PCBs, and organochloride residues were abundant, indicative of intermediate carbon transformations that generate accessible cellular currencies in acetyl-CoA and succinyl-CoA, potentially from complex, multi-ringed carbon compounds. The significant expression of transposon-related transcripts in polluted

sediments was a key finding and may be linked to microbial community adaption. Distinctions in microbial gene expression between natural and legacy contaminated sediments are fascinating and lend importance to biomonitoring studies that seek to utilize omic tools (Weisener et al., 2017). However, it should be noted that despite a strong contaminant gradient, the majority of mRNA transcripts remained statistically unchanged across sediment regions; a strong case for the functional redundancy of microorganisms. Despite this resilience, ecosystems will experience tipping points in the face of multiple stressors that diminish their beneficial services, and signs of these transitions can be observed and quantified from microbial function. Future work may seek to combine multiple omic tools (metatranscriptomics, metagenomics, and proteomics) with relevant geochemical data, over more defined spatial and temporal scales to better understand baseline characteristics of polluted and pristine sediments.

Conflicts of interest

The authors declare no conflict of interest.

Acknowledgements

The authors would like to thank the Great Lakes Sustainability Fund and Canada-COA Funds for supporting the original sediments surveys, and Genome Quebec for support in the Illumina HiSeq 2000 platform for RNAseq.

FIGURES AND TABLES

Table 1

Mean concentrations of total organic and metal contaminants across sediment designations. Concentrations stated in $\mu\text{g g}^{-1}$ dry weight, except for TOC which is stated as a percentage (\pm standard error).

	Total PAH	Total PCB	Total OGCs	As	Cd	Cr	Cu	Fe	Hg	Mn	Ni	Pb	Zn	TOC%
COLD	4.04 ^H (1.13)	0.16 ^H (0.05)	0.05 (0.01)	6.81 (1.89)	1.07 ^H (0.14)	22.12 ^H (2.6)	22.42 ^H (4.38)	17421.52 ^H (1414.9)	0.19 ^H (0.03)	287.62 (29.09)	19.61 ^H (1.52)	15.89 ^H (3.59)	78.17 ^H (12.31)	3.66 ^H (0.32)
INT	7.27 ^H (1.41)	0.16 ^H (0.03)	0.07 (0.02)	9.61 (2.87)	1.33 ^H (0.09)	24.16 ^H (2.72)	26.74 ^H (6.45)	18423 ^H (2720.7)	0.22 ^H (0.05)	269.77 (45.96)	22.08 ^H (3.71)	14.94 ^H (1.58)	84.54 ^H (9.3)	4.03 ^H (0.55)
HOT	14.02 ^a (1.47)	0.51 ^a (0.07)	0.08 (0.02)	5.26 (1.2)	1.68 ^a (0.2)	31.62 ^a (3.8)	30.72 ^a (2.77)	22815.98 ^a (2005.6)	0.4 ^a (0.04)	301.78 (19.38)	25.9 ^a (0.82)	23.81 ^a (1.55)	153.59 ^a (14.83)	4.72 ^a (0.21)

PAH = polycyclic aromatic hydrocarbons, PCB = polychlorinated biphenyls, OGC = organochlorides

^c= significant difference from COLD mean

^l= significant difference from INTERMEDIATE mean

^H= significant difference from HOT mean

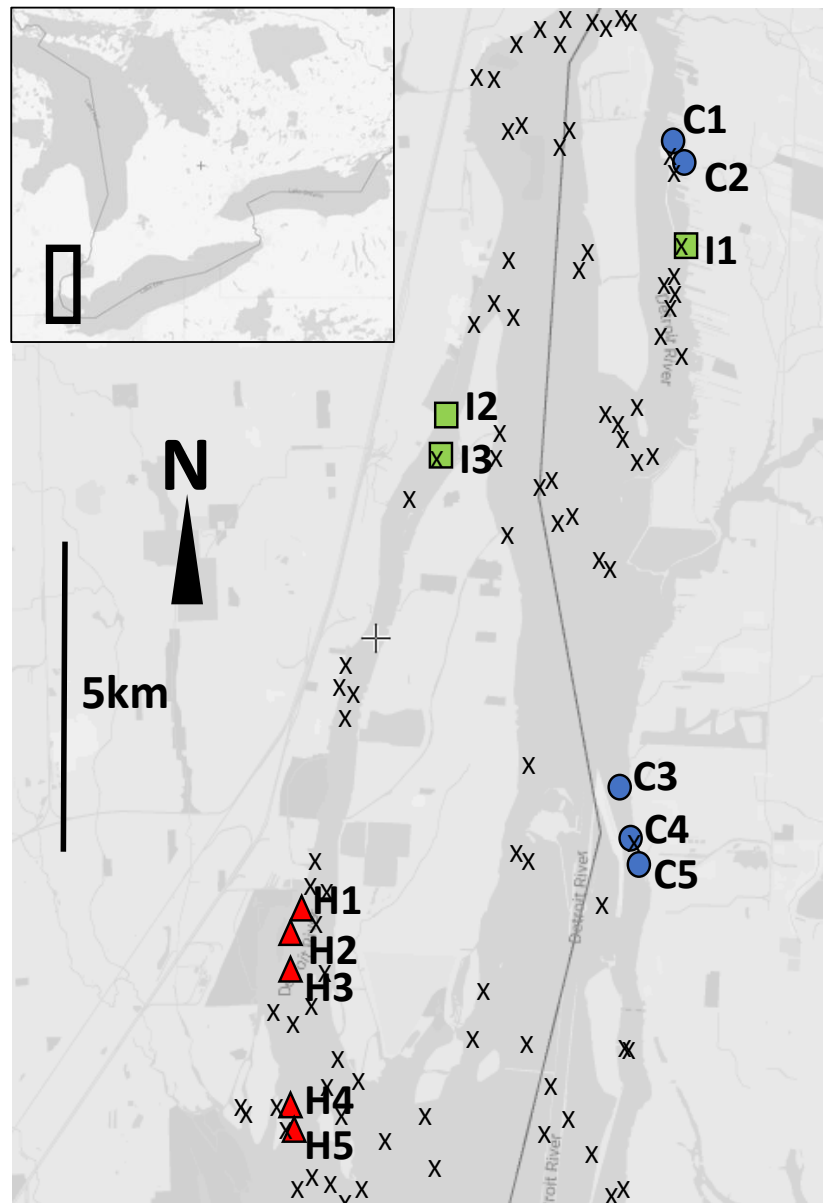


Figure 1: Sediment sampling locations from the present study and their contaminant designation in the lower Detroit River. Inset map shows the location of the Detroit River within the Lower Great Lakes (Circles C=Cold, Squares I=Intermediate, Triangles H=HOT, X= previous sediment sampling locations from 1999 and 2009 surveys from which contaminant designations were derived).

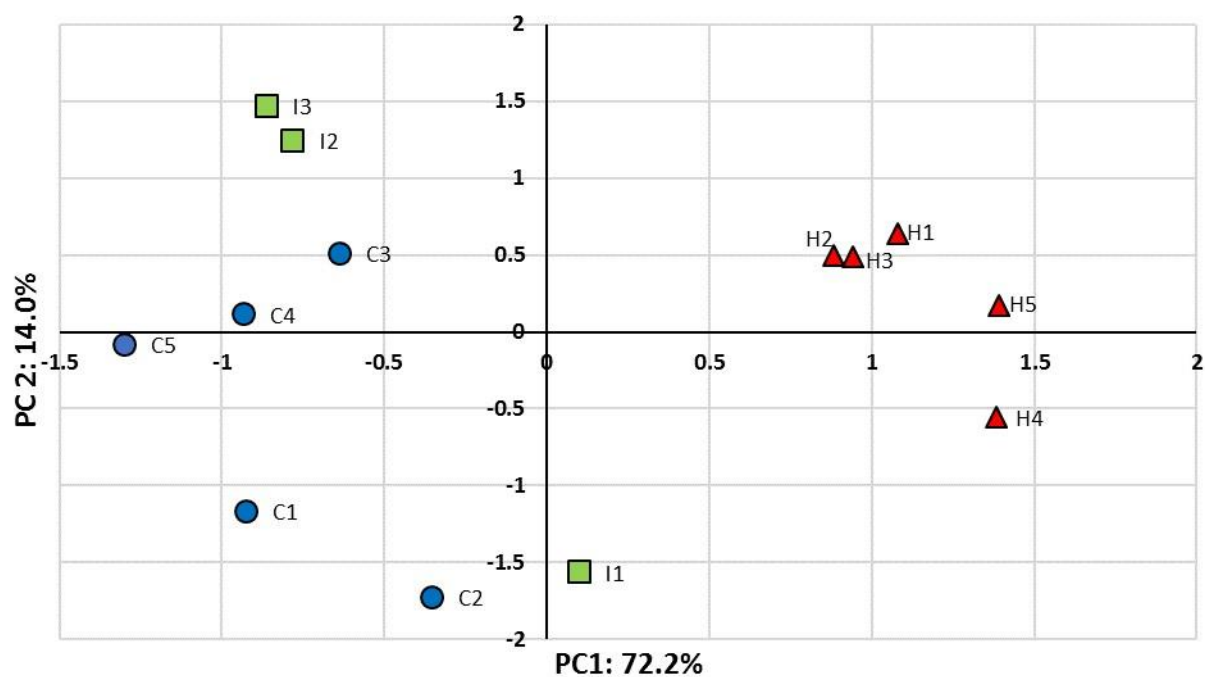


Figure 2: PC1 and PC2 scores of sediment samples based on total interpolated concentrations of metals and organic contaminants. Circles = COLD sites, squares = INT sites, triangles = HOT sites.

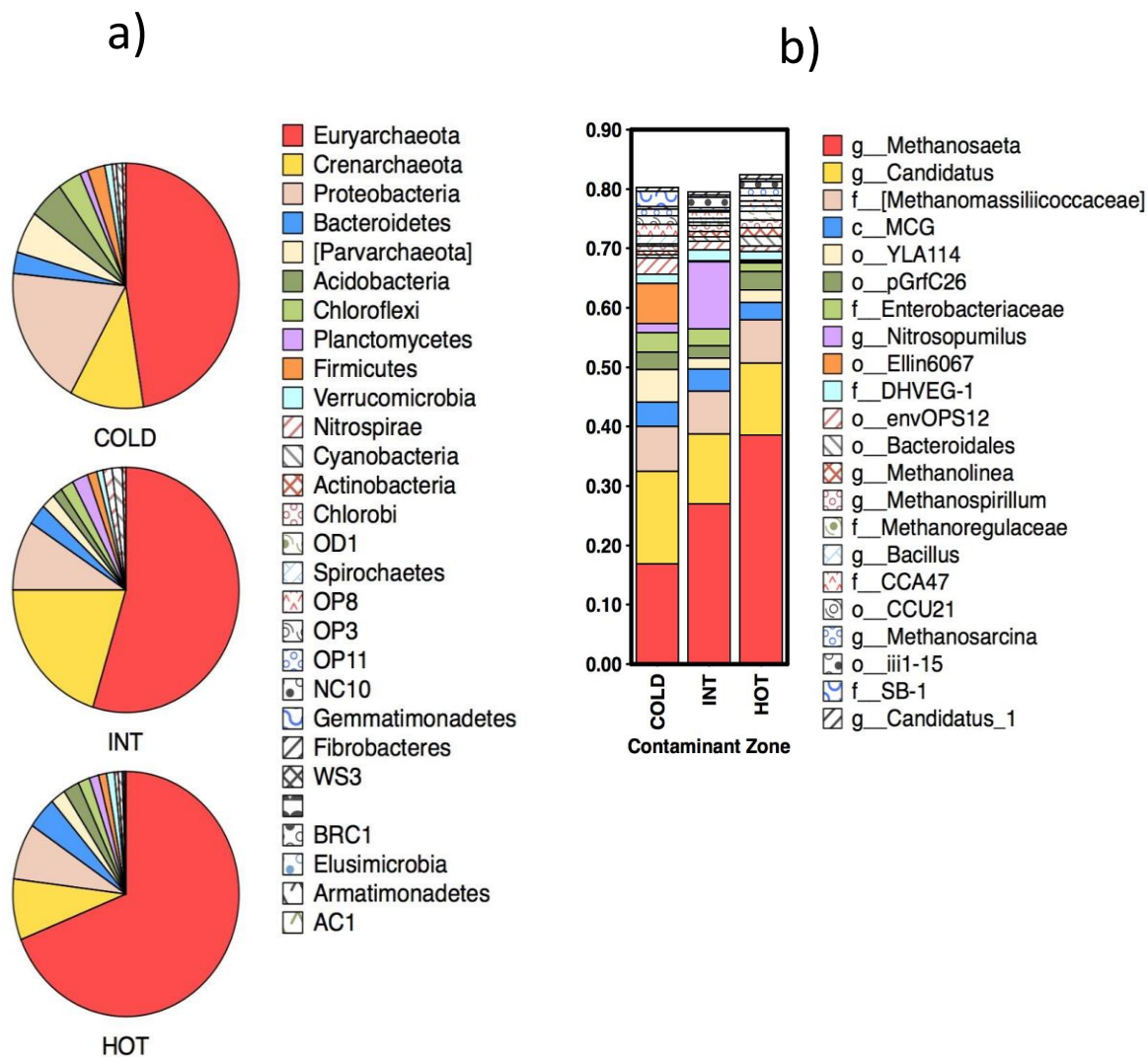


Figure 3: RNA-based microbial taxonomy %abundances at a) phylum resolution and b) class-genus resolution across contaminant regions.

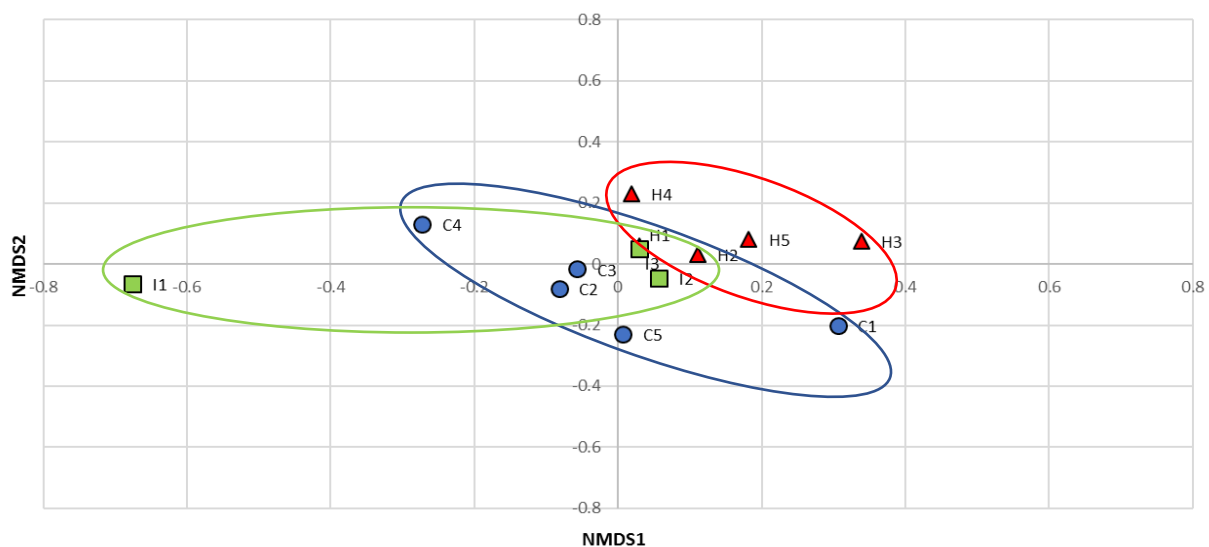


Figure 4: Non-metric multidimensional scaling (stress = 0.103) of all 13 sediment samples for total metatranscriptomic profiles based on COG abundance count matrix. Circles = COLD sites, squares = INT sites, triangles = HOT sites.

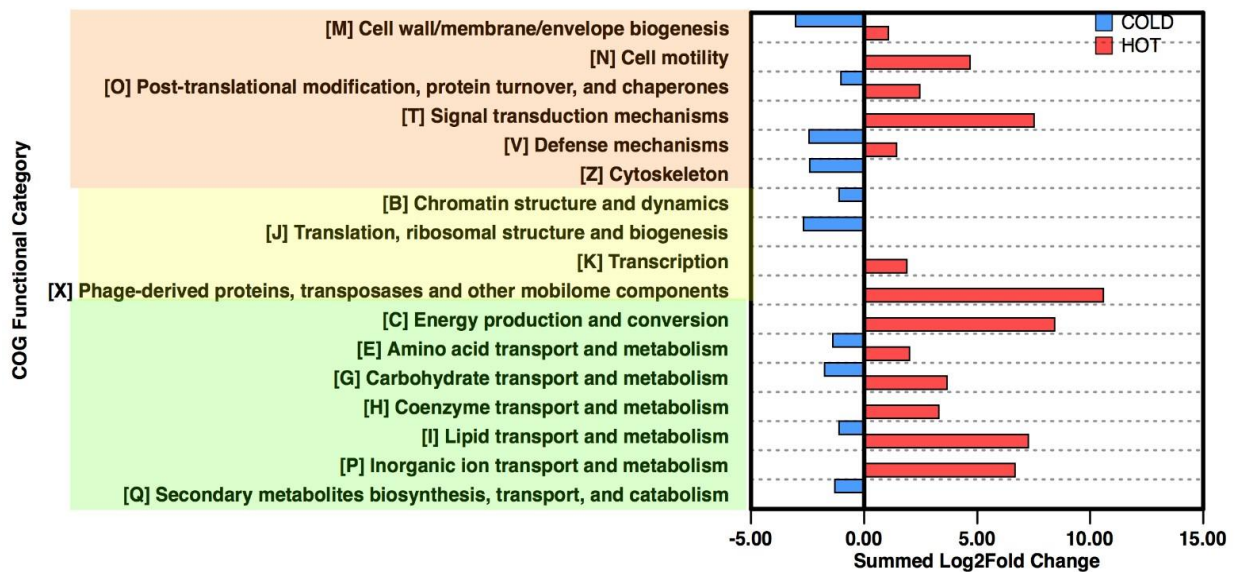


Figure 5: Summed Log₂Fold change values across COG Functional Categories for low (COLD, n=5) and high (HOT, n=5) contaminated sediments. Negative values represent COLD sediments and positive values represent HOT sediments. Broad highlighted boxes represent; [M] – [Z] Cellular Processes and Signalling, [B] – [X] Information Storage and Processing, [C] – [Q] Metabolism.

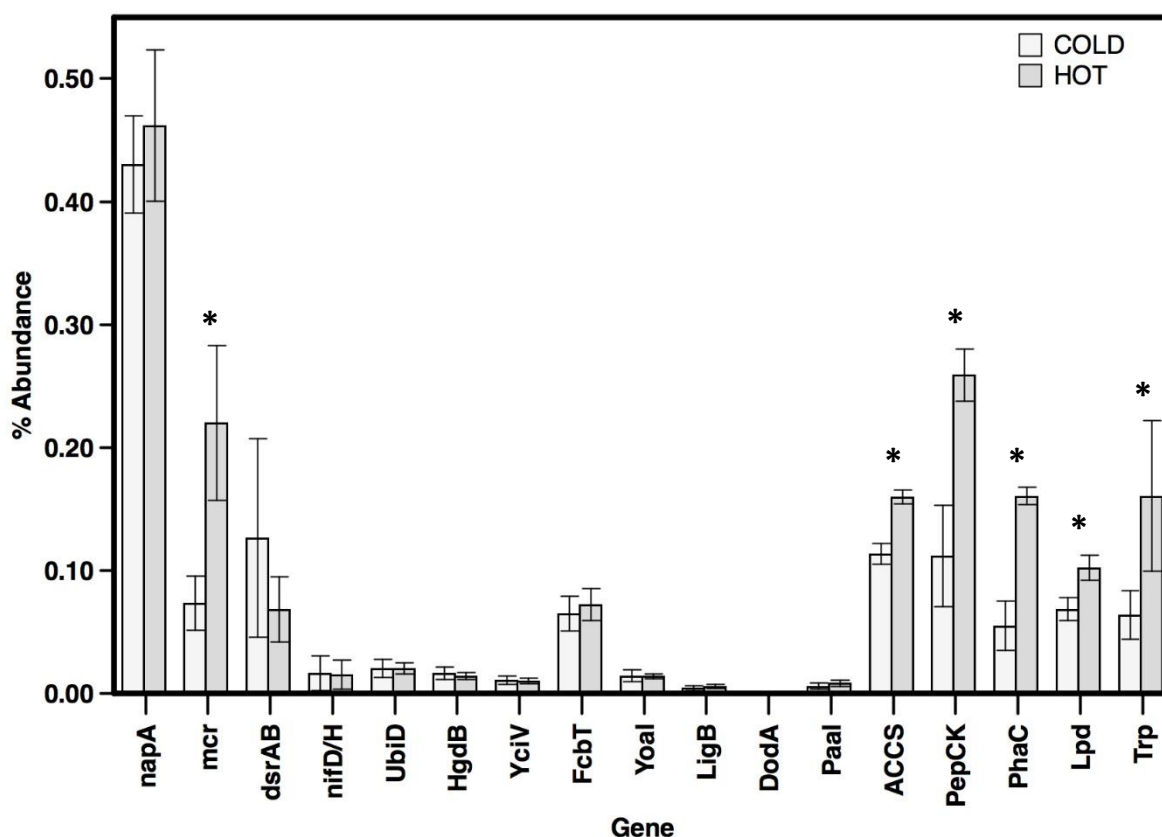


Figure 6: Average relative abundance of select genes across COLD and HOT sediments. Asterisks denote differential expression ($p < 0.05$) between COLD and HOT. napA: periplasmic nitrate reductase, mcr: methylcoenzyme M reductase, dsrAB: dissimilatory sulfite reductase alpha and beta subunit, nifD/H: Nitrogenase molybdenum-iron protein, alpha and beta chains. Aromatic degradation genes; UbiD: 3-polypropenyl-4-hydroxybenzoate decarboxylase, HgdB: benzoyl-CoA reductase/2-hydroxyglutaryl-CoA dehydratase subunit, YciV: predicted metal-dependent phosphoesterase, FcbT: TRAP-type mannitol/chloroaromatic compound transport system, Yoal: aromatic ring hydroxylase, LigB: aromatic ring-opening dioxygenase, catalytic subunit, DodA: aromatic ring-cleaving dioxygenase, Paal: acyl-coenzyme A thioesterase PaaI, contains HGG motif. ACCS: Acyl-CoA synthetase, PepCK: phosphoenolpyruvate carboxykinase, PhaC: poly 3-hydroxyalkanoate synthetase, Lpd: pyruvate/2-oxoglutarate dehydrogenase complex, Trp: transposases.

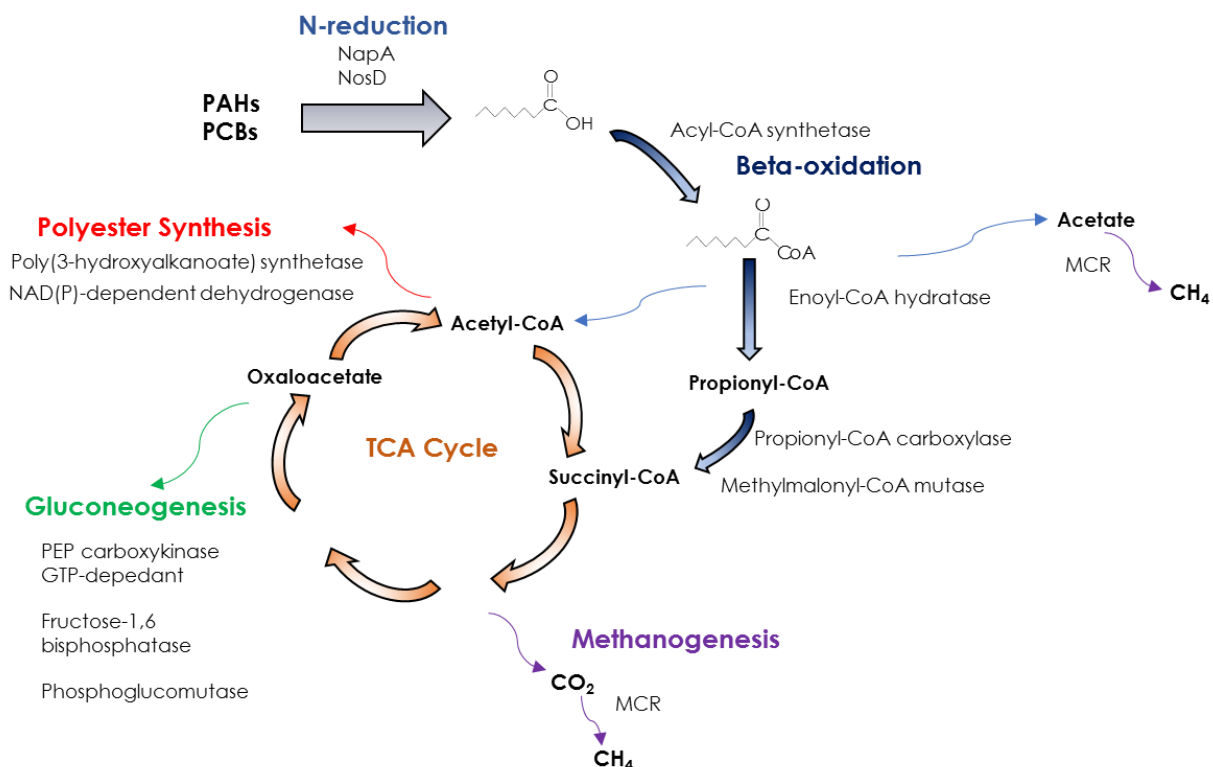


Figure 7: Proposed carbon transformation pathways in legacy contaminated sediments of the Detroit River. Transcripts shown are involved in N-reduction, beta-oxidation, methanogenesis, polyester synthesis, and gluconeogenesis exhibited differential expression ($p > 0.05$) in HOT sediments compared to less contaminated environments as quantified through *DESeq2*.

References

- Abramowicz, D.A., 1990. Aerobic and Anaerobic Biodegradation of PCBs: A Review. *Crit. Rev. Biotechnol.* 10, 241–251. <https://doi.org/10.3109/073885590009038210>
- Antwis, R.E., Griffiths, S.M., Harrison, X.A., Aranega-Bou, P., Arce, A., Bettridge, A.S., Brailsford, F.L., de Menezes, A., Devaynes, A., Forbes, K.M., Fry, E.L., Goodhead, I., Haskell, E., Heys, C., James, C., Johnston, S.R., Lewis, G.R., Lewis, Z., Macey, M.C., McCarthy, A., McDonald, J.E., Mejia-Florez, N.L., O'Brien, D., Orland, C., Pautasso, M., Reid, W.D.K., Robinson, H.A., Wilson, K., Sutherland, W.J., 2017. Fifty important research questions in microbial ecology. *FEMS Microbiol. Ecol.* 93, 1–10. <https://doi.org/10.1093/femsec/fix044>
- Birrer, S.C., Dafforn, K.A., Johnston, E.L., 2017. Microbial Community Responses to Contaminants and the Use of Molecular Techniques, in: *Microbial Ecotoxicology*. Springer International Publishing, Cham, pp. 165–183. https://doi.org/10.1007/978-3-319-61795-4_8
- Chen, G.-Q., Jiang, X.-R., 2017. Engineering bacteria for enhanced polyhydroxyalkanoates (PHA) biosynthesis. *Synth. Syst. Biotechnol.* 2, 192–197. <https://doi.org/10.1016/J.SYNBIO.2017.09.001>
- Cheng, J., Charles, T.C., 2016. Novel polyhydroxyalkanoate copolymers produced in *Pseudomonas putida* by metagenomic polyhydroxyalkanoate synthases. *Appl. Microbiol. Biotechnol.* 100, 7611–7627. <https://doi.org/10.1007/s00253-016-7666-6>
- Colborne, S.F., Maguire, T.J., Mayer, B., Nightingale, M., Enns, G.E., Fisk, A.T., Drouillard, K.G., Mohamed, M.N., Weisener, C.G., Wellen, C., Mundle, S.O.C., 2019. Water and sediment as sources of phosphate in aquatic ecosystems: The Detroit River and its role in the Laurentian Great Lakes. *Sci. Total Environ.* 647, 1594–1603. <https://doi.org/10.1016/J.SCITOTENV.2018.08.029>
- Davis, M.P.A., van Dongen, S., Abreu-Goodger, C., Bartonicek, N., Enright, A.J., 2013. Kraken: A set of tools for quality control and analysis of high-throughput sequence

- data. *Methods* 63, 41–49. <https://doi.org/10.1016/J.YMETH.2013.06.027>
- Deppenmeier, U., Johann, A., Hartsch, T., Merkl, R., Schmitz, R.A., Martinez-Arias, R., Henne, A., Wiezer, A., Bäumer, S., Jacobi, C., Brüggemann, H., Lienard, T., Christmann, A., Bömeke, M., Steckel, S., Bhattacharyya, A., Lykidis, A., Overbeek, R., Klenk, H.-P., Gunsalus, R.P., Fritz, H.-J., Gottschalk, G., 2002. The genome of *Methanosarcina mazei*: evidence for lateral gene transfer between bacteria and archaea. *J. Mol. Microbiol. Biotechnol.* 4, 453–61.
- Díaz, E., 2004. Bacterial degradation of aromatic pollutants: A paradigm of metabolic versatility. *Int. Microbiol.* 7, 173–180. <https://doi.org/im2304027> [pii]
- Drouillard, K.G., Tomczak, M., Reitsma, S., Haffner, G.D., 2006. A River-wide Survey of Polychlorinated Biphenyls (PCBs), Polycyclic Aromatic Hydrocarbons (PAHs), and Selected Organochlorine Pesticide Residues in Sediments of the Detroit River — 1999. *J. Great Lakes Res.* 32, 209–226. [https://doi.org/10.3394/0380-1330\(2006\)32](https://doi.org/10.3394/0380-1330(2006)32)
- Edgar, R.C., 2010. Search and clustering orders of magnitude faster than BLAST. *Bioinformatics* 26, 2460–2461. <https://doi.org/10.1093/bioinformatics/btq461>
- Falk, N., Chaganti, S.R., Weisener, C.G., 2018. Evaluating the microbial community and gene regulation involved in crystallization kinetics of ZnS formation in reduced environments. *Geochim. Cosmochim. Acta* 220. <https://doi.org/10.1016/j.gca.2017.09.039>
- Fuchs, G., Boll, M., Heider, J., 2011. Microbial degradation of aromatic compounds — from one strategy to four. *Nat. Rev. Microbiol.* 9, 803–816. <https://doi.org/10.1038/nrmicro2652>
- Furlong, E.T., Carter, D.S., Hites, R.A., 1988. ORGANIC CONTAMINANTS IN SEDIMENTS FROM THE TRENTON CHANNEL. *J. Great Lakes Res.* 14, 489–501. [https://doi.org/10.1016/S0380-1330\(88\)71581-6](https://doi.org/10.1016/S0380-1330(88)71581-6)
- Ghosal, D., Ghosh, S., Dutta, T.K., Ahn, Y., 2016. Current state of knowledge in microbial degradation of polycyclic aromatic hydrocarbons (PAHs): A review. *Front.*

- Microbiol. 7. <https://doi.org/10.3389/fmicb.2016.01369>
- Gibbons, S.M., Jones, E., Bearquiver, A., Blackwolf, F., Roundstone, W., Scott, N., Hooker, J., Madsen, R., Coleman, M.L., Gilbert, J.A., 2014. Human and environmental impacts on river sediment microbial communities. *PLoS One* 9, 1–9. <https://doi.org/10.1371/journal.pone.0097435>
- Gieg, L.M., Fowler, S.J., Berdugo-Clavijo, C., 2014. Syntrophic biodegradation of hydrocarbon contaminants. *Curr. Opin. Biotechnol.* 27, 21–29. <https://doi.org/10.1016/j.copbio.2013.09.002>
- Hemme, C.L., Deng, Y., Gentry, T.J., Fields, M.W., Wu, L., Barua, S., Barry, K., Tringe, S.G., Watson, D.B., He, Z., Hazen, T.C., Tiedje, J.M., Rubin, E.M., Zhou, J., 2010. Metagenomic insights into evolution of a heavy metal-contaminated groundwater microbial community. *ISME J.* 4, 660–672. <https://doi.org/10.1038/ismej.2009.154>
- Kessler, B., Weusthuis, R., Witholt, B., Eggink, G., 2001. Production of Microbial Polyesters: Fermentation and Downstream Processes. Springer, Berlin, Heidelberg, pp. 159–182. https://doi.org/10.1007/3-540-40021-4_5
- Kim, Y.B., Lenz, R.W., 2001. Polyesters from Microorganisms. Springer, Berlin, Heidelberg, pp. 51–79. https://doi.org/10.1007/3-540-40021-4_2
- Kopylova, E., Noé, L., Touzet, H., 2012. SortMeRNA: fast and accurate filtering of ribosomal RNAs in metatranscriptomic data. *Bioinformatics* 28, 3211–3217. <https://doi.org/10.1093/bioinformatics/bts611>
- Korlević, M., Zucko, J., Dragić, M.N., Blažina, M., Pustijanac, E., Zeljko, T.V., Gacesa, R., Baranasic, D., Starcevic, A., Diminic, J., Long, P.F., Cullum, J., Hranueli, D., Orlić, S., 2015. Bacterial diversity of polluted surface sediments in the northern Adriatic Sea. *Syst. Appl. Microbiol.* 38, 189–197. <https://doi.org/10.1016/j.syapm.2015.03.001>
- Love, M.I., Huber, W., Anders, S., 2014. Moderated estimation of fold change and dispersion for RNA-seq data with DESeq2. *Genome Biol.* 15, 550.

<https://doi.org/10.1186/s13059-014-0550-8>

- Lozupone, C. a, Knight, R., 2007. Global patterns in bacterial diversity. *Proc. Natl. Acad. Sci. U. S. A.* 104, 11436–11440. <https://doi.org/10.1073/pnas.0611525104>
- Lynch, M.D.J., Neufeld, J.D., 2015. Ecology and exploration of the rare biosphere. *Nat. Rev. Microbiol.* 13, 217–229. <https://doi.org/10.1038/nrmicro3400>
- Maphosa, F., de Vos, W.M., Smidt, H., 2010. Exploiting the ecogenomics toolbox for environmental diagnostics of organohalide-respiring bacteria. *Trends Biotechnol.* 28, 308–316. <https://doi.org/10.1016/j.tibtech.2010.03.005>
- Martinez, X., Pozuelo, M., Pascal, V., Campos, D., Gut, I., Gut, M., Azpiroz, F., Guarner, F., Manichanh, C., 2016. MetaTrans: an open-source pipeline for metatranscriptomics. *Sci. Rep.* 6, 26447. <https://doi.org/10.1038/srep26447>
- McDonald, D., Price, M.N., Goodrich, J., Nawrocki, E.P., DeSantis, T.Z., Probst, A., Andersen, G.L., Knight, R., Hugenholtz, P., 2012. An improved Greengenes taxonomy with explicit ranks for ecological and evolutionary analyses of bacteria and archaea. *ISME J.* 6, 610–618. <https://doi.org/10.1038/ismej.2011.139>
- Metcalf, T.L., Metcalfe, C.D., Bennett, E.R., Haffner, G.D., 2000. Distribution of Toxic Organic Contaminants in Water and Sediments in the Detroit River. *J. Great Lakes Res.* 26, 55–64. [https://doi.org/10.1016/S0380-1330\(00\)70672-1](https://doi.org/10.1016/S0380-1330(00)70672-1)
- Michas, A., Vestergaard, G., Trautwein, K., Avramidis, P., Hatzinikolaou, D.G., Vorgias, C.E., Wilkes, H., Rabus, R., Schlöter, M., Schöler, A., 2017. More than 2500 years of oil exposure shape sediment microbiomes with the potential for syntrophic degradation of hydrocarbons linked to methanogenesis. *Microbiome* 5, 118. <https://doi.org/10.1186/s40168-017-0337-8>
- Olsen, R.L., Chappell, R.W., Loftis, J.C., 2012. Water quality sample collection, data treatment and results presentation for principal components analysis – literature review and Illinois River watershed case study. *Water Res.* 46, 3110–3122. <https://doi.org/10.1016/J.WATRES.2012.03.028>

- Reid, T., Chaganti, S.R., Droppo, I.G., Weisener, C.G., 2018. Novel insights into freshwater hydrocarbon-rich sediments using metatranscriptomics: Opening the black box. *Water Res.* 136, 1–11. <https://doi.org/10.1016/J.WATRES.2018.02.039>
- Rho, M., Tang, H., Ye, Y., 2010. FragGeneScan: predicting genes in short and error-prone reads. *Nucleic Acids Res.* 38, e191–e191. <https://doi.org/10.1093/nar/gkq747>
- Sawulski, P., Clipson, N., Doyle, E., 2014. Effects of polycyclic aromatic hydrocarbons on microbial community structure and PAH ring hydroxylating dioxygenase gene abundance in soil. *Biodegradation* 25, 835–847. <https://doi.org/10.1007/s10532-014-9703-4>
- Schimel, J., Balser, T.C., Wallenstein, M., 2007. Microbial Stress-Response Physiology and its Implications for Ecosystem Function. *Ecology* 88, 1386–1394. <https://doi.org/10.1890/06-0219>
- Scott, N.M., Hess, M., Bouskill, N.J., Mason, O.U., Jansson, J.K., Gilbert, J.A., 2014. The microbial nitrogen cycling potential is impacted by polyaromatic hydrocarbon pollution of marine sediments. *Front. Microbiol.* 5, 1–8. <https://doi.org/10.3389/fmicb.2014.00108>
- Smith, C.J., Nedwell, D.B., Dong, L.F., Osborn, A.M., 2007. Diversity and abundance of nitrate reductase genes (narG and napA), nitrite reductase genes (nirS and nrfA), and their transcripts in estuarine sediments. *Appl. Environ. Microbiol.* 73, 3612–22. <https://doi.org/10.1128/AEM.02894-06>
- Sotsky, J.B., Greer, C.W., Atlas, R.M., 1994. Frequency of genes in aromatic and aliphatic hydrocarbon biodegradation pathways within bacterial populations from Alaskan sediments. *Can. J. Microbiol.* 40, 981–5. <https://doi.org/10.1139/m94-157>
- Szalinska, E., Drouillard, K.G., Anderson, E.J., Haffner, G.D., 2011. Factors influencing contaminant distribution in the Huron-Erie Corridor sediments. *J. Great Lakes Res.* 37, 132–139. <https://doi.org/10.1016/j.jglr.2010.11.005>
- Szalinska, E., Drouillard, K.G., Fryer, B., Haffner, G.D., 2006. Distribution of Heavy

- Metals in Sediments of the Detroit River. *J. Great Lakes Res.* 32, 442–454.
[https://doi.org/10.3394/0380-1330\(2006\)32](https://doi.org/10.3394/0380-1330(2006)32)
- Szalinska, E., Grgicak-Mannion, A., Haffner, G.D., Drouillard, K.G., 2013. Assessment of decadal changes in sediment contamination in a large connecting channel (Detroit River, North America). *Chemosphere* 93, 1773–1781.
<https://doi.org/10.1016/j.chemosphere.2013.06.009>
- Wang, H., Cheng, M., Dsouza, M., Weisenhorn, P., Zheng, T., Gilbert, J.A., 2018. Soil Bacterial Diversity Is Associated with Human Population Density in Urban Greenspaces. *Environ. Sci. Technol.* 52, acs.est.7b06417.
<https://doi.org/10.1021/acs.est.7b06417>
- Weisener, C., Lee, J., Chaganti, S.R., Reid, T., Falk, N., Drouillard, K., 2017. Investigating sources and sinks of N₂O expression from freshwater microbial communities in urban watershed sediments. *Chemosphere* 188, 697–705.
<https://doi.org/10.1016/j.chemosphere.2017.09.036>
- Weisener, C.G., Reid, T., 2017. Combined imaging and molecular techniques for evaluating microbial function and composition: A review. *Surf. Interface Anal.* 49, 1416–1421. <https://doi.org/10.1002/sia.6317>
- Widenfalk, A., Bertilsson, S., Sundh, I., Goedkoop, W., 2008. Effects of pesticides on community composition and activity of sediment microbes - responses at various levels of microbial community organization. *Environ. Pollut.* 152, 576–584.
<https://doi.org/10.1016/j.envpol.2007.07.003>
- Zeglin, L.H., 2015. Stream microbial diversity in response to environmental changes: review and synthesis of existing research. *Front. Microbiol.* 6, 454.
<https://doi.org/10.3389/fmicb.2015.00454>

CHAPTER 3: INTEGRATING MICROBIAL DNA COMMUNITY ANALYSES INTO TIME-INTEGRATED SUSPENDED SEDIMENT SAMPLING METHODS

3.1 Introduction

Riverine fine-grained suspended sediment ($< 63 \mu\text{m}$) can often be associated with pollutants and pathogens of concern due to its high adsorption capacity, cohesive properties, dissolved organic carbon content, and high surface area to volume ratio (Krein et al. 2003; Droppo et al. 2015). Thus, the timing and magnitude of anthropogenic disturbances in lotic systems from sewage infrastructure, industrial effluent, and agricultural/urban runoff can be better understood and managed by incorporating information about the suspended sediment phase (SSP).

Filtration of grab samples is conventionally performed to discern the SSP from that of dissolved constituents. However, analytical procedures that seek to quantify particle-size distributions and/or concentrations of particulate contaminants require large collection volumes, especially where total suspended solids (TSS) measurements are low. To overcome these limitations, time-integrated collections of the SSP can be performed. In some instances, continuous flow centrifugation (CFC) allows for larger volumes of water to be collected and particulate matter separated in the field for physicochemical analysis (Plach et al. 2011; Reid et al. 2020), however this method may be impractical where access to sampling sites is problematic as the units are heavy and require powered generators. A low maintenance alternative was implemented by Phillips et al. 2000 which used a deployable passive unit installed in the field to collect a representative subsample of the time integrated SSP load over time periods of days to weeks. The samplers, hereafter called Phillips Tube (PT) samplers are similar to vertical sediment traps used in deep lotic environments (Wilhelm et al. 2014) but differ in that they have a horizontal orientation to capture TSS under convective transport with stream flow.

Phillips Tube samplers have been used to monitor physicochemical characteristics of the SSP including grain size distributions and concentrations of particulate phosphorus, metals, and radionuclides (Ballantine et al., 2008; Collins et al., 2010; Owens et al., 2012; Smith and Owens, 2014). However, the microbial component of the SSP has not yet been assessed. The transport and fate of these organisms can have ecological and human health implications. For example, the flow of living and dead microbial biomass downstream is a fundamental component of aquatic biogeochemical cycling of macronutrients (i.e. carbon,

nitrogen, phosphorus), and may alter receiving environments where deposited communities impose new functions (Zhang et al. 2020). In terms of human health, particles can serve as attachment substrates for pathogenic species which may be mobilized from soils or the bed sediment phase (BSP) and transported to sites of municipal water intakes or recreational areas (Bradford et al. 2013; Pandey et al. 2018; VanMensel et al. 2020). Thus, it is important to advance the understanding of microbial SSP collection techniques.

To date, there have been no studies to evaluate the suitability of PT samplers for microbiological characterization of suspended sediment. In addition, microbial communities are known to influence and be influenced by redox conditions in sediments, which can change the availability and mobility of chemical species of interest including metals (Gadd 2010), nutrients (C, N, P) (Peura et al. 2015; Ding et al. 2018; Rahutomo et al. 2018), and organic contaminants (Ghosal et al. 2016). Therefore, interpretations of the SSP accumulated in fine sediment samplers may be incomplete without considering the function of microbial assemblages.

In this study, multiple PT samplers were deployed in an agricultural-influenced, low order stream through the spring/summer of 2018. The collected SSP was subject to microbial community analysis via DNA-metabarcoding with three primary study objectives; 1) testing the precision and replicability between individual PT samplers, 2) contrasting BSP and SSP communities over space and time within the stream segment, 3) understanding changes within PT samplers influenced by redox/microbial effects that may improve interpretations of SSP chemical measurements. The third objective was further tested by assessing seasonal water quality parameters and meteorological conditions using continuous DO/temperature loggers and climate data.

3.2 Methods

3.2.1 Site and Sampling Information

Big Creek is a low order stream that flows roughly 25 km north from its headwaters in central Essex County, Ontario, to its outlet at Lake St. Clair, where it merges briefly with the Thames River (Fig. 1A, B, Table S1). Its gross drainage area is 57 km², with the surrounding catchment being flat (elevation change along the river being < 1 m km⁻¹) and characterized by Brookstone Clay, dominated by row crop corn and soybean rotation.

Much of the catchment has been altered to allow for artificial drainage around farm plots, and limited wooded areas exist along the river length (land use > 70 % agriculture, <10 % forested) (Falk et al. 2021). The study reach of Big Creek runs for 0.7 km starting close to the headwaters with a maximum width and depth of 4 m and 0.5 m, respectively. Access to the segment was approved by landowners. Five sub-sites were chosen along the segment to assess longitudinal variability in BSP and SSP microbial communities: S1 and S2 flanked a road overpass, S3 and S4 were positioned adjacent to a soybean plot with little riparian buffer, and S5 adjacent to the plot surrounded by higher riparian buffer. The sites were sampled monthly from April – July 2018, and once in November 2018.

3.2.2 Water and Bed Sediment Sampling

Water quality parameters including TSS, soluble reactive phosphorus (SRP), temperature, dissolved oxygen (DO), oxidation-reduction potential (ORP), and pH were measured at a downstream (S1), midpoint (S3), and upstream (S5) sub-site for each site visit. TSS and SRP were measured via grab samples collected approximately 10 cm below the surface. The remaining parameters were measured using a TROLL 9500 Multiparameter Sonde (In-Situ, Inc.). TSS was measured by filtration through 0.45 μm cellulose acetate filters and massing of filters after drying at 100 °C for 24 hrs with SRP measured on a SmartChem 170 Direct Read Discrete Analyzer via the phosphomolybdenum blue method, using ammonium molybdate, potassium antimony titrate as a catalyst, and ascorbic acid as the reducing agent.

Bed sediments were collected from the same points as surface water parameters with a pre-sterilized trowel from the top 5 cm of the sediment water interface (SWI) and stored in 200 mL polyethylene containers. Care was taken to minimize the loss of fines during collection. Sediments were immediately sub-sampled ($n = 3-5$) into 5 mL cryogenic tubes and flash frozen in liquid nitrogen and transported back to the laboratory for storage at -80 °C until DNA extraction (Falk et al. 2019). Additional details on field methods can be found in Appendix B.

3.2.3 Suspended Sediment Sampling by Time-Integrated Passive Samplers

Phillips Tube samplers were used to collect suspended sediment over the monthly time intervals April-May (AM), May-June (MJ), and June-July (JJ). The samplers as

described by Phillips et al. 2000 consist of a 1 m long, polyvinylchloride tube with a fitted threaded conical head cap (facing upstream) and end plug, with 4 mm diameter openings at either end for passage of water through the unit. Water passes through the main body of the tube where the flow velocity is decreased by a factor of 600 promoting sedimentation of suspended sediment particles. The samplers are inexpensive, easy to deploy, and are ideal for collection of higher concentrations of TSS than grab or autosamplers. Further, they enable a time-integrated sample that is believed to be representative of ambient stream characteristics.

At the first sampling time point in April, seven PT samplers were deployed over the five sub-sites: two replicate samplers each at sites S1 and S5, and one at sites S2, S3, and S4. Samplers were placed at approximately 60% of the water depth at the time of deployment by securing to rebar stakes driven into the bed sediment (Fig. 1C). At each subsequent time point, samplers were removed, and the collected material emptied into 20-gallon buckets, sub-sampled, and transported back to the laboratory on ice. The samplers were cleaned and sterilized and returned to their position in the study reach. In the lab, samples were filtered for TSS as described previously. Several parameters were calculated from the PT samplers including mean accumulated TSS (mg L^{-1}) and mean time-averaged suspended sediment TSS load (g day^{-1}), calculated by dividing accumulated sampler TSS by days of deployment. Mean total volume passed (TVP) through the PT samplers was also estimated by dividing the mean accumulated sampler TSS mass by the average TSS concentration of the stream water during the collection period. Several filters from each sampler were preserved by placement in sealed cryogenic vials, flash frozen in liquid nitrogen, and stored at $-80\text{ }^{\circ}\text{C}$ until DNA extraction. The frozen TSS filters were used to profile the suspended sediment microbial communities.

3.2.4 DNA Extraction

Bed and suspended sediments were extracted for total DNA using the QIAGEN DNeasy PowerLyzer PowerSoil Kit following the manufacturers instructions. For bed sediments, approximately 0.25 g of sample was used. For suspended sediment, filters were cut into smaller pieces using sterile tweezers and inserted into QIAGEN PowerBead Tubes, with intermittent vortexing to ensure the filter pieces, beads, and PowerBead solution were

well homogenized prior to the first bead beating step. Polymerase Chain Reaction (PCR) was performed on total DNA to amplify an approx. 300 base pair (bp) segment of the hypervariable 16S bacterial rRNA gene. Forward primer V5F (5–ATTAGATACCCNGGTAG-3) and reverse primer V6R (5–CGACAGAGCCATGCANCACCT-3) were used in the PCR reaction with 1 µL of DNA, with additional reagents and reaction parameters specified in the methods of Falk et al. (2018). Resulting DNA was visualized on 1% agarose gels to confirm amplification and successful samples were subject to a modified bead cleaning based on the Agencourt AMPure XP PCR Purification protocol to remove DNA fragments < 50 bases. Samples were then barcoded with a unique base sequence through a second PCR reaction for downstream multiplexing. All samples were combined, purified, and excised through a final 2% agarose gel extraction (QIAquick Gel Extraction Kit), normalized, and sequenced on an Ion Torrent Personal Genome Machine (Life Technologies) and output in single-end FASTQ file format.

3.2.5 Microbial Community Taxonomy and Diversity Metrics

Resulting FASTQ files were imported and processed using the Quantitative Insights into Microbial Ecology (QIIME) pipeline, QIIME2 ver. 2019.1. In brief, demultiplexed FASTQ files were imported using the “SingleEndFastqManifestPhred33” format and filtered and quality controlled using DADA2 to remove chimeras and low-quality sequences (Callahan et al. 2016). Multiple sequence alignment was performed on the resulting amplicon sequence variants (ASVs) with mafft (Katoh et al. 2002) and used in phylogenetic tree construction with fasttree2 (Price et al. 2010) with the q2-phylogeny plugin. Alpha diversity metrics (Shannon, Pielou’s evenness, Faith phylogenetic diversity (pd)) and beta diversity (Bray-Curtis dissimilarity) were estimated using the q2-diversity plugin after rarefying to 5000 sequences per sample (Faith 1991; Lozupone and Knight 2005; Lozupone et al. 2007). Alpha diversity is used as an approximation of within-sample diversity, and thus can be calculated for each sample individually, whereas beta diversity is a measurement of between, or pairwise, sample dissimilarity, and thus is used in comparisons when there is more than one sample. Microbial taxonomy was assigned to ASVs from the SILVA ribosomal RNA database (Silva release 132_99_16S) (Quast et al.

2013) through a Naive Bayes classifier via the q2-feature-classifier plugin (Bokulich et al. 2018) trained on sequences extracted using the primers specified in section 2.4.

Pairwise alpha diversity between sample communities was tested with the Kruskal-Wallis test. Bray-Curtis distances were used to test for differences in community compositions between groups via PERMANOVA with 999 permutations. Both tests implement the Benjamini-Hochberg correction for multiple comparisons. Additional multivariate analyses and biomarker discovery of microbial samples was performed through MicrobiomeAnalyst (Dhariwal et al. 2017; Chong et al. 2020). Principal coordinate analysis (PCoA) was used to visualize Bray-Curtis distances between samples, and linear discriminant analysis Effect Size (LEfSe), a method designed for metagenomic data, was used to identify significant biomarker taxa across groups (Segata et al. 2011). Differences in subsite water quality and sediment parameters were assessed through Mann-Whitney U tests.

3.2.6 In-Situ DO measurements from PT Samplers

Onset/HOBO Optical Dissolved Oxygen/Temperature Loggers (model # U26-001) were used to log both ambient stream DO concentration and concentration within a PT sampler to confirm suspected DO changes. A unit was deployed at Big Creek from May-June 2021 for 38 days, with one logger placed inside the unit and another fixed to the outside. Both loggers were pre-calibrated as per the manufacturers instructions and programmed to measure and record DO and temperature every 5 minutes.

3.3 Results

3.3.1 Seasonal Water Quality Parameters

Water quality parameters were measured monthly to provide estimates of average stream conditions through the study period. Environmental parameters from monthly grab samples and sonde data are shown in Table 1, along with parameters calculated from the PT samplers. TVP for samples AM, MJ, and JJ, was 413 L, 146 L, and 13.2 L, respectively, however, these values are only estimates as sampler calibration has shown that accumulated sampler TSS characteristics are not 100% proportional to in-stream characteristics (Phillips et al. 2000). Water quality parameters were not measured in

replicate at every sub-site for each sampling period, however, sub-sites that were measured showed no measurable differences between upstream and downstream locations on the same sampling day for any variable (Mann-Whitney U, $p > 0.05$). The only exception was a TSS grab sample in July which was higher at S1 (downstream) (581.6 mg L^{-1}) than S5 (upstream) (331.9 mg L^{-1}). SRP monthly averages were 8.9, 66.8, 5.6, and $4.8 \text{ } \mu\text{g L}^{-1}$ for April, May, June, and July site visits, respectively. Daily precipitation and max daily air temperature values obtained from local meteorological stations through the 2018 collection period are displayed in Fig. 2A. Continuous DO and temperature measurements from inside (Sampler) and outside (Stream) the Phillips unit deployed in 2021 are displayed in Fig. 2B alongside daily precipitation and max daily air temperature.

3.3.2 Microbial Community Diversity in Bed and Suspended Sediments

After quality control, 65 DNA samples passed the chosen threshold of 5000 sequences and were used for microbial community comparisons among groups. Samples had an average sequence count of 38,188.8. Community alpha diversity was not different between BSP or between SSP sub-sites at any one time point (Kruskal-Wallis pairwise $p > 0.05$, Table S2). Adjacent (i.e., replicate) sampler SSP communities, tested from April-May samples at S1 and S5, also showed no measurable differences in alpha diversity. Community composition was not statistically different between subs-sites of BSP samples or between subs-sites of SSP samples (PERMANOVA pairwise adjusted p -values > 0.05 , Table S3). Due to the absence of measurable dissimilarity between upstream and downstream sub-sites and adjacent suspended sediment samplers, DNA samples were grouped by sampling month and source (i.e., BSP or SSP) in all subsequent analyses, for a total of eight groups.

For monthly microbial community analyses, there were no differences in community evenness within or between BSPs and SSPs. April-May SSPs had lower Shannon diversity than April and July BSPs. Faith-pd diversity showed more differences between groups; April-May samples had lower diversity than June-July, April, June, July, and November bed samples, while May beds had lower diversity than April, June, and July beds (Table S2, Fig. S1). Monthly microbial community composition was significantly

different within and between all SSPs and BSPs, except for between May and June BSPs (PERMANOVA pairwise adjusted p-values > 0.05, Table S3).

When sampling month was removed as a variable and all samples were grouped by only sediment source (i.e., bed or suspended sediment) microbial communities showed higher Shannon and Faith-phylogenetic diversity in BSPs than SSPs, but no difference in evenness. In addition, community composition was significantly different between BSP and SSP communities. This separation is represented in the Bray-Curtis distance PCoA plot in Fig. 3.

3.3.3 Microbial Community Analysis

Classification of ASVs across samples resulted in 4160 unique taxonomic features. For additional microbial community analysis, singleton features were removed, and default low count and low variance filters were applied, yielding 573 taxonomic features. Overall, communities were dominated by Proteobacteria, which comprised > 50 % of all ASVs in sample groups, except for November BSPs (Fig. 4). Acidobacteria, Verrucomicrobia, Bacteroidetes, Planctomycetes, Nitrospirae, and Actinobacteria were the other dominant phyla across groups. As samples shared many of the same microbial taxa, LEfSe biomarker analysis was performed to identify the differentially abundant taxa across groups ($p < 0.05$), with a Linear Discriminant Analysis (LDA) score of ± 2 as the cut off value. Nineteen phyla were observed as biomarkers of sediment source, with seven identified as significant indicators of suspended sediments and 12 for bed sediments (Fig. 5). Within SSP samples, the Verrucomicrobia, Planctomycetes, Patescibacteria, Fibrobacteres, and Cyanobacteria were significant biomarker phyla. In contrast, BSP samples showed significant phyla belonging to Proteobacteria, Nitrospirae, Euryarchaeota, Chloroflexi, and unclassified taxa. When samples were grouped by sediment source and month, 271 taxa assigned to genus or the next highest classification level were found to be significant biomarkers. This distribution is displayed in Fig. 6. July BSP samples had the highest number of differential biomarkers (52) with May BSP samples yielding the fewest (14). On average, SSP samples (AM, MJ, JJ) had more significant biomarkers than bed sediments. The 50 most significant biomarker taxa (at genus or next highest classification level) as determined by LDA score are displayed in Fig. 7 and are sub-labelled to identify the sample group with the highest

association. SSPs showed high differential abundance of an unclassified *Burkholderiaceae*, and *Arenimonas*, *Prostheobacter*, *Sphingomonas*, and an unclassified *Pedosphaeraceae*. For BSPs, *Thiobacillus*, unclassified *Gallionellaceae*, *Sulfurifustis*, *Aquabacterium*, and *Gallionella* were the top five identified taxonomic groups.

3.4 Discussion

3.4.1 Precision and Replicability of Microbial SSP in Phillips Tube Samplers

In microbial community studies, calculation of within and between sample diversity is often the initial assessment of whether groups are composed of different abundances or types of species and can guide additional inquiries into why these differences may exist. These additional inquiries can be based on collections of physical, chemical, or biological variables that define the groups. Microbial alpha diversity and community composition did not vary significantly upstream to downstream for any timepoint within each sediment compartment, suggesting that the suspended and bed sediments studied represented consistent spatial niches, and slight changes in creek morphology or surrounding geography did not impose any observable selection on sub-sites. This observation is reasonable for a short segment such as that studied here (0.7 km), however as river lengths increase, microbial communities tend to diverge, and become dissimilar over distance, even within the same watercourse (Gibbons et al. 2014; Liao et al. 2020). Replicate (i.e., side by side) sediment samplers showed no significant differences in suspended phase microbial communities by alpha and beta diversity tests. It's noted that replicate samplers were placed in consistently flowing sections, and that if placement was at stream bends, this could have altered the receiving load between samplers, as water velocity on the inside and outside of bends can alter particle size distribution and settling (Deng and Singh 2002; Zhang et al. 2020). However, as the goal of the suspended samplers was to collect a time-integrated signal of total microbial biomass transported downstream, fine scale differences in loads due to channel morphology are not believed to influence the overarching SSP microbial community. In addition, paired t-tests showed no significant differences between replicate sampler TSS concentrations. Thus, replicate PT samplers in this study (n=7) showed good precision and replicability with respect to the microbial community and load collected.

3.4.2 Microbial Characteristics of Bed and Suspended Sediments

3.4.2.1 *Alpha and Beta Diversity*

Although microbial assemblages were consistent spatially within bed and within suspended sediments, there was a marked difference between the sediment compartments, as well as clear seasonal shifts. Bed sediments were more diverse than suspended sediments on average. Benthic sediments are often influenced by abrupt light and redox gradients, and rapid oxygen consumption over shallow depths (on the micron scale) can select for a variety of species that adapt to niches of available organic and inorganic energy sources (Zeglin 2015). Alternatively, suspended sediment communities, though potentially originating from erosion of beds, are subject to more uniform stream conditions with respect to light and/or DO over similar spatial scales. This finding aligns with recent studies that compared benthic and water column communities, where benthic communities exhibited higher diversity (Clinton et al. 2020; Laperriere et al. 2020). This was not always the case, however, as June-July SSP communities displayed the highest average diversity of any sample group. The June-July time interval was the longest, had the warmest water temperatures, and the lowest DO, and these characteristics may have played a role in an expansion or shift to opportunistic facultative microbial niches within the suspended phase. In studies of agricultural tributaries in Ontario, alterations in rainfall and DO have been known to influence microbial community composition (Chen et al. 2018). The lower water level and flow rate also would have caused less connectivity between suspended sediment samplers at sub-sites, and this decreased linkage may be partly responsible for differences in the microbial June-July suspended sediment community, leading to high alpha diversity. This hypothesis contrasts with observations that higher flows, often in spring, contribute to the greatest in-stream microbial diversity, as allochthonous terrestrial matter input from rain events adds more cells from soil/litter into streams (Laperriere et al. 2020; Caillon et al. 2021). However, these observations are commonly based on grab samples that would collect both living and dead/dormant cells recently flushed from the land. Here, the high incidence of rainfall events during the April-May spring sampling interval could have served to flush the samplers, resetting the in-situ microbial community, leading to a lower diversity than expected compared to more calm intervals where communities had greater time to establish. Thus, contrasting alpha diversity measurements across studies can be

influenced by sampling methodology, with grab sampling reflecting nascent stream conditions, and time-integrated collections representative of longer periods.

Time points had close to equal alpha diversity, but the species types and abundances varied. PCoA plots demonstrate this separation between both sediment compartments and season, with greater overlap existing for BSP sample groups. The smaller distances and distinct clusters of SSP groups by month reflect the nature of the suspended environment, which can be more dynamic temporally than bed sediments. As water column physicochemical parameters vary seasonally, so do water column microbial communities (Staley et al. 2015), and it is shown here that time-integrated SSP-associated communities shifted in the same fashion. This is reflected in temporal community composition comparisons, where SSP groups were distinct from each other. Even bed sediments were nearly always dissimilar, with the exception of May and June bed communities which did not pass the threshold of statistical difference. Thus, although beta diversity points to community differences in both sediment compartments, temporal shifts were greater in SSP communities. Therefore, studies of suspended microbial assemblages likely require higher frequency monitoring than bed sediments.

3.4.2.2 Microbial Biomarkers of Bed and Suspended Sediments

Biomarker tests such as LEfSe use a combined assessment of class discrimination using non-parametric tests and linear discriminant analysis (LDA) and can shed more light on differentially abundant genomic features than observations from % abundances and/or alpha diversity measures alone. LEfSe showed that suspended and bed communities could be differentiated even at the phylum level, with Verrucomicrobiota and Proteobacteria being the highest discriminating groups, respectively. Studies of water column assemblages, some in southern Ontario lakes and rivers, have found Proteobacteria, Cyanobacteria, Actinobacteria, and Bacteroidetes to be dominant phyla (Zeglin 2015; Mohiuddin et al. 2019; Fasching et al. 2020). In this study, Cyanobacteria and Actinobacteria were indicative of SSPs when timepoints were combined (LDA scores of +4.4 and +4.32, respectively), but the Bacteroidetes were equally present in both BSPs and SSPs, and Proteobacteria were overrepresented in BSPs (LDA score -5.37). Thus, suspended sediments share similarities with microbial groups sourced from surface waters

but also have characteristics akin to bed sediments, as particle flocculation and aggregation can produce semi-reduced microenvironments (Chen et al. 2018). Further, suspended flocs have often been described as suspended biofilms (Droppo et al. 2015) with similar functions to sessile biofilms such as O₂ gradients. This corroborates with the Phillips' unit DO log from 2021, which showed that oxygen levels within the sampler decreased over time.

Stream DO oscillated daily following in-stream respiration/photosynthesis, whereas sampler DO began decreasing from ambient (~12 mg L⁻¹) to hypoxic conditions (1-3 mg L⁻¹) by the third week of deployment (Fig. 2B). This was likely driven by the absence of light in the sampler, which forced the environment into net respiration where oxygen was gradually consumed.

The low in-situ sampler DO measured in 2021 corresponds with trends observed in the suspended microbial community in 2018. At the genus level, SSPs were defined by groups tolerant of or reliant on semi-aerobic environments, including *Arenimonas*, *Prostheobacter*, *Polynucleobacter*, *Methylothera*, *Rheinheimera*, and *JGI_0001001_H03*. Many are cited to be capable of N-reduction, including *Sphingomonas*, *Methylothera*, *Rheinheimera*, and *Pseudomonas*, which is a valuable metabolic option where oxygen is gradually depleted (Lv et al. 2017; Huang et al. 2018). Alternatively, bed sediments were defined by *Thiobacillus*, *Sulfurifustis*, *Gallionella*, *Methanosaeta*, *Sideroxydans*, *Geobacter*, and *Desulfatiglans*, all of which are classified as chemolithotrophic and/or anaerobic members (Hiibel et al. 2011; Jin et al. 2012; Jewell et al. 2016; Umezawa et al. 2016; Jochum et al. 2018; Falk et al. 2019; Cooper et al. 2020). Fe and S-metabolizing groups were common in bed sediments as were nitrate reducers, which is expected where oxygen depletion occurs rapidly and consistently at the sediment water interface and energy generation is driven by cycling of terminal electron acceptors such as nitrate, iron oxyhydroxides, and sulfate. This is further corroborated by the prevalence of *betaproteobacteria* groups in BSPs, particularly during April and July. Taxa within this class of the proteobacteria are often numerically prevalent in sediments and play key roles in geochemical alterations due to their wide metabolic diversity (Custodio et al. 2022). Thus, BSP communities appear to be adapted to lower redox niches, but SSP taxa

represent an assortment of aerobic and semi-aerobic groups that can utilize N-species in addition to oxygen. The identification of these taxa in the SSP aligns with the DO depletion pattern observed in the sampler in 2021 and suggests that the sampler environment can become distinct from ambient stream conditions if deployed too long, potentially making biogeochemical measurements erroneous.

The total number of differentially abundant genera per sampling group, is displayed in Fig. 6. SSP samples had more unique identifying genera overall than did BSPs, except for July bed sediments, where the number was equally high. November bed samples also had a large portion of differentially expressed genera compared to other bed sediment groups, with the highest representation by *Geobacter* and *MND1*. July and November represented the warmest and coldest sampling periods, respectively, thus the high number of unique genera in bed sediments, as determined through LEfSe biomarker analysis, corresponds with the environmental extremes of the study. Similar results have been observed for riverine microbial communities (Feris et al. 2009; Butler et al. 2019; Sun et al. 2019), and also for macro bioindicators (Cuffney et al. 2010), where irregularities in physicochemical parameters correlate with unique sets of taxa. Here we show that the same trend occurred for benthic microbial assemblages. There also was an opposing trend where BSP samples had fewer biomarker taxa overall than SSPs, despite BSPs having higher average alpha diversity. Since alpha diversity metrics account for both species' evenness and abundance, it is hypothesized that a more uniform community would have less microbial outliers as detected by LEfSe. Future work that correlates diversity analyses with biomarker signatures in aquatic microbial assemblages should build on this observation.

3.4.3 Precipitation, Redox, and Microbial Effects on Phillips Tube Samplers

Additional diel measurements collected from the 2021 data loggers showed the significant impacts of high rainfall on both in-stream and in-sampler DO. In several instances, in-stream DO cycles were disrupted after these events, including events at the ends of weeks 1 and 2, and through week 5 and 6 (Fig. 2B). Identical results have been observed in low order streams where high flow events associated with rainfall cause diel DO trends to cease, with recovery taking several days (Utz et al. 2020). High flow events can disrupt in-stream metabolism via scouring of biofilms and increased turbidity than can

impede photosynthesis and respiration, and that is likely the cause of the stream DO anomalies identified in 2021. However, PT sampler DO concentrations showed temporary increases after these events, which may have been caused by an increased flux of oxygenated water that persisted in the tube for several days before oxygen was again gradually consumed. If similar patterns emerged after precipitation events recorded during the April-May interval of 2018, periodic reintroduction of oxygen could have caused a disturbance to in-sampler microbial communities, and lead to the lower diversity exhibited compared to the dryer June and July intervals. Events such as these are not necessarily a drawback to time-integrated sampling. Rather, they align with the original objective of the PT samplers which is to collect a time-average fine sediment load during high flow events, and disturbances to the collected microbial consortium may in fact prevent biological alteration of the constituents in-situ. This lends additional evidence that deployments of PT samplers during quiescent stream periods can confound physicochemical measurements, as conditions within the samplers can diverge from the in-stream environment.

The decreasing DO concentrations over time within the Phillips unit during the 2021 deployment provide confidence to previous results that suggest that conservative, non-redox sensitive geochemical variables, or a combination thereof, are best utilized in sediment fingerprinting studies (Smith and Owens 2014; Williamson et al. 2020). Therefore, robust methods that eliminate high variance geochemical variables in sediment source-tracking studies are encouraged (Walling et al. 2008), and the use of total elemental concentrations of metals, C, nutrients, etc. are more accurate than using dissolved/mobilized species. For example, initial calibration studies that utilized total C measurements showed good agreement between point suspended sediment grabs and accumulated sampler suspended sediment (Phillips et al. 2000), while subsequent work showed redox-sensitive species such as arsenic and selenium (Babechuk et al. 2009; Franzblau et al. 2014) to be less reliable tracers (Smith and Owens 2014).

3.5 Conclusions

This is the first study to apply a passive sediment sampling technique for the assessment of the microbiological component of fluvial systems. Samplers accumulated adequate sediment volumes for microbial DNA-metabarcoding surveys over the

deployment intervals (21 - 43 days) and showed no significant differences in alpha diversity or community composition between upstream and downstream sites. In future work, fewer replicate samplers than used in this study (n=7) would suffice for watercourse segments of similar lengths (≈ 0.7 km).

Suspended sediment microbial communities varied monthly and were more unique and less diverse than bed sediment communities. Biomarker analysis through LEfSe identified indicator taxa across sediment source and months and revealed microbial genera that were representative of geochemical niches in suspended vs. bed sediment compartments, as well as those indicative of seasonality. These observations can aid in sediment source tracking, particularly in differentiating between terrestrial-sourced vs. bed-scoured material. Further, incorporating microbial community analyses can serve as a sentinel of potential geochemical and/or redox shifts within samplers. Future studies may apply both DNA and RNA-based microbial techniques to compare the active vs. dead/dormant community members collected in the suspended particulate phase and assess temporal relationships between microbial function and in-stream processing of central nutrients such as C, N, and P.

A Phillips unit subsequently deployed with dissolved oxygen sensors in 2021 showed gradual depletion of in-situ DO to hypoxic conditions after three weeks, with precipitation pulses periodically reintroducing oxygen into the sampler for several days. This observation is valuable to future applications of these sampler types, as redox state is a principal driver of sediment biogeochemistry and contaminant mobility. It is proposed that similar events contributed to microbial community changes in the samplers in 2018, however additional paired measurements of DO, precipitation, and microbial communities within and between samplers is required to confirm this hypothesis due to the discrepancy in sampling years. Regardless, it is recommended that in the absence of further calibration trials under different flow conditions, deployment intervals not exceed three weeks, and that if intervals capture quiescent stream conditions, then in-situ biogeochemical measurements be interpreted with caution.

Acknowledgements

The authors would like to acknowledge Tom Reid, Lauren Goddard, Sara Butler, Chelsea Salter, Princess Vergara, Savannah Knorr, and Luke Mawhinney for aid in field and laboratory work, as well as Shelby Mackie in the GLIER Environmental Genomics Facility for library preparation and sequencing. This work was supported through a NSERC Strategic partners Grant (STP 521430-18).

FIGURES AND TABLES

Table 1
Big Creek Water Quality Parameters from grab samples and time-integrated suspended sediment samplers (\pm standard deviation).

	Grab Samples					Time-Integrated Passive Samples		
	TSS mg L ⁻¹	Temp °C	pH	DO mg L ⁻¹	ORP mV	Cond µS cm ⁻¹	TSS mg L ⁻¹	TSS Load g day ⁻¹
April	55.2 (6.8)	12.9 (0.45)	7 (0.06)	9.2 (0.62)	199.8 (3.3)	825.5 (3.5)	AM (1594.8)	1.9
May	146.1 (37.2)	19.3 (2.4)	6.8 (0.22)	8.7 (0.03)	192 (17.0)	539.4 (76.1)	MJ (3174.3)	0.57
June	23.7 (12.7)	12.6 (0.51)	7.2 (0.09)	8 (0.19)	86.3 (5.9)	864.2 (13.5)	JJ (108.8)	0.07
July	431.7 (139.8)	22.4 (0.31)	7.1 (0.25)	3.2 (1.6)	120.7 (65.3)	855.5 (29.7)		

TSS = Total Suspended Solids, DO = Dissolved Oxygen, ORP = Oxidation/Reduction Potential, Cond = Conductivity, AM = April-May, MJ = May-June, JJ = June-July.

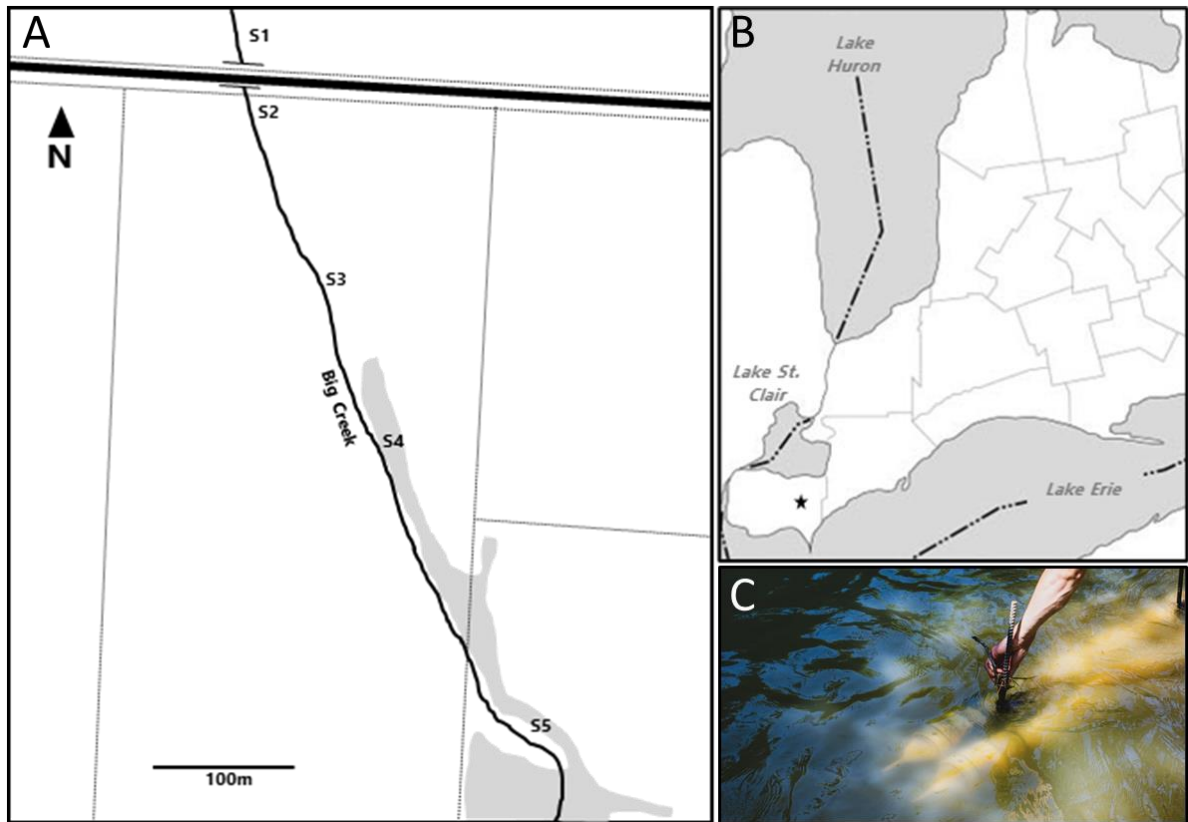


Figure 1: A) Big Creek subsite sampling locations, downstream (S1) to upstream (S5). B) Location of Big Creek in Essex County, Ontario, Canada. C) Replicate suspended sediment samplers being submerged at S1.

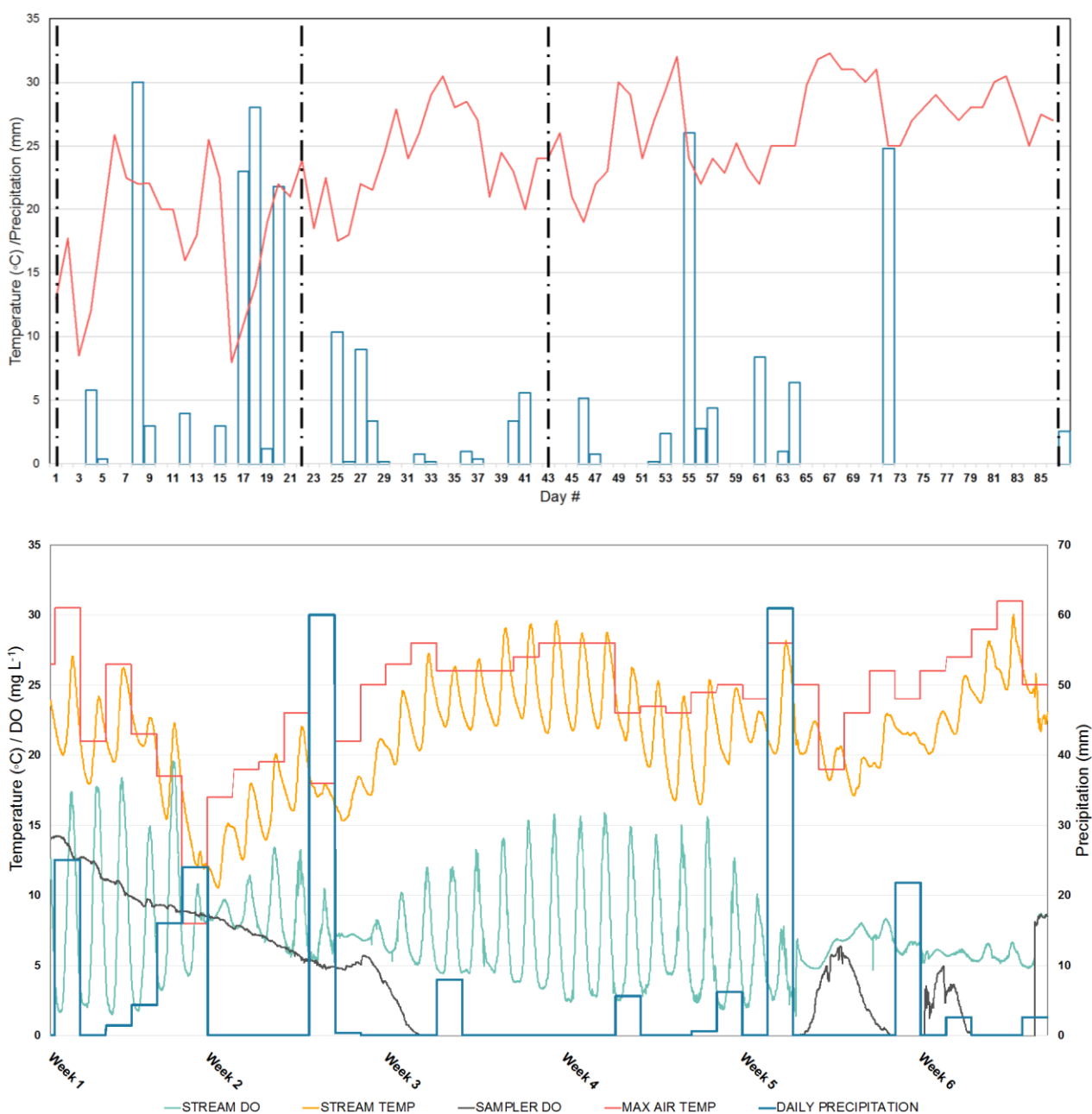


Figure 2: Big Creek physicochemical time series data. A) 2018 max daily air temperature (line) and precipitation (bars) during the 86-day sampling period from April to July. Sampling timepoints are denoted by dashed lines. B) 2021 deployment max daily air temperature, precipitation, and stream temperature and dissolved oxygen (DO) with Sampler DO. Recorded Sampler temperature was identical to Stream temperature.

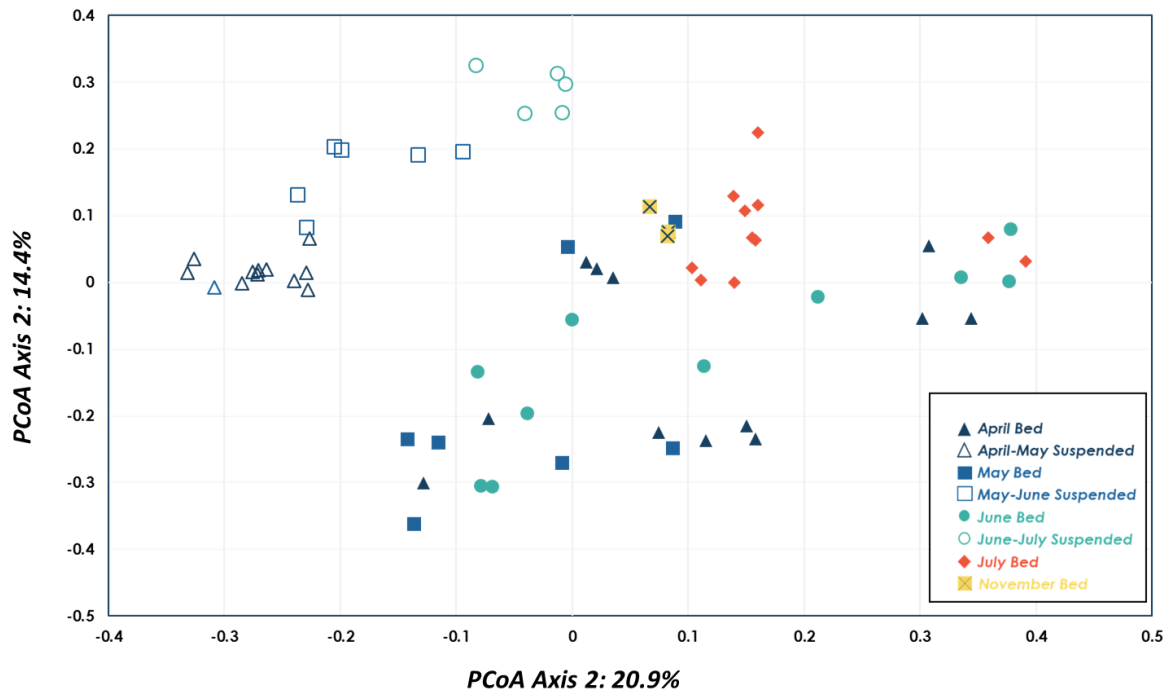


Figure 3: PCoA with Bray-Curtis distances of feature-level microbial community composition across samples. Labelled by Source and Month. Closed and open symbols represent bed and suspended phase microbial samples, respectively

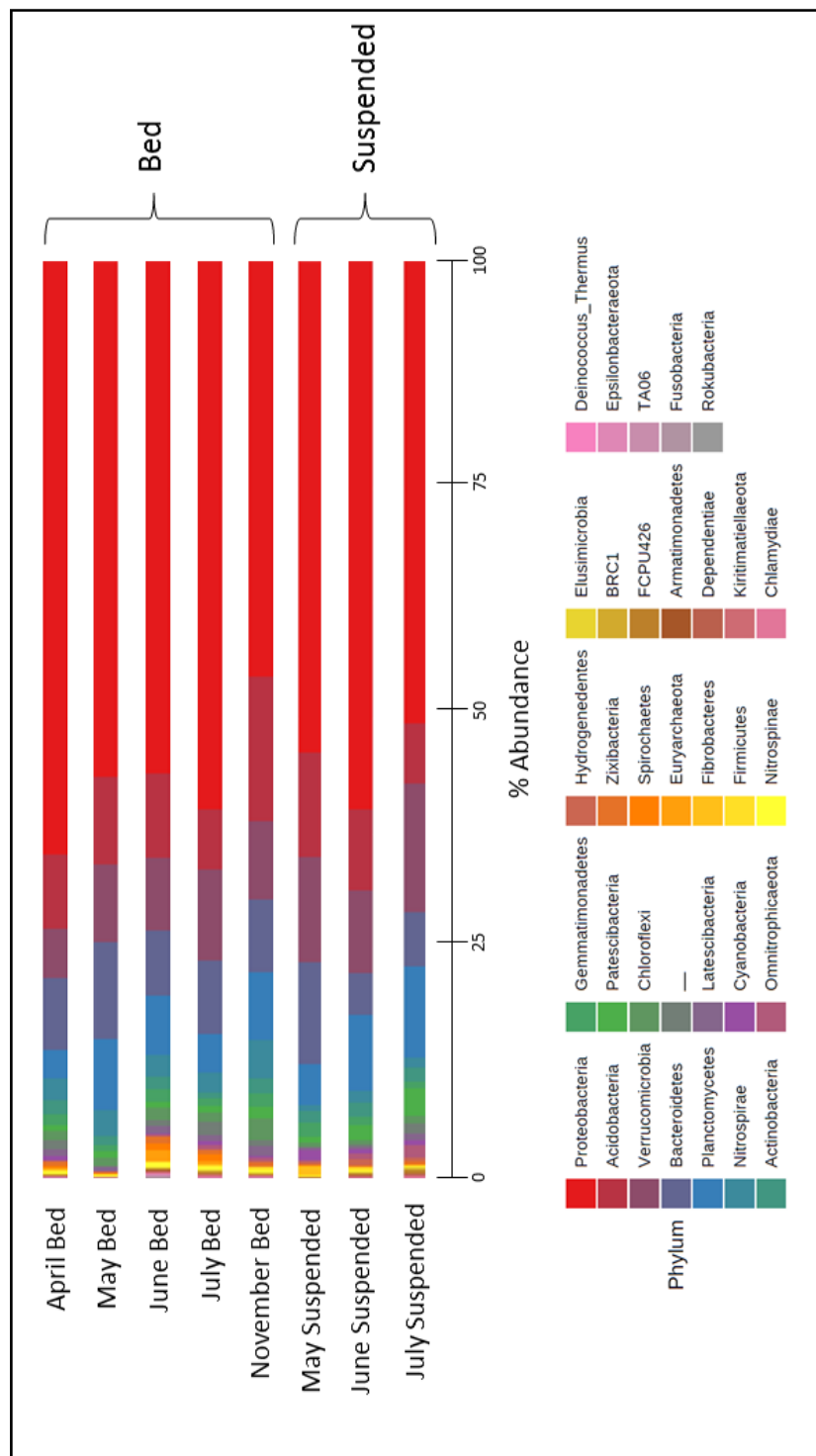


Figure 4: Microbial phylum distribution across months and sediment source displayed as % abundance.

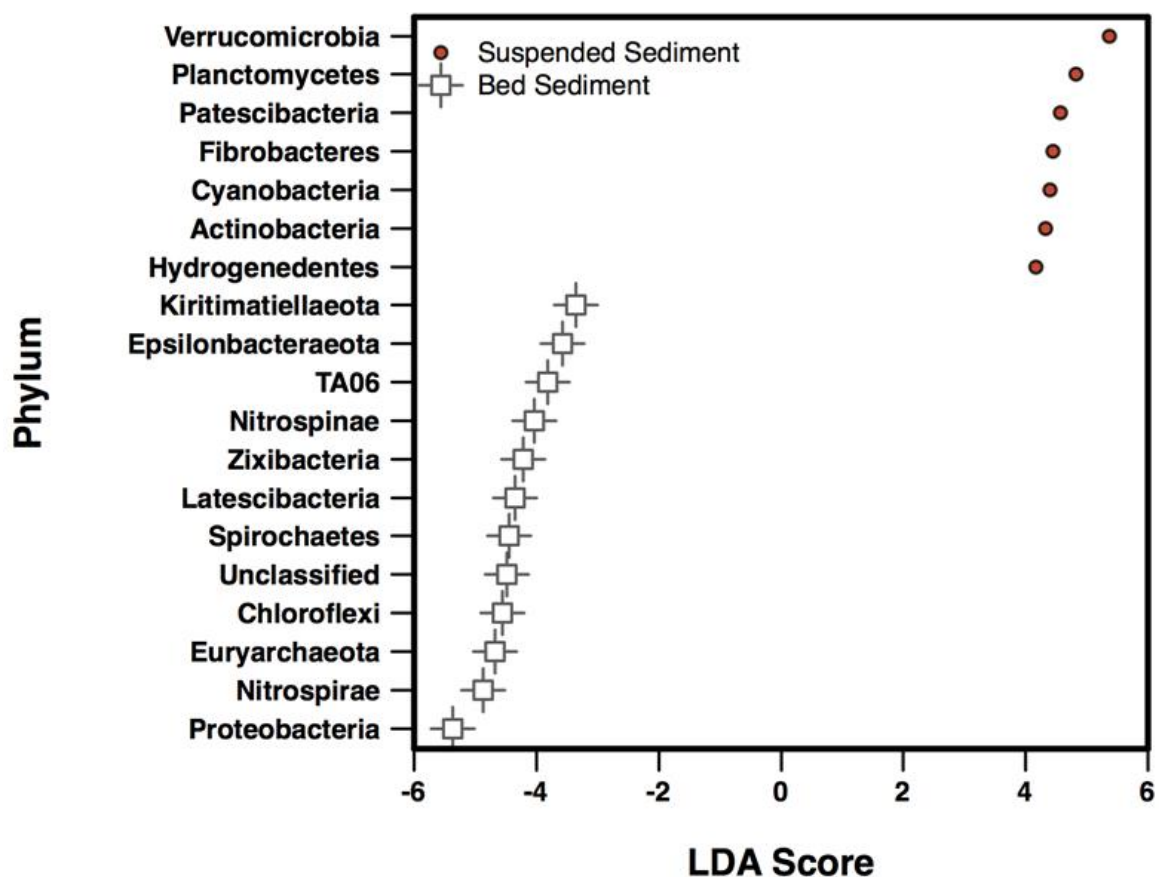


Figure 5: LEfSe biomarker analysis identifying significantly different phyla between suspended and bed sediments over all sampling timepoints. A default log linear discriminant analysis (LDA) score of ± 2 was used as the default cut-off for differential expression with a false detection rate-adjusted p-value cut-off of 0.05. Suspended and bed sediment phyla are arbitrarily designated with positive (+) and negative (-) LDA scores, respectively.

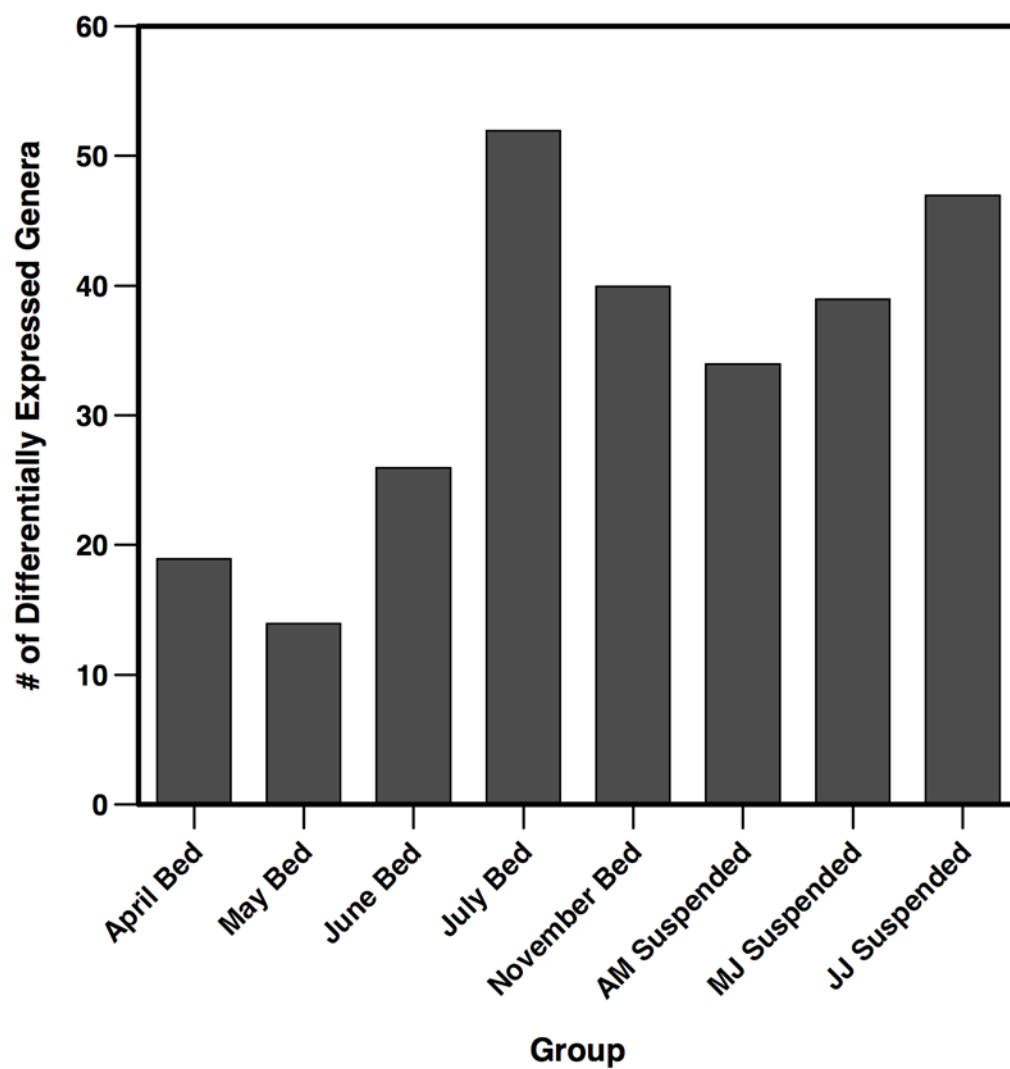


Figure 6: Distribution of the number of differentially expressed genera (n=271) across months and sediment source as determined through LEfSe. AM = April-May, MJ = May-June, JJ = June-July.

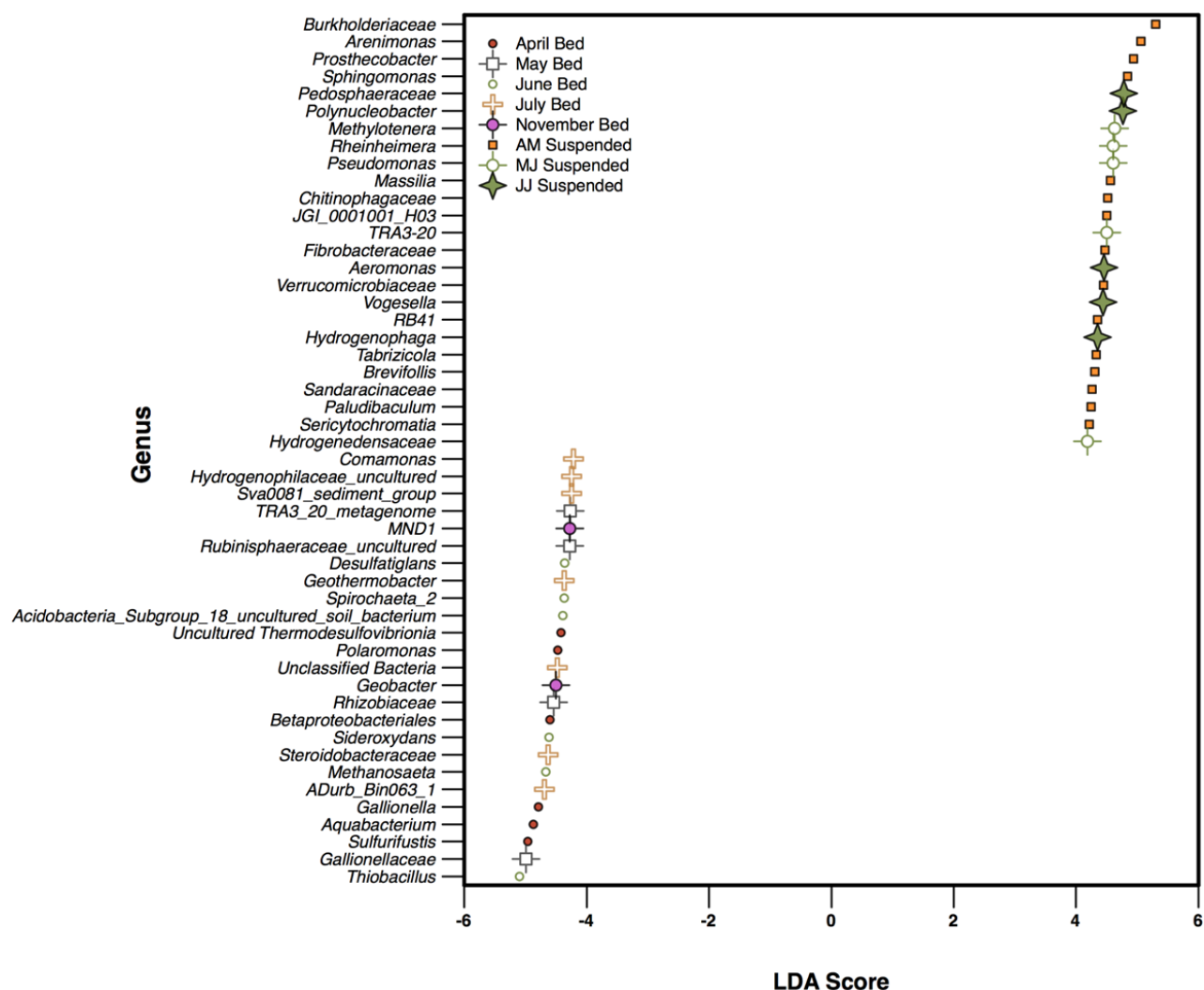


Figure 7: LEfSe biomarker analysis identifying the top 50 significantly different genera between sediment source and month. A default log linear discriminant analysis (LDA) score of ± 2 was used as the default cut-off for differential expression with a false detection rate-adjusted p-value cut-off of 0.05. Suspended and bed sediment phyla are arbitrarily designated with positive (+) and negative (-) LDA scores, respectively. AM = April-May, MJ = May-June, JJ = June-July

References

- Babechuk, M.G., Weisener, C.G., Fryer, B.J., Paktunc, D., Maunders, C., 2009. Microbial reduction of ferrous arsenate: Biogeochemical implications for arsenic mobilization. *Appl. Geochemistry* 24, 2332–2341. <https://doi.org/10.1016/j.apgeochem.2009.09.006>
- Ballantine, D.J., Walling, D.E., Collins, A.L., Leeks, G.J.L., 2008. The phosphorus content of fluvial suspended sediment in three lowland groundwater-dominated catchments. *J. Hydrol.* 357, 140–151. <https://doi.org/10.1016/j.jhydrol.2008.05.011>
- Bokulich, N.A., Kaehler, B.D., Rideout, J.R., Dillon, M., Bolyen, E., Knight, R., Huttley, G.A., Gregory Caporaso, J., 2018. Optimizing taxonomic classification of marker-gene amplicon sequences with QIIME 2's q2-feature-classifier plugin. *Microbiome* 6, 1–17. <https://doi.org/10.1186/s40168-018-0470-z>
- Bradford, S.A., Morales, V.L., Zhang, W., Harvey, R.W., Packman, A.I., Mohanram, A., Welty, C., 2013. Transport and Fate of Microbial Pathogens in Agricultural Settings. *Crit. Rev. Environ. Sci. Technol.* 43, 775–893. <https://doi.org/10.1080/10643389.2012.710449>
- Butler, T.M., Wilhelm, A.C., Dwyer, A.C., Webb, P.N., Baldwin, A.L., Techtmann, S.M., 2019. Microbial Community Dynamics During Lake Ice Freezing. *Sci. Rep.* 9, 1–11. <https://doi.org/10.1038/s41598-019-42609-9>
- Caillon, F., Besemer, K., Peduzzi, P., Schelker, J., 2021. Soil microbial inoculation during flood events shapes headwater stream microbial communities and diversity. *Microb. Ecol.* 82, 591–601. <https://doi.org/10.1007/s00248-021-01700-3>
- Callahan, B.J., McMurdie, P.J., Rosen, M.J., Han, A.W., Johnson, A.J.A., Holmes, S.P., 2016. DADA2: High-resolution sample inference from Illumina amplicon data. *Nat. Methods* 13, 581–583. <https://doi.org/10.1038/nmeth.3869>
- Chen, W., Wilkes, G., Khan, I.U.H., Pintar, K.D.M., Thomas, J.L., Lévesque, C.A., Chapados, J.T., Topp, E., Lapen, D.R., 2018. Aquatic bacterial communities

- associated with land use and environmental factors in agricultural landscapes using a metabarcoding approach. *Front. Microbiol.* 9, 2301.
<https://doi.org/10.3389/fmicb.2018.02301>
- Chong, J., Liu, P., Zhou, G., Xia, J., 2020. Using MicrobiomeAnalyst for comprehensive statistical, functional, and meta-analysis of microbiome data. *Nat. Protoc.* 15, 799–821. <https://doi.org/10.1038/s41596-019-0264-1>
- Clinton, S., Johnson, J., Lambirth, K., Sun, S., Brouwer, C., Keen, O., Redmond, M., Fodor, A., Gibas, C., 2020. Sediment microbial diversity in urban piedmont North Carolina watersheds receiving wastewater input. *Water (Switzerland)* 12, 1557.
<https://doi.org/10.3390/W12061557>
- Collins, A.L., Zhang, Y., Walling, D.E., Grenfell, S.E., Smith, P., 2010. Tracing sediment loss from eroding farm tracks using a geochemical fingerprinting procedure combining local and genetic algorithm optimisation. *Sci. Total Environ.* 408, 5461–5471. <https://doi.org/10.1016/j.scitotenv.2010.07.066>
- Cooper, R.E., Stefan, C.W., Poulin, R.X., Ueberschaar, N., Wurlitzer, J.D., Stettin, D., Wichard, T., Pohnert, G., Küsel, K., 2020. Iron is not everything : unexpected complex metabolic responses between iron-cycling microorganisms. *ISME J.* 14, 2675–2690. <https://doi.org/10.1038/s41396-020-0718-z>
- Cuffney, T.F., Brightbill, R.A., May, J.T., Waite, I.R., 2010. Responses of benthic macroinvertebrates to environmental changes associated with urbanization in nine metropolitan areas. *Ecol. Appl.* 20, 1384–1401. <https://doi.org/10.1890/08-1311.1>
- Custodio, M., Espinoza, C., Peñaloza, R., Peralta-Ortiz, T., Sánchez-Suárez, H., Ordinola-Zapata, A., Vieyra-Peña, E., 2022. Microbial diversity in intensively farmed lake sediment contaminated by heavy metals and identification of microbial taxa bioindicators of environmental quality. *Sci. Rep.* 12, 1–12.
<https://doi.org/10.1038/s41598-021-03949-7>
- Deng, Z.Q., Singh, V.P., 2002. Optimum channel pattern for environmentally sound training and management of alluvial rivers. *Ecol. Modell.* 154, 61–74.

[https://doi.org/10.1016/S0304-3800\(02\)00053-4](https://doi.org/10.1016/S0304-3800(02)00053-4)

Dhariwal, A., Chong, J., Habib, S., King, I.L., Agellon, L.B., Xia, J., 2017.

MicrobiomeAnalyst: A web-based tool for comprehensive statistical, visual and meta-analysis of microbiome data. *Nucleic Acids Res.* 45, W180–W188.

<https://doi.org/10.1093/nar/gkx295>

Ding, S., Chen, M., Gong, M., Fan, X., Qin, B., Xu, H., Gao, S.S., Jin, Z., Tsang,

D.C.W., Zhang, C., 2018. Internal phosphorus loading from sediments causes seasonal nitrogen limitation for harmful algal blooms. *Sci. Total Environ.* 625, 872–884. <https://doi.org/10.1016/j.scitotenv.2017.12.348>

Droppo, I.G., D'Andrea, L., Krishnappan, B.G., Jaskot, C., Trapp, B., Basuvaraj, M.,

Liss, S.N., 2015. Fine-sediment dynamics: towards an improved understanding of sediment erosion and transport. *J. Soils Sediments* 15, 467–479.

<https://doi.org/10.1007/s11368-014-1004-3>

Faith, D.P., 1991. Conservation evaluation and phylogenetic diversity. *Biol. Conserv.* 61, 1–10. [https://doi.org/10.1016/0003-2697\(75\)90168-2](https://doi.org/10.1016/0003-2697(75)90168-2)

Falk, N., Chaganti, S.R., Weisener, C.G., 2018. Evaluating the microbial community and gene regulation involved in crystallization kinetics of ZnS formation in reduced environments. *Geochim. Cosmochim. Acta* 220, 201–216.

<https://doi.org/10.1016/j.gca.2017.09.039>

Falk, N., Day, M., Weisener, C.G., 2021. Evaluating Sediment Phosphorus Exchange in Rural Ontario Headwaters by Paired Sequential Extraction and Sorption Isotherms. *Water, Air, Soil Pollut.* 232, 1–14. <https://doi.org/10.1007/s11270-021-05381-z>

Falk, N., Reid, T., Skoyles, A., Grgicak-Mannion, A., Drouillard, K., Weisener, C.G., 2019. Microbial metatranscriptomic investigations across contaminant gradients of the Detroit River. *Sci. Total Environ.* 690, 121–131.

<https://doi.org/10.1016/j.scitotenv.2019.06.451>

Fasching, C., Akotoye, C., Bižić, M., Fonvielle, J., Ionescu, D., Mathavarajah, S.,

- Zoccarato, L., Walsh, D.A., Grossart, H.P., Xenopoulos, M.A., 2020. Linking stream microbial community functional genes to dissolved organic matter and inorganic nutrients. *Limnol. Oceanogr.* 65, S71–S87.
<https://doi.org/10.1002/lno.11356>
- Feris, K.P., Ramsey, P.W., Gibbons, S.M., Frazar, C., Rillig, M.C., Moore, J.N., Gannon, J.E., Holben, W.E., 2009. Hyporheic microbial community development is a sensitive indicator of metal contamination. *Environ. Sci. Technol.* 43, 6158–6163.
<https://doi.org/10.1021/es9005465>
- Franzblau, R.E., Loick, N., Weisener, C.G., 2014. Investigating the effects of Se solid phase substitution in jarosite minerals influenced by bacterial reductive dissolution. *Minerals* 4, 17–36. <https://doi.org/10.3390/min4010017>
- Gadd, G.M., 2010. Metals, minerals and microbes: Geomicrobiology and bioremediation. *Microbiology* 156, 609–643. <https://doi.org/10.1099/mic.0.037143-0>
- Ghosal, D., Ghosh, S., Dutta, T.K., Ahn, Y., 2016. Current state of knowledge in microbial degradation of polycyclic aromatic hydrocarbons (PAHs): A review. *Front. Microbiol.* 1369. <https://doi.org/10.3389/fmicb.2016.01369>
- Gibbons, S.M., Jones, E., Bearquiver, A., Blackwolf, F., Roundstone, W., Scott, N., Hooker, J., Madsen, R., Coleman, M.L., Gilbert, J.A., 2014. Human and environmental impacts on river sediment microbial communities. *PLoS One* 9, 1–9.
<https://doi.org/10.1371/journal.pone.0097435>
- Hiibel, S.R., Pereyra, L.P., Breazeal, M.V.R., Reisman, D.J., Reardon, K.F., Pruden, A., 2011. Effect of Organic Substrate on the Microbial Community Structure in Pilot-Scale Sulfate-Reducing Biochemical Reactors Treating Mine Drainage. *Environ. Eng. Sci.* 28, 563–572. <https://doi.org/10.1089/ees.2010.0237>
- Huang, S., Chen, C., Jaffé, P.R., 2018. Seasonal distribution of nitrifiers and denitrifiers in urban river sediments affected by agricultural activities. *Sci. Total Environ.* 642, 1282–1291. <https://doi.org/10.1016/j.scitotenv.2018.06.116>

- Jewell, T.N.M., Karaoz, U., Brodie, E.L., Williams, K.H., Beller, H.R., 2016. Metatranscriptomic evidence of pervasive and diverse chemolithoautotrophy relevant to C , S , N and Fe cycling in a shallow alluvial aquifer. *ISME J.* 10, 2106–2117. <https://doi.org/10.1038/ismej.2016.25>
- Jin, R., Yang, G., Zhang, Q., Ma, C., Yu, J., Xing, B., 2012. The effect of sulfide inhibition on the ANAMMOX process. *Water Res.* 47, 1459–1469. <https://doi.org/10.1016/j.watres.2012.12.018>
- Jochum, L.M., Schreiber, L., Marshall, I.P.G., Jørgensen, B.B., Schramm, A., Kjeldsen, K.U., 2018. Single-cell genomics reveals a diverse metabolic potential of uncultivated *Desulfatiglans*-related deltaproteobacteria widely distributed in marine sediment. *Front. Microbiol.* 9, 1–16. <https://doi.org/10.3389/fmicb.2018.02038>
- Katoh, K., Misawa, K., Kuma, K.I., Miyata, T., 2002. MAFFT: A novel method for rapid multiple sequence alignment based on fast Fourier transform. *Nucleic Acids Res.* 30, 3059–3066. <https://doi.org/10.1093/nar/gkf436>
- Krein, A., Petticrew, E., Udelhoven, T., 2003. The use of fine sediment fractal dimensions and colour to determine sediment sources in a small watershed. *Catena* 53, 165–179. [https://doi.org/10.1016/S0341-8162\(03\)00021-3](https://doi.org/10.1016/S0341-8162(03)00021-3)
- Laperriere, S.M., Hilderbrand, R.H., Keller, S.R., Trott, R., Santoro, A.E., 2020. Headwater stream microbial diversity and function across agricultural and urban land use gradients. *Appl. Environ. Microbiol.* 86, 1–17. <https://doi.org/10.1128/AEM.00018-20>
- Liao, H., Yen, J.Y., Guan, Y., Ke, D., Liu, C., 2020. Differential responses of stream water and bed sediment microbial communities to watershed degradation. *Environ. Int.* 134, 105198. <https://doi.org/10.1016/j.envint.2019.105198>
- Lozupone, C., Knight, R., 2005. UniFrac: A new phylogenetic method for comparing microbial communities. *Appl. Environ. Microbiol.* 71, 8228–8235. <https://doi.org/10.1128/AEM.71.12.8228-8235.2005>

- Lozupone, C.A., Hamady, M., Kelley, S.T., Knight, R., 2007. Quantitative and qualitative β diversity measures lead to different insights into factors that structure microbial communities. *Appl. Environ. Microbiol.* 73, 1576–1585.
<https://doi.org/10.1128/AEM.01996-06>
- Lv, P., Luo, J., Zhuang, X., Zhang, D., Huang, Z., Bai, Z., 2017. Diversity of culturable aerobic denitrifying bacteria in the sediment, water and biofilms in Liangshui River of Beijing, China. *Sci. Rep.* 7, 1–12. <https://doi.org/10.1038/s41598-017-09556-9>
- Mohiuddin, M.M., Botts, S.R., Paschos, A., Schellhorn, H.E., 2019. Temporal and spatial changes in bacterial diversity in mixed use watersheds of the Great Lakes region. *J. Great Lakes Res.* 45, 109–118. <https://doi.org/10.1016/j.jglr.2018.10.007>
- Owens, P.N., Blake, W.H., Giles, T.R., Williams, N.D., 2012. Determining the effects of wildfire on sediment sources using ^{137}Cs and unsupported ^{210}Pb : The role of landscape disturbances and driving forces. *J. Soils Sediments* 12, 982–994.
<https://doi.org/10.1007/s11368-012-0497-x>
- Pandey, P., Soupir, M.L., Wang, Y., Cao, W., Biswas, S., Vaddella, V., Atwill, R., Merwade, V., Pasternack, G., 2018. Water and Sediment Microbial Quality of Mountain and Agricultural Streams. *J. Environ. Qual.* 47, 985–996.
<https://doi.org/10.2134/jeq2017.12.0483>
- Peura, S., Sinclair, L., Bertilsson, S., Eiler, A., 2015. Metagenomic insights into strategies of aerobic and anaerobic carbon and nitrogen transformation in boreal lakes. *Sci. Rep.* 5, 1–6. <https://doi.org/10.1038/srep12102>
- Phillips, J.M., Russell, M.A., Walling, D.E., 2000. Time-integrated sampling of fluvial suspended sediment: A simple methodology for small catchments. *Hydrol. Process.* 14, 2589–2602. [https://doi.org/10.1002/1099-1085\(20001015\)14:14<2589::AID-HYP94>3.0.CO;2-D](https://doi.org/10.1002/1099-1085(20001015)14:14<2589::AID-HYP94>3.0.CO;2-D)
- Plach, J.M., Elliott, A.V.C., Droppo, I.G., Warren, L.A., 2011. Physical and ecological controls on freshwater floc trace metal dynamics. *Environ. Sci. Technol.* 45, 2157–2164. <https://doi.org/10.1021/es1031745>

- Price, M.N., Dehal, P.S., Arkin, A.P., 2010. FastTree 2 - Approximately maximum-likelihood trees for large alignments. *PLoS One* 5, e9490.
<https://doi.org/10.1371/journal.pone.0009490>
- Quast, C., Pruesse, E., Yilmaz, P., Gerken, J., Schweer, T., Yarza, P., Peplies, J., Glöckner, F.O., 2013. The SILVA ribosomal RNA gene database project: Improved data processing and web-based tools. *Nucleic Acids Res.* 41, 590–596.
<https://doi.org/10.1093/nar/gks1219>
- Rahutomo, S., Kovar, J.L., Id, M.L.T., 2018. Varying redox potential affects P release from stream bank sediments 13, e0209208.
<https://doi.org/10.1371/journal.pone.0209208>
- Reid, T., Droppo, I.G., Weisener, C.G., 2020. Tracking functional bacterial biomarkers in response to a gradient of contaminant exposure within a river continuum. *Water Res.* 168, 115167. <https://doi.org/10.1016/j.watres.2019.115167>
- Segata, N., Izard, J., Waldron, L., Gevers, D., Miropolsky, L., Garrett, W.S., Huttenhower, C., 2011. Metagenomic biomarker discovery and explanation. *Genome Biol.* 12, 1–18. <https://doi.org/10.1186/gb-2011-12-6-r60>
- Smith, T.B., Owens, P.N., 2014. Flume- and field-based evaluation of a time-integrated suspended sediment sampler for the analysis of sediment properties. *Earth Surf. Process. Landforms* 39, 1197–1207. <https://doi.org/10.1002/esp.3528>
- Staley, C., Gould, T.J., Wang, P., Phillips, J., Cotner, J.B., Sadowsky, M.J., 2015. Species sorting and seasonal dynamics primarily shape bacterial communities in the Upper Mississippi River. *Sci. Total Environ.* 505, 435–445.
<https://doi.org/10.1016/j.scitotenv.2014.10.012>
- Sun, X., Li, B., Han, F., Xiao, E., Xiao, T., Sun, W., 2019. Impacts of Arsenic and Antimony Co-Contamination on Sedimentary Microbial Communities in Rivers with Different Pollution Gradients. *Microb. Ecol.* 78, 589–602.
<https://doi.org/10.1007/s00248-019-01327-5>

- Umezawa, K., Watanabe, T., Miura, A., Kojima, H., Fukui, M., 2016. The complete genome sequences of sulfur-oxidizing Gammaproteobacteria *Sulfurifustis variabilis* skN76T and *Sulfuricaulis limicola* HA5T. *Stand. Genomic Sci.* 11, 1–8.
<https://doi.org/10.1186/s40793-016-0196-0>
- Utz, R.M., Bookout, B.J., Kaushal, S.S., 2020. Influence of temperature, precipitation, and cloud cover on diel dissolved oxygen ranges among headwater streams with variable watershed size and land use attributes. *Aquat. Sci.* 82, 1–16.
<https://doi.org/10.1007/s00027-020-00756-6>
- VanMensel, D., Chaganti, S.R., Droppo, I.G., Weisener, C.G., 2020. Exploring bacterial pathogen community dynamics in freshwater beach sediments: A tale of two lakes. *Environ. Microbiol.* 22, 568–583. <https://doi.org/10.1111/1462-2920.14860>
- Walling, D.E., Collins, A.L., Stroud, R.W., 2008. Tracing suspended sediment and particulate phosphorus sources in catchments. *J. Hydrol.* 350, 274–289.
<https://doi.org/10.1016/j.jhydrol.2007.10.047>
- Wilhelm, S.W., Lecleir, G.R., Bullerjahn, G.S., McKay, R.M., Saxton, M.A., Twiss, M.R., Bourbonniere, R.A., 2014. Seasonal changes in microbial community structure and activity imply winter production is linked to summer hypoxia in a large lake. *FEMS Microbiol. Ecol.* 87, 475–485. <https://doi.org/10.1111/1574-6941.12238>
- Williamson, T.N., Dobrowolski, E.G., Gellis, A.C., Sabitov, T., Gorman Sanisaca, L., 2020. Monthly suspended-sediment apportionment for a western Lake Erie agricultural tributary. *J. Great Lakes Res.* 46, 1307–1320.
<https://doi.org/10.1016/j.jglr.2020.06.011>
- Zeglin, L.H., 2015. Stream microbial diversity in response to environmental changes: review and synthesis of existing research. *Front. Microbiol.* 6, 454.
<https://doi.org/10.3389/fmicb.2015.00454>
- Zhang, W., Wang, H., Li, Y., Lin, L., Hui, C., Gao, Y., Niu, L., Zhang, H., Wang, L., Wang, P., Wang, C., 2020. Bend-induced sediment redistribution regulates

deterministic processes and stimulates microbial nitrogen removal in coarse sediment regions of river. *Water Res.* 170, 115315.
<https://doi.org/10.1016/j.watres.2019.115315>

CHAPTER 4: BIOGEOCHEMICAL MECHANISMS ASSOCIATED WITH IN-SITU SEDIMENT P RELEASE IN SOUTHERN ONTARIO HEADWATERS

4.1 Introduction

Freshwater environments worldwide are frequently impaired by non-point pollution of agricultural phosphorus (P) (Withers et al. 2014). Watersheds of the Great Lakes' Huron-Erie Corridor (HEC) are no exception, with nutrient loadings often correlating with the number and extent of cyanobacterial blooms and water column anoxia in both Lake Erie and Lake St. Clair (Michalak et al. 2013; Kane et al. 2014; Winter et al. 2015). Recent loading estimates suggest that the St. Clair and Thames Rivers of southern Ontario are the two largest sources of P loads to Lake St. Clair, representing 71.5% and 12.1% of the total average annual load (Bocaniov et al. 2019), and that the Detroit River, the outlet for Lake St. Clair, transports 41% and 31% of the total P (TP) and dissolved reactive P (DRP), respectively, to Lake Erie; the shallowest and most eutrophic of the Great Lakes. However, nutrient retention and transport in smaller, headwater tributaries of the HEC are less understood. Focused studies within these upstream watershed regions can help understand the initial fate of non-point P and improve understanding of nutrient sinks and sources early in the river continuum (Zhang et al. 2019).

To date, models have shown that a large proportion of P is retained within Great Lake headwater regions, as tributary loads entering the lower Great Lakes are often less than total estimated terrestrial P exports (Van Staden et al. 2021). Thus, these networks of lower order streams in agriculturally dense regions can serve as vital sinks of nutrients. Bed sediments are the primary interface for matter exchange to the water column of lotic systems and are particularly important in nutrient equilibrium due to diffusion and adsorption to and from aquatic plants, microbial biofilms, and the sediment matrix. Suspended sediment, composed of a complex mixture of particle flocs, organic material, and microorganisms, is also known to adhere and transport particulate P (PP), which can be derived from bed and/or rivers banks and soils (Richards et al. 2008). Fine grained suspended sediment (particle size $<63\ \mu\text{m}$) is especially poised to adsorb DRP due to its high specific area and cohesiveness. Yet studies that seek to account for headwater nutrient loads are often focused on soil erosion and edge of field P mechanisms (Zhang et al. 2020; Macrae et al. 2021; Shrestha et al. 2021) and less on the in-stream interactions with bed and suspended sediments (Stutter et al. 2021). It is thus unclear whether headwater sediments represent semi-permanent P sinks or increasingly vulnerable sources, and how

nutrient legacies, Nitrogen (N) cycling, and microbial communities interact with these reservoirs.

Legacy agriculture can serve to prime bed and suspended sediments with P, diminishing their buffering ability over time (Chen et al. 2018). Non-point Nitrogen in headwaters can also affect the fate of P, as both are primary macro nutrients for aquatic biota and have a tightly linked stoichiometry (Dodds and Smith 2016). Communities of sediment-bound microorganisms have a profound effect on N and P cycling in lotic systems as well, as sediment and water column redox is influenced by microbial metabolism which can alter the chemical speciation of nutrients. For example, microbes are responsible for the conversion of inert dinitrogen (N_2) to bioavailable forms (NH_3 , NO_3) and can indirectly influence the release of immobile sediment P by reduction of metal-oxide mineral phases (Wang et al. 2022). Thus, the spatial and temporal interactions of these variables must be quantified for a better understanding of P fate in headwaters.

To address these research gaps a study within three southern Ontario headwater segments was performed through the spring/summer of 2018 – 2020. Two agriculturally impacted sites (one influenced by inorganic/chemical fertilizer, and one influenced by organic/manure amendment) and one forested control site were compared and contrasted for sediment P-buffering capacity, legacy nutrient loads, sediment redox, N speciation, and sediment microbial community composition. It was hypothesized that site sediments would act primarily as P-sinks, and that the reference forested site would have the greatest P-buffering capacity. It was further hypothesized that the agricultural sites would have more similar microbial communities than the forested site, and that they would comprise more N-metabolizing taxa indicative of non-point fertilizer impacts. Further, we tested the assumption that the agricultural watercourse segments sites could be more prone to redox-driven P release by assessing vertical sediment redox profiles and in-stream physico-chemical variables (i.e. dissolved oxygen (DO), temperature). By assessing a multitude of variables over time in differently impacted headwater segments, we seek a better understanding of sediment P-buffering and the biogeochemical factors that can contribute to P storage/release in Great Lakes headwaters.

4.2 Methods

4.2.1 Site Selection and Watershed Characteristics

Three watercourses that drain into the HEC in southern Ontario were sampled in 2018-2020; Big Creek (BC) located in Essex County, Nissouri Creek (NC) located in Oxford County (both tributaries of the Thames River), and the Saugeen River (SR) located in Grey County (outlets to Lake Huron) (Fig S3). The BC watershed is flat (average slope $\sim 0.4 \text{ m km}^{-1}$) characterized by clay loam soils (Brookston Clay) and is dominated by crops of soybean, wheat, and corn, with low livestock density. The NC watershed has higher slopes ($\sim 0.9 \text{ m km}^{-1}$) characterized by loam/silt loam soils (Guelph Loam) and is dominated by pasture, corn, soybean, wheat, and hay, with a higher density of beef, dairy, and swine livestock operations. Both BC and NC have been incorporated into past and ongoing non-point source nutrient monitoring initiatives and are considered to be representative of the prevailing watershed agricultural practices (Falk et al. 2021; Nelligan et al. 2021). SR represents a more natural baseline watercourse devoid of direct agricultural influences, with higher average slopes in the drainage basin ($\sim 7 \text{ m km}^{-1}$), characterized by sandy, well-drained loam soils (Sargent Loam, Harriston Loam, Pike Lake Loam) with a higher percentage of watershed forested land (35%) than BC and NC (<10%). General climate and drainage basin data, and additional watercourse characteristics can be found in Table S1.

4.2.2 Point Sampling of Bed Sediment and Surface Water

Point sampling was performed at BC only in 2018, and for all three sites in 2019 and 2020. As sampling dates were not identical across sites, timepoints were classified as early spring (ESP), mid spring (MSP), early summer (ES), mid summer (MS), late summer (LS), or fall (F). Timepoints were selected when preceding weekly precipitation was low to capture conditions of baseflow. In this way, the effects of external nutrient loading from the surrounding catchment could be minimized and observations could be based on in-stream processes. At each point sampling, surface water was collected from the middle of the watercourse roughly 20% below the surface in high-density polyethylene (HDPE) bottles in triplicate, with bottles being rinsed thoroughly in the same waterbody beforehand and with no head space to limit oxygen diffusion. General water quality parameters were measured using a YSI EXO2 Multiparameter Water Quality Sonde. Bed sediment samples

were collected using a shallow hand corer or trowel from the upper 1–5 cm layer of sediment and stored in 200 mL polyethylene containers. Both water and bed sediment samples were stored on ice until the end of the sampling day, after which they were stored at $-4\text{ }^{\circ}\text{C}$ or at $-20\text{ }^{\circ}\text{C}$ if analyses were not performed within several days.

4.2.3 Suspended Sediment Collection

To collect an adequate volume of suspended sediment for particulate phosphorus measurements, sediment traps were placed at sites in 2019 and 2020 at the first point sampling and were retrieved, emptied, and replaced after every ensuing sampling. Phillips Tube (PT) samplers were used, which consist of hollow poly-vinyl chloride (PVC) tubes approx. 1 m in length sealed with a threaded conical head and flat end plug with 4 mm diameter openings for fluid flow-through. The design allows for collection of fine suspended sediment ($< 63\text{ }\mu\text{m}$) from the water column in larger quantities than possible from point grab samples (Phillips et al. 2000). At Big Creek and Nissouri Creek, PT samplers were first deployed in mid spring and collected at each subsequent point sampling, thus representative suspended sediment was collected during the intervals mid spring-early summer (MSP-ES), early summer-mid summer (ES-MS), mid summer-late summer (MS-LS), and mid summer-fall (MS-LF). For SR, the mid spring (MSP) sampling timepoint was not performed in 2019. PT samplers were secured above the watercourse bed as described by Falk et al., with the accumulated water-sediment slurry collected at each point sampling in 20-gallon buckets, and the samplers cleaned and returned to their position in the watercourse after collection (Falk et al. 2022). PT sampler water-sediment slurries were subsampled and preserved in the same fashion as surface water.

4.2.4 Physico-Chemical Analyses of Water and Sediment

4.2.4.1 Select Water Chemistry

All water and PT sampler samples were measured for total suspended solids (TSS) and for bioavailable P as soluble reactive phosphorus (SRP). TSS (mg L^{-1}) was calculated by filtration of a recorded volume of water through pre-weighed $0.45\text{ }\mu\text{m}$ cellulose acetate filters and massing of filters after drying for 24 hrs. SRP was measured, after filtration, on a SmartChem 170 Direct Read Discrete Analyzer via the phosphomolybdenum blue method, using ammonium molybdate, potassium antimony titrate as a catalyst, and ascorbic acid as the reducing agent. TP and TN were measured by colorimetry after

digestion in sulphuric acid and potassium persulphate (Method ref. no. E3116), with analyses performed at the Ontario Ministry of the Environment, Conservation and Parks (OMEC) Laboratory Services Branch. Additional analytical methods for select metals, anions, and residue/turbidity can be found in (Chow et al., 2009).

4.2.4.2 Sediment Phosphorus Equilibrium

Estimates of sediment buffering capacity were done by the Zero Equilibrium Phosphorus Concentration (EPC₀) assay following the sorption isotherm method (Falk et al. 2021). In brief, individual 5 grams sub-samples of bed sediment were spiked with increasing initial concentrations of SRP (SRP_{ini}) (4, 15, 30, 70, 150, 500, 2000 µg L⁻¹) with a 0.0005 M CaCl₂ background solution (total volume of 40 mL) and placed on an orbital shaker for 24 h. Treatments were then centrifuged (2500 × g, 15 min) and the supernatant removed, filtered, and measured for the final SRP concentration (SRP_{fin}). The amount of P-sorbed per gram of sediment for each spike was calculated as:

$$1) P_{\text{sorb}} (\mu\text{g g}^{-1}) = \frac{(\text{SRP}_{\text{ini}} - \text{SRP}_{\text{fin}}) \times V (\text{L})}{\text{mass (g)}}$$

To calculate EPC₀ values (µg L⁻¹), SRP_{fin} was regressed against P_{sorb} on an x–y coordinate system using a linear or Freundlich model depending on the higher r². SRP_{fin} at P_{sorb} = 0 (x-intercept) was calculated as the EPC₀ value, i.e., the concentration of SRP where zero net sorption to/from the sediment occurs after the 24 h incubation, or where SRP_{fin} = SRP_{ini}. For PT sampler sediment, the same methodology was used except that 35 mL of sediment-water slurry was spiked rather than the 5 g of sediment. This was due to the difficulty in removing the fine sediment load from suspension. Thus, SRP_{ini} was calculated as the sum of the spiked concentration and the initial SRP concentration of the sediment-water slurry, and the slurry TSS concentration to calculate the suspended sediment mass (normalized for volume of the sample). The background CaCl₂ solution was used to make up the final 40 mL volume, with all dilution effects accounted for in calculations of EPC₀ values. Sediments and surface waters are considered to be in equilibrium with respect to dissolved P if the difference between SRP in the water column and EPC₀ does not exceed 20% (Jarvie et al. 2005; Weigelhofer et al. 2018). This criterion is used here to define site sediment as sinks (SRP > EPC₀ by 20%) or sources (SRP < EPC₀ by 20%) of SRP, or in equilibrium (SRP within 20% of EPC₀).

4.2.4.3 In-situ Sediment Redox

To assess in-situ bed sediment dissolved oxygen (DO) and oxidation-reduction potential (ORP) Unisense microsensors/microelectrodes were used with a motorized vertical field MicroProfiling system and Field Microsensor Multimeter (FMM) (<https://unisense.com/>). Sensors were glass-type with 100 μm tips (OX-100 and RD-100 for DO, ORP, respectively) and were calibrated in the field before profiling. For field measurements, the MicroProfiler was adhered to the linear stage and hand pressed firmly into an undisturbed section of sediment no farther than 2 meters from where bed sediment was collected. The sensors were mounted to the motor stage at an initial position approximately 1 cm above the sediment water interface (SWI). Duplicate vertical profile sequences were 2 - 3 cm in depth with measurements recorded every 0.3 mm. Sensors were programmed with a measure and stabilization period of 3 seconds, with all measurements logged on the FMM. Rates of variable change over the SWI were calculated by dividing the variable difference (μmol for DO and mV and for ORP) by the depth interval (mm). Stable measurements before and after the SWI (represented by unchanging values) were omitted in rate calculations to only capture conditions over the SWI.

4.2.5 Bed Sediment Microbial Community Analysis

Bed sediments collected across the three sites in 2019 were extracted for total DNA using the QIAGEN DNeasy PowerLyzer PowerSoil Kit following the manufacturers instructions. Forward V5F (5-ATTAGATACCCNGGTAG-3) and reverse V6R (5-CGACAGAGCCATGCANACCT-3) primers were used for amplification of a 300 base pair (bp) segment of the hypervariable 16S bacterial rRNA gene for taxonomic identification using the SILVA ribosomal RNA database (Silva release 132_99_16S) (Quast et al. 2013). Sequencing was performed on an Ion Torrent Personal Genome Machine (Life Technologies) and resulting reads were processed using the Quantitative Insights into Microbial Ecology (QIIME) pipeline, QIIME2 ver. 2019.1 with details of filtering, alignment, and phylogenetic tree construction in Falk et al. 2022 (Falk et al. 2022). Principal coordinate analysis (PCoA) was used to visualize Bray-Curtis distances between 2019 samples with beta diversity dissimilarity tested via PERMANOVA with 999 permutations. Linear discriminant analysis Effect Size (LEfSe), a method designed for

metagenomic data, was used to further identify significant biomarker taxa across sample groups (Segata et al. 2011).

4.2.6 Historical Watershed and Climate Data

To assess historical water quality trends for watersheds, past data collected as part of the Ontario Provincial (Stream) Water Quality Monitoring Network (PWQMN) was obtained from the publicly accessible open data catalogue from the Ministry of Environment, Conservation and Parks (MECP) (<https://data.ontario.ca/dataset/provincial-stream-water-quality-monitoring-network>). Station IDs 04001303302 and 08012305702 were used for Big Creek and the Saugeen River, respectively, with station 04001304102 (Middle Thames River) representing the Nissouri Creek watershed, as data for Nissouri Creek was unavailable. The Middle Thames station lies 14 km downstream from the Nissouri Creek sampling site. Local precipitation data was obtained from the nearest weather station to the sampling sites from the Government of Canada Historical Data Archive (Government of Canada).

4.2.7 Data Analysis

Data analysis and statistics were performed in R (v. 4.1.2) and Past3 software. Additional microbial community tests and visualizations were produced through MicrobiomeAnalyst (Dhariwal et al. 2017; Chong et al. 2020).

4.3 Results

4.3.1 Legacy TN and TP Concentrations

Surface water TN, TP, and TN:TP ratios were analyzed for this study and calculated from PWQMN historical data available from 2000-2020. Trends are displayed by variable, broken down by site in Figure 1. Data from the current study as well as historical data show higher nutrient levels at the agriculturally influenced sites than the Saugeen River. TN was highest at Nissouri Creek, with TP dominating at Big Creek, and this trend was apparent from both current and historical data. This is reflected in the TN:TP ratios, which were higher at Nissouri Creek than Big Creek (Table S3 and Table S4).

4.3.2 Bed and Suspended Sediment Buffering Capacity by EPC₀

Annual averaged site data for water SRP vs. bed sediment EPC₀ are displayed in Figure 2. Mean SRP values for Big Creek 2018, 2019, and 2020 (0.023, 0.087, and 0.065

mg L⁻¹) were all greater than 20% than corresponding mean EPC₀ values (0.015, 0.0096, 0.0051 mg L⁻¹) and assigned as dissolved P sinks. For Nissouri Creek 2019, mean EPC₀ (0.037 mg L⁻¹) was over 20% greater than SRP (0.030 mg L⁻¹) and defined as a source, but higher average SRP than EPC₀ was measured in 2020 (0.095 and 0.015 mg L⁻¹, respectively) and defined a sink. The Saugeen River showed lower average concentrations for both metrics, with 2019 values of 0.0017 and 0.0024 mg L⁻¹ (P-source) and 2020 values of 0.015 and 0.00079 mg L⁻¹ (P-sink), for SRP and EPC₀, respectively.

The point sampling breakdown values of SRP, bed and suspended sediment EPC₀, and precipitation are shown in Figure 3. Stacked columns show the total interval precipitation (i.e., mm of precipitation between point sampling) with the 7-day preceding precipitation shown as the top portion of the column. At Big Creek in 2018, bed sediments were defined as P-sources in Early Spring and Mid Summer, and P-sinks in Mid Spring and Early Summer. In 2019 and 2020, all SRP concentrations exceeded bed sediment EPC₀ values by > 20% at Big Creek and were defined as P-sinks. Nissouri Creek bed sediments were defined as P-sources in Mid Spring and Fall 2019, P-sinks in Mid Summer 2019 and all of 2020, and in equilibrium in Early Spring and Late Summer 2019. Nissouri Creek was a notably high source of P in Mid Spring 2019 with EPC₀ exceeding SRP by 246% (0.039 and 0.011 mg L⁻¹ for EPC₀ and SRP, respectively). Saugeen River surface water SRP and bed EPC₀ concentrations were lower than both BC and NC, however, were defined as P-sources in Late Summer and Fall 2019, P-sinks in Mid Summer 2019 and all 2020, and in equilibrium in Early Summer 2019.

For time-integrated suspended sediment, 2019 EPC₀ values at Big Creek were significantly higher than for bed sediments, with values of 0.33, 0.35, 0.05, and 0.08, and mg L⁻¹ for the Mid Spring-Early Summer (P-source), Early Summer-Mid Summer (P-source), Mid-Summer-Late (P-Sink) Summer, and Late Summer-Fall (P-sink) intervals, and 1.9 mg L⁻¹ for the Mid Summer-Fall interval of 2020 (P-source) (Figure 3). Values at Nissouri Creek were lower and closer to bed sediment concentrations, measuring 0.03, 0.08, 0.06, 0.04 mg L⁻¹ for the 2019 intervals (in chronological order) and 0.26 mg L⁻¹ for the 2020 interval. Nissouri Creek suspended sediment was deemed a P-source for the Early Summer-Mid Summer 2019 interval and Mid Summer-Fall 2020 interval. Saugeen River

exhibited lower EPC_0 values for suspended sediment than bed sediment for all intervals, measuring 1.55×10^{-4} , 6.96×10^{-4} , and 0.0016 mg L^{-1} for Early Summer-Mid Summer, Mid Summer-Late Summer, and Late Summer-Fall 2019. All intervals for SR suspended sediment were defined as P-sinks. The Saugeen River PT sampler was dislodged during deployment in 2020, thus no suspended sediment data was retrieved.

4.3.3 Site Physico-chemical Water Quality Variable Correlations

In-stream variables known to influence sediment redox and potentially influence sediment-P desorption were subject to correlation analysis via Spearman's Rank test for all observations. Significant correlations are displayed in Table 1. SRP was positively correlated with TP (ρ 0.94, $p < 0.05$) with no correlations to redox parameters. TP was also correlated with DO (ρ -0.97, $p < 0.05$), TSS (ρ 0.83, $p < 0.05$), and minimum (Min) ORP (ρ -0.76, $p < 0.05$). EPC_0 was slightly but significantly correlated to NO_3 and DO rate.

4.3.4 Vertical Microsensor Redox and DO Profiling

Vertical microsensor profile data is summarized in the inset bar chart in Figure 4, with average values provided for DO rate, ORP rate, and Min ORP calculated for each site from all measurements over 2019-2020. Average DO rates were -56.4, -76.2, and -38.32 $\mu\text{mol L}^{-1} \text{ mm}^{-1}$ over the SWI for Big Creek, Nissouri Creek, and the Saugeen River, respectively, with ORP rates of 19.1, -10.3, and -9.9 mV mm^{-1} . Average Min ORP values were -116.9, 74.0, and -55.6 mV for Big Creek, Nissouri Creek, and Saugeen River bed sediments. Sample vertical profiles from Mid Spring 2019 for each site are shown in Figure 4.

4.3.5 Temporal and Spatial Bed Sediment Microbial Community Analysis

Microbial community DNA sequencing yielded 69 samples for 2019 bed sediments, with an average count of 37,676 sequence per sample, resulting in identification of 454 microbial features after filtering. Ordination of samples by PCoA using Bray Curtis distance is displayed in Figure 5A, with the first 2 axes representing 29% and 14.2% of the variation in the dataset. Nissouri Creek and Saugeen River communities showed greater similarity to each other than to Big Creek communities in the resulting ordination, with Big Creek showing a wide distribution across Axis 1. There was overlap across many site

timepoints, except for Mid Spring Nissouri Creek samples, which showed a unique radiation to the top left quadrant. Biomarker analysis indicated that this timepoint was significantly abundant in the phyla Pseudomonadota (formerly Proteobacteria), Actinobacteria, Firmicutes, and Thaumarchaeota. Biomarker genera from this timepoint are listed in Table S2 and included the notable Ammonia Oxidizing Archaea (AOA) *Candidatus Nitrosocosmicus*, and the denitrifiers *Dechloromonas*, *Rhodoferrax*, and *Thauera*. Figure 5B displays the abundance of *C. Nitrosocosmicus* across samples, highlighting its differential association within Nissouri Creek Mid Spring samples. The class Bacteroidia was the only taxonomic feature found to be a significant bioindicator of P-sink sediments across all samples (Figure S1), with no significant bioindicators of P-source events observed.

As Nissouri Creek was characterized by high TN concentrations, measured N chemistries for 2019 were further assessed. Ammonium, nitrate, and nitrite concentrations are displayed in Figure 6. Ammonium was highest in Mid Spring (0.163 mg L^{-1}) and Late Summer (0.093 mg L^{-1}), with nitrate concentrations measured above 6 mg L^{-1} for all timepoints.

4.4 Discussion

4.4.1 Legacy Nutrient Trends

Site trends for TN, TP, and TN:TP molar ratios in this study were consistent with 20-year data from the PWQMN. Big Creek continues to be characterized by high TP, with Nissouri Creek showing higher TN, and the Saugeen River having relatively lower nutrient concentrations, and represents an appropriate reference watercourse. Higher N concentrations in the Nissouri Creek watershed over the last 20 years are suggested to be linked to increased manure output from higher livestock densities (IJC 2018; Nelligan et al. 2021). High outlier values that were contained within the historical PWQMN network dataset were not seen in this study. Such extreme values generally represent external nutrient loading events associated with fall precipitation and winter melts (Maccoux et al. 2016; Muenich et al. 2016; Nelligan et al. 2021). As the goal of this study was to assess mainly baseflow internal P dynamics in the watercourses, the lack of outlier values confirms that trends here are mostly representative of in-stream processes and less influenced by external loading events. This is further supported by the lack of correlation

between 7-day precipitation and SRP and nitrate concentrations across the study. However, there were some instances of high precipitation preceding point samplings, such as in Mid Spring at Big Creek and Nissouri Creek in 2018 and 2019, respectively.

4.4.2 Headwater Bed Sediment P Buffering

Big Creek and Nissouri Creek, had higher values of SRP and EPC_0 than the more forested Saugeen River site, and this was evident at practically all sampling timepoints. Waterbody sediments affected by non-point P sources commonly accumulate legacy P (Palmer-Felgate et al. 2009), and it's confirmed here that the sites with higher present and historical levels of surface water nutrients also exhibited reduced sediment P buffering potential as measured by zero phosphorus equilibrium tests. However, the range of EPC_0 values observed across the three years of data collection ($0.7 - 60 \mu\text{g/L}$) were in the lower end of other studies of similar non-point P lotic systems ($4 - 200 \mu\text{g/L}$). This suggests that although 25% of bed sediments analyzed here were defined as P-sources ($EPC_0 > \text{SRP}$ by 20%) the magnitude of these internal release events are relatively moderate (Falk et al. 2021; Simpson et al. 2021). There was no clear trend in higher EPC_0 values or sediment P sources with dryer, warmer timepoints, as has been suggested in other studies (Zhang et al. 2015; Stutter et al. 2021). Temperature and precipitation did not show any significant correlations with bed sediment EPC_0 or surface water SRP, and P-source designations occurred more during spring and fall timepoints than during the summer. In addition, the experimental design called for sampling when the preceding weekly precipitation was low to capture baseflow effects, yet still only several P-source events were recorded. Thus, it was confirmed that headwater bed sediments studied here behaved primarily as P-sinks (75% of observations), and that the Saugeen River represents an appropriate baseline compared to agriculturally influenced systems. However, observations at Big Creek and Nissouri Creek suggest that there are site-specific factors that may contribute to P loading downstream, which are outlined below.

4.4.2.1 Non-point P from Suspended Sediment at Big Creek

Despite bed sediments at Big Creek having lower EPC_0 values (i.e., were better P buffers) than Nissouri Creek, water column SRP was equally high, and TP was much greater, both presently and over the last 20 years of data collection. This suggests that P at Big Creek originates externally. External non-point P at Big Creek could be from a

combination of sources. For one, there is a large extent of tile-drainage in the BC watershed due to clay soils, and tile drains have been shown to act as conduits of soil P to waterbodies (King et al. 2015). Tile drain effluent was collected in mid spring and early summer at BC when it was noticed that tiles were flowing, with measured SRP concentrations of 0.07 and 0.03 mg L⁻¹, respectively. Mid Spring 2019 tile SRP concentration was higher than the water column concentration, offering evidence that tiles can contribute to high SRP at Big Creek. However, more observations from tile drains across southern Ontario watershed are necessary to make this connection.

Another likely source of P at Big Creek is from suspended sediment. TSS concentrations were consistently high at BC, likely due to the high clay content of the surrounding soils, with fine-grained sediment less likely to deposit in lotic systems and remain in suspension. Correlations across sites showed that TSS and TP were significantly correlated (ρ 0.83, $p < 0.05$), as were SRP and TP (ρ 0.94, $p < 0.05$). In addition, determination of suspended sediment EPC₀ values showed that the fine particulate phase could be a much greater accumulator and source of SRP than bed sediments, and that in many cases, the sediment slurry accumulated within the PT samplers at Big Creek were at or near saturation with respect to dissolved P (Figure 3). For example, suspended sediment EPC₀ values at Big Creek were found to be as high as 200 times greater than corresponding bed sediment values, and suspended sediment collected during the 2020 interval was measured to have an EPC₀ over 2000% greater than corresponding surface water SRP, constituting a major internal P-source. It's possible that suspended sediment is an overlooked source of internal P in suspension at Big Creek, as has been the case in other regional watersheds of the lower Great Lakes (Shinohara et al. 2018; Markovic et al. 2020).

Fine suspended sediment ($< 63 \mu\text{m}$) has higher affinity for dissolved species compared to coarser benthic sediments due to the high surface area to volume ratio of this phase (Wang et al. 2006; Agudelo et al. 2011; Droppo et al. 2015). However, it is also possible that the exceedingly high suspended sediment EPC₀ values observed originate from the methodology (i.e., PT time-integrated samplers). Specifically, suspended sediment EPC₀ values appeared to increase with longer deployment and with higher TSS accumulations. This may seem intuitive, but the mass-normalization portion of the P-sorb

equation (Equation 1) should remove mass effects, or in other words, a larger amount of sediment should not increase the amount of P-sorbed per mass. Therefore, it is possible that additional SRP is being adsorbed to sediment within the PT sampler, and essentially, the collected fine suspended sediment is behaving as an SRP filter and retaining more SRP during the interval than there would be present naturally. This could explain the SRP saturation effects observed here, and also high saturation seen in other studies that use this methodology (Emelko et al. 2016). In addition to SRP filter effects, the redox state of the PT samplers can also confound measurements of redox-sensitive species (such as P adsorbed to Fe and Mn-oxy/hydroxides) (Falk et al. 2022). Microbial effects could also impact redox state, as suspended sediments can comprise and be shaped by biofilms. To better evaluate suspended phase EPC_0 values, sampling methods that can obtain appropriate sediment masses (such as point centrifugation) can be paired with observations from time-integrated SS samplers. Despite these drawbacks, suspended sediment as a source of dissolved P should not be ignored in agricultural catchments, as the shorter collection intervals in this study still suggest high P-desorption potentials. Calculations here show that if particulate phosphorus is transported to receiving waterbodies of lower SRP concentrations, then the magnitude of diffusive release of bioavailable P from fine sediment in Big Creek can be over 100 times greater than bed sediments.

4.4.2.2 Non-point P at Nissouri Creek from Bed Sediments

Lower TP, TSS, and suspended sediment EPC_0 values, but higher bed sediment EPC_0 values suggest that Nissouri Creek is influenced by different mechanisms than Big Creek. Correlation analysis for all data observations yielded a significant correlation between EPC_0 and vertical sediment DO depletion rate as measured by microsensor redox profiles. Thus, the more rapidly that DO decreased through the SWI, EPC_0 values were generally higher. At Nissouri Creek in Mid Spring 2019, the DO depletion rate was $158.4 \mu\text{mol L}^{-1} \text{mm}^{-1}$, the highest value recorded from any site, and bed sediment was determined to be a source of SRP ($EPC_0 > \text{SRP}$ by 246%). Local sediment anoxia has been shown in field and laboratory studies to increase P desorption from the sediment matrix, as reductive dissolution of oxides and hydroxides of Fe and Mn can release immediately bioavailable P-species adsorbed to these minerals (Ding et al. 2018; Casillas-Ituarte et al. 2019). P fluxes from sediments associated with these biogeochemical redox processes have been cited over

a wide, yet somewhat inconsistent Eh range, from as great as 300 mV to – 200 mV (Hill and Robinson 2012; Parsons et al. 2017; Ding et al. 2018). ORP microsensor profiles showed that NC sediment reached an average minimum of 110 mV in Mid Spring 2019 (study average of 74.0 mV), indicating weekly reducing conditions, but within ranges of previously recorded microbially-mediated Fe/Mn reduction. Thus, there was a plausible link between higher EPC_0 values and increased sediment anoxia at this location.

However, ORP routinely reached lower values at Big Creek (average Min ORP of -117 mV), yet bed sediments there were only deemed a source of SRP at 2 of the 11 timepoints. In addition, there was no significant correlation between ORP rate or minimum ORP with sediment EPC_0 in this study. Another suggested mechanism for the higher EPC_0 values at Nissouri Creek is that N-driven production results in a relative limitation of bioavailable P (McDowell et al. 2017) and this is influencing the diffusion gradient of SRP from sediments. As N-species remain high while SRP is gradually depleted, P may begin to diffuse from bed sediments, or more immobile forms of P may be scavenged by microorganisms. This would manifest in a P-source designation, as sediment P reservoirs would be intermittently greater than water column P in these scenarios. This mechanism would also explain the high DO depletion rates at the Nissouri Creek SWI in Mid Spring 2019, as oxygen would be rapidly consumed by microbial metabolism, leaving nitrate as the next most favourable terminal electron acceptor. The abundance of nitrate in the Nissouri Creek system would also promote the higher ORP values observed compared to Big Creek and the Saugeen River. In effect, higher N-species available for microbial metabolism would prevent reductive Fe/Mn dissolution that would release bioavailable P; a form of redox buffering (Hill and Robinson 2012; Orihel et al. 2017; Dupas et al. 2018). Thus, one hypothesis is that Nissouri Creek sediments represent a catch 22 of sorts: high N pollution can cause ecosystem stress as an overabundant macronutrient for primary production, yet simultaneously serve to buffer sediments from internal P release. Thus, Nissouri Creek and other locations influenced by high N-loading from manure application represent vulnerable systems where nutrient reduction strategies must take into account interactions between surface water N and sediment P; a reduction in either nutrient will affect the other.

4.4.5 Microbial Community Effects

Nissouri Creek and Saugeen River shared more similar bed sediment microbial communities than Big Creek, with Big Creek exhibiting greater intra-community differences as displayed by the wide ellipses in Figure 5A. Despite the differences in N and P concentrations between Nissouri Creek and the Saugeen River, analysis of study-wide water quality parameters showed that these two watercourses were actually more chemically similar than BC (Figure S2), characterized by high concentrations of calcium, magnesium, and dissolved inorganic carbon. Previous non-point pollution research within the Huron-Erie corridor has identified Ca, Mg, and HCO_3 as indicators of the Thames River, of which both Big Creek and Nissouri Creek drain into (Maguire et al. 2019). However, the stark differences in agricultural land use and geology between BC and NC appear to dominate the discrepancies in water chemistry and this is also reflected in the divergent microbial communities. The more similar soil characteristics, geography, and source waters perhaps contribute to similarities in NC and SR. Thus, a general “agricultural” land use designation should be avoided when studying catchments with differing fertilizer practices. Nissouri Creek microbial communities did however diverge from Saugeen River communities at times, particularly at the previously identified Mid Spring 2019 timepoint, which was unique in its higher 7-day preceding precipitation, sediment DO depletion rate, and P-source designation. Biomarker analysis identified *Dechloromonas*, *Rhodoferrax*, and *Thauera* as top indicator genera of this timepoint, all of which are capable of denitrification (Holmes et al. 2009; Fuchs et al. 2011; Sanford et al. 2012; Weisener et al. 2017; Palacin-Lizarbe et al. 2019; Yang et al. 2019). The ammonia oxidizing archaea (AOA) *Candidatus Nitrosocosmicus* was also identified as one of the differentially expressed genera that characterized the Nissouri Creek 2019 Mid Spring timepoint. The proposed link between Nitrate-driven production and internal P loading from bed sediments at Nissouri Creek is supported by the abundance of these taxa, which could be actively involved in coupled nitrification and denitrification. This is further supported by the high concentrations of ammonium and nitrate measured at NC during Mid Spring 2019, potentially derived from field manure application in the watershed. The 7-day precipitation preceding the NC Mid Spring timepoint was the highest recorded across the study, and many of the indicator taxa groups have been cited in studies of manure-

influenced systems (Lopatto et al. 2019; Liao et al. 2020; Ye et al. 2021). Thus, transfer of N-laden manure from fields to waterbodies was likely. In summary, though sites did not share a general biomarker community indicative of internal P-loading events, investigations of timepoint-specific events were supported by unique taxa sets and may be indicators of internal P release in other manure-afflicted systems.

4.5 Conclusions

Tributary loads of P entering the lower Great Lakes are often lower than estimated based on terrestrial inputs. Thus, watercourse bed and suspended sediments must play vital roles in retaining P in upland, agriculturally intensive watersheds. This study over three years within an inorganic fertilizer-influenced, manure fertilizer-influenced, and a reference forested watercourse revealed site-specific biogeochemical mechanisms associated with sediment phosphorous release and retention and the key variables at play.

Overall, site sediments acted as P-sinks during the growing season. The inorganic fertilizer-influenced stream was defined by high TP, SRP, and TSS, and had a higher risk of internal P-release from suspended sediments than from bed sediments. High clay content in surrounding soils likely promoted P-sorption to the fine suspended sediment phase, which could be poised to diffusive desorption when transported through the river continuum. The manure-influenced site was defined by higher TN and higher bed sediment EPC_0 values, but ORP at the sediment water interface was buffered by high nitrate concentrations, which could reduce the potential for anoxia-driven P-desorption. N-driven production at this site could however serve to remove SRP from the water column and promote diffusive flux of SRP from loosely-bound sediment-P phases. An ammonia oxidizing archaea (AOA) genus was shown to be a significant biomarker during this N-driven, P-desorption mechanism, and could play a role in sustaining high NO_3 concentrations within sediment pore waters. Physicochemical spatial differences precluded the classification of bioindicator taxa associated with bed sediment P-sources across the three sites; however site-specific investigations may yield specific sets of taxa that correlate with P-sourcing events in watercourses defined by either inorganic or manure fertilizer application.

In summary, this study provides a case study of P-retention trends in low-order, upland watercourses in southern Ontario, and revealed site-specific vulnerabilities associated with internal release of P from bed and suspended sediments.

Acknowledgements

The authors thank Nargis Ismail, Jonathon Leblanc, and Shelby Mackie for technical support at the Great Lakes Institute for Environmental Research (GLIER). The authors also acknowledge Ryan Sorichetti for helping with sample analysis logistics, and the Weisener Lab Group staff and students for field and lab assistance. This work was supported through a NSERC Strategic partners Grant (STP 521430-18).

FIGURES AND TABLES

Table 1
Significant Sediment and Water Quality Variable Correlations

Variables		P-Value	Statistic p (rho)
TP	SRP	5.48E-05	0.93939
TP	DO	0.000165	-0.96667
TSS	DO	0.000795	-0.78901
Min ORP	ORP Rate	0.001637	0.85455
TSS	TP	0.00294	0.8303
NO ₃	EPC ₀	0.005801	0.65588
Precip Pre	ORP	0.007559	0.62293
NO ₃	DO	0.012593	-0.69231
Min ORP	DO	0.021776	0.80952
Temp	ORP	0.024715	-0.54167
Min ORP	TP	0.036756	-0.7619
DO rate	EPC ₀	0.04254	-0.64848

TP = surface water total phosphorus

SRP = surface water soluble reactive phosphorus

DO = surface water dissolved oxygen

Min ORP = bed sediment minimum oxidation-reduction potential

OPR rate = bed sediment oxidation-reduction potential rate

TSS = surface water total suspended solids

NO₃ = surface water nitrate

EPC₀ = bed sediment zero equilibrium phosphorus concentration

Temp = surface water temperature

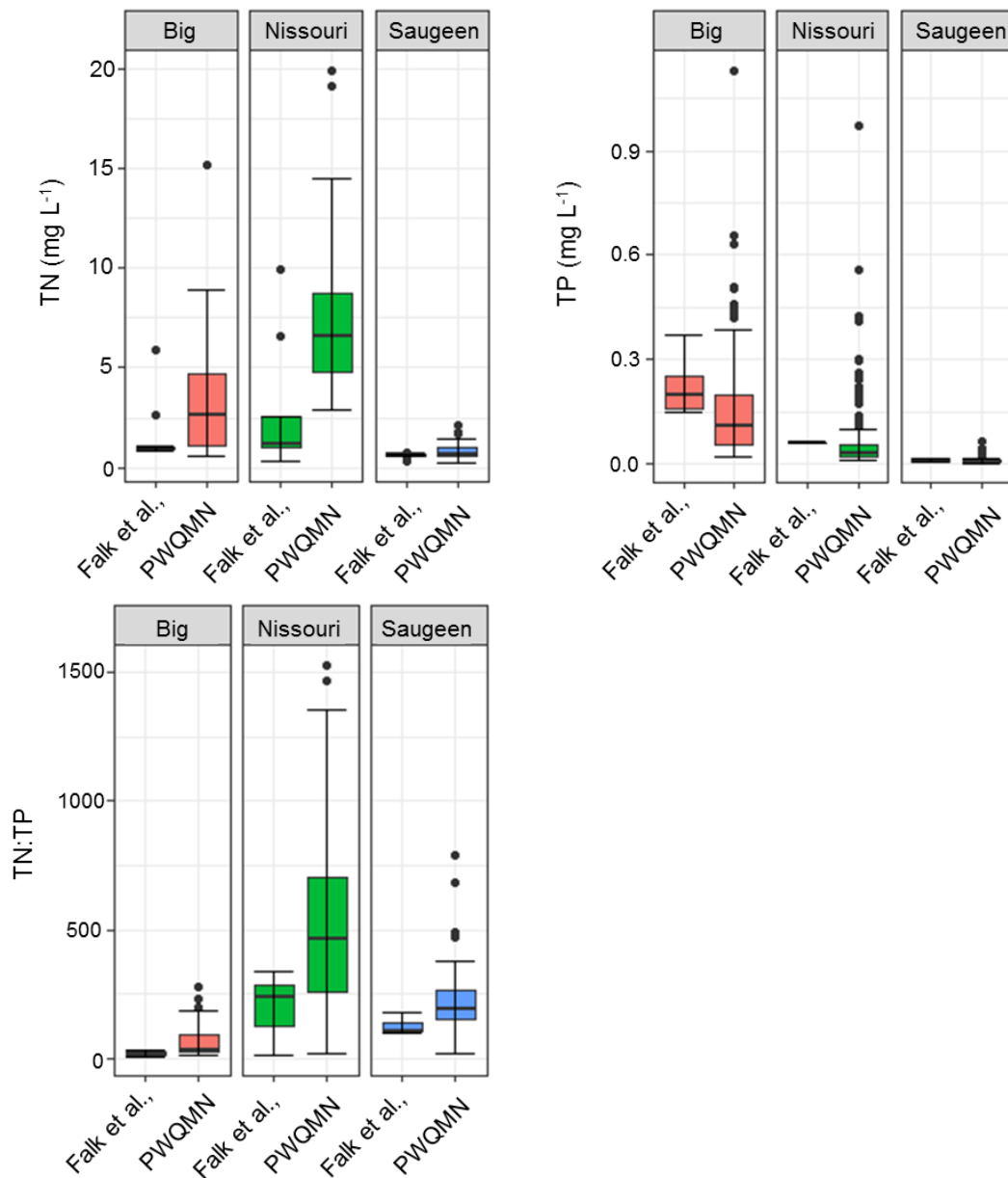


Figure 1: Total Nitrogen (TN), Total Phosphorus (TP), and TN:TP for Big Creek, Nissouri Creek, and the Saugeen River. Falk et al., data represents the range of values collected as part of this study, with Provincial Water Quality Monitoring Network (PWQMN) data representing values obtained for 2000 – 2020 from the open data catalogue from the Ministry of Environment, Conservation and Parks (MECP) (<https://data.ontario.ca/dataset/provincial-stream-water-quality-monitoring-network>).

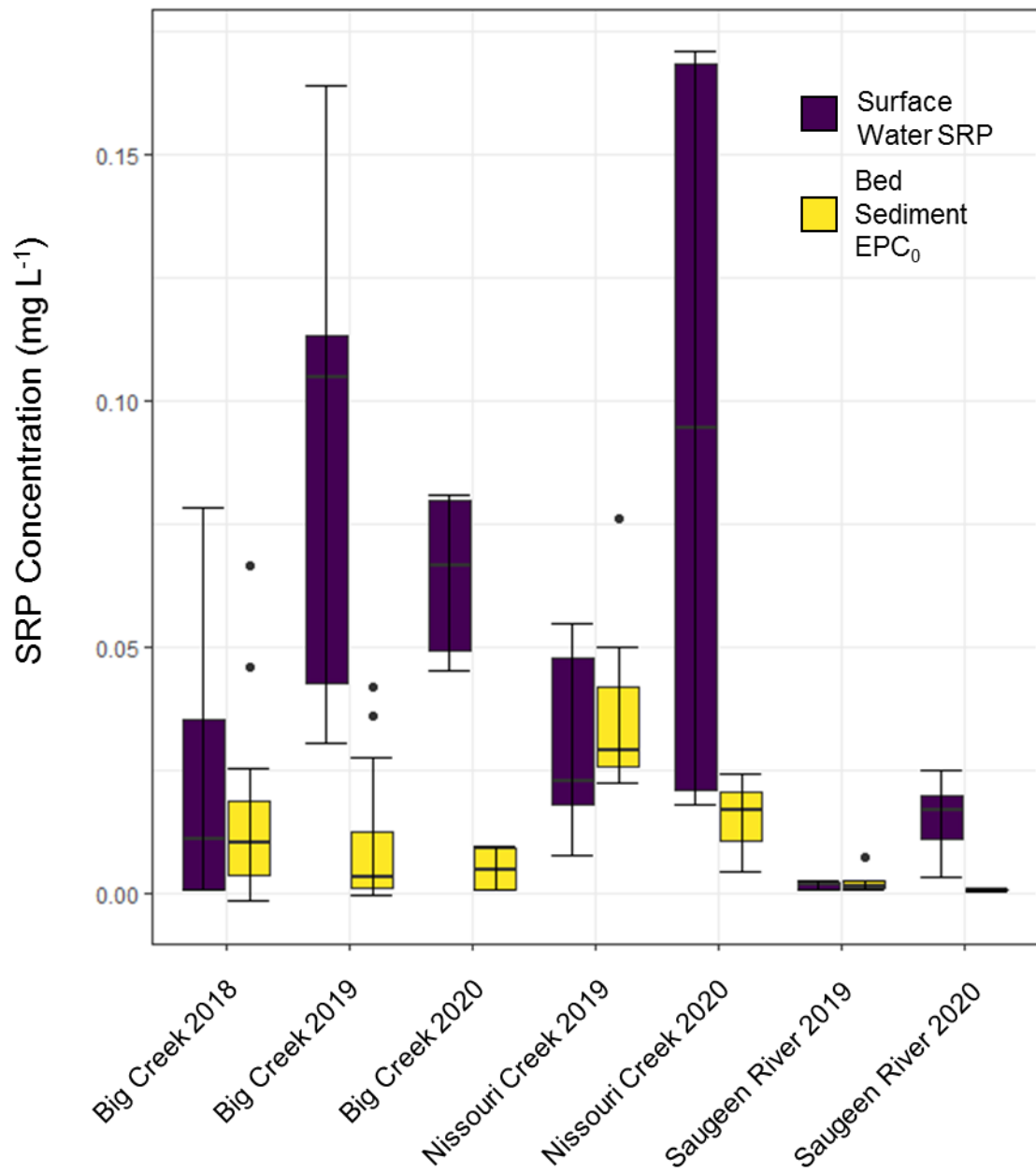


Figure 2: Box plot annual distributions of surface water soluble reactive phosphorus (SRP) and bed sediment zero equilibrium phosphorus concentrations (EPC_0) for Big Creek, Nissouri Creek, and the Saugeen River sampling sites.

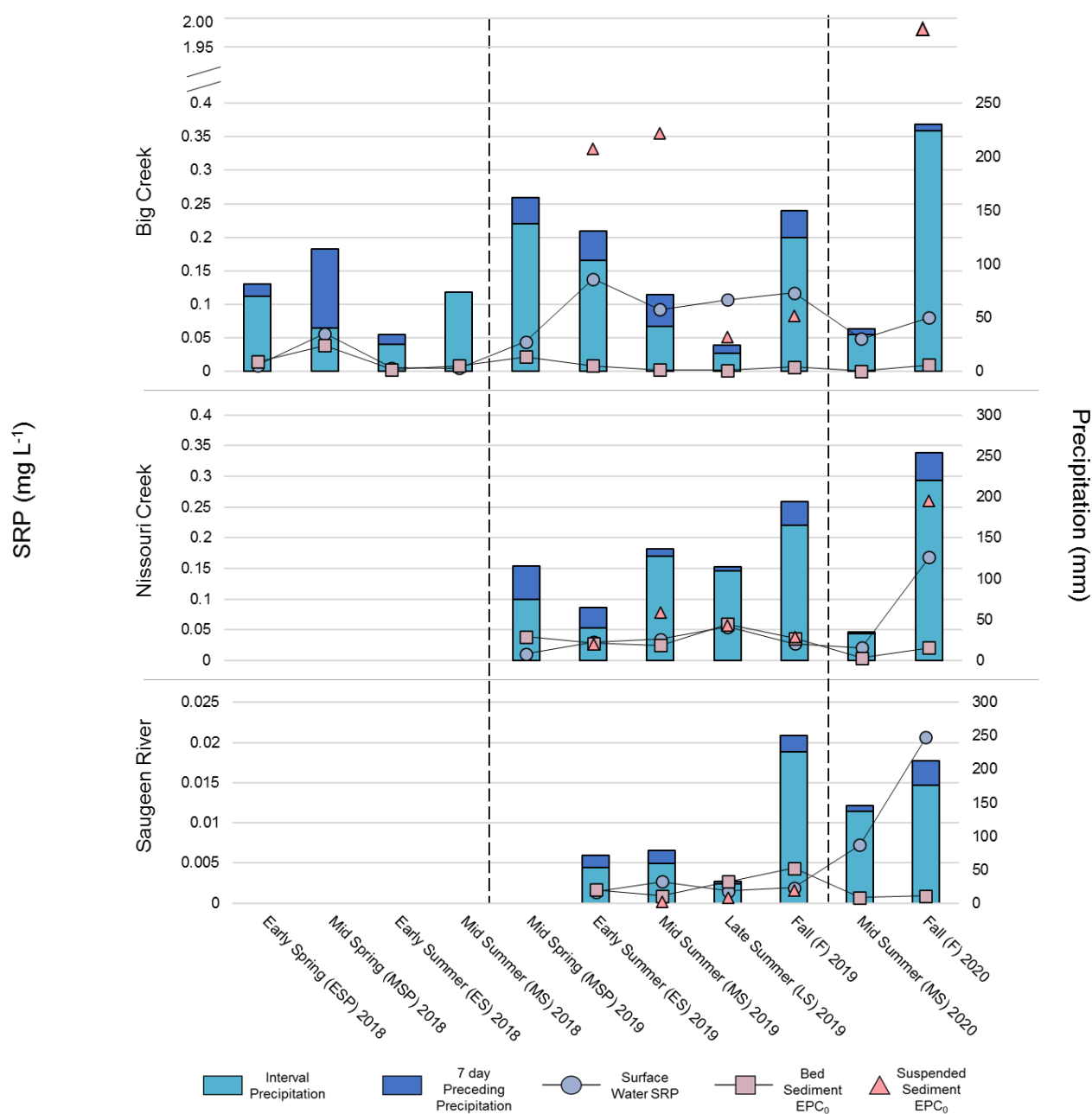


Figure 3: Seasonal point sampling characteristics for Big Creek, Nissouri Creek, and the Saugeen River for 2018 through 2020. Stacked bars represent the total interval precipitation (mm) with top sections specifying the seven-day precipitation amount preceding sampling. Dashed lines separate sampling years: Nissouri Creek and the Saugeen River were not sampled in 2018. EPC₀ measured as mg L⁻¹ SRP.

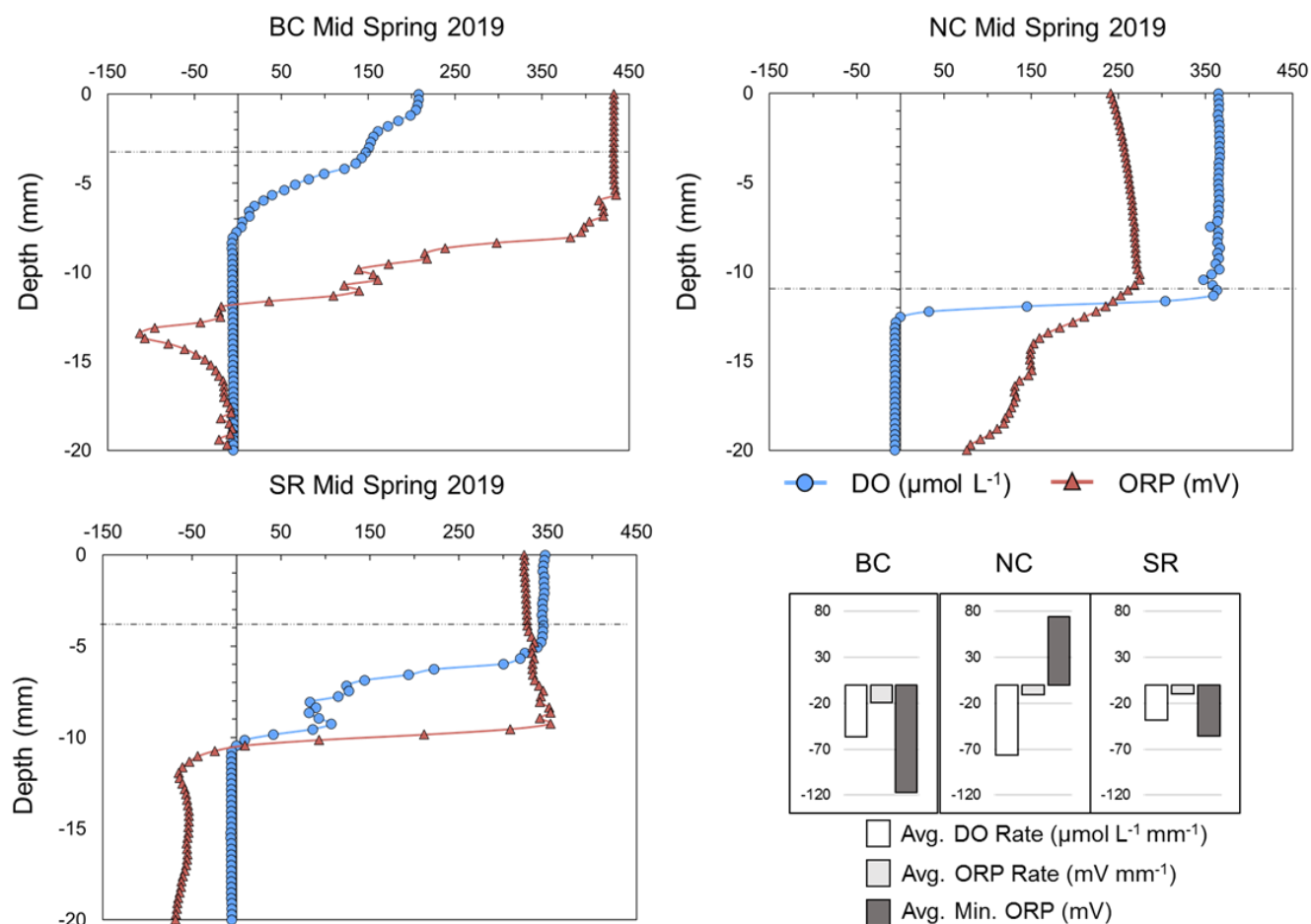


Figure 4: Mid Spring 2019 vertical microsensor profiles for dissolved oxygen (DO) and oxidation-reduction potential (ORP). Horizontal dashed lines represent the location of the sediment water interface (SWI). Inset bar graph shows average DO and ORP depletion rates with depth, and average minimum (Min) recorded ORP across all measurements for Big Creek (BC), Nissouri Creek (NC), and the Saugeen River (SR).

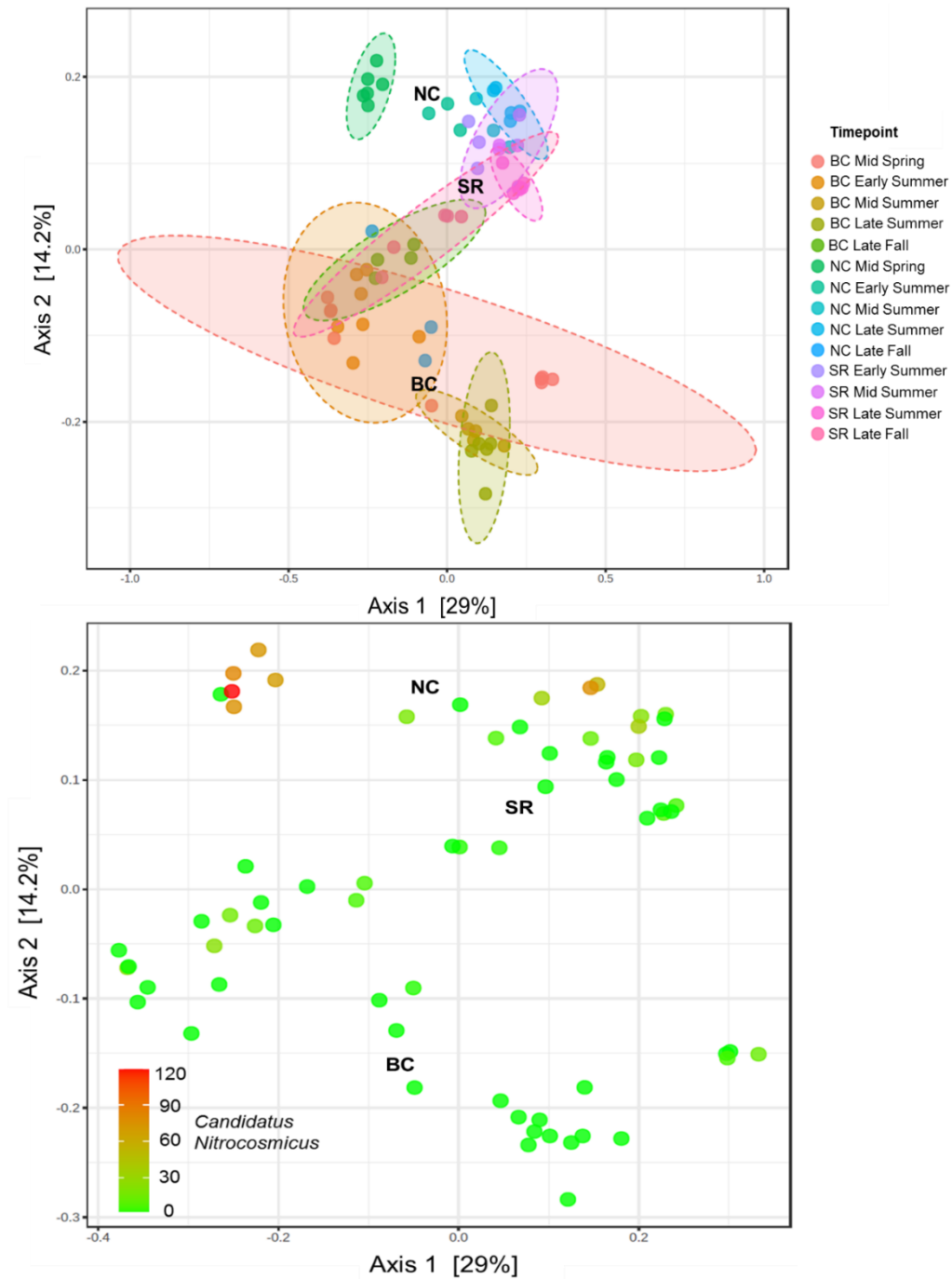


Figure 5: PCoA with Bray-Curtis distances of genus-level microbial community composition across samples. A) Samples labelled by site and timepoint with 95% confidence ellipses. BC = Big Creek, NC = Nissouri Creek, SR = Saugeen River. B) Samples labelled by the cumulative sum scaled abundance of the ammonia oxidizing archaea (AOA) *Candidatus Nitrosocosmicus*.

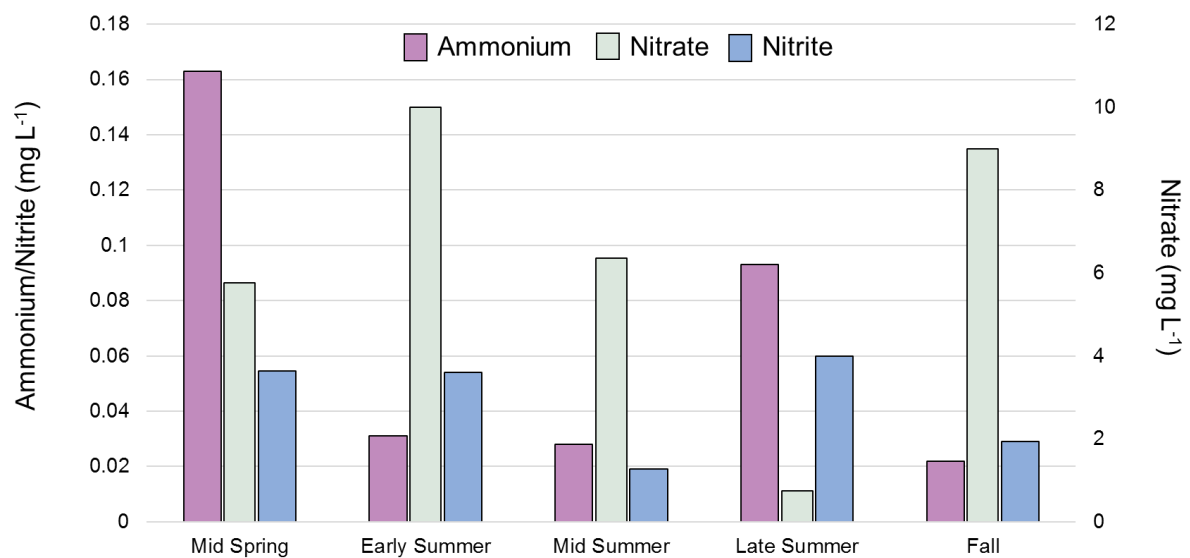


Figure 6: Nissouri Creek 2019 concentrations of ammonium, nitrate, and nitrite.

References

- Agudelo, S.C., Nelson, N.O., Barnes, P.L., Keane, T.D., Pierzynski, G.M., 2011. Phosphorus Adsorption and Desorption Potential of Stream Sediments and Field Soils in Agricultural Watersheds. *J. Environ. Qual.* 40, 144–152. <https://doi.org/10.2134/jeq2010.0153>
- Bocaniov, S.A., Van Cappellen, P., Scavia, D., 2019. On the Role of a Large Shallow Lake (Lake St. Clair, USA-Canada) in Modulating Phosphorus Loads to Lake Erie. *Water Resour. Res.* 55, 10548–10564. <https://doi.org/10.1029/2019WR025019>
- Casillas-Ituarte, N.N., Sawyer, A.H., Danner, K.M., King, K.W., Covault, A.J., 2019. Internal Phosphorus Storage in Two Headwater Agricultural Streams in the Lake Erie Basin. *Environ. Sci. Technol.* <https://doi.org/10.1021/acs.est.9b04232>
- Chen, D., Shen, H., Hu, M., Wang, J., Zhang, Y., Dahlgren, R.A., 2018. Legacy Nutrient Dynamics at the Watershed Scale: Principles, Modeling, and Implications, 1st ed, *Advances in Agronomy*. Elsevier Inc. <https://doi.org/10.1016/bs.agron.2018.01.005>
- Chong, J., Liu, P., Zhou, G., Xia, J., 2020. Using MicrobiomeAnalyst for comprehensive statistical, functional, and meta-analysis of microbiome data. *Nat. Protoc.* 15, 799–821. <https://doi.org/10.1038/s41596-019-0264-1>
- Dhariwal, A., Chong, J., Habib, S., King, I.L., Agellon, L.B., Xia, J., 2017. MicrobiomeAnalyst: A web-based tool for comprehensive statistical, visual and meta-analysis of microbiome data. *Nucleic Acids Res.* 45, W180–W188. <https://doi.org/10.1093/nar/gkx295>
- Ding, S., Chen, M., Gong, M., Fan, X., Qin, B., Xu, H., Gao, S.S., Jin, Z., Tsang, D.C.W., Zhang, C., 2018. Internal phosphorus loading from sediments causes seasonal nitrogen limitation for harmful algal blooms. *Sci. Total Environ.* 625, 872–884. <https://doi.org/10.1016/j.scitotenv.2017.12.348>
- Dodds, W.K., Smith, V.H., 2016. Nitrogen, phosphorus, and eutrophication in streams. *Int. Waters* 6, 155–164. <https://doi.org/10.5268/IW-6.2.909>
- Droppo, I.G., D'Andrea, L., Krishnappan, B.G., Jaskot, C., Trapp, B., Basuvaraj, M., Liss, S.N., 2015. Fine-sediment dynamics: towards an improved understanding of sediment erosion and transport. *J. Soils Sediments* 15, 467–479. <https://doi.org/10.1007/s11368-014-1004-3>
- Dupas, R., Tittel, J., Jordan, P., Musolff, A., Rode, M., 2018. Non-domestic phosphorus release in rivers during low-flow: Mechanisms and implications for sources identification. *J. Hydrol.* 560, 141–149. <https://doi.org/10.1016/j.jhydrol.2018.03.023>
- Emelko, M.B., Stone, M., Silins, U., Allin, D., Collins, A.L., Williams, C.H.S., Martens, A.M., Bladon, K.D., 2016. Sediment-phosphorus dynamics can shift aquatic ecology

- and cause downstream legacy effects after wildfire in large river systems. *Glob. Chang. Biol.* 22, 1168–1184. <https://doi.org/10.1111/gcb.13073>
- Falk, N., Day, M., Weisener, C.G., 2021. Evaluating Sediment Phosphorus Exchange in Rural Ontario Headwaters by Paired Sequential Extraction and Sorption Isotherms. *Water, Air, Soil Pollut.* 232, 1–14. <https://doi.org/10.1007/s11270-021-05381-z>
- Falk, N., Droppo, I.G., Drouillard, K.G., Weisener, C.G., 2022. Integrating microbial DNA community analyses into time - integrated suspended sediment sampling methods. *J. Soils Sediments*. <https://doi.org/10.1007/s11368-022-03293-x>
- Fuchs, G., Boll, M., Heider, J., 2011. Microbial degradation of aromatic compounds — from one strategy to four. *Nat. Rev. Microbiol.* 9, 803–816. <https://doi.org/10.1038/nrmicro2652>
- Hill, C.R., Robinson, J.S., 2012. Phosphorus flux from wetland ditch sediments. *Sci. Total Environ.* 437, 315–322. <https://doi.org/10.1016/j.scitotenv.2012.06.109>
- Holmes, D.E., Williams, K.H., Wilkins, M.J., Long, P.E., Lovley, D.R., 2009. Influence of Heterogeneous Ammonium Availability on Bacterial Community Structure and the Expression of Nitrogen Fixation and Ammonium Transporter Genes during in Situ Bioremediation of Uranium-Contaminated Groundwater 43, 4386–4392.
- IJC, 2018. Fertilizer application patterns and trends and their implications for water quality in the western Lake Erie basin, International Joint Commission (IJC).
- Jarvie, H.P., Jurgens, M.D., Williams, R.J., Neal, C., Davies, J.J.L., Barrett, C., White, J., 2005. Role of river bed sediments as sources and sinks of phosphorus across two major eutrophic UK river basins : the Hampshire Avon and Herefordshire Wye. *J. Hydrol.* 304, 51–74. <https://doi.org/10.1016/j.jhydrol.2004.10.002>
- Kane, D.D., Conroy, J.D., Peter Richards, R., Baker, D.B., Culver, D.A., 2014. Re-eutrophication of Lake Erie: Correlations between tributary nutrient loads and phytoplankton biomass. *J. Great Lakes Res.* 40, 496–501. <https://doi.org/10.1016/j.jglr.2014.04.004>
- King, K.W., Williams, M.R., Fausey, N.R., 2015. Contributions of Systematic Tile Drainage to Watershed-Scale Phosphorus Transport. *J. Environ. Qual.* 44, 486–494. <https://doi.org/10.2134/jeq2014.04.0149>
- Liao, H., Yen, J.Y., Guan, Y., Ke, D., Liu, C., 2020. Differential responses of stream water and bed sediment microbial communities to watershed degradation. *Environ. Int.* 134, 105198. <https://doi.org/10.1016/j.envint.2019.105198>
- Lopatto, E., Choi, J., Colina, A., Ma, L., Howe, A., Hinsla-Leasure, S., 2019. Characterizing the soil microbiome and quantifying antibiotic resistance gene dynamics in agricultural soil following swine CAFO manure application. *PLoS One* 14. <https://doi.org/10.1371/journal.pone.0220770>
- Maccoux, M.J., Dove, A., Backus, S.M., Dolan, D.M., 2016. Total and soluble reactive

- phosphorus loadings to Lake Erie: A detailed accounting by year, basin, country, and tributary. *J. Great Lakes Res.* 42, 1151–1165.
<https://doi.org/10.1016/j.jglr.2016.08.005>
- Macrae, M., Jarvie, H., Brouwer, R., Gunn, G., Reid, K., Joosse, P., King, K., Kleinman, P., Smith, D., Williams, M., Zwonitzer, M., 2021. One size does not fit all: Toward regional conservation practice guidance to reduce phosphorus loss risk in the Lake Erie watershed. *J. Environ. Qual.* 50, 529–546. <https://doi.org/10.1002/jeq2.20218>
- Maguire, T.J., Spencer, C., Grgicak-Mannion, A., Drouillard, K., Mayer, B., Mundle, S.O.C., 2019. Distinguishing point and non-point sources of dissolved nutrients, metals, and legacy contaminants in the Detroit River. *Sci. Total Environ.* 681, 1–8.
<https://doi.org/10.1016/j.scitotenv.2019.04.311>
- Markovic, S., Blukacz-Richards, A.E., Dittrich, M., 2020. Speciation and bioavailability of particulate phosphorus in forested karst watersheds of southern Ontario during rain events. *J. Great Lakes Res.* 46, 824–838.
<https://doi.org/10.1016/j.jglr.2020.05.001>
- McDowell, R.W., Elkin, K.R., Kleinman, P.J.A., 2017. Temperature and Nitrogen Effects on Phosphorus Uptake by Agricultural Stream-Bed Sediments. *J. Environ. Qual.* 46, 295–301. <https://doi.org/10.2134/jeq2016.09.0352>
- Michalak, A.M., Anderson, E.J., Beletsky, D., Boland, S., Bosch, N.S., Bridgeman, T.B., Chaffin, J.D., Cho, K., Confesor, R., Daloglu, I., DePinto, J. V., Evans, M.A., Fahnenstiel, G.L., He, L., Ho, J.C., Jenkins, L., Johengen, T.H., Kuo, K.C., LaPorte, E., Liu, X., McWilliams, M.R., Moore, M.R., Posselt, D.J., Richards, R.P., Scavia, D., Steiner, A.L., Verhamme, E., Wright, D.M., Zagorski, M.A., 2013. Record-setting algal bloom in Lake Erie caused by agricultural and meteorological trends consistent with expected future conditions. *Proc. Natl. Acad. Sci.* 110, 6448–6452.
<https://doi.org/10.1073/pnas.1216006110>
- Muenich, R.L., Kalcic, M., Scavia, D., 2016. Evaluating the Impact of Legacy P and Agricultural Conservation Practices on Nutrient Loads from the Maumee River Watershed. *Environ. Sci. Technol.* 50, 8146–8154.
<https://doi.org/10.1021/acs.est.6b01421>
- Nelligan, C., Sorichetti, R.J., Yousif, M., Thomas, J.L., Wellen, C.C., Parsons, C.T., Mohamed, M.N., 2021. Then and now: Revisiting nutrient export in agricultural watersheds within southern Ontario’s lower Great Lakes basin. *J. Great Lakes Res.*
<https://doi.org/10.1016/j.jglr.2021.08.010>
- Orihel, D.M., Baulch, H.M., Casson, N.J., North, R.L., Parsons, C.T., Seckar, D.C.M., Venkiteswaran, J.J., 2017. Internal phosphorus loading in canadian fresh waters: A critical review and data analysis. *Can. J. Fish. Aquat. Sci.* 74, 2005–2029.
<https://doi.org/10.1139/cjfas-2016-0500>
- Palacin-Lizarbe, C., Camarero, L., Hallin, S., Jones, C.M., Cáliz, J., Casamayor, E.O., Catalan, J., 2019. The DNRA-denitrification dichotomy differentiates nitrogen

- transformation pathways in mountain lake benthic habitats. *Front. Microbiol.* 10, 1–15. <https://doi.org/10.3389/fmicb.2019.01229>
- Palmer-Felgate, E.J., Jarvie, H.P., Withers, P.J.A., Mortimer, R.J.G., Krom, M.D., 2009. Stream-bed phosphorus in paired catchments with different agricultural land use intensity. *Agric. Ecosyst. Environ.* 134, 53–66. <https://doi.org/10.1016/J.AGEE.2009.05.014>
- Parsons, C.T., Rezanezhad, F., O’Connell, D.W., Van Cappellen, P., 2017. Sediment phosphorus speciation and mobility under dynamic redox conditions. *Biogeosciences* 14, 3585–3602. <https://doi.org/10.5194/bg-14-3585-2017>
- Phillips, J.M., Russell, M.A., Walling, D.E., 2000. Time-integrated sampling of fluvial suspended sediment: A simple methodology for small catchments. *Hydrol. Process.* 14, 2589–2602. [https://doi.org/10.1002/1099-1085\(20001015\)14:14<2589::AID-HYP94>3.0.CO;2-D](https://doi.org/10.1002/1099-1085(20001015)14:14<2589::AID-HYP94>3.0.CO;2-D)
- Quast, C., Pruesse, E., Yilmaz, P., Gerken, J., Schweer, T., Yarza, P., Peplies, J., Glöckner, F.O., 2013. The SILVA ribosomal RNA gene database project: Improved data processing and web-based tools. *Nucleic Acids Res.* 41, 590–596. <https://doi.org/10.1093/nar/gks1219>
- Richards, R.P., Baker, D.B., Crumrine, J.P., Kramer, J.W., Ewing, D.E., Merryfield, B.J., 2008. Thirty-Year Trends in Suspended Sediment in Seven Lake Erie Tributaries. *J. Environ. Qual.* 37, 1894. <https://doi.org/10.2134/jeq2007.0590>
- Sanford, R.A., Wagner, D.D., Wu, Q., Chee-sanford, J.C., Thomas, S.H., Cruz-garcía, C., Rodríguez, G., Massol-deyá, A., Krishnani, K.K., Ritalahti, K.M., 2012. Unexpected nondenitri fi er nitrous oxide reductase gene diversity and abundance in soils. <https://doi.org/10.1073/pnas.1211238109>
- Segata, N., Izard, J., Waldron, L., Gevers, D., Miropolsky, L., Garrett, W.S., Huttenhower, C., 2011. Metagenomic biomarker discovery and explanation. *Genome Biol.* 12, 1–18. <https://doi.org/10.1186/gb-2011-12-6-r60>
- Shinohara, R., Ouellette, L., Nowell, P., Parsons, C.T., Matsuzaki, S. ichiro S., Paul Voroney, R., 2018. The composition of particulate phosphorus: A case study of the Grand River, Canada. *J. Great Lakes Res.* 44, 527–534. <https://doi.org/10.1016/j.jglr.2018.03.006>
- Shrestha, N.K., Rudra, R.P., Daggupati, P., Goel, P.K., Shukla, R., 2021. A comparative evaluation of the continuous and event-based modelling approaches for identifying critical source areas for sediment and phosphorus losses. *J. Environ. Manage.* 277, 111427. <https://doi.org/10.1016/j.jenvman.2020.111427>
- Simpson, Z.P., McDowell, R.W., Condron, L.M., McDaniel, M.D., Jarvie, H.P., Abell, J.M., 2021. Sediment phosphorus buffering in streams at baseflow: A meta-analysis. *J. Environ. Qual.* 50, 287–311. <https://doi.org/10.1002/jeq2.20202>

- Stutter, M., Richards, S., Ibiyemi, A., Watson, H., 2021. Spatial representation of in-stream sediment phosphorus release combining channel network approaches and in-situ experiments. *Sci. Total Environ.* 795, 148790. <https://doi.org/10.1016/j.scitotenv.2021.148790>
- Van Staden, T.L., Van Meter, K.J., Basu, N.B., Parsons, C.T., Akbarzadeh, Z., Van Cappellen, P., 2021. Agricultural phosphorus surplus trajectories for Ontario, Canada (1961–2016), and erosional export risk. *Sci. Total Environ.* 151717. <https://doi.org/10.1016/j.scitotenv.2021.151717>
- Wang, S., Jin, X., Bu, Q., Zhou, X., Wu, F., 2006. Effects of particle size, organic matter and ionic strength on the phosphate sorption in different trophic lake sediments. *J. Hazard. Mater.* 128, 95–105. <https://doi.org/10.1016/j.jhazmat.2005.07.048>
- Wang, X., Zhi, Y., Chen, Y., Shen, N., Wang, G., Yan, Y., 2022. Realignment of phosphorus in lake sediment induced by sediment microbial fuel cells (SMFC). *Chemosphere* 291, 132927. <https://doi.org/10.1016/j.chemosphere.2021.132927>
- Weigelhofer, G., Ramião, J.P., Pitzl, B., Bondar-Kunze, E., O’Keeffe, J., 2018. Decoupled water-sediment interactions restrict the phosphorus buffer mechanism in agricultural streams. *Sci. Total Environ.* 628–629, 44–52. <https://doi.org/10.1016/j.scitotenv.2018.02.030>
- Weisener, C., Lee, J., Chaganti, S.R., Reid, T., Falk, N., Drouillard, K., 2017. Investigating sources and sinks of N₂O expression from freshwater microbial communities in urban watershed sediments. *Chemosphere* 188, 697–705. <https://doi.org/10.1016/j.chemosphere.2017.09.036>
- Winter, J.G., Palmer, M.E., Howell, E.T., Young, J.D., 2015. Long term changes in nutrients, chloride, and phytoplankton density in the nearshore waters of Lake Erie. *J. Great Lakes Res.* 41, 145–155. <https://doi.org/10.1016/j.jglr.2014.11.028>
- Withers, P.J.A., Neal, C., Jarvie, H.P., Doody, D.G., 2014. Agriculture and eutrophication: Where do we go from here? *Sustain.* 6, 5853–5875. <https://doi.org/10.3390/su6095853>
- Yang, Y., Li, S., Gao, Y., Chen, Y., Zhan, A., 2019. Environment-driven geographical distribution of bacterial communities and identification of indicator taxa in Songhua River. *Ecol. Indic.* 101, 62–70. <https://doi.org/10.1016/j.ecolind.2018.12.047>
- Ye, G., Banerjee, S., He, J.Z., Fan, J., Wang, Z., Wei, X., Hu, H.W., Zheng, Y., Duan, C., Wan, S., Chen, J., Lin, Y., 2021. Manure application increases microbiome complexity in soil aggregate fractions: Results of an 18-year field experiment. *Agric. Ecosyst. Environ.* 307, 107249. <https://doi.org/10.1016/j.agee.2020.107249>
- Zhang, B., Shrestha, N.K., Rudra, R., Shukla, R., Daggupati, P., Goel, P.K., Dickinson, W.T., Allataifeh, N., 2020. Threshold storm approach for locating phosphorus problem areas: An application in three agricultural watersheds in the Canadian Lake Erie basin. *J. Great Lakes Res.* 46, 132–143.

<https://doi.org/10.1016/j.jglr.2019.12.003>

Zhang, W., Pueppke, S.G., Li, H., Geng, J., Diao, Y., Hyndman, D.W., 2019. Modeling phosphorus sources and transport in a headwater catchment with rapid agricultural expansion. *Environ. Pollut.* 255, 113273.

<https://doi.org/10.1016/j.envpol.2019.113273>

Zhang, Z., Wang, H., Zhou, J., Li, H., He, Z., Van Nostrand, J.D., Wang, Z., Xu, X., 2015. Redox potential and microbial functional gene diversity in wetland sediments under simulated warming conditions: implications for phosphorus mobilization. *Hydrobiologia* 743, 221–235.

<https://doi.org/10.1007/s10750-014-2039-6>

CHAPTER 5: MICROBIAL COMMUNITY-DRIVEN NUTRIENT
TRANSFORMATIONS IN SOUTHERN ONTARIO TRIBUTARY SEDIMENTS; AN
RNA-DNA APPROACH

5.1 Introduction

Nutrient runoff from agriculture is recognized as a leading cause of degraded river quality worldwide. Excess loads of nitrogen (N) and phosphorus (P) from fertilizers can impair both surface waters and sediments and lead to eutrophication, anoxia, and disruption of ecosystem services (Newcomer Johnson et al., 2016). Understanding the fate of N and P within the river continuum is vital to effectively combat the detrimental effects of nutrients on all receiving waterbodies and can aid in remediation (Kelly et al., 2021; Stutter et al., 2021).

Microbial communities in rivers are actively involved in the biogeochemical transformations of Nitrogen (N) and Phosphorus (P). Denitrifying bacteria convert NO_3 and NO_2 to N_2 gas, effectively removing N from aquatic systems, while dissimilatory nitrate reducers and nitrifying bacteria cycle and retain ammonia (NH_3) in surface waters and sediments (Huang et al., 2018). In addition, N-fixation is microbially mediated and necessary for the assimilation and biosynthesis of a multitude of life-sustaining N-containing compounds. P is essential to nearly all microbial processes, and is a vital component of nucleic acids, membranes, and ATP. Thus, P is often considered the limiting nutrient for primary production in aquatic systems (Records et al., 2016). Microbes transport, cycle, and store P in large quantities (McMahon and Read, 2013; Sanz-Luque et al., 2020), and these processes are important to understand when quantifying sinks and sources of P through rivers. Characterizing the function of microbial communities is therefore central to the understanding of N and P processes.

The extraction and sequencing of nucleic acids (DNA and RNA) from water and sediments can inform both on the populations of microbes present and the types of genes being transcribed involving N and P transformations. Many beneficial results have come from these studies and have allowed for a better understanding of anthropogenic impacts on microbial communities in freshwater environments (Gibbons et al., 2014; Laperriere et al., 2020). However, most studies utilize only DNA or only RNA as the biomarker of present microbes. DNA-based investigations cast a wide net and uncover sequences originating from active, but also dead and dormant cells, while RNA-based investigations target only the most active community members at a specific time and place. Although

both approaches are valid depending on the research questions at hand, there is a gap in studies that utilize both methods. Comparing microbial communities from co-extracted RNA and DNA can help elucidate what share of the community is active vs. non-active, making additional interpretations of gene expression more robust (Birrer et al., 2018). Further, understanding the proportions of neutral and active cells across river niches (i.e., in surface waters, suspended sediments, and bed sediments) can help unveil processes involved in species sorting.

In this study, microbial communities within bed sediments, suspended sediments, and surface waters from three watercourses in Southern Ontario, Canada were analyzed via DNA and RNA metabarcoding over two seasons (summer vs. fall). In addition, total RNA shotgun sequencing (metatranscriptomics) was performed on bed sediment samples to further evaluate microbial function tied to N and P cycling. We hypothesized that the RNA-based microbial community would represent a smaller subset of the DNA-based community, and that the RNA communities would have lower diversity in all river reservoirs. We also predicted that both DNA and RNA communities would show greater seasonal difference in community composition within surface waters and suspended sediments than within bed sediments, as dispersal would be greater in the water column. Finally, we explore the variations in bed sediment microbial N and P cycling genes across the agriculturally impacted and reference sites to illuminate the key processes at play at the sediment water interface.

5.2 Methods

5.2.1 Site Overview

Three watercourses in southern Ontario were sampled in summer and fall 2020; Big Creek (BC), Nissouri Creek (NC), and the Saugeen River (SR). Watercourses were selected based on the prevailing watershed agricultural practice. In brief, BC and NC are within agricultural catchments (> 70% agricultural landcover) characterized by inorganic fertilizer application and a manure/inorganic fertilizer mix, respectively, with the SR sampling site located in a higher forested catchment (< 35% agricultural landcover). Both BC and NC are tributaries of the Thames River, which serves as a primary conduit of P to Lake St. Clair and the Detroit River of the Great Lakes Huron-Erie Corridor (HEC) (Bocaniov et al., 2019). The SR sampling point lies in an upstream segment of the river

approx. 140 km from its outlet to lower Lake Huron. Sampling access sites were wadable and did not exceed 0.7 m in depth.

5.2.2 Surface Water and Bed Sediment Sampling

At summer and fall timepoints, surface water and bed sediment samples were obtained in the field for chemical and microbial analyses. Surface water was collected in triplicate from the midsection of the watercourse segment in sterile HDPE bottles, with a set of samples filtered through 0.45 µm cellulose-acetate filters. Bed sediment was collected using a pre-sterilized trowel that was used to remove and shovel sediment into sterile, wide mouth HDPE containers at the sediment-water interface (SWI). General water quality parameters were recorded via a YSI EXO2 Multiparameter Water Quality Sonde. N chemistry (NO₃, NO₂, NH₄, Total Organic Nitrogen (TON)), P chemistry (soluble reactive P (SRP), Total P (TP)) and SO₄ were measured on a Thermo Gallery Plus Beermaster Autoanalyzer, with Total N (TN) measured on a Shimadzu TOC-L/TNM-L CPH Model Analyzer according to EPA standards (Supplementary Methods). Analyses were performed at the University of Alberta's Natural Resources Analytical Laboratory (NRAL). The isotopic composition of N and O in NO₃ was determined by the denitrifier method at the University of Calgary's Isotope Science Laboratory – Applied Geochemistry Group (ISL-AGg) (Casciotti et al., 2002; Sigman et al., 2001). Water samples were injected into vials containing *Pseudomonas aureofaciens* (ATCC# 13985), with the produced N₂O pre-concentrated (PreCon®), separated (HP 6890® gas chromatogram), and analyzed on a Thermo DeltaVPlus® mass spectrometer. Stable isotope ratios ¹⁵N/¹⁴N and ¹⁸O/¹⁶O were used to calculate delta (δ) ¹⁵N and ¹⁸O values using:

$$\delta^{15}\text{N or } \delta^{18}\text{O (‰)} = \left[\left(\frac{R_{\text{sample}}}{R_{\text{standard}}} \right) - 1 \right] \times 1000$$

where R = ¹⁵N/¹⁴N or ¹⁸O/¹⁶O and standards being atmospheric N₂ and Vienna standard mean ocean water (VSMOW) for N and O, respectively.

5.2.3 Time-Integrated Suspended Sediment Collection

Phillips Tube (PT) sampler sediment traps were used to collect suspended sediment in between the summer and fall point sampling. The traps consist of hollow poly-vinyl chloride (PVC) tubes fitted with 4 mm diameter openings on both ends to enable flow

through the unit. Flow within the unit is decreased by a factor of 600 enabling fine suspended sediment ($< 63 \mu\text{m}$) to settle and collect within the tube (Phillips et al., 2000). A single sampler was placed at each site at the summer point sampling, secured to bed sediments with rebar at approximately 60% of the depth of the watercourse, and retrieved at the fall sampling. The collected water-sediment slurry was emptied into 20-litre buckets and immediately sampled for water quality parameters and microbial community analysis.

5.2.4 Microbial Sampling and Preservation

For bed sediment microbial community analysis, bed sediment from the HDPE containers were subsampled in the field into 4-6 replicate cryotubes (5 mL volume) using sterilized spatulas and immediately flash-frozen in a liquid nitrogen dewar (4 L capacity). For discrete surface water and PT sampler microbial community analysis, water samples were filtered in the field through $0.22 \mu\text{m}$ Sterivex Filters using sterile luer lock 40 mL syringes. Water was passed through Sterivex filters until moderate resistance was reached up to a maximum of 500 mL. For each site, 5-6 replicate filters were collected, sealed with sterile putty, placed in Ziploc bags and flash frozen in liquid nitrogen.

5.2.5 DNA and rDNA Metabarcoding for Microbial Community Analysis

5.2.5.1 Extraction and Sequencing

All bed sediment samples and suspended sediment and surface water Sterivex filters were extracted for total microbial RNA and DNA using the Qiagen RNeasy PowerSoil Total RNA and RNeasy PowerSoil DNA Elution Kits. Bed sediments were processed per the manufacturer's instructions using 2 g of sediment per extraction. For suspended sediment and surface water, Sterivex filter units were cracked open using pre-sterilized pliers, and filters were cut and removed with clean scalpels and tweezers and then processed the same as bed sediments. Each extraction yielded a paired total RNA and total DNA sample. An aliquot of total RNA was converted to copy DNA (hereafter called rDNA) using the High-Capacity RNA-to-cDNA kit (Applied BiosystemsTM). All DNA and rDNA samples were subject to Polymerase Chain Reaction (PCR) to amplify an approx. 300 base pair (bp) segment of the hypervariable 16S prokaryote rRNA gene. Forward primer V5F (5-ATTAGATACCCNGGTAG-3) and reverse primer V6R (5-CGACAGAGCCATGCANCACCT-3) were used in the PCR reaction with 1 μL of DNA or rDNA, with additional reagents and reaction parameters specified elsewhere (Falk et al.,

2022). Resulting amplicons were visualized on 1% agarose gels to confirm sequence length, followed by a modified bead cleaning based on the Agencourt AMPure XP PCR Purification protocol to remove DNA fragments < 50 base pairs. A second PCR was performed to attach unique barcode and adapter nucleotides to each sample for sequencing in multiplex. Samples were then combined and excised through a final 2% agarose gel extraction (QIAquick Gel Extraction KitTM), normalized for concentration on an Agilent 2100 Bioanalyzer, and sequenced on an Ion Torrent Personal Genome Machine (Life Technologies) and output in single-end FASTQ file format.

5.2.5.2 Microbial Community Profiling

DNA and rDNA FASTQ files were processed through the Quantitative Insights into Microbial Ecology (QIIME) pipeline, QIIME2 ver. 2021.4 following the methodology in Falk et al., (Falk et al., 2022). After filtering (Callahan et al., 2016) and alignment (Kato et al., 2002), samples were rarefied to 10000 sequences for estimation of alpha (Shannon) and beta (Bray-Curtis distance) diversity using the q2-phylogeny plugin (Faith, 1991; Lozupone and Knight, 2005; Lozupone et al., 2007). Microbial taxonomy was then assigned to amplicon sequence variants (ASVs) using the SILVA ribosomal RNA database (Silva release 132_99_16S) (Quast et al., 2013) with a Naive Bayes classifier (Bokulich et al., 2018) trained on sequences extracted using the primers specified. The resulting hierarchical taxonomy-by-sample table was used for all DNA and rDNA-based community analysis.

5.2.5.3 Active, Neutral, and Non-Active Taxa Classification

DNA and rDNA communities were compared to classify microbial taxa as Active, Neutral, or Non-Active across sites, season, and substrate. Samples were first normalized by cumulative sum scaling (CSS) and then subject to biomarker analysis via linear discriminant analysis Effect Size (LEfSe) (Segata et al., 2011). LEfSe is a form of differential feature analysis that calculates which ecological features are statistically different in abundance between groups. Differential abundance results for each feature were then categorized under 3 possible conditions: 1) rDNA abundance > DNA abundance, 2) rDNA abundance < DNA abundance, and 3) RNA = 0, DNA > 0. The first condition implies active taxa, where the feature is detected in higher abundance from rDNA sequences (originating from rRNA) than DNA sequences (originating from chromosomal

DNA). The second condition implies neutral taxa, where the feature is detected in higher abundance in DNA sequences, but also detected in rDNA. The third condition implies non-active taxa, where it is only detected in DNA sequences with no corresponding detection from rDNA. This methodology was applied to phylum and genus level features for bed sediments, suspended sediments, and surface waters for each timepoint and location. The methodology is shown graphically in Figure S1.

5.2.5.4 Additional Microbial Community Analysis and Statistics

Pairwise alpha diversity between sample communities was tested with the Kruskal-Wallis test, with community composition tested via PERMANOVA with 999 permutations on the Bray-Curtis distances. Additional multivariate analyses and biomarker discovery of microbial samples was performed through MicrobiomeAnalyst (Chong et al., 2020; Dhariwal et al., 2017) and R (v. 4.1.2). Non-metric multidimensional scaling (NMDS) was used to visualize distances between samples, and Mantel tests used to assess the correlation (Spearman) between DNA and rDNA communities, with both methods using Bray-Curtis distance matrices produced from hierarchical taxonomy tables.

5.2.6 mRNA Sequencing and Metatranscriptomics of Bed Sediments

For each sampling point, an aliquot of bed sediment total RNA was analyzed for total prokaryotic gene function via mRNA metatranscriptomics. After extraction, RNA purity and quantity was confirmed on an Agilent 2100 Bioanalyzer and sent to the Centre d'expertise et de services Génome Québec (<https://cesgq.com/home>) for bacterial rRNA depletion (Ribo-Zero rRNA removal kit), cDNA reverse transcription, and shotgun sequencing on an Illumina NovaSeq 6000 System (Montréal (Québec) Canada). Sequence reads were processed through the MG-RAST (Metagenomics Rapid Annotations using Subsystems Technology) pipeline (Meyer et al., 2008). Details of preprocessing, dereplication, and gene calling can be found in Keegan et al., (Keega et al., 2016). Clustering of proteins was performed at 90% similarity using uclust (Edgar, 2010), with protein identification and annotation mapping done via sBLAT and using the M5NR database. Annotations were selected using the “Representative Hit”, classification, with functional profiles of feature hits across samples produced using the hierarchical SEED Subsystems classification (Overbeek et al., 2014). Subsystems uses a four-level hierarchy organization, with functional prediction increasing in specificity as levels increase. The

highest level (L1) represents a broad functional category containing many features surrounding a central cellular process, while the lowest level (L4) produces a functional assignment (often a protein-coding gene) to a single feature.

5.3 Results

5.3.1 Water Quality Parameters

Select seasonal water quality parameters for summer and fall 2020 across sites are displayed in Table 1. Total Nitrogen (TN) was higher at the agricultural sites and greater in the summer than the fall, with Nissouri Creek defined by higher nitrate concentrations (4.65 mg L⁻¹ and 1.01 mg L⁻¹ for summer and fall, respectively), but with Big Creek defined by higher ammonium (130 mg L⁻¹ and 36.3 mg L⁻¹ for summer and fall). Total phosphorus (TP) and soluble reactive phosphorus (SRP) concentrations were also higher at the agricultural sites, with Big Creek exhibiting greater levels in the summer (0.16 mg L⁻¹ and 0.05 mg L⁻¹ for TP and SRP, respectively) and Nissouri Creek higher levels in the fall (0.46 mg L⁻¹ and 0.17 mg L⁻¹). Stable isotope analysis for surface waters were consistent seasonally for Nissouri Creek and the Saugeen River but varied from summer to fall for Big Creek, showing an increase in $\delta^{15}\text{N}$ and $\delta^{18}\text{O}$ values.

5.3.2 DNA and rDNA Microbial Community Comparisons

DNA and rDNA metabarcoding produced 111 samples with an average sequence count of 49,687 sequences per sample (max = 282460, min = 6193), with all sample groups having a minimum of three replicates. Annotation in QIIME2 yielded 5624 taxonomic features, comprising 3453 genera within 76 phyla. Shannon diversity was greater overall in DNA samples compared to rDNA samples ($p = 0.00483$), and substrate diversity was in the order bed sediment > suspended sediment > surface water (Figure 1). NMDS ordination of samples by nucleic acid type and substrate is shown in Figure 2. There was greater overlap between DNA and rDNA samples for bed sediments than for suspended sediments or surface water.

PERMANOVA test showed high dissimilarity between sample groups. Substrate type (i.e., bed sediment, suspended sediment, or surface water) and nucleic acid type (i.e., DNA vs. rDNA) accounted for most differences between samples. Communities were nearly always significantly different between summer and fall within a site, with the

exception of Saugeen River bed sediments, where summer DNA and fall DNA communities were not significantly different, nor were summer rDNA and fall rDNA communities, and for Nissouri Creek bed sediments, where summer DNA and fall DNA communities were not significantly different ($p > 0.05$). Surface water microbial communities were all statistically different between summer to fall within a site.

Mantel test results for DNA and rDNA-generated distance matrices by substrate are shown in Figure 3. Suspended sediments yielded the highest Spearman correlation between DNA and rDNA communities ($r = 0.7619$, $p = 0.007$), followed by surface waters ($r = 0.548$, $p = 0.001$) and bed sediments ($r = 0.2609$, $p = 0.007$).

5.3.3 Active Microbial Community Investigations

Figure 4 displays the abundance of active, neutral, and non-active microbial genera across samples, as determined by comparing DNA and rDNA communities. On average, bed sediment samples had a higher abundance of active and neutral taxa (39% and 44%, respectively), surface waters had a higher abundance of non-active and active taxa (39% and 38%) and suspended sediments had a higher abundance of active taxa (43%). For surface waters, the proportion of non-active taxa was higher in Fall samples than summer samples. The proportion of non-active and neutral taxa was greater than 50% of the community in all sample groups.

Bed sediment active microbial genera for summer and fall are displayed in Figure 5a and 5b, respectively, for the three sites and ordered by LEfSe LDA score. There were more active genera observed in summer than fall. For summer sediments, only 3 genera were shared across sites, *Dechloromonas*, *Chryseolinea*, and *Brevinema*. The rest of the active taxa were either shared by two of the three sites, or unique to one. At Big Creek, Nissouri Creek, and Saugeen River, 28, 13, and 38 unique active genera were identified, respectively. For Big Creek, *Thiobacillus*, *Aquabacterium*, *Rhizobacter*, *Comamonas*, and *Leptothrix* were identified as the top 5 active biomarker genera. For Nissouri Creek, *Magnetococcus*, *Nitrosospira*, *Azoarcus*, *Zoogloea*, and *Roseimarinus* were the top 5. For the Saugeen River, the genera were *Ferritrophicum*, *OLB12*, *Calothrix_UAM_374*, *Acidibacter*, and *Bacteroidetes_bacterium_GWF2_49_14*. For Fall bed sediments, no active genera were shared by all three sites, with only *Limnobacter*, *Nitrosomonas*, and

pLW_20 being common across Big Creek and Nissouri Creek. Big Creek and Nissouri Creek had 20 and 17 active genera, respectively, with Saugeen River only exhibiting a single significant active biomarker, Thioploca. Big Creek was characterized by Sulfuritalea, Aquabacterium, Thiobacillus, Sideroxydans, and Dechloromonas, with Nissouri Creek by an uncultured_soil_bacterium, MND1, Methanoregula, Pirellula, and Smithella.

5.3.4 Metatranscriptomics Overview

Summer and Fall bed sediments metatranscriptomics samples are summarized in Table S1. Samples had an average protein-coding read count of 115,712, with one sample removed due to low sequences. Figure 6 shows a heatmap of Level1 functional categories across sample groups, scaled based on the deviation of the samples from the average normalized expression of the functional category. For Big Creek, summer sediments showed high relative expression of Nitrogen Metabolism, Protein Metabolism, and Sulfur Metabolism genes, as well as genes related to the Phages Prophages Transposable Elements Plasmids and Stress Response categories. Fall Big Creek sediments showed greatest expression within Photosynthesis, Respiration, and Phosphorus Metabolism categories. For Nissouri Creek, summer showed higher expression of the categories Carbohydrates, Motility and Chemotaxis, and Cell Division and Cell Cycle, with fall sediments characterized by Virulence Disease and Defence and Potassium Metabolism. For the Saugeen River, summer sediment showed lower relative expression across categories compared to other samples, but with high expression within Nitrogen Metabolism and Motility and Chemotaxis. Fall sediments showed similar trends to Nissouri Creek fall sediments, highlighted by high relative expression within Metabolism of Aromatic Compounds, Amino Acids and Derivatives, and Fatty Acids Lipids and Isoprenoids. Overall, differential feature analysis using DESeq2 showed more significant L1 differences between BC and NC ($n = 17$) and BC and SR ($n = 14$) than NC and SR ($n = 7$) ($p < 0.05$). L4 genes classified under nitrogen, phosphorus, and sulfur metabolism were further analyzed for differential expression across sites and seasons.

5.3.5 Spatial and Temporal Expression in N, P, and S Metabolism in Bed Sediments

5.3.5.1 Summer Metatranscriptomic Profiling

For Summer there were 20 genes differentially expressed across site sediments: 6 N-metabolism genes, 2 P-metabolism genes, and 12 S-metabolizing genes (Figure 7A). For N-metabolism, dissimilatory nitrate reduction to ammonia (DNRA) was the main pathway that showed differences across sites. Big Creek exhibited significantly greater abundance of the membrane-bound nitrate reductase (*narH*) alpha and beta chain genes involved in the microbial conversion of nitrate to nitrite, as well as greater abundance of the periplasmic nitrate reductase (*napA*) along with the Saugeen River. A Ferredoxin 3 gene and hydroxylamine reductase (*hao*) classified under nitrosative stress were significantly more abundant at Nissouri Creek, though *hao* was also greater at Big Creek than the Saugeen River. Nitrous-oxide reductase (*nosZ*) involved in the final step of denitrification showed greater abundance at Big Creek and the Saugeen River than Nissouri Creek. For P-metabolism, a pyrophosphate-energized proton pump gene (*hppA*) was significantly more abundant at Nissouri Creek, and a phosphate ABC transporter, periplasmic phosphate-binding protein (*PstS*) showed higher abundance at Big Creek. For S-metabolism genes, a set of sulfur-oxidation and reduction genes showed greater abundance at Big Creek than both Nissouri Creek and the Saugeen River (*SoxA*, *SoxB*, molybdopterin C, *SoxX*, *SoxZ*, *SoxD*, *SoxY*, glutamate synthase (with sulfite), and alkyl hydroperoxide reductase). Sulfate adenylyltransferase (dissimilatory-type) and adenylylsulfate reductase (alpha-subunit) were highly abundant across all 3 sites, but greatest at Nissouri Creek.

5.3.5.2 Fall Metatranscriptomic Profiling

For Fall sediments, 42 genes exhibited differential abundance across sites: 16 N-metabolism genes, 12 P-metabolism genes, and 14 S-metabolism genes (Figure 7B). DNRA was again the main pathway showing differences within N-metabolism, with *narH* (beta chain) and *napA* exhibiting greater abundance at Big Creek, but a nitrate ABC transporter and nitrite reductase *nir* (large subunit) being higher at Nissouri Creek and the Saugeen River. Under nitrosative stress, *hao*, which is also involved in ammonia transformation, was highly expressed across all sediments, but lowest at Nissouri Creek. Ferredoxin 3 and a nitric oxide-dependent regulator (*DnrN* or *NorA*) were also lower at Nissouri Creek than Big Creek and the Saugeen River. Like summer, the denitrification

pathway showed a higher abundance of *nosZ* at Big Creek and Nissouri Creek, but also shifts in a Cu-containing nitrite reductase (*nirK*) and a nitric-oxide reductase (*norB*, quinol-dependent), which were most expressed at Big Creek and Saugeen River, respectively. Significant genes involved in ammonia assimilation/oxidation were glutamate-ammonia-ligase adenylyltransferase (*glnE*), nitrogen regulation protein NR(I), and an ammonium transporter, all of which showed greater abundance at Nissouri Creek and the Saugeen River and low expression at Big Creek. The N-fixation pathway showed a similar trend to ammonia assimilation/oxidation: *nifE*, *nifA*, and *nifB* all showed high abundance at Nissouri and Saugeen and less expression at Big Creek.

For P-metabolism, two primary pathways comprised differences between sites: Phosphate/Phosphonate Metabolism and P-uptake and Transport. Under Phosphate/Phosphonate Metabolism, *hppa* was highly expressed across sites, but most abundant at Big Creek, with a similar trend seen in an inorganic pyrophosphatase (PPase), and an NAD(P) transhydrogenase alpha subunit. A Mn-depednent PPase and a low-affinity inorganic phosphate transporter were more abundant at Big and Nissouri Creek and less abundant at the Saugeen River. An exopolyphosphatase and 2-aminoethylphosphonate:pyruvate aminotransferase (*phnW*) were more abundant at Nissouri and Saugeen, and less expressed at Big Creek. Under P-uptake and Transport, all significant genes were in higher abundance at Nissouri Creek and the Saugeen River, with low relative expression at Big Creek. This included an alkaline phosphatase (ALP) and *PstS* involved in P-uptake, and a phosphate regulon sensor (*SphS*), and phosphate transport permeases (*PstA*, *PstC*) involved in the high affinity phosphate (PHO) transporter regulon.

For S-metabolism, fewer genes involving sulfur-oxidation/reduction were differentially expressed across sediments than in the summer. *SoxY*, a sulfide dehydrogenase, *DsrK*, and a glutamate synthase [NADPH] clustered with sulfite reductase were all more abundant at Big Creek than Nissouri Creek, with intermediate expression at Saugeen River. Within “Inorganic Sulfur Assimilation”, sulfate adenylyltransferase (dissimilatory-type) and adenylylsulfate reductase (alpha-subunit) were again highly abundant across all 3 sites, but greatest abundance was measured at Big Creek opposed to Nissouri Creek as seen in the summer. The 4Fe-4S ferredoxin also exhibited this trend.

However, a putative sulfate permease and a sulfate/thiosulfate import ATP-binding protein (CysA) showed higher abundance at Nissouri Creek and Saugeen River. The remaining S-metabolism genes spread across “Glutathione Utilization”, “Taurine Utilization”, “Alkanesulfonate Assimilation”, and “Thioredoxin-disulfide Reductase” were more abundant at Nissouri Creek and the Saugeen River and in low abundance at Big Creek. The exception was alkyl hydroperoxide reductase, which was higher expressed at Big Creek and Saugeen River and lower at Nissouri Creek.

5.4 Discussion

5.4.1 Microbial Diversity Across Source Material and DNA/RNA

rDNA microbial communities in this study showed lower diversity than their DNA counterparts across bed sediments, suspended sediments, and surface waters. This observation aligns with our hypothesis that RNA extraction-based communities should represent only a subset of the entire microbial community at any given time. The contrast between DNA and rDNA community diversity was greatest in surface water samples, which is suggested to be caused by the dynamic nature of lotic systems. Niche theory dictates that species selection is high when environments are influenced by extreme deterministic factors, such as in rivers, where flow is the primary control of environmental filtering (Stegen et al., 2012). Thus, biota will become more specialized if they are to survive and reproduce. This specialization shrinks the diversity of the active community, which is observed here in low rDNA Shannon diversity in surface waters across sites. The higher surface water diversity observed from DNA is likely driven by the allochthonous members; microorganisms that are sourced from banks, soils, vegetation, etc. or even from bed sediments. These microbes may not be relevant to in-stream biogeochemical functioning, as their niche belongs outside of the river environment. As they are only transient community members, caution should be taken if inferences about in-situ stream functioning is based solely on DNA metabarcoding or metagenomics from surface water collection, as the proportion of estimated dead taxa in these samples was 39% of detected features, a value that is very similar to studies of soils microbiomes that recorded 40% “relic” DNA (Carini et al. 2016). One exception however is the effect of dead/dormant allochthonous microorganisms on stream food webs, where they can serve as an additional source of labile carbon/nutrients even when deceased (Lennon et al., 2018).

Bed sediments are more stable than surface waters yet vary physically and chemically over small spatial scales (Oest et al., 2018), which supports a variety of niches. Additionally, dispersal is more restricted, and cells are retained in the environment even if they are not active (Wang et al., 2021). These factors likely drove the high diversity and higher relatedness between DNA and rDNA bed sediment communities across sites, as observed visually in the NMDS and from PERMANOVA results that showed fewer community differences between bed sediments than surface waters over time. Suspended sediments have attributes of both bed sediments and surface waters and rDNA alpha diversity was intermediate between the two. In summary, DNA-based surveys likely provide better insights into microbial functioning in sediments than in surface waters but may require higher sample numbers due to physico-chemical heterogeneity.

Mantel tests found a higher correlation between suspended sediment DNA/rDNA distance matrices ($R=0.7619$) and between surface water DNA/rDNA distance matrices ($R=0.548$), with a weaker correlation between bed sediment DNA/rDNA ($R=0.2609$) (Figure 3). These results seemingly contradicted the observations from NMDS ordination and PERMANOVA tests, which both suggested that bed sediment microbes share a higher degree of similarity between DNA and rDNA samples. One explanation for this is in the interpretation of the Mantel test results. A higher correlation between two community composition distance matrices, in this case DNA and rDNA matrices, means that the taxa within the samples of the groups may respond in similar ways over space and time, and not that they are similar in taxa abundance or community composition. In other words, the primary selective pressures on suspended sediment and surface water microbes are more consistent regardless of site, season, or nucleic acid type, whereas in bed sediments, the forces that differentiate communities are more nuanced and difficult to quantify. Thus, Mantel correlation statistics fail to align bed sediment microbial samples with the site-specific factors that drive them, due to the high diversity and heterogeneity in this environment. Alternatively, the less diverse surface water sample communities are influenced in similar ways even at different sites and when analyzed from different nucleic acids. In all, Mantel test results support the alpha and beta diversity comparisons of microbial communities and show that lotic systems can exhibit discrepancies between DNA and RNA-based metabarcoding methods.

5.4.2 Significantly Active Taxa across Season and Sites

Analysis of the rDNA samples showed a greater variety of active bacterial genera detected in summer sediments than fall sediments across sites as observed in Figures 5a, 5b. This could be due to temperature and/or substrate availability, as surface waters were warmer and concentrations of TN and SO₄ were higher in the summer, resources which increase productivity and cellular growth potential (Muscarella et al., 2019). Yet despite the diversity exhibited in active bed sediment taxa, only 3 genera were common among the 3 sites in the summer (*Dechloromonas*, *Chryseolinea*, and *Brevinema*), and none in the fall. *Dechloromonas* is a mainstay taxon identified in many sediment contamination studies and is known to have wide metabolic versatility, including denitrification (Huang et al., 2018; Zhang et al., 2021), and has been shown to interact with keystone taxa in metal-stressed environments (Cyriac et al., 2020). It's confirmed here that *Dechloromonas* is not only present, but is active across site sediments, lending additional support that this genus is a key player in lotic sediment biogeochemical cycling. *Chryseolinea*, and *Brevinema* are less frequently mentioned taxa across literature searches, but have been identified in higher abundance in wastewater treatment bioreactors and constructed wetlands where C:N ratios are low (Xu et al., 2018; Yang et al., 2018; Zhong et al., 2016). Saugeen River sediments were characterized by many unique active genera in the summer, but only one (*Thioploca*) in the fall, while Big Creek had more of the same active genera detected seasonally. Saugeen River served as the natural reference site with lower agricultural impacts while Big Creek was considered the most altered landscape based on nutrient concentrations and altered drainage from tiling. The contrasting seasonal turnover in active genera may be influenced by these factors, with Big Creek exhibiting less of a change in it's sediment microbiome due to consistent anthropogenic stressors year-round, while the Saugeen River undergoes a more natural temporal shift.

5.4.3 Metatranscriptomic Analysis of Sediment Microbial Gene Expression

5.4.3.1 Overview

Bed sediments of lotic systems provide a medium for matter accumulation and exchange with the water column and were shown to contain highly diverse microbial communities. Thus, gene expression investigations via shotgun metatranscriptomics were carried out in bed sediments during summer and fall across the three sites.

5.4.3.2 Big Creek

Nitrate reduction coupled to Sulfur oxidation was found to be a main microbial metabolic pathway in Big Creek bed sediments. Both denitrification and DNRA are likely co-occurring, but the extent of DNRA coupled to sulfur oxidation is dominant as evidenced by differential expression of *narH* and *napA* transcripts, higher concentrations of ammonia in the water column, and a lower redox state which favours DNRA (Biessy et al., 2022). It's also likely that respiratory DNRA is occurring over fermentive DNRA due to the lower availability of total organic carbon (TOC) and NO_3 at BC. Reduced FeS mineral phases could be the electron donors for nitrate reduction (Bosch et al., 2012), as Fe oxidation-reduction fronts were visualized in surface sediments, as were micron-sized framboid-like minerals from previous scanning electron microscope (SEM) investigations (Figure S2). Concomitant S-reduction may also be occurring at lower sediment depths to cycle SO_4 and/or elemental S back into reduced FeS, as genes for sulfate reduction were also differentially expressed, and Big Creek sediments have exhibited low oxidation-reduction potentials (ORP) in the range expected for sulfate reduction. These observations are further supported by the abundance of active S-oxidizing and N-reducing taxa observed in the summer and fall from rDNA analysis, including *Thiobacillus*, *Sulfuritalea*, *Aquabacterium*, *Sideroxydans*, and *Dechloromonas*, as well as a trend of elevated $\delta^{15}\text{N}$ and $\delta^{18}\text{O}$ values from summer to fall which is a signature of microbially mediated N-reduction (Mayer et al., 2002). Studies within Big Creek have observed decreasing N loads over time (Nelligan et al., 2021) which is supported here by the differential expression of a *nosZ* gene involved in the conversion of N_2O to N_2 , which can remove N from the system. In summary, DNRA as an ammonia producing pathway and denitrification as a N removal pathway are tightly coupled to S oxidation-reduction in Big Creek sediments, and the microbial genera responsible have been identified.

The periplasmic phosphate-binding protein PstS showed higher expression at Big Creek in the summer compared to expression at Nissouri Creek and the Saugeen River. This could be a single of P-stress (Steffen et al., 2017), as Big Creek shows current and historical high loads of TP.

5.4.3.3 Nissouri Creek

The L1 functional heatmap showed a more varied bed sediment microbial community at Nissouri Creek, with lower N and S metabolism than Big Creek, but high expression of Carbohydrate, Motility and Chemotaxis, Cell Division, and RNA metabolism pathways in the summer, and Potassium Metabolism, Virulence Disease and Defence, and DNA Metabolism in the fall. This suggests a diverse and growing community less centrally reliant on N and S cycling. Higher NO₃ concentrations in the water column and higher sediment TOC and labile P observed in a previous study (Falk et al., 2021) may be driving the functional diversity observed in sediments at Nissouri Creek, as has been seen in analogous research (Meng et al., 2020; Tu et al., 2022). Despite NO₃ being readily available, denitrification and DNRA genes were detected in lower abundance than Big Creek and Saugeen River sediments, as were S-oxidation genes. Rather, Nissouri Creek sediments were characterized by nitrosative stress and S-assimilation genes in the summer, when TN and SO₄ concentrations were high. The S-assimilation genes (Sulfate adenylyltransferase and adenylylsulfate reductase) are known to be involved in sulfate reduction, which may be favoured in summer Nissouri Creek sediments in the absence of NO₃ reduction. Further, microbial communities seem to be affected by reactive nitrogen oxide species in the summer, thus rather than abundant NO₃ being reduced completely to N₂, N-intermediates are accumulating in cells; evidence of an N-excess (VanMensel et al., 2020). Contributing to this may be the N-oxidizing genus *Nitropsira*, which was in high abundance in summer Nissouri Creek sediments and corresponded with increased expression of the ammonia oxidizing *hao* gene. These N-stress effects however appeared dampened in the fall, coinciding with lower NO₃ and TN concentrations in the water column. These trends also support increase N-fixation genes at Nissouri Creek in the fall, which could provide bioavailable N to sediments under seasonal limitation.

P genes at Nissouri Creek showed that the membrane-bound pyrophosphatase *hpa* and the periplasmic phosphate-binding protein *PstS* were in higher abundance in summer when SRP was lower relative to the fall. Alternatively, several P-uptake and transport genes (*ALP*, *SphS*, *PstA*, *PstC*) were differentially expressed in the fall in response to higher relative SRP concentrations. Contradictory to observations at Big Creek, *PstS* appeared to increase in response to lower seasonal SRP concentrations at Nissouri Creek (0.02 mg L⁻¹

in the Summer vs. 0.17 mg L⁻¹ in the fall), indicating a response to P-limitation that has been observed in other studies (Harke et al., 2016).

5.4.3.4 Saugeen River

Saugeen River sediments exhibited increased N and S metabolism pathways in the summer and increased P-metabolism in the Fall. Saugeen was also characterized by a large seasonal shift in many cellular processes including those under Amino Acids and Derivatives, Cofactors Vitamins Prosthetic Groups Pigments, and Fatty Acid Lipids and Isoprenoids (Figure 6). N cycling genes under DNRA and denitrification appeared to be consistent seasonally, however ammonia processing and N-fixation genes showed an increase relative to Big Creek and Nissouri Creek in the fall. As external sources of TN are lower within the Saugeen River due to less intensive agriculture, N-fixation may be necessary to supply bioavailable NH₄⁺, which also increased the expression of ammonia oxidation (hao) in the fall. Lower average available NO₃ may also require microbial communities to utilize low-affinity N-reductases, such as napA which showed high differential expression in Saugeen River sediments in summer and fall. Interestingly, the only differentially expressed active bacterial genera detected in fall Saugeen sediments was the N-reducing and S-oxidizing Thioploca (which was also active in summer Saugeen River sediments). This genus can accumulate NO₃ within intracellular vacuoles to be used as electron acceptors (Devol, 2015; Zhu et al., 2018). Thioploca is thus likely behind the abundance of napA expression and sulfur-oxidation at Saugeen, particularly during the fall. Further, Thioploca may be a keystone microbe in fall Saugeen sediments and provide oxidized S species to the community in scenarios where SO₄ concentrations are low, such as was observed at this site. Though this role needs to be further investigated, Thioploca is no doubt an important member of Saugeen River sediment communities.

With respect to P-cycling, Saugeen River sediment microbial assemblages responded to higher relative fall SRP concentrations with increased uptake and transport genes. However, the phosphate-binding protein PstS did not change significantly between summer and fall, as it did at Big Creek and Nissouri Creek. The expression of PstS in sediment microbial communities is therefore predicted to be site-specific, and perhaps is dependent on past states of P-availability rather than measurements of present SRP in the

water column (i.e., a hysteresis effect). For example, the Nissouri Creek SRP concentration measured in summer 2020 (0.02 mg L^{-1}) was slightly lower compared to the growing season site average of 2019 (0.03 mg L^{-1}), as was the sediment EPC_0 average (0.037 mg L^{-1} in 2019 vs. 0.015 mg L^{-1} in 2020). The same could be said about Big Creek sediments, where both surface water SRP and EPC_0 values were lower in summer 2020 compared to previous measurements in 2019. Thus, the tipping point for PstS expression indicating sediment P-limitation may coincide with both a lower surface water concentration of SRP, as well as a lower P-desorption potential, and perhaps reside within the values measured here. In this case, Big Creek P-limitation may involve an SRP concentration $< 0.08 \text{ mg L}^{-1}$ and an $\text{EPC}_0 < 0.0008 \text{ mg L}^{-1}$, while at Nissouri Creek involve an SRP concentration $< 0.02 \text{ mg L}^{-1}$ and an $\text{EPC}_0 < 0.004 \text{ mg L}^{-1}$. However, these values need further data collection for confirmation. Saugeen River sediments showed no significant seasonal change in PstS expression yet was higher than Big Creek and Nissouri Creek in the fall when SRP concentrations were higher than average. It's concluded that the mechanisms involved in this phosphate-binding protein cannot be explained by water column SRP concentrations alone, and that further investigations of sediment bioavailable P are necessary to fully understand expression patterns. However, its relevance in systems of dynamic nutrient regimes should not be ignored.

5.4.3.5 Land-Use Implications

Sediments within non-manure amended systems may be characterized by lower total organic carbon (TOC), and by extension, lower organic P, as was observed from sediments from the sites of this study (Falk et al., 2021). Lower TOC can impact microbial community energetics, and specifically in this case, can favour respiratory DNRA over denitrification, which removes less N from headwaters but produces ammonia. In manure-amended systems, fertilizer can be applied on an N-based rate (Agudelo et al., 2011), thus excess P may be added to soils and stored in streams of these watersheds. Previous research has suggested this, with Nissouri Creek sediments being elevated in total P compared to Big Creek and the Saugeen River, with higher composition of labile and reducible P, which is more bioavailable. As abundant NO_3^- exists within the Nissouri Watershed, a shift to a dominant denitrifying microbial community could serve to decrease NO_3^- over time (a shift that is occurring at Big Creek) and reduce the redox buffering capacity of N-species on

sediment P-release. Thus, any N-reduction strategies in manure-amended watersheds should take into account sediment P-reservoirs and P-forms (including sediment porewater), as well as sediment redox conditions.

5.5 Conclusions

The fate of N and P in river waters and sediments are intrinsically tied to the functioning of microbial assemblages. Here, both DNA and RNA-based extractions of microbial communities in surface waters, suspended sediments, and bed sediments, have identified the most active taxa as a proportion of the whole community in each river reservoir, and have identified the key metabolic pathways associated with N and P cycling in bed sediments over two seasons via metatranscriptomics.

Alpha diversity was found to be highest in bed sediment and lowest in surface waters, and 17% and 39% of detected features were estimated to be non-active in sediments and surface waters, respectively. Suspended sediments and surface water samples however showed a higher Mantel test correlation between DNA and rDNA communities across all samples, suggesting that environments characterized by flow are more similar to each other over space and time with respect to the selective pressures on microbial communities than are bed sediments. The high abundance of non-active taxa detected in surface waters suggests that DNA-based approaches alone should not be used to infer function in these environments.

Site bed sediments showed a diverse community of active taxa from RNA extractions, with the reference forested site, Saugeen River, showing the greatest number of unique bioindicator taxa in the summer, but the least in the fall, suggesting a high seasonal turnover. The bacterial genera *Dechloromonas*, *Chryseolinea*, and *Brevinema* were the only active taxa detected across all sites in the summer, with *Limnobacter*, *Nitrosomonas*, and pLW_20 shared between the agriculturally-impacted sites in the fall. These represent possible keystone genera in Southern Ontario river bed sediments, particularly *Dechloromonas*, which possesses a functionally diverse genome.

Metatranscriptomics identified that N-cycling genes contributed more to differences between site bed sediments than P-cycling genes. Big Creek sediments were

characterized by abundant DNRA linked to sulfur oxidation, likely driven by *Thiobacillus*, *Sulfuritalea*, *Aquabacterium*, *Sideroxydans*, and *Dechloromonas*, which could serve to remove NO_3 but produce NH_4 . Nissouri Creek bed sediments microbial communities experienced seasonal nitrosative stress, possibly a symptom of legacy summertime N-pollution in the watershed, with the N-oxidizing genus *Nitropsira* being highly active. Saugeen River bed sediments showed a strong presence of DNRA, denitrification, and N-fixation genes seasonally, which is suggested to be in responses to low available N in the system. The N-reducing and S-oxidizing genera *Thioploca* was detected as a bioindicator in Saugeen sediments, thus is likely highly integrated with N and S cycling. Many P metabolism and uptake/transport genes showed high expression cross sites, indicating their importance to universal cell functioning, with increased abundance at Nissouri Creek and Saugeen River in the fall coinciding with relative rises in water column SRP concentrations.

Finally, when the active microbial communities were more diverse across sites in the summer, there were fewer detectable difference in N, P, and S cycling genes between sites. This suggests that a more diverse community broadens its function horizons and becomes less specialized, resulting in a higher functional overlap with communities of similarly high diversity (Figure 8). This concept however is only testable using RNA-based microbial techniques, as they represent the living community members that contribute to functional diversity.

In summary, assemblages of microbes in river waters and sediments respond to and alter vital macronutrients including N and P. Combining genomic techniques (DNA/RNA metabarcoding, metatranscriptomics) with measurements of N and P speciation, including isotopic compositions of waters, can illuminate the primary metabolic pathways involved in nutrient transformations in stressed environments, and in the future, guide assessments and remediations surrounding freshwater resources.

Acknowledgments

The authors acknowledge Great Lakes Institute for Environmental Research (GLIER) technicians Sharon Lackie (SEM), Jonathon Leblanc (IGF), and Nargis Ismail

(OANL) for aid in sample preparation and analysis, and field and lab assistants Stephanie Aldea and Bryce Ducharme. Research was supported through a NSERC Strategic partners Grant (STP 521430-18).

FIGURES AND TABLES

Table 1

Seasonal Water Quality Parameters for Big Creek, Nissouri Creek, and the Saugeen River

Parameter	Season	Big Creek	Nissouri Creek	Saugeen River
Temp (°C)	Summer	26 (0.1)	20.4 (0.2)	24.0 (0)
	Fall	13.8 (0)	10.1 (0)	9.7 (0)
ORP (mV)	Summer	104.2 (0.7)	19.7 (1.6)	18.3 (1.6)
	Fall	109.4 (0.3)	258.4 (0.4)	213.1 (0)
Conductivity (µS cm ⁻¹)	Summer	506.8 (1)	578.8 (2.4)	238.8 (21.1)
	Fall	517.8 (0.1)	508.9 (0.2)	327.9 (0.1)
pH	Summer	8.67 (0)	9.06 (0.04)	9.12 (0.01)
	Fall	8.91 (0.01)	9.43 (0.03)	9.35 (0.03)
DO (mg L ⁻¹)	Summer	9.01 (0.03)	10.46 (0.08)	10.89 (0.05)
	Fall	10.55 (0.02)	12.34 (0.03)	11.39 (0.01)
fDOM (µg L ⁻¹)	Summer	69.73 (0.55)	33.62 (0.13)	60.46 (0.04)
	Fall	86.57 (0.31)	83.36 (0.03)	114.06 (0.11)
NO ₃ (mg L ⁻¹)	Summer	1.8 (0.14)	4.65 (0.07)	0.2 (0)
	Fall	0.35 (0.005)	1.01 (0.004)	0.23 (0.003)
NO ₂ (µg L ⁻¹)	Summer	< 25	< 25	< 25
	Fall	3.1 (0.19)	1.5 (0.3)	0.9 (0.05)
NH ₄ (µg L ⁻¹)	Summer	130 (0)	30 (0)	20 (0)
	Fall	36.3 (14)	16.4 (3)	24.5 (3)
TON (mg L ⁻¹)	Summer	0.95 (0.07)	0.3 (0)	0.4 (0.14)
	Fall	0.35 (0.005)	1.02 (0.004)	0.23 (0.003)
TN (mg L ⁻¹)	Summer	2.75 (0.21)	4.95 (0.07)	0.6 (0.14)
	Fall	0.94 (0.02)	1.21 (0.02)	0.62 (0.01)
δ ¹⁵ N (‰)	Summer	5.6	13.9	5.6
	Fall	11.7	11.1	7.4
δ ¹⁸ O (‰)	Summer	3.3	3.2	1.8
	Fall	18.8	3.1	2.2
SRP (mg L ⁻¹)	Summer	0.05 (0.004)	0.02 (0.004)	0.007 (0.005)
	Fall	0.08 (0.0006)	0.17 (0.004)	0.02 (0.004)
TP (mg L ⁻¹)	Summer	0.16 (0.01)	0.06 (0)	0.005 (0)
	Fall	0.19	0.46	0.05
SO ₄ (mg L ⁻¹)	Summer	32 (0)	30 (0)	5 (0)
	Fall	19.4 (0.2)	8.4 (0)	1.7 (0)

ORP = oxidation-reduction potential

DO = dissolved oxygen

TON = total organic nitrogen

SRP = soluble reactive phosphorus

fDOM = Fluorescent Dissolved Organic Matter

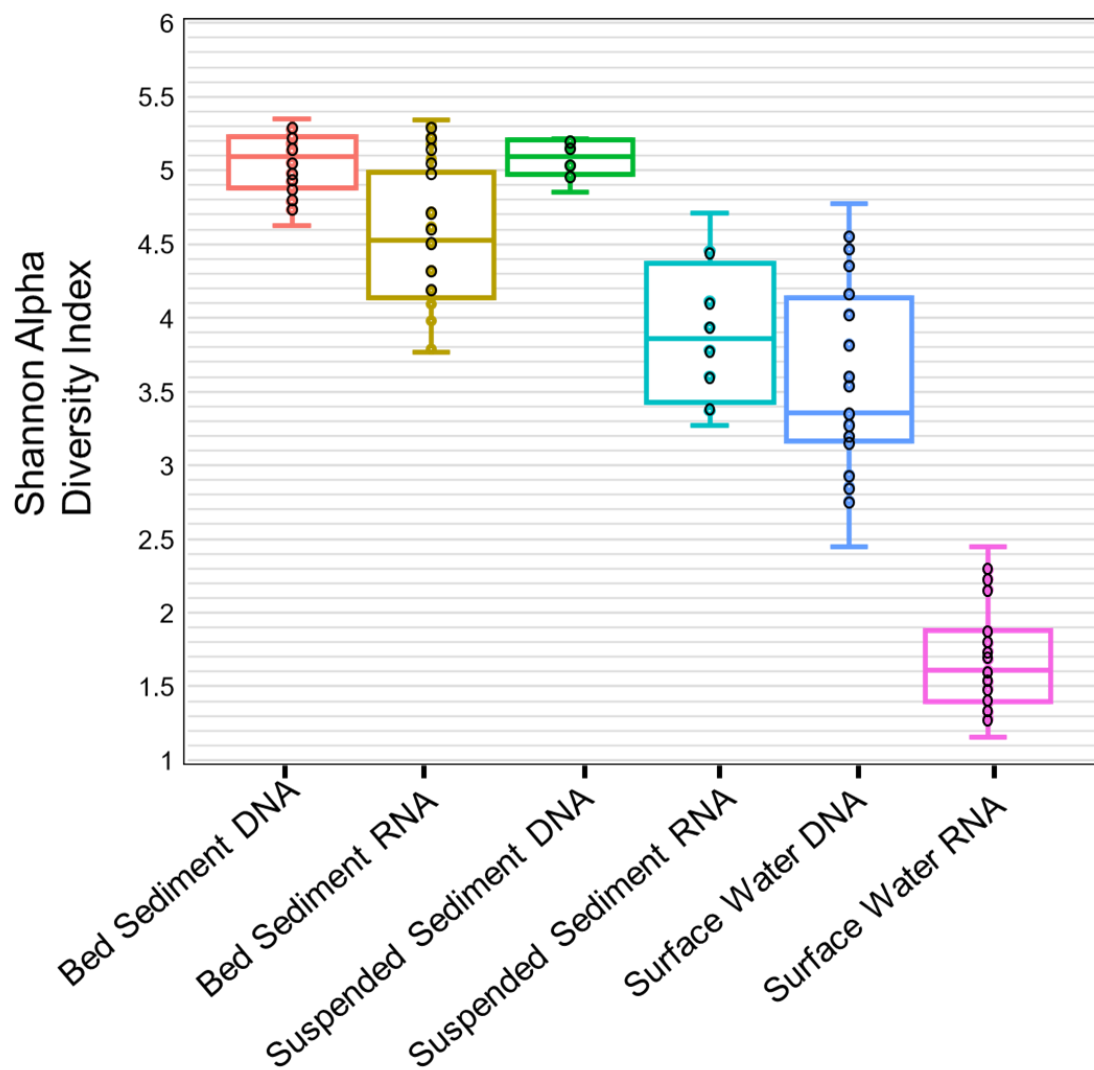


Figure 1: Microbial community Shannon (H) alpha diversity distribution for substrate (bed sediment, suspended sediments, surface water) and nucleic acid type (DNA, RNA) across samples.

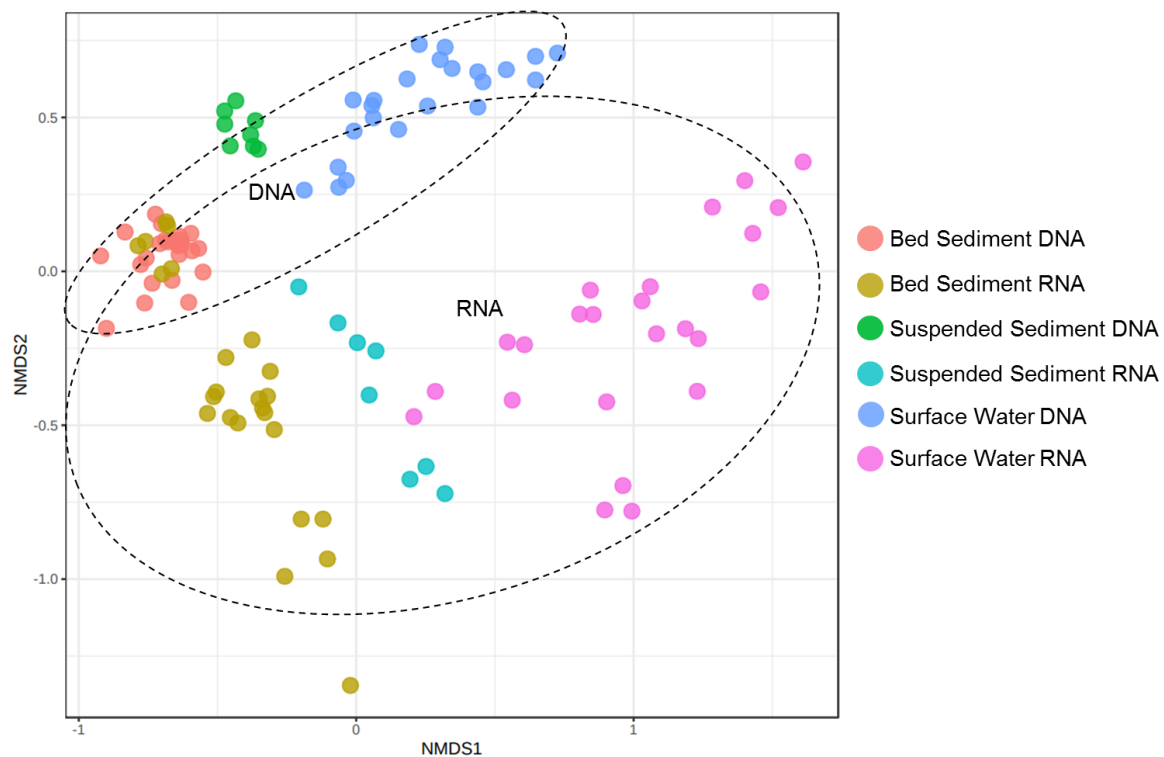


Figure 2: NMDS ordination of microbial community samples across substrate (bed sediment, suspended sediments, surface water) and nucleic acid type (DNA, RNA). Ellipses represent 95% confidence intervals for DNA and RNA-based samples.

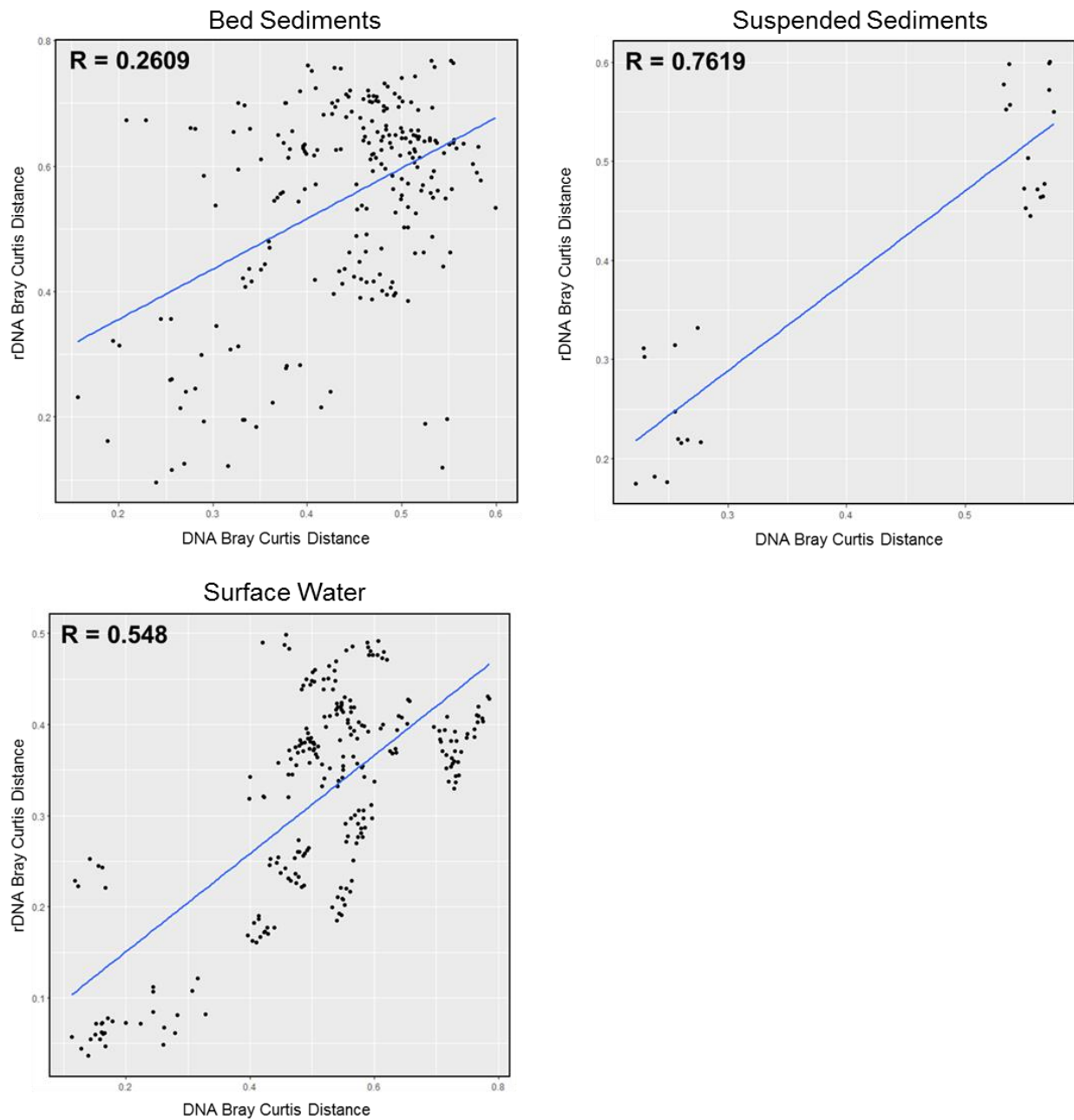


Figure 3: Mantel tests between DNA and RNA microbial community Bray Curtis distances for bed sediments, suspended sediments, and surface water samples. R value represents the Spearman correlation between distance matrices.

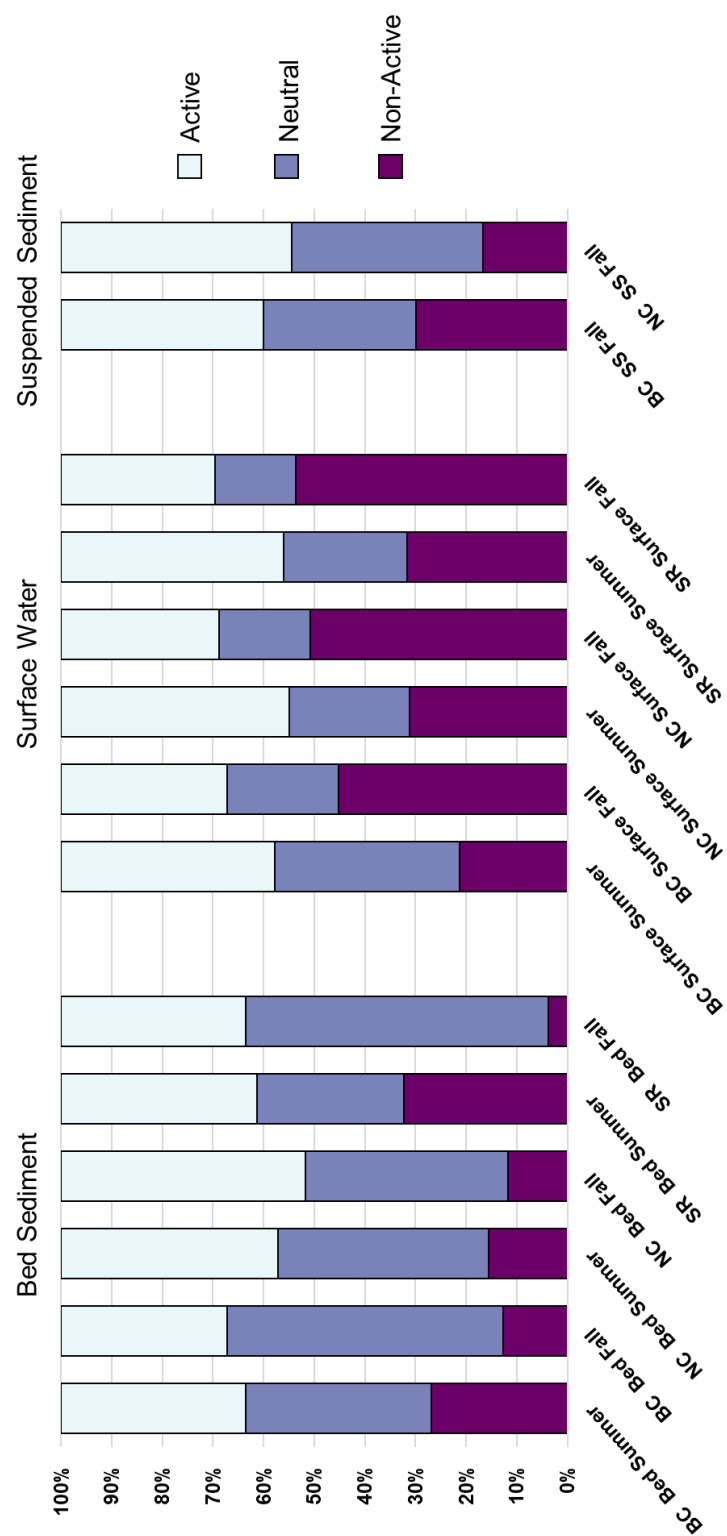


Figure 4: Abundances of active, neutral, and non-active microbial genera across sample groups.



Figure 5a: Summer shared and unique active microbial genera for Big Creek, Nissouri Creek, and Saugeen River bed sediments, ordered by LefSe LDA score. LDA scores represent the effect size of the genera abundance, with higher LDA scores indicating a stronger association with the site.

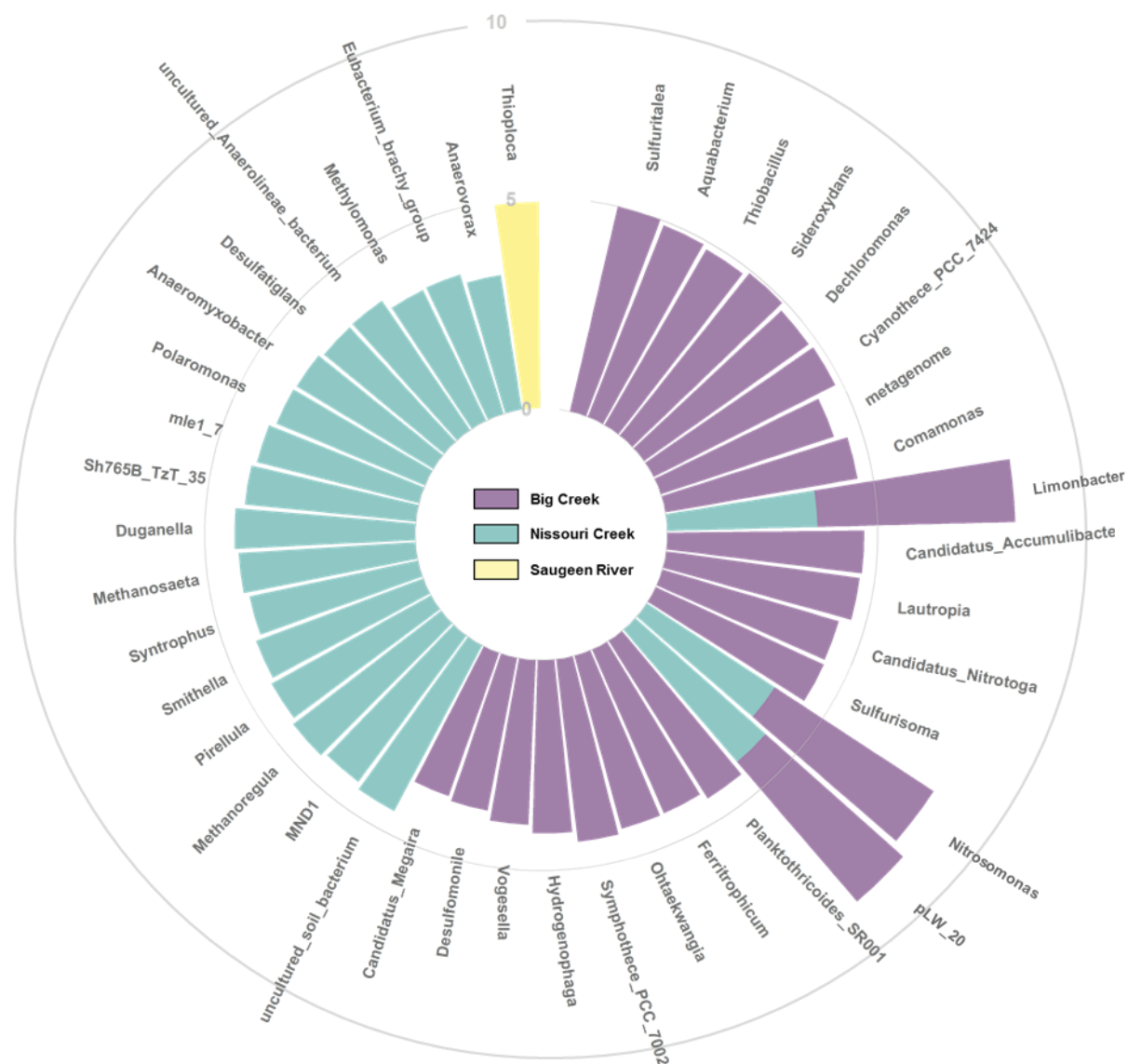


Figure 5b: Fall shared and unique active microbial genera for Big Creek, Nissouri Creek, and Saugeen River bed sediments, ordered by LefSe LDA score. LDA scores represent the effect size of the genera abundance, with higher LDA scores indicating a stronger association with the site.

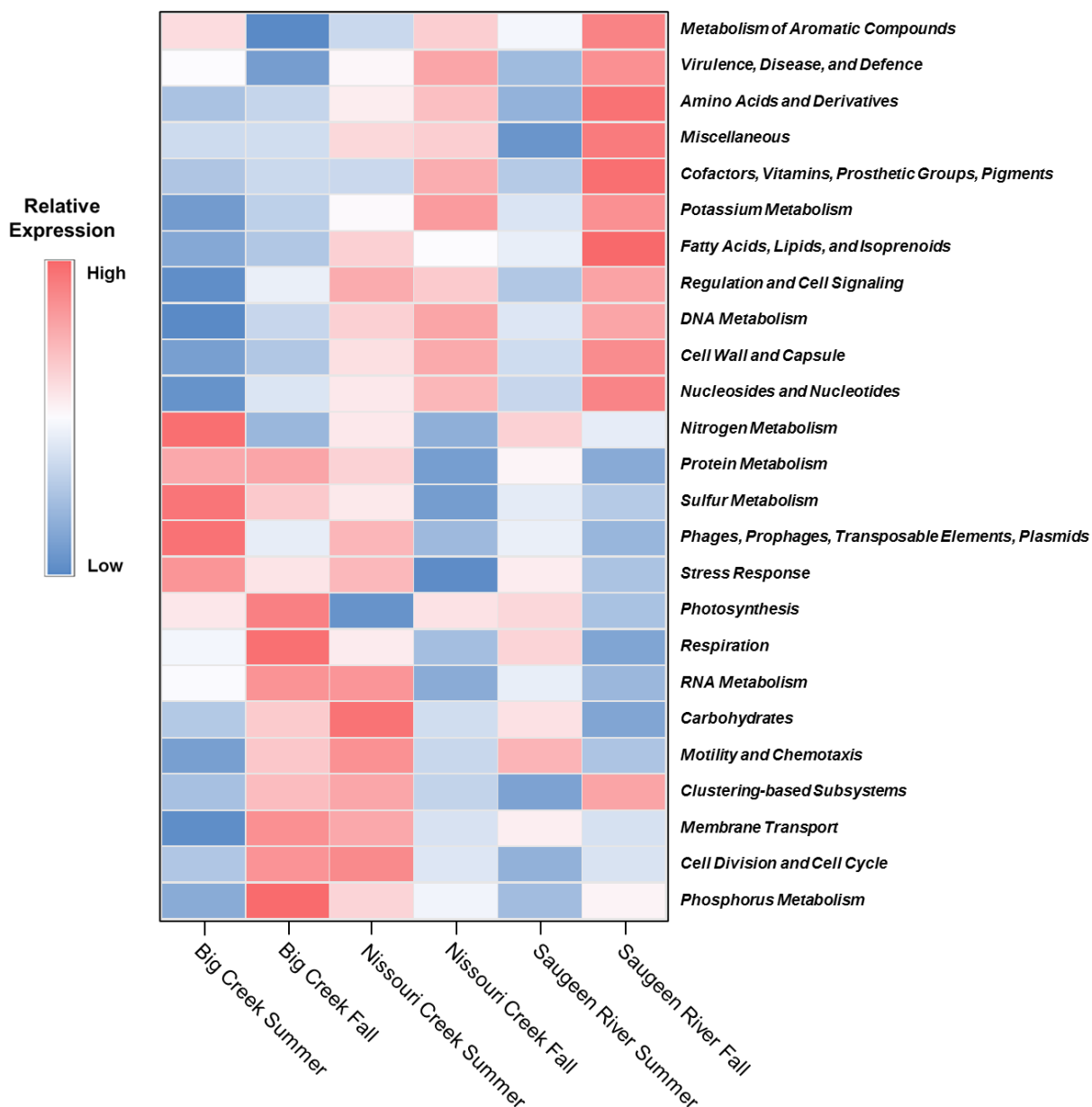


Figure 6: Relative expression heatmap of primary microbial functional categories across river sites and seasons. High expression (red) indicates greater than average abundance with low expression (blue) indicating lower than average abundance across samples.

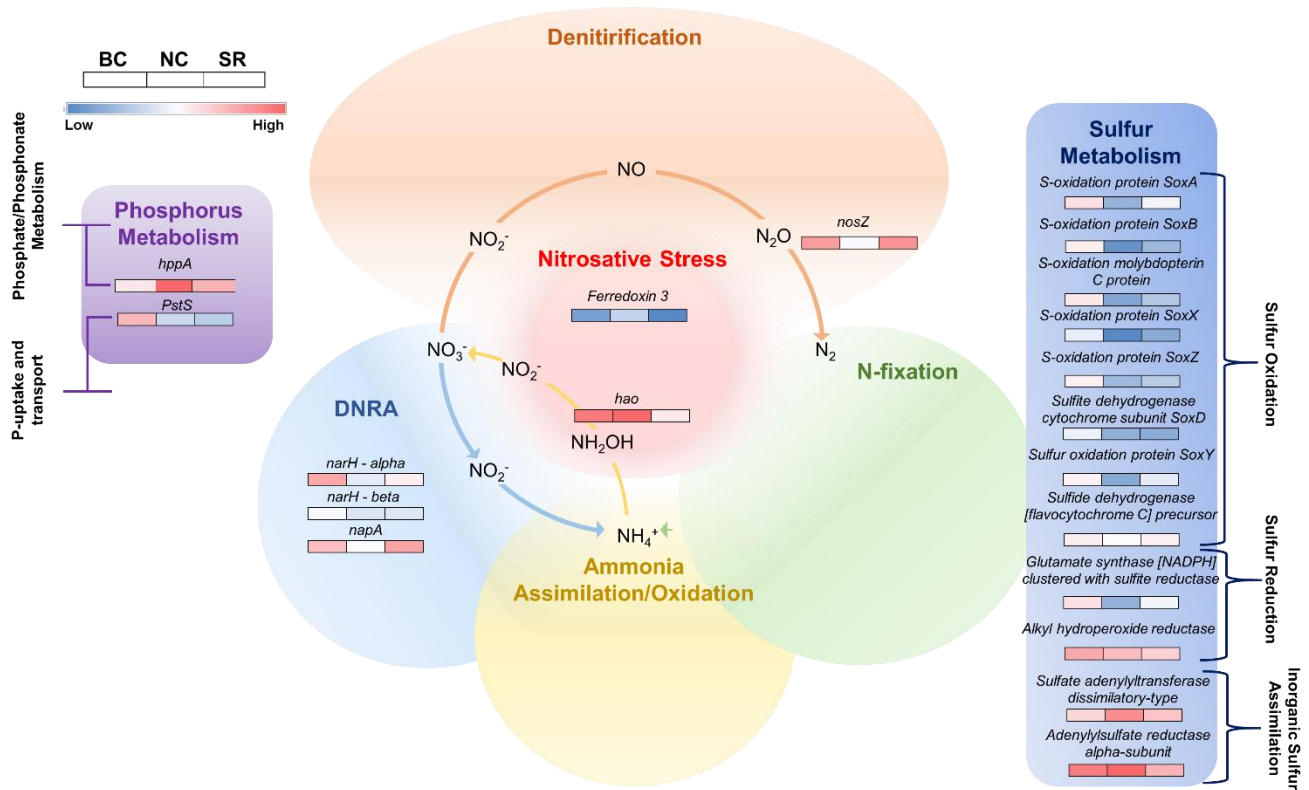


Figure 7a: Summer differentially expressed genes within primary Phosphorus, Nitrogen, and Sulfur Metabolism across big Creek (BC) Nissouri Creek (NC) and Saugeen River (SR) bed sediments. Secondary metabolic pathways are denoted by brackets within phosphorus and sulfur metabolism. Nitrogen secondary pathways of denitrification, dissimilatory nitrate reduction to ammonia (DNRA), nitrosative stress, N-fixation, and Ammonia Assimilation/Oxidation are denoted within the N-cycling pathway diagram. High expression (red) indicates greater than average abundance with low expression (blue) indicating lower than average abundance across samples.

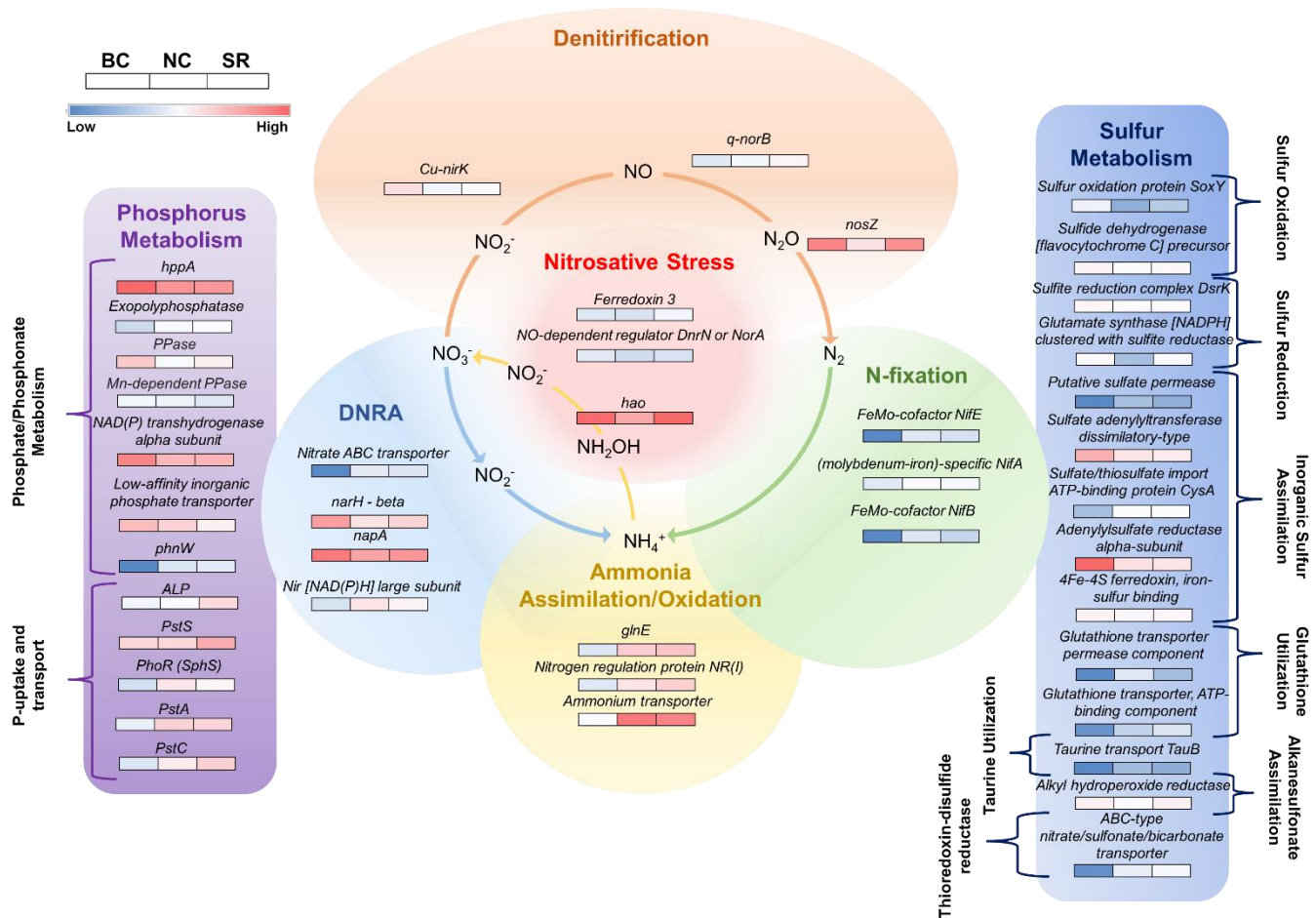


Figure 7b: Fall differentially expressed genes within primary Phosphorus, Nitrogen, and Sulfur Metabolism across big Creek (BC) Nissouri Creek (NC) and Saugeen River (SR) bed sediments.

References

- Agudelo, S.C., Nelson, N.O., Barnes, P.L., Keane, T.D., Pierzynski, G.M., 2011. Phosphorus Adsorption and Desorption Potential of Stream Sediments and Field Soils in Agricultural Watersheds. *J. Environ. Qual.* 40, 144–152. <https://doi.org/10.2134/jeq2010.0153>
- Biessy, L., Pearman, J.K., Waters, S., Vandergoes, M.J., Wood, S.A., 2022. Metagenomic insights to the functional potential of sediment microbial communities in freshwater lakes. *Metabarcoding and Metagenomics* 6, 59–74. <https://doi.org/10.3897/MBMG.6.79265>
- Birrer, S.C., Dafforn, K.A., Simpson, S.L., Kelaher, B.P., Potts, J., Scanes, P., Johnston, E.L., 2018. Interactive effects of multiple stressors revealed by sequencing total (DNA) and active (RNA) components of experimental sediment microbial communities. *Sci. Total Environ.* 637–638, 1383–1394. <https://doi.org/10.1016/j.scitotenv.2018.05.065>
- Bocaniov, S.A., Van Cappellen, P., Scavia, D., 2019. On the Role of a Large Shallow Lake (Lake St. Clair, USA-Canada) in Modulating Phosphorus Loads to Lake Erie. *Water Resour. Res.* 55, 10548–10564. <https://doi.org/10.1029/2019WR025019>
- Bokulich, N.A., Kaehler, B.D., Rideout, J.R., Dillon, M., Bolyen, E., Knight, R., Huttley, G.A., Gregory Caporaso, J., 2018. Optimizing taxonomic classification of marker-gene amplicon sequences with QIIME 2's q2-feature-classifier plugin. *Microbiome* 6, 1–17. <https://doi.org/10.1186/s40168-018-0470-z>
- Bosch, J., Lee, K.Y., Jordan, G., Kim, K.W., Meckenstock, R.U., 2012. Anaerobic, nitrate-dependent oxidation of pyrite nanoparticles by thiobacillus denitrificans. *Environ. Sci. Technol.* 46, 2095–2101. <https://doi.org/10.1021/es2022329>
- Callahan, B.J., McMurdie, P.J., Rosen, M.J., Han, A.W., Johnson, A.J.A., Holmes, S.P., 2016. DADA2: High-resolution sample inference from Illumina amplicon data. *Nat. Methods* 13, 581–583. <https://doi.org/10.1038/nmeth.3869>

- Casciotti, K.L., Sigman, D.M., Hastings, M.G., Böhlke, J.K., Hilkert, A., 2002. Measurement of the oxygen isotopic composition of nitrate in seawater and freshwater using the denitrifier method. *Anal. Chem.* 74, 4905–4912. <https://doi.org/10.1021/ac020113w>
- Chong, J., Liu, P., Zhou, G., Xia, J., 2020. Using MicrobiomeAnalyst for comprehensive statistical, functional, and meta-analysis of microbiome data. *Nat. Protoc.* 15, 799–821. <https://doi.org/10.1038/s41596-019-0264-1>
- Cyriaque, V., Geron, A., Billon, G., Nesme, J., Werner, J., Gillan, D.C., Sørensen, S.J., Wattiez, R., 2020. Metal-induced bacterial interactions promote diversity in river-sediment microbiomes. *FEMS Microbiol. Ecol.* 96, 1–12. <https://doi.org/10.1093/femsec/fiaa076>
- Devol, A.H., 2015. Denitrification, anammox, and N₂ production in marine sediments. *Ann. Rev. Mar. Sci.* 7, 403–423. <https://doi.org/10.1146/annurev-marine-010213-135040>
- Dhariwal, A., Chong, J., Habib, S., King, I.L., Agellon, L.B., Xia, J., 2017. MicrobiomeAnalyst: A web-based tool for comprehensive statistical, visual and meta-analysis of microbiome data. *Nucleic Acids Res.* 45, W180–W188. <https://doi.org/10.1093/nar/gkx295>
- Edgar, R.C., 2010. Search and clustering orders of magnitude faster than BLAST. *Bioinformatics* 26, 2460–2461. <https://doi.org/10.1093/bioinformatics/btq461>
- Faith, D.P., 1991. Conservation evaluation and phylogenetic diversity. *Biol. Conserv.* 61, 1–10. [https://doi.org/10.1016/0003-2697\(75\)90168-2](https://doi.org/10.1016/0003-2697(75)90168-2)
- Falk, N., Day, M., Weisener, C.G., 2021. Evaluating Sediment Phosphorus Exchange in Rural Ontario Headwaters by Paired Sequential Extraction and Sorption Isotherms. *Water, Air, Soil Pollut.* 232, 1–14. <https://doi.org/10.1007/s11270-021-05381-z>
- Falk, N., Droppo, I.G., Drouillard, K.G., Weisener, C.G., 2022. Integrating microbial DNA community analyses into time - integrated suspended sediment sampling

- methods. *J. Soils Sediments*. <https://doi.org/10.1007/s11368-022-03293-x>
- Gibbons, S.M., Jones, E., Bearquiver, A., Blackwolf, F., Roundstone, W., Scott, N., Hooker, J., Madsen, R., Coleman, M.L., Gilbert, J.A., 2014. Human and environmental impacts on river sediment microbial communities. *PLoS One* 9, 1–9. <https://doi.org/10.1371/journal.pone.0097435>
- Harke, M.J., Davis, T.W., Watson, S.B., Gobler, C.J., 2016. Nutrient-Controlled Niche Differentiation of Western Lake Erie Cyanobacterial Populations Revealed via Metatranscriptomic Surveys. *Environ. Sci. Technol.* <https://doi.org/10.1021/acs.est.5b03931>
- Huang, S., Chen, C., Jaffé, P.R., 2018. Seasonal distribution of nitrifiers and denitrifiers in urban river sediments affected by agricultural activities. *Sci. Total Environ.* 642, 1282–1291. <https://doi.org/10.1016/j.scitotenv.2018.06.116>
- Katoh, K., Misawa, K., Kuma, K.I., Miyata, T., 2002. MAFFT: A novel method for rapid multiple sequence alignment based on fast Fourier transform. *Nucleic Acids Res.* 30, 3059–3066. <https://doi.org/10.1093/nar/gkf436>
- Keega, K.P., Glass, E.M., Meyer, F., 2016. MG-RAST, a Metagenomics Service for Analysis of Microbial Community Structure and Function. *Microb. Environ. Genomics (MEG)*, *Methods Mol. Biol.* 1399, 167–182. <https://doi.org/10.1007/978-1-4939-3369-3>
- Kelly, M.C., Zeglin, L.H., Husic, A., Burgin, A.J., 2021. High Supply, High Demand: A Fertilizer Waste Release Impacts Nitrate Uptake and Metabolism in a Large River. *J. Geophys. Res. Biogeosciences* 126, 1–16. <https://doi.org/10.1029/2021JG006469>
- Laperriere, S.M., Hilderbrand, R.H., Keller, S.R., Trott, R., Santoro, A.E., 2020. Headwater stream microbial diversity and function across agricultural and urban land use gradients. *Appl. Environ. Microbiol.* 86, 1–17. <https://doi.org/10.1128/AEM.00018-20>
- Lennon, J.T., Muscarella, M.E., Placella, S.A., Lehmkuhl, B.K., 2018. How, when, and

- where relic DNA affects microbial diversity. *MBio* 9.
<https://doi.org/10.1128/mBio.00637-18>
- Lozupone, C., Knight, R., 2005. UniFrac: A new phylogenetic method for comparing microbial communities. *Appl. Environ. Microbiol.* 71, 8228–8235.
<https://doi.org/10.1128/AEM.71.12.8228-8235.2005>
- Lozupone, C.A., Hamady, M., Kelley, S.T., Knight, R., 2007. Quantitative and qualitative β diversity measures lead to different insights into factors that structure microbial communities. *Appl. Environ. Microbiol.* 73, 1576–1585.
<https://doi.org/10.1128/AEM.01996-06>
- Mayer, B., Boyer, E.W., Goodale, C., Jaworski, N.A., Van Breemen, N., Howarth, R.W., Seitzinger, S., Billen, G., Lajtha, K., Nadelhoffer, K., Van Dam, D., Hetling, L.J., Nosal, M., Paustian, K., 2002. Sources of nitrate in rivers draining sixteen watersheds in the northeastern U.S.: Isotopic constraints. *Biogeochemistry* 57–58, 171–197. <https://doi.org/10.1023/A:1015744002496>
- McMahon, K.D., Read, E.K., 2013. Microbial contributions to phosphorus cycling in eutrophic lakes and wastewater. *Annu. Rev. Microbiol.* 67, 199–219.
<https://doi.org/10.1146/annurev-micro-092412-155713>
- Meng, L., Zuo, R., Wang, J. sheng, Yang, J., Li, Q., Chen, M., 2020. The spatial variations of correlation between microbial diversity and groundwater quality derived from a riverbank filtration site, northeast China. *Sci. Total Environ.* 706, 135855. <https://doi.org/10.1016/j.scitotenv.2019.135855>
- Meyer, F., Paarmann, D., D’Souza, M., Olson, R., Glass, E.M., Kubal, M., Paczian, T., Rodriguez, A., Stevens, R., Wilke, A., Wilkening, J., Edwards, R.A., 2008. The metagenomics RAST server - A public resource for the automatic phylogenetic and functional analysis of metagenomes. *BMC Bioinformatics* 9, 1–8.
<https://doi.org/10.1186/1471-2105-9-386>
- Muscarella, M.E., Boot, C.M., Broeckling, C.D., Lennon, J.T., 2019. Resource heterogeneity structures aquatic bacterial communities. *ISME J.* 13, 2183–2195.

<https://doi.org/10.1038/s41396-019-0427-7>

- Nelligan, C., Sorichetti, R.J., Yousif, M., Thomas, J.L., Wellen, C.C., Parsons, C.T., Mohamed, M.N., 2021. Then and now: Revisiting nutrient export in agricultural watersheds within southern Ontario's lower Great Lakes basin. *J. Great Lakes Res.* <https://doi.org/10.1016/j.jglr.2021.08.010>
- Newcomer Johnson, T.A., Kaushal, S.S., Mayer, P.M., Smith, R.M., Sviridchi, G.M., 2016. Nutrient retention in restored streams and rivers: A global review and synthesis. *Water (Switzerland)* 8, 1–28. <https://doi.org/10.3390/w8040116>
- Oest, A., Alsaffar, A., Fenner, M., Azzopardi, D., Tiquia-Arashiro, S.M., 2018. Patterns of change in metabolic capabilities of sediment microbial communities in river and lake ecosystems. *Int. J. Microbiol.* 2018, 5–7. <https://doi.org/10.1155/2018/6234931>
- Overbeek, R., Olson, R., Pusch, G.D., Olsen, G.J., Davis, J.J., Disz, T., Edwards, R.A., Gerdes, S., Parrello, B., Shukla, M., Vonstein, V., Wattam, A.R., Xia, F., Stevens, R., 2014. The SEED and the Rapid Annotation of microbial genomes using Subsystems Technology (RAST). *Nucleic Acids Res.* 42, 206–214. <https://doi.org/10.1093/nar/gkt1226>
- Phillips, J.M., Russell, M.A., Walling, D.E., 2000. Time-integrated sampling of fluvial suspended sediment: A simple methodology for small catchments. *Hydrol. Process.* 14, 2589–2602. [https://doi.org/10.1002/1099-1085\(20001015\)14:14<2589::AID-HYP94>3.0.CO;2-D](https://doi.org/10.1002/1099-1085(20001015)14:14<2589::AID-HYP94>3.0.CO;2-D)
- Quast, C., Pruesse, E., Yilmaz, P., Gerken, J., Schweer, T., Yarza, P., Peplies, J., Glöckner, F.O., 2013. The SILVA ribosomal RNA gene database project: Improved data processing and web-based tools. *Nucleic Acids Res.* 41, 590–596. <https://doi.org/10.1093/nar/gks1219>
- Records, R.M., Wohl, E., Arabi, M., 2016. Phosphorus in the river corridor. *Earth-Science Rev.* 158, 65–88. <https://doi.org/10.1016/j.earscirev.2016.04.010>
- Sanz-Luque, E., Bhaya, D., Grossman, A.R., 2020. Polyphosphate: A Multifunctional

- Metabolite in Cyanobacteria and Algae. *Front. Plant Sci.* 11, 1–21.
<https://doi.org/10.3389/fpls.2020.00938>
- Segata, N., Izard, J., Waldron, L., Gevers, D., Miropolsky, L., Garrett, W.S., Huttenhower, C., 2011. Metagenomic biomarker discovery and explanation. *Genome Biol.* 12, 1–18. <https://doi.org/10.1186/gb-2011-12-6-r60>
- Sigman, D.M., Casciotti, K.L., Andreani, M., Barford, C., Galanter, M., Böhlke, J.K., 2001. A bacterial method for the nitrogen isotopic analysis of nitrate in seawater and freshwater. *Anal. Chem.* 73, 4145–4153. <https://doi.org/10.1021/ac010088e>
- Steffen, M.M., Davis, T.W., McKay, R.M.L., Bullerjahn, G.S., Krausfeldt, L.E., Stough, J.M.A., Neitzey, M.L., Gilbert, N.E., Boyer, G.L., Johengen, T.H., Gossiaux, D.C., Burtner, A.M., Palladino, D., Rowe, M.D., Dick, G.J., Meyer, K.A., Levy, S., Boone, B.E., Stumpf, R.P., Wynne, T.T., Zimba, P. V., Gutierrez, D., Wilhelm, S.W., 2017. Ecophysiological Examination of the Lake Erie Microcystis Bloom in 2014: Linkages between Biology and the Water Supply Shutdown of Toledo, OH. *Environ. Sci. Technol.* 51, 6745–6755. <https://doi.org/10.1021/acs.est.7b00856>
- Stegen, J.C., Lin, X., Konopka, A.E., Fredrickson, J.K., 2012. Stochastic and deterministic assembly processes in subsurface microbial communities. *ISME J.* 6, 1653–1664. <https://doi.org/10.1038/ismej.2012.22>
- Stutter, M., Richards, S., Ibiyemi, A., Watson, H., 2021. Spatial representation of in-stream sediment phosphorus release combining channel network approaches and in-situ experiments. *Sci. Total Environ.* 795, 148790. <https://doi.org/10.1016/j.scitotenv.2021.148790>
- Tu, C., Jin, Z., Che, F., Cao, X., Song, X., Lu, C., 2022. Characterization of phosphorus sorption and microbial community in lake sediments during overwinter and recruitment periods of cyanobacteria . *Chemosphere* 307, 135777. <https://doi.org/10.1016/j.chemosphere.2022.135777>
- VanMensel, D., Chaganti, S.R., Droppo, I.G., Weisener, C.G., 2020. Exploring bacterial pathogen community dynamics in freshwater beach sediments: A tale of two lakes.

- Environ. Microbiol. 22, 568–583. <https://doi.org/10.1111/1462-2920.14860>
- Wang, L., Han, M., Li, X., Yu, B., Wang, H., Ginawi, A., Ning, K., Yan, Y., 2021. Mechanisms of niche-neutrality balancing can drive the assembling of microbial community. *Mol. Ecol.* 30, 1492–1504. <https://doi.org/10.1111/mec.15825>
- Xu, J., He, J., Wang, M., Li, L., 2018. Cultivation and stable operation of aerobic granular sludge at low temperature by sieving out the batt-like sludge. *Chemosphere* 211, 1219–1227. <https://doi.org/10.1016/j.chemosphere.2018.08.018>
- Yang, Z., Yang, L., Wei, C., Wu, W., Zhao, X., Lu, T., 2018. Enhanced nitrogen removal using solid carbon source in constructed wetland with limited aeration. *Bioresour. Technol.* 248, 98–103. <https://doi.org/10.1016/j.biortech.2017.07.188>
- Zhang, S., Amanze, C., Sun, C., Zou, K., Fu, S., Deng, Y., Liu, X., Liang, Y., 2021. Evolutionary, genomic, and biogeographic characterization of two novel xenobiotics-degrading strains affiliated with *Dechloromonas*. *Heliyon* 7, e07181. <https://doi.org/10.1016/j.heliyon.2021.e07181>
- Zhong, Z., Wu, X., Gao, L., Lu, X., Zhang, B., 2016. Efficient and microbial communities for pollutant removal in a distributed-inflow biological reactor (DBR) for treating piggy wastewater. *RSC Adv.* 6, 95987–95998. <https://doi.org/10.1039/c6ra20777d>
- Zhu, J., He, Y., Zhu, Y., Huang, M., Zhang, Y., 2018. Biogeochemical sulfur cycling coupling with dissimilatory nitrate reduction processes in freshwater sediments. *Environ. Rev.* 26, 121–132. <https://doi.org/10.1139/er-2017-0047>

CHAPTER 6: DISSERTATION CONCLUSIONS, DISCUSSION AND FUTURE DIRECTIONS

This chapter will conclude the thesis by summarizing the main findings with respect to the hypotheses and research objectives of the preceding chapters. It will also review the limitations of the studies included and discuss future directions.

6.1 Chapter Summaries and Significance

6.1.1 Data Chapter 2

Initial hypotheses:

H2.1: Microbial community diversity is not different in low vs. high contaminant sediment regions in the lower Detroit River.

H2.2: Microbial expression of PAH-degrading genes is not different in low vs. high contaminant regions.

In Chapter 2, the study of microbial community gene expression in the Detroit River showed that microbial function was different between low contaminated (i.e., COLD) and high contaminated (i.e., HOT) riverbed sediments. It was also shown that community alpha diversity was lower in HOT sites compared to COLD sites, rejecting hypothesis H2.1 (see above). This confirms that microbial activity can be affected by strong environmental variables over medium spatial scales (in this case 5-10 km) and adds to the body of evidence that metatranscriptomics agree well with stress gradients. However, it was not tested whether or not the lower microbial diversity was a negative consequence in an ecosystem context. Low diversity is generally assumed to be less desirable in populations compared to higher diversity, as higher diversity often results in increased resilience and resistance to disturbance (Maron et al. 2018). Yet this trend is not clear when it comes to microorganisms, as in some cases anthropogenic stress results in increased diversity (Beattie et al. 2020; Cyriaque et al. 2020). Whether or not this is good or bad depends entirely on the desirable outcomes relative to human expectations. For example, wastewater treatment relies partially on microbial communities to perform nitrification to remove ammonia and nitrite from wastewater (Ray et al. 2012). If a treatment cell is observed to perform optimally within a specified diversity range (measured consistently by an alpha diversity metric such as Shannon H), then any deviation from that range, either

by increases or decreases in diversity, would be considered detrimental to the desired outcome. Thus, diversity is useful only if it is constrained and interpreted within a monitored system. For Detroit River sediments, additional mesocosm studies that use collected sediments spiked with mixtures of contaminants paired with measurements of contaminant concentration and microbial diversity could further elucidate the connection between microbial heterogeneity and persistent organic pollution degradation. Such an approach has been used previously to understand the response of the total and active bacterial/eukaryotic communities to metals and organic enrichments (Birrer et al. 2018). With regards to hypothesis H2.2, eight genes present in the COLD and HOT metatranscriptomes that have been shown to be involved in microbial PAH degradation showed no differential expression between the two groups. Thus, hypothesis H2.2 could not be rejected based on the evidence gathered here. The eight genes (*Ubid*, *HgdB*, *YciV*, *FcbT*, *Yoal*, *LigB*, *DodA*, and *Paal*) were observed to be in low abundance, and thus not highly expressed in non-contaminated or contaminated sediments. As discussed in Chapter 2, other gene pathways were more prevalent that represented secondary metabolism that would occur after primary breakdown of PAHs. It was thus predicted that the primary POP degradation signal was not captured by the RNA-snapshot from sediments, and that cleavage of these complex organic compounds occurs sparingly, as the resources microbial communities require to do so (e.g., high-energy terminal electron acceptors such as O₂ and or NO₃) are in low and fleeting abundance in the Detroit River subsurface. This was supported by an analysis of the concentrations of PAHs by molecular weight in contaminated sediments, where the HOT zone sediments had higher concentrations of heavier PAHs, evidence that these are only sparingly broken down.

The most important finding from Data Chapter 2 is the confirmation that total RNA-gene function changes identified by a metatranscriptomic approach can align with independent chemical datasets of contamination in Great Lakes watersheds. Further, this study embodies an ideal meso-scale to large-scale experimental design for environmental metatranscriptomics, with an appropriate number of total mRNA extraction replicates (n= 3-5) covering a well constrained contaminant gradient.

6.1.2 Data Chapter 3

Initial hypotheses:

H3.1: Microbial community composition is not different between individual suspended sediment samplers along the river segment.

H3.2: Suspended and bed sediment phase microbial communities do not differ in their composition.

H3.3: The oxidation-reduction potential inside the suspended sediment sampler is not different from that in the stream environment.

In Chapter 3, the established Phillips Tube (PT) sampler method of fine suspended sediment in fluvial systems was tested for its ability to collect adequate volumes of sediment for DNA extraction and analysis of microbial communities. As no study had before assessed the microbial source tracking potential of these type of samplers, this research is important for initial calibration and proof of concept. Comparing between seven individual samplers spread over a 0.7 km river segment, it was observed that the microbial community collected within samplers was identical from upstream to downstream for each time interval, meaning that hypothesis H3.1 was not rejected, and that the samplers had good spatial precision and are promising for source tracking studies where inter-sampler consistency is required. The collected suspended microbial community composition was consistently different from that collected from bed sediments (as measured by beta-diversity tests of community composition) thus hypothesis H3.2 was rejected. Suspended load microbial communities were also less diverse than bed sediment communities on average. This was also observed in Chapter 5 across three sites and two seasons, where bed sediments showed higher diversity than both water column and suspended load (i.e., PT sampler) communities. This is evidence that bed sediments can harbour more metabolically diverse taxa, likely driven by the complex heterogeneity in this environment, providing more niches than suspended sediment flocs.

Some drawbacks of the Chapter however include that, 1) it was not adequately tested whether individual PT samplers collected a representative microbial community over the deployment time, and 2) it was not confirmed whether the sampler environment

imposed some form of selection on the in-situ microorganisms. For these concerns, subsequent studies would need to collect a high frequency of suspended sample from the PT samplers during its deployment time to address potential community turnover from initial set up to retrieval. This could also be paired with point suspended sediment sampling of the surface water via grab samples and filtration to obtain enough sediment mass, or the use of field centrifugation. In this way, it could be tested whether the microbial community changes within the tube environment compared to what is expected to be in suspension. The issue with this approach however is that in low total suspended sediment (TSS) systems, it would be difficult to frequently obtain a high mass of suspended sediment; a situation for which the PT samplers were designed in the first place. The use of flume experiments could aid in microbial PT sampler calibration, as they allow for a controlled setup where the concentration of TSS can be more or less controlled based on flow velocity, and corrections can be made that are not possible in field experiments. Flume set ups would also permit the use of valves to cut off supply to a parallel flow-through PT tube circuit, enabling fine control on the temporal sampling of the in-situ microbial community. Experiments such as these could further clarify the ideal deployment times for microbial source tracking of suspended sediments based on different stream parameters (flow rate, particle size distributions, shear stress, TSS concentration, floc characteristics). In the absence of these studies, inferences about the microbial community turnover within samplers must be made based on the current study data.

The consistency of the collected microbial community in the separate samplers for each timepoint in the study suggests that selective pressures that could have altered the in-situ community were low, as it's unlikely that samplers spread over space would have developed the same microbial community merely by chance. Thus, either the same selection is at play in each sampler, or the samplers are all collecting and accumulating the same source material. Since a portion of community establishment can be random (e.g., founder effects within the tubes), it's further unlikely that the separate tubes would have developed the same microbial community by chance. These theories provide evidence that the PT samplers do indeed collect a microbial community that is representative of what is in suspension in the stream environment, and that in-situ sampler divergence of the community is limited. Yet, this is only assured during higher flow periods. There was a

scenarios where microbial communities differed between replicate samplers during the warmest and longest deployment time of the late summer period. In this setting, the connectivity between samplers in the stream segment was reduced, and it appeared that random selection and divergence of microbial communities within samplers outpaced the collection of a representative suspended sediment sample. In other words, the samplers did not act as passive collectors, but rather behaved as in-situ incubators. It was concluded that the samplers collect a more consistent microbial load under higher flows, but under low flow, the communities within tubes can diverge, and this corresponded with in-situ decreased in PT sampler dissolved oxygen (thus H3.3 was rejected). Thus, it's confirmed that the PT samplers be reserved for collection under high flow events, as initially intended, and not be used frequently in ephemeral lotic systems.

In summary, suspended sediment contains abundant and detectable microbial communities, and these are and should be considered a part of the in-stream meta community and as an inherent component of sediment flocs and aggregates. In addition, these microbes can be selected for and can change based on the collection method and stream connectivity, and it's recommended that, in the absence of further calibration trials, deployment times for microbial source tracking studies do not exceed two weeks.

6.1.3 Data Chapter 4

Initial hypotheses:

H4.1: Big Creek, Nissouri Creek, and the Saugeen River show no difference in past and present total N and total P concentrations.

H4.2: Bed and suspended sediments are primarily sinks of P with no difference in EPC_0 values across sites and seasons.

H4.3: Bed sediment microbial community composition is not different between sites and not affected by internal P loading risk.

Chapter 4 of this thesis summarized data from three seasons of field work at three different stream segments: Big Creek, Nissouri Creek (both agriculturally impacted), and the Saugeen River (a forested reference site). As detailed in the methods, each watershed

is characterized by a different fertilizer treatment, with Big Creek dominated by inorganic/chemical fertilizer, Nissouri Creek dominated by a manure/chemical fertilizer mix, and the Saugeen River segment experiencing limited fertilizer amendment. Analysis from 2000 to the present based on Provincial Water Quality Monitoring Network (PWQMN) archived data showed that Big Creek had the highest Total Phosphorus (TP) levels while Nissouri Creek had higher Total Nitrogen (TN) levels, with the Saugeen River segment maintaining low concentrations for both parameters. For additional context, Ontario water quality guidelines for TP indicate that concentrations should be maintained below 0.01 mg L^{-1} ($10 \mu\text{g L}^{-1}$) to protect against aesthetic deterioration, and concentrations exceeding 0.03 mg L^{-1} ($30 \mu\text{g L}^{-1}$) can lead to nuisance algae concentrations and excessive plant growth (Government of Ontario, 2016). Big Creek median TP concentrations observed in this study (0.197 mg L^{-1}) and from past PWQMN data (0.109) both greatly exceed these thresholds, while values for Nissouri Creek (0.0605 and 0.031 mg L^{-1} , respectively) exceeded guidelines by smaller margins. Additionally, Big Creek TP concentrations were significantly greater than Nissouri Creek and Saugeen River concentrations, both presently and historically (Appendix C, Table S4). In terms of Nitrogen, the largest component of TN in freshwaters is most often nitrate (NO_3^-), thus quality guidelines are often centered around this ion rather than TN. The drinking water guideline for nitrate is a maximum concentration of 10 mg L^{-1} nitrate-nitrogen (Health Canada, 2013), with long-term surface water quality guidelines stated at 3 mg L^{-1} (CCME) (equivalent to 45 and $13 \text{ mg L}^{-1} \text{NO}_3^-$, respectfully, where the ionic concentration is used). Big Creek, Nissouri Creek, and Saugeen River median nitrate-nitrogen concentrations in this study were 3.1 , 6.4 , and 0.27 mg L^{-1} , respectively, with 20-year PWQMN data median values of 1.15 , 3.55 , and 0.26 . Thus, Nissouri Creek has experienced current and long-term exceedances for surface water nitrate-nitrogen, while Big Creek may be experiencing increases over time. The Saugeen River has shown to be consistently within limits of nitrate-nitrogen surface water quality guidelines and is unchanging based on this data. Additionally, Big Creek and Nissouri Creek nitrate-nitrogen concentrations were shown to be significantly greater than the Saugeen River both from current study and PWQMN 20-year data with Nissouri Creek only showing greater concentrations than Big Creek in PWQMN 20-year data (Appendix C, Table S4). These additional calculations support the

rejection of H4.1 and provide evidence that the sites within predominantly agricultural watersheds are experiencing greater nutrient stress than the reference Saugeen River, with Big Creek and Nissouri Creek afflicted more by P and N stressors, respectively. These sites may serve as analogues for lotic systems in adjacent watersheds that are characterized by similar land use trends. Additional contributions of this work include the collating of multi-year PWQMN data into a manageable format for future analysis of a variety of water quality parameter in R statistical software.

For H4.2, bed sediments tested through 2018 – 2020 were primarily characterized as sinks of surface water P or were at equilibrium with surface water P, as measured by the Zero Equilibrium Phosphorus Concentration (EPC₀) assay. However, the magnitude of EPC₀ values did vary spatially and temporally, ranging from 0.7 – 60 µg/L, with higher values observed at the agriculturally-impacted sites. Thus, the first portion of H4.2 cannot be rejected, as bed sediments were not seen as chronic P-sources, however the second portion can be rejected, as EPC₀ values were different over space and time.

Although the EPC₀ assay can provide a reliable relative measure of bioavailable P adsorption/desorption potential across sediments, it has several drawbacks. For one, benthic sediments can be heterogenous in their biological, physical, and chemical properties, thus sampling design must consider spatial variation in rivers/lakes and collect sediment from several points, preferably with paired measures of variables that can influence P-flux and/or sediment P diagenesis (i.e., grain size, total organic carbon (TOC), mineralogy). High spatial variability in these variables would necessitate a greater number of replicates. In term of the EPC₀ assay itself, the incubation period requires constant mixing of the sediment within the spiked solution of P, a simulation that is not exactly consistent with processes at the sediment water interface (SWI). The mixing disrupts vertical redox zonation that establishes under deposition of beds when oxygen is increasingly limited with depth, which can control P bioavailability. For example, mixing may promote oxidated Fe/Mn mineral phases that enhance P-sorption, thus overestimating the buffering capacity for bioavailable P. Alternatively, mixing may promote dissolution of P from the sediment matrix, which could underestimate buffering capacity. To overcome these limitations, the use of in-situ SWI P-flux measurement techniques, including

diffusive gradients in thin films (DGT) or diffusive equilibration in thin film (DET), can be paired with EPC_0 measurements, as well as mesocosm experiments involving core incubations (Orihel et al. 2017). In terms of interpretations of EPC_0 results, the 20% rule (where sediments are deemed a sink or source of SRP if EPC_0 values are below or exceed surface water concentrations by 20%, respectively) is arbitrary and is not often supported by paired observations of water quality/watershed impacts tied to the release or retention of P. In general, P-source designations are considered unfavourable, however, exchange of nutrients between the SWI is a natural biogeochemical process, and P release is necessary for maintaining primary production in freshwater systems (Froelich 1988). Thus, if the EPC_0 assay is to be useful as a management tool, it must be paired with measures of watershed health indicators to distinguish correlation and causation. For example, this research observed scenarios of P-release from Saugeen River sediments, however, analysis of 20-year TP and TN measurements from this site showed that water quality has maintained good status, and this corroborates with watershed report cards from the Saugeen Conservation Authority that indicate good conditions for surface water quality (Saugeen Conservation, 2018). On the other hand, Nissouri Creek exhibited an equal number of P-source events to the Saugeen River, yet surface water TP and TN have exceeded provincial guidelines and the Nissouri watershed is deemed as steady or in slight decline from watershed report cards from the Upper Thames River Conservation Authority (Upper Thames River Conservation Authority, 2017). Both scenarios may warrant additional monitoring, as the Saugeen River can serve as a baseline reference with Nissouri Creek requiring further study to assess the connection of internal P-loading to watershed impairments. This is the first study to establish spatial and temporal trends of P-sink/source behaviour in southern Ontario lotic systems, and has shown that, though the EPC_0 measure is efficient and easily compared across multiple sites, it should be coupled with other chemical, physical, and biological indicators of lotic health.

In terms of suspended sediment (SS) analysis, this research is the first to report EPC_0 measurements of time-integrated SS in Southern Ontario watersheds. With respect to H4.2, SS collected through PT samplers did vary in P-source potential seasonally and across the three sites, thus it is rejected. EPC_0 values for Big Creek SS were especially high, and though measurements of water column TP include SS particulate P, this research

demonstrated the high P-desorption potential of this P reservoir. Many studies have acknowledged the concern of particulate P (Markovic et al. 2020; Owens 2020), but this work suggests that the magnitude of P-release from transported, fine grained suspended sediments in agricultural watersheds is higher than anticipated. Additional studies could collect SS using PT samplers over a greater scale, perhaps along the entirety of Big Creek for example, to assess spatial variations in SS EPC₀ and judge whether 1) particulate P may experience deposition along the river continuum, altering SS EPC₀ values spatially, or 2) whether it is transported and subsequently desorbed into down stream Lake St. Clair. In the case of 1), this particulate P reservoir may help explain a missing sink of P in lower Great Lakes watersheds (Van Staden et al. 2021), and in the case of 2), may open the door to greater interest in the role of particulate P in nutrient loading to lentic bodies. Data collected here from Big Creek may also aid in understanding particulate P processes in Northwestern Ohio, where soils are similar in their high clay content and where agricultural practises are similar, but more intensive. The high TSS at Big Creek, which was shown to correlate with TP, was hypothesized to be influenced by the high clay composition of surrounding agricultural plots, as fine-grained particles are more likely to remain in suspension.

H4.3 was rejected as ordination and beta diversity tests showed that bed sediment microbial community composition was different between sites. No microbial taxonomic groups or features were identified as bioindicators of P-desorption events in bed sediments. Only the class Bacteroidia showed increased abundance when sediments were deemed P-sinks. The Bacteroidia, a class of the Bacteroidota phylum, have a wide diversity and do not fit into any single niche, thus it is difficult to speculate on what features of Bacteroidia may cause them to be more abundant in P-sink environments other than random chance. With the observation that EPC₀ values positively correlated with NO₃ concentration and negatively correlated with DO depletion rate, it is hypothesized that increases in EPC₀ would coincide with oxygen depletion over the SWI, and that this could select against obligate aerobic taxa within the Bacteroidia. The absence of a bacterial group is not a reliable bioindicator, however it does align with the concept of dysbiosis, a term usually reserved for an unbalance in the gut microbial community (Shin et al. 2015). It's an intriguing idea that the decrease in Bacteroidia could be a symptom of sediment P-release,

and a greater sampling size over many sites and seasons is required to test this hypothesis. This also goes for *Candidatus Nitrosocosmicus*, the ammonia oxidizing archaeon identified in high abundance during the strong P-source activity at Nissouri Creek. This research provides additional evidence for the use of microbial taxa as bioindicators of stress. One challenge in bioindicator research is scale resolution. If too few sites are studied, identified bioindicators may not be powerful enough to be used in assessments over large regions, particularly with respect to microbial communities which exhibit vast diversity over space and substrate (Lozupone and Knight 2007). Alternatively, if too many sites are assessed, regional or stressor-specific microbial bioindicator taxa may be washed out from data as not applicable to multiple sites, thus a taxon such as *Candidatus Nitrosocosmicus* may have been overlooked, despite its site-specific relevance to Nissouri Creek. In summary, microbial communities as bioindicators of anthropogenic stress is an emerging method in ecosystem assessment (Birrer et al. 2018; Cavaco et al. 2019; Yang et al. 2019; Kraemer et al. 2020; Wood et al. 2021), and this research adds to knowledge taxa relevant to N and P stress in lotic systems. However, future bioindicators must be fine tuned to specific management goals, whether it is regional or over national/international scales.

6.1.4 Data Chapter 5

Initial hypotheses:

H5.1: Alpha diversity within a site is not different between substrate type (i.e., surface waters, suspended sediments, and bed sediments) or between the nucleic acid extraction method (i.e., RNA vs. DNA).

H5.2: Alpha diversity between DNA metabarcoding and RNA metabarcoding samples is not different across all samples.

H5.3: Abundance of N, P, and S-metabolism genes are not different between sites and seasons.

In Chapter 5, H5.1 was rejected, as alpha diversity (Shannon H) was different in samples collected from bed sediments, suspended sediments, and surface waters, as well as between DNA and RNA-based community assessments. Bed sediments represented the most diverse microbial reservoir, as detected by the oligo primers used, followed by

suspended sediments, and then surface waters. DNA samples also showed significantly greater diversity than RNA samples within sites and when all samples were grouped, rejecting H5.2.

The explanation for the high bed sediment diversity was discussed in section 5.4.1. However, the significant difference between suspended sediments and surface waters needs further clarification. Samples classified as suspended sediment were collected in a passive manner from the PT samplers previously described, thus they represent a time-integrated collection of suspended particulate matter that would have passed through each stream segment over the 2-month deployment time. Samples classified as surface water were instantaneous grab samples that were filtered through a 0.2 μm filter, with all the material collected on the filter used for the nucleic acid extraction and downstream microbial community analysis. Thus, the surface water samples represented all particle-attached microbial community members (where particles were $> 0.2 \mu\text{m}$ in size) as well as any free-living microbes (where cell size was $> 0.2 \mu\text{m}$). Some studies of surface water microbial communities have separated particle-attached and free-living microbial communities from grab samples by a 2-step filtering approach using first a coarse filter size (2-3 μm) followed by a fine filter size (Savio et al. 2015; Laas et al. 2022). Analysis of the coarse filter represented the particle-attached microbial community, with the second being the free-living community. This method is useful in that it is efficient and replicable and provides an operationally defined distinction between the two niches. Savio et al., found that the two groups decreased in diversity as a function of distance downstream, but that the particle-attached community was more diverse. Other studies have used centrifugation in the lab and field to separate particle-attached and free-living communities (Droppo et al. 2009; VanMensel et al. 2022). Many other studies have shown that the majority of microorganisms in the aqueous phase are attached to and are active on particles (Caron et al. 1986; Liu et al. 2013; Dang and Lovell 2016; Zhang et al. 2021). The importance of the particle-attached microbial community is clear and represents an integral part of the surface water community. Thus, this work advocates that both free-living and particle-attached microorganisms be considered as a meta-community in surface waters, and that separation of the two is unnecessary when describing in-stream microbial biodiversity. The suggestion that particle-attached communities are only hitchhikers in lotic systems is not entirely valid,

as this study and others have detected and analyzed rRNA and mRNA from this phase, showing an actively metabolizing community. It was observed in Chapter 5 that surface waters comprised the highest proportion of non-active taxa, on average. As performed in this study, future work may separate non-active and active taxa by DNA and RNA extractions, respectively, and not by the substrate to which they are attached.

With respect to suspended sediment sampling methodology, results from this chapter support findings that PT sampler microbial communities not be used for source tracking or biomarkers if deployment time exceeds two weeks, in the absence of further calibration studies. Despite the observation of high microbial diversity within the PT sampler communities across the three sites, the DNA and RNA community compositions were significantly different, and the PT sampler communities were different from the point grab samples of surface water collected at the beginning and end of the deployment. This suggests that the active community within the sampler over time may be a product of in-situ conditions, most notably oxygen-depletion, and may not represent the in-stream particulate community. Evidence of denitrification in the PT samplers from stable isotope analysis also suggest a shifting community reliant on alternative terminal electron acceptors (in this case NO_3^-). Both Big Creek and Nissouri Creek TP sampler water was analyzed for $\delta^{15}\text{N}$ and $\delta^{18}\text{O}$ after the deployment time, and both showed significantly larger values compared to paired surface water measurements before and after deployment. For example, fall Big Creek PT sampler measurements were 23.2 ‰ and 21 ‰ for $\delta^{15}\text{N}$ and $\delta^{18}\text{O}$, respectively, compared to 5.6 ‰ and 3.3 ‰ in the summer and 11.7 ‰ and 18.8 ‰ in the fall for surface water. Nissouri Creek fall PT sampler measurements were 30.2 ‰ and 11.3 ‰ for $\delta^{15}\text{N}$ and $\delta^{18}\text{O}$, compared to 13.9 ‰ and 3.2 ‰ in the summer and 11.1 ‰ and 3.1 ‰ in the fall for surface water. The Saugeen River PT sampler was dislodged in 2020, however stable isotope measurements performed earlier in the 2020 sampling year within the sampler were 6.4 ‰ and 13.4 ‰, which were elevated compared to surface water values (5.6 ‰ and 1.8 ‰ summer, and 7.4 ‰ and 2.2 ‰ fall). These isotopic observations pair with results from Chapter 3 that cited high abundances of denitrifiers within the samplers at BC.

Metatranscriptomic investigations of bed sediments revealed interesting trends in seasonal and site-specific N, P, and S metabolism, as well as whole-transcriptome patterns. For one, transcriptomes exhibited large shifts from summer and fall within sites (Figure 5.6). This seasonal variability could discredit some of the generalizations made in Chapter 2 from Detroit River metatranscriptomes, as that study relied on only a single sampling timepoint in the early fall. In other words, as microbial community function can vary rapidly over time, a single timepoint may not capture the full metabolic potential of the community. To remedy this, DNA-based metagenomics could be paired with RNA-based metatranscriptomics. Although this is currently a costly and computationally heavy approach, improvements in both sequencing technologies and processing (e.g., ease of access to dedicated bioinformatic pipelines on external servers) could make this pairing a routine approach. In fact, initial sequencing and assembly of metagenomes from sediments, for example, could serve as scaffold for follow up transcriptomes to be assembled against (i.e., reference-based assembly transcriptomics).

Functional RNA-seq data supported observations from rDNA metabarcoding, microsensor profiles of oxidation-reduction (ORP) and DO, and scanning electron microscopy, that Big Creek sediments were undergoing dissimilatory nitrate reduction to ammonia (DNRA) as an ammonia producing pathway and denitrification as a N removal pathway. This was also suspected to be coupled to S oxidation/reduction as evidenced by the high observed abundance of S-metabolism genes. Nissouri Creek sediments showed high expression of N-stress transcripts, believed to be active due to the abundance of reactive N intermediates produced via the incomplete reduction of NO_3 . This pattern was seasonally affected, with less N-stress genes identified in the fall when TN and NO_3 concentrations were lower. Saugeen River sediments showed microbial responses to lower nutrient availability, including higher expression of N-fixation and low-affinity N-reductases. Investigations in Chapter 4 showed the Saugeen River this maintaining low to adequate concentrations of TN, thus the aforementioned genes may be signs of an appropriate reference systems with respect to non-point N loading.

N-metabolism genes paired well with physico-chemical observations of the three sites with respect to nutrient sources and mobility. However, P-metabolism was not as

informative, and microbial functional trends seen in other studies of P-affected sediments were not observed here. One explanation is that N-metabolism genes, such as those involved in ammonia and NO_3/NO_2 transformations are more phylogenetically conserved (Amend et al. 2016; Isobe et al. 2019), whereas P-metabolism is widespread across organisms. Thus, N-metabolism genes could be more useful in management as they respond to point non-point N additions, while P-metabolism genes are responsible for a vast number of cellular processes that can convolute functional-response studies.

In all, H5.3 was rejected as sites exhibited different trends in N, P, and S metabolism as analysed via RNA-seq metatranscriptomics. It is maintained that metatranscriptomics is most valuable when 1) experiments are based on a reference vs. treatment system, which is optimal for current statistical tests that seek to quantify differential expression between two groups, 2) 3-5 biological replicates are used per group, 3) observations are paired with physico-chemical measurements of the system. If environmental metatranscriptomes are interpreted alone, it is excellent for generating hypotheses for future studies, but often lacks context.

6.2 Conclusion

Advances in genomic tools expand our knowledge of the inner workings of microbial communities daily. A fundamental challenge in microbial ecology is how to utilize the immense volume of sequence data that currently exists while keeping pace with the increasing number of newly discovered genomes, and how this information can be integrated into the management and monitoring of ecosystems. The data comprising this thesis has added to exiting evidence that microbial communities, regardless of unit of extraction or analysis (DNA or RNA, amplicon sequencing or metatranscriptome) respond to anthropogenic stressors via alterations in their composition and function. This work also maintains that microbial communities vary spatially and temporally. Thus, routine microbial surveys are necessary if they are to inform and work towards the desired outcomes of natural and constructed environments. RNA-seq metatranscriptomics provide a bounty of information on microbial function, yet the capricious nature of microorganisms and the current cost constraints of shotgun sequencing makes this approach most useful for hypothesis generation, especially when coupled with novel techniques such as

microsensors technologies or stable isotope analysis. Amplicon sequencing of the 16S rRNA gene in prokaryotes (or the equivalent archaeal or fungal rRNA) remains a reliable and replicable method to survey microbial populations in vulnerable freshwater environments, and this technique is best paired with chemical parameters, such as salinity, nutrients, xenobiotics, and microplastics, that are known to contribute to ecosystem degradation and may trigger change in microbial abundances. The combining of both RNA and DNA-based amplicon sequencing, as introduced in this thesis work, is promising as a finer-tuned assessment of the microbial taxa that most contribute or respond to environmental vectors, as it captures highly active but also dead/dormant community members. The development of a bioinformatic tool that equates differences between DNA and RNA 16S sequence abundance (adjusting for gene copy number) to identify the most influential microbial taxa in an environmental sample could serve as an inexpensive addition (or replacement) to culture-based techniques. As this method would continue to rely on well-curated databases of known 16S rRNA gene sequences, the continued discovery of novel genomes via metagenomics would not hinder its relevance, so long as databases are kept updated.

The application of such a tool, or an equivalent technology using protein-coding genes, relies on continued communication and collaboration between research institutions, industry, and government. Above all, scientific progress depends on the curiosity of individuals, and the open and accepting sharing of their ideas, both good and bad.

References

- Amend, A.S., Martiny, A.C., Allison, S.D., Berlemont, R., Goulden, M.L., Lu, Y., Treseder, K.K., Weihe, C., Martiny, J.B.H., 2016. Microbial response to simulated global change is phylogenetically conserved and linked with functional potential. *ISME J.* 10, 109–118. <https://doi.org/10.1038/ismej.2015.96>
- Beattie, R.E., Bandla, A., Swarup, S., Hristova, K.R., 2020. Freshwater Sediment Microbial Communities Are Not Resilient to Disturbance From Agricultural Land Runoff. *Front. Microbiol.* 11, 1–14. <https://doi.org/10.3389/fmicb.2020.539921>
- Birrer, S.C., Dafforn, K.A., Simpson, S.L., Kelaher, B.P., Potts, J., Scanes, P., Johnston, E.L., 2018. Interactive effects of multiple stressors revealed by sequencing total (DNA) and active (RNA) components of experimental sediment microbial communities. *Sci. Total Environ.* 637–638, 1383–1394. <https://doi.org/10.1016/j.scitotenv.2018.05.065>
- Caron, D.A., Davis, P.G., Madin, L.P., Sieburth, J.M., 1986. Enrichment of microbial populations in macroaggregates (marine snow) from surface waters of the North Atlantic. *J. Mar. Res.* 44, 543–565. <https://doi.org/10.1357/002224086788403042>
- Cavaco, M.A., St. Louis, V.L., Engel, K., St. Pierre, K.A., Schiff, S.L., Stibal, M., Neufeld, J.D., 2019. Freshwater microbial community diversity in a rapidly changing High Arctic watershed. *FEMS Microbiol. Ecol.* 95, 1–13. <https://doi.org/10.1093/femsec/fiz161>
- Cyriaque, V., Geron, A., Billon, G., Nesme, J., Werner, J., Gillan, D.C., Sørensen, S.J., Wattiez, R., 2020. Metal-induced bacterial interactions promote diversity in river-sediment microbiomes. *FEMS Microbiol. Ecol.* 96, 1–12. <https://doi.org/10.1093/femsec/fiaa076>
- Dang, H., Lovell, C.R., 2016. Microbial Surface Colonization and Biofilm Development in Marine Environments. *Microbiol. Mol. Biol. Rev.* 80, 91–138. <https://doi.org/10.1128/mmbr.00037-15>
- Droppo, I.G., Liss, S.N., Williams, D., Nelson, T., Jaskot, C., Trapp, B., 2009. Dynamic existence of waterborne pathogens within river sediment compartments. Implications for water quality regulatory affairs. *Environ. Sci. Technol.* 43, 1737–1743. <https://doi.org/10.1021/es802321w>
- Froelich, P.N., 1988. Kinetic control of dissolved phosphate in natural rivers and estuaries: A primer on the phosphate buffer mechanism. *Limnol. Oceanogr.* 33, 649–668. <https://doi.org/10.4319/lo.1988.33.4part2.0649>
- Isobe, K., Allison, S.D., Khalili, B., Martiny, A.C., Martiny, J.B.H., 2019. Phylogenetic conservation of bacterial responses to soil nitrogen addition across continents. *Nat. Commun.* 10, 1–8. <https://doi.org/10.1038/s41467-019-10390-y>

- Kraemer, S.A., Barbosa da Costa, N., Shapiro, B.J., Fradette, M., Huot, Y., Walsh, D.A., 2020. A large-scale assessment of lakes reveals a pervasive signal of land use on bacterial communities. *ISME J.* 14, 3011–3023. <https://doi.org/10.1038/s41396-020-0733-0>
- Laas, P., Ugarelli, K., Travieso, R., Stumpf, S., Gaiser, E.E., Kominoski, J.S., Stingl, U., 2022. Water Column Microbial Communities Vary along Salinity Gradients in the Florida Coastal Everglades Wetlands. *Microorganisms* 10. <https://doi.org/10.3390/microorganisms10020215>
- Liu, T., Xia, X., Liu, S., Mou, X., Qiu, Y., 2013. Acceleration of denitrification in turbid rivers due to denitrification occurring on suspended sediment in oxic waters. *Environ. Sci. Technol.* 47, 4053–4061. <https://doi.org/10.1021/es304504m>
- Lozupone, C. a, Knight, R., 2007. Global patterns in bacterial diversity. *Proc. Natl. Acad. Sci. U. S. A.* 104, 11436–11440. <https://doi.org/10.1073/pnas.0611525104>
- Markovic, S., Blukacz-Richards, A.E., Dittrich, M., 2020. Speciation and bioavailability of particulate phosphorus in forested karst watersheds of southern Ontario during rain events. *J. Great Lakes Res.* 46, 824–838. <https://doi.org/10.1016/j.jglr.2020.05.001>
- Maron, P.-A., Sarr, A., Kaisermann, A., Lévêque, J., Mathieu, O., Guigue, J., Karimi, B., Bernard, L., Dequiedt, S., Terrat, S., Chabbi, A., Ranjard, L., 2018. High Microbial Diversity Promotes Soil Ecosystem Functioning. *Appl. Environ. Microbiol.* 84, 1–13.
- Orihel, D.M., Baulch, H.M., Casson, N.J., North, R.L., Parsons, C.T., Seckar, D.C.M., Venkiteswaran, J.J., 2017. Internal phosphorus loading in canadian fresh waters: A critical review and data analysis. *Can. J. Fish. Aquat. Sci.* 74, 2005–2029. <https://doi.org/10.1139/cjfas-2016-0500>
- Owens, P.N., 2020. Soil erosion and sediment dynamics in the Anthropocene: a review of human impacts during a period of rapid global environmental change. *J. Soils Sediments* 20, 4115–4143. <https://doi.org/10.1007/s11368-020-02815-9>
- Ray, R., Henshaw, P., Biswas, N., 2012. Effects of reduced aeration in a biological aerated filter. *Can. J. Civ. Eng.* 39, 432–438. <https://doi.org/10.1139/L2012-022>
- Savio, D., Sinclair, L., Ijaz, U.Z., Parajka, J., Reischer, G.H., Stadler, P., Blaschke, A.P., Blöschl, G., Mach, R.L., Kirschner, A.K.T., Farnleitner, A.H., Eiler, A., 2015. Bacterial diversity along a 2600km river continuum. *Environ. Microbiol.* 17, 4994–5007. <https://doi.org/10.1111/1462-2920.12886>
- Shin, N.R., Whon, T.W., Bae, J.W., 2015. Proteobacteria: Microbial signature of dysbiosis in gut microbiota. *Trends Biotechnol.* 33, 496–503. <https://doi.org/10.1016/j.tibtech.2015.06.011>
- Van Staden, T.L., Van Meter, K.J., Basu, N.B., Parsons, C.T., Akbarzadeh, Z., Van

- Cappellen, P., 2021. Agricultural phosphorus surplus trajectories for Ontario, Canada (1961–2016), and erosional export risk. *Sci. Total Environ.* 151717. <https://doi.org/10.1016/j.scitotenv.2021.151717>
- VanMensel, D., Droppo, I.G., Weisener, C.G., 2022. Identifying chemolithotrophic and pathogenic-related gene expression within suspended sediment flocs in freshwater environments: A metatranscriptomic assessment. *Sci. Total Environ.* 807, 150996. <https://doi.org/10.1016/j.scitotenv.2021.150996>
- Wood, S.A., Biessy, L., Pingram, M.A., Hamer, M.P., Wagenhoff, A., Clapcott, J., Pearman, J.K., 2021. Temporal and spatial variation in bacterial communities on uniform substrates in non- - wadeable rivers 1–12. <https://doi.org/10.1002/edn3.227>
- Yang, Y., Li, S., Gao, Y., Chen, Y., Zhan, A., 2019. Environment-driven geographical distribution of bacterial communities and identification of indicator taxa in Songhua River. *Ecol. Indic.* 101, 62–70. <https://doi.org/10.1016/j.ecolind.2018.12.047>
- Zhang, R., Xu, X., Jia, D., Lyu, Y., Hu, J., Chen, Q., Sun, W., 2021. Sediments alleviate the inhibition effects of antibiotics on denitrification: Functional gene, microbial community, and antibiotic resistance gene analysis. *Sci. Total Environ.* 804, 150092. <https://doi.org/10.1016/j.scitotenv.2021.150092>

APPENDICES

Appendix A (Chapter 2)

Table S1

Sample Site Characteristics and Library Depth

Sampling Site ID	UTM Coordinates (mE, mN)	DEPTH (m)	Number of Reads HiSeq
C1	326164.36, 4677019.76	4.4	2.07E+07
C2	326012.84, 4677011.6	3.2	2.25E+07
C3	325141.65, 4666449.25	2.5	2.39E+07
C4	325205.56, 4665864.02	2.6	2.60E+07
C5	325229.49, 4665731.21	4.7	1.93E+07
I1	326126.93, 4675376.04	5.7	2.15E+07
I2	322298.22, 4672345.58	2.8	2.09E+07
I3	322183.63, 4672153.8	4.9	2.28E+07
H1	319599.37, 4664753.54	2.1	2.30E+07
H2	319423.78, 4664257.02	1.5	1.92E+07
H3	319316.17, 4663870.21	1.5	2.33E+07
H4	319333.59, 4660985.31	1.9	2.23E+07
H5	319230.1, 4660780.51	1.6	2.07E+07

Table S2

Loadings of correlation coefficients from significant PCA axes for contaminants. Bolded values represent strong axis correlations (> 0.7).

	PC 1	PC 2
Tot PAH	0.8866	0.36597
Tot PCB	0.84199	0.37802
Tot OGCs	0.58219	0.73727
As	-0.56265	0.62714
Cd	0.8659	0.34217
Cr	0.9502	-0.10775
Cu	0.83264	-0.31555
Fe	0.94308	-0.23183
Hg	0.97647	0.11937
Mn	0.4889	-0.62885
Ni	0.94083	-0.12331
Pb	0.92446	-0.18728
Zn	0.98471	0.028813
TOC%	0.90653	0.022065

Table S3

SIMPER Analysis of select metals and total organic contaminants in Detroit River
Sediments

Contaminant	Average dissimilarity	Contrib. %	Cumulative %
Fe	10.34	96.95	96.95
Zn	0.1364	1.279	98.23
Mn	0.09478	0.8886	99.12
Tot PAH	0.01834	0.1719	99.29
Cu	0.0179	0.1678	99.46
Cr	0.01748	0.1639	99.62
Pb	0.01664	0.156	99.78
Ni	0.01195	0.112	99.89
As	0.00759	0.07115	99.96
TOC%	0.001994	0.0187	99.98
Cd	0.001083	0.01016	99.99
Tot PCB	0.0006406	0.006006	100
Hg	0.0003764	0.003529	100
Tot OGC	7.00E-05	0.0006563	100

Table S4

MetaTrans output of differentially expressed Cluster of Orthologous Groups (COGs) between COLD and HOT sediment regions. SD= standard deviation.

COG ID	baseMean COLD	baseMean HOT	SD COLD	SD HOT	log2FoldChange	pvalue	Annotation	COG Functional Category
COG1249	203.7671118	304.7188687	9.052612	27.48662	0.579266502	0.000558111	Pyruvate/2-oxoglutarate dehydrogenase complex, dihydrolipoamid	C - Energy production and conversion
COG2863	39.33630193	111.4980285	15.28949	35.63203	1.409907614	0.000807102	Cytochrome c553	C - Energy production and conversion
COG3658	16.28177114	58.74253953	6.908652	24.07258	1.681968113	0.000898818	Cytochrome b	C - Energy production and conversion
COG1274	332.7187554	771.602167	148.1516	74.54208	1.17036658	0.001363912	Phosphoenolpyruvate carboxykinase, GTP-dependent	C - Energy production and conversion
COG3245	14.74178544	46.94568855	6.080926	17.13404	1.516777189	0.002279992	Cytochrome c5	C - Energy production and conversion
COG1042	337.8980019	475.6608316	45.20153	31.14818	0.488448783	0.021511752	Acyl-CoA synthetase (NDP forming)	C - Energy production and conversion
COG1049	64.42484253	118.6207152	13.25561	31.46397	0.846715662	0.024691383	Aconitase B	C - Energy production and conversion
COG1139	31.94672723	54.56608699	6.290039	4.275917	0.723752602	0.048070759	L-lactate utilization protein LutB, contains a ferredoxin-type	C - Energy production and conversion

COG3087	0.633396964	7.211585123	0.928914	2.272091	2.457158267	0.010604682	Cell division protein FtsN	D - Cell cycle control and mitosis
COG4303	35.85405662	88.69276233	13.85613	18.60736	1.251423384	0.003535565	Ethanolamine ammonia-lyase, large subunit	E - Amino Acid metabolism and transport
COG0345	48.5298576	82.01773602	7.800854	10.64523	0.760872722	0.011234489	Pyrroline-5-carboxylate reductase	E - Amino Acid metabolism and transport
COG1449	81.43313351	146.4046972	3.506164	10.45924	0.841245969	4.32733E-06	Alpha-amylase/alpha-mannosidase, GH57 family	G - Carbohydrate metabolism and transport
COG0158	78.55992612	203.478721	19.56588	49.49272	1.338837537	4.35306E-06	Fructose-1,6-bisphosphatase	G - Carbohydrate metabolism and transport
COG0033	83.56712837	152.0308255	22.03969	20.97276	0.844657306	0.007323726	Phosphoglucumutase	G - Carbohydrate metabolism and transport
COG0296	176.538443	281.8789018	37.76998	15.25148	0.6551316	0.008725799	1,4-alpha-glucan branching enzyme	G - Carbohydrate metabolism and transport
COG4058	217.9557235	654.6786415	68.52338	185.6054	1.539957721	2.2333E-06	Methyl coenzyme M reductase, alpha subunit	H - Coenzyme metabolism
COG4547	3.160887298	12.35529271	1.842885	5.530542	1.755339228	0.030387943	Cobalamin biosynthesis protein CobT (nicotinate-mononucleotide	H - Coenzyme metabolism
COG4770	88.54880193	262.998724	15.98627	54.90812	1.525353626	1.074E-10	Acetyl/propionyl-CoA carboxylase, alpha subunit	I - Lipid metabolism
COG3243	163.9714713	478.6458697	68.69766	36.04585	1.487061398	8.27104E-06	Poly(3-hydroxyalkanoate) synthetase	I - Lipid metabolism
COG2030	79.701997	204.4580951	25.1546	35.41528	1.308468112	1.69693E-05	Acyl dehydratase	I - Lipid metabolism

COG2185	149.8332768	327.4090196	23.57567	86.48302	1.096782921	0.000154267	Methylmalonyl-CoA mutase, C-terminal domain/subunit (cobalamin)	I - Lipid metabolism
COG4395	64.98508538	134.6148631	17.76924	26.48986	1.0186162	0.002490516	Predicted lipid-binding transport protein, Tim44 family	I - Lipid metabolism
COG1024	224.2621519	299.310607	13.573	27.05746	0.417858631	0.038758264	Enoyl-CoA hydratase/carnithine racemase	I - Lipid metabolism
COG1028	745.8432252	997.2033917	89.17037	53.22289	0.412492191	0.029954211	NAD(P)-dependent dehydrogenase, short-chain alcohol dehydrogen	IQR - Lipid metabolism
COG2214	96.78088546	213.0935859	19.7412	89.41936	1.101504527	0.010276777	Curved DNA-binding protein CbpA, contains a DnaJ-like domain	K - Transcription
COG1309	77.52762279	137.794443	14.7169	34.08077	0.796884839	0.029003988	DNA-binding transcriptional regulator, AcrR family	K - Transcription
COG1961	30.11333155	71.12169954	4.340385	33.53916	1.171867797	0.022822043	Site-specific DNA recombinase related to the DNA invertase Pin	L - Replication and repair
COG2176	14.59108158	34.50761332	6.800331	4.014558	1.160475168	0.025312508	DNA polymerase III, alpha subunit (gram-positive type)	L - Replication and repair

COG4227	2.468190743	11.63395181	1.992797	5.129082	1.843957487	0.029051406	Antirestriction protein ArdC	L - Replication and repair
COG4974	78.48335887	158.2748077	12.68015	62.10563	0.974055349	0.037822097	Site-specific recombinase XerD	L - Replication and repair
COG1686	33.05755122	74.03550352	15.85074	14.41556	1.078178073	0.035523374	D-alanyl-D-alanine carboxypeptidase	M - Cell wall/membrane/envelop biogenesis
COG1192	108.0788968	412.2945924	15.48999	238.5798	1.800961196	0.000373132	Cellulose biosynthesis protein BcsQ	N - Cell motility
COG3168	11.19980169	36.19963505	3.435382	10.35669	1.555067092	0.00070447	Tfp pilus assembly protein PilP	NW - Cell motility
COG5008	23.74052191	65.52947915	13.79948	15.91474	1.328161075	0.014107367	Tfp pilus assembly protein, ATPase PilU	NW - Cell motility
COG1703	44.14180288	93.05814375	11.38315	15.84058	1.053251778	0.000929478	Putative periplasmic protein kinase ArgK or related GTPase of	O - Post-translational modification, protein turnover, chaperone functions
COG0354	6.467982249	18.80349934	2.405486	1.204045	1.409473944	0.009734813	Folate-binding Fe-S cluster repair protein YgfZ, possible role	O - Post-translational modification, protein turnover, chaperone functions
COG4097	4.557719127	28.51183314	1.150471	2.730683	2.438887854	1.64025E-08	Predicted ferric reductase	P - Inorganic ion transport and metabolism
COG3420	7.852215375	25.56969341	2.756224	4.788148	1.560502391	0.001060897	Nitrous oxidase accessory protein NosD, contains tandem CASH d	P - Inorganic ion transport and metabolism

COG3025	7.758971557	35.83803133	5.946609	16.06176	1.999261826	0.002304375	Inorganic triphosphatase YgiF, contains CYTH and CHAD domains	P - Inorganic ion transport and metabolism
COG2897	72.58442165	113.9371021	17.75098	11.7107	0.670781285	0.034508598	3-mercaptopyruvate sulfurtransferase SseA, contains two rhodan	P - Inorganic ion transport and metabolism
COG3608	10.94990904	118.4593938	7.709465	72.13603	3.126173755	1.09847E-08	Predicted deacylase	R - General Functional Prediction only
COG2413	3.689496237	28.92662692	3.24705	9.646601	2.808840379	4.25728E-07	Predicted nucleotidyltransferase	R - General Functional Prediction only
COG2321	46.48731238	127.8107785	24.86104	42.72685	1.401868848	0.005072275	Predicted metalloprotease	R - General Functional Prediction only
COG1988	0.942302642	14.01381364	1.788783	13.63571	2.494483386	0.02086932	Membrane-bound metal-dependent hydrolase Ybcl, DUF457 family	R - General Functional Prediction only
COG3864	0.84789884	6.915424773	0.550928	3.97755	2.21877249	0.025747137	Predicted metal-dependent peptidase	R - General Functional Prediction only
COG5490	22.75191032	355.3755785	19.18954	198.1675	3.553707649	1.99101E-11	Uncharacterized protein	S - Function Unknown
COG2823	201.745497	651.8847947	38.38115	209.9399	1.646376659	1.38357E-08	Osmotically-inducible protein OsmY, contains BON domain	S - Function Unknown
COG5276	37.73943313	99.24151525	7.014211	50.78676	1.333231321	0.005393991	Uncharacterized conserved protein	S - Function Unknown

COG0011	19.89300371	87.7363047	14.17375	63.36568	1.888927664	0.005682767	Uncharacterized conserved protein YqgV, UPF0045/DUF77 family	S - Function Unknown
COG4803	36.08933154	95.49040759	16.75405	28.14114	1.342332572	0.005682767	Uncharacterized membrane protein	S - Function Unknown
COG3071	3.7193457	12.71027548	2.039409	1.945679	1.564126937	0.024788333	Uncharacterized conserved protein HemY, contains two TPR repea	S - Function Unknown
COG4457	0.480903447	5.977797373	0.753388	4.553487	2.442482619	0.029954211	Uncharacterized protein	S - Function Unknown
COG3159	3.720827665	14.24041927	3.081051	4.591488	1.66476778	0.034545277	Uncharacterized conserved protein YigA, DUF484 family	S - Function Unknown
COG5473	6.018667905	26.02121782	2.470627	23.39473	1.795201662	0.03753977	Uncharacterized membrane protein	S - Function Unknown
COG1718	14.03115067	45.33077827	7.504189	20.7593	1.573354706	0.006409264	Serine/threonine-protein kinase RIO1	T - Signal Transduction
COG4831	1.328179132	8.873244912	0.886315	6.761561	2.05196502	0.042406558	Roadblock/LC7 domain	T - Signal Transduction
COG3456	3.620817986	107.1212838	2.747866	73.70255	3.888697003	2.08479E-08	Predicted component of the type VI protein secretion system, c	TU - Intracellular trafficking and secretion
COG3634	11.70768909	34.14946121	4.306785	10.30399	1.450512574	0.003893458	Alkyl hydroperoxide reductase subunit AhpF	V - Defence Mechanisms
COG3666	44.03618357	119.2412661	10.39698	39.11824	1.392133256	7.66169E-05	Transposase	X - Phage-derived proteins, transposases and other mobilome components

COG2963	14.56647179	39.47666581	5.040678	8.936976	1.301306204	0.002908904	Transposase and inactivated derivatives	X - Phage-derived proteins, transposases and other mobilome components
COG3677	1.628368315	13.53643061	1.319378	10.05882	2.450726165	0.003329644	Transposase	X - Phage-derived proteins, transposases and other mobilome components
COG5421	51.16397891	155.1255443	16.6481	74.75796	1.504408096	0.004058836	Transposase	X - Phage-derived proteins, transposases and other mobilome components
COG4679	18.468553	58.72357924	4.042532	31.62276	1.545522236	0.005393991	Phage-related protein	X - Phage-derived proteins, transposases and other mobilome components
COG4644	7.918912283	27.46854483	4.839554	8.2528	1.587874634	0.00715701	Transposase and inactivated derivatives, TnpA family	X - Phage-derived proteins, transposases and other mobilome components
COG3547	70.65435603	124.1550722	9.331512	32.96589	0.791467121	0.028271998	Transposase	X - Phage-derived proteins, transposases and other mobilome components
COG2036	364.0033367	159.7318538	124.7439	74.35505	-1.138521448	0.014304828	Archaeal histone H3/H4	B - Chromatin Structure and dynamics
COG0685	143.0425779	85.28697058	18.4139	25.59377	-0.73227538	0.048070759	5,10-methylenetetrahydrofolate reductase	E - Amino Acid metabolism and transport
COG3033	106.0502537	65.90098923	25.62764	3.47513	-0.675514044	0.053621618	Tryptophanase	E - Amino Acid metabolism and transport

COG2160	68.99874886	36.72023182	17.84738	7.838313	-0.859847693	0.046124214	L-arabinose isomerase	G - Carbohydrate metabolism and transport
COG2152	59.9251471	30.66026764	17.33655	8.485003	-0.908691491	0.050160703	Predicted glycosyl hydrolase, GH43/DUF377 family	G - Carbohydrate metabolism and transport
COG1947	68.56961874	30.58524145	25.39754	4.263135	-1.122489189	0.01090368	4-diphosphocytidyl-2C-methyl-D-erythritol kinase	I - Lipid metabolism
COG2606	599.2279578	296.2787345	281.5576	30.1205	-0.977684707	0.025698494	Cys-tRNA(Pro) deacylase, prolyl-tRNA editing enzyme YbaK/EbsC	J - Translation, ribosomal structure, and biogenesis
COG0193	119.1512891	54.73897424	59.61012	16.92208	-1.075681967	0.048070759	Peptidyl-tRNA hydrolase	J - Translation, ribosomal structure, and biogenesis
COG2238	79.60474848	50.23030345	4.671522	11.25668	-0.649784158	0.057901979	Ribosomal protein S19E (S16A)	J - Translation, ribosomal structure, and biogenesis
COG0739	148.4009655	100.3879011	8.315403	7.20832	-0.564314588	0.006579847	Murein DD-endopeptidase MepM and murein hydrolase activator NI	M - Cell wall/membrane/envelop biogenesis
COG4678	21.73071636	2.107625915	17.06777	3.38563	-2.474496602	0.013190193	Muramidase (phage lambda lysozyme)	MX - Cell wall/membrane/envelop biogenesis
COG3227	168.5677506	79.97399249	48.73245	19.08365	-1.03714441	0.00403955	Zn-dependent metalloprotease	O - Post-translational modification, protein turnover, chaperone functions
COG3508	43.95817972	17.15669647	14.84714	4.258077	-1.301634084	0.004552302	Homogentisate 1,2-dioxygenase	Q - Secondary Structure

COG0535	1399.643513	367.6140822	372.8115	83.23274	-1.88112626	2.12775E-12	Radical SAM superfamily enzyme, MoaA/NifB/PqqE/SkfB family	R - General Functional Prediction only
COG3450	35.97354674	11.28647872	8.101467	3.647472	-1.561770275	0.000244911	Predicted enzyme of the cupin superfamily	R - General Functional Prediction only
COG4784	54.66934291	21.73292084	22.70105	5.621388	-1.286861645	0.008762571	Putative Zn-dependent protease	R - General Functional Prediction only
COG0673	758.3394134	529.0406952	52.9791	70.94518	-0.513271664	0.008825192	Predicted dehydrogenase	R - General Functional Prediction only
COG2331	87.43833488	35.79446053	21.74793	15.71272	-1.222199591	0.010373748	Predicted nucleic acid-binding protein, contains Zn-ribbon dom	R - General Functional Prediction only
COG2013	73.75031475	43.71852688	10.43204	8.443006	-0.738838995	0.031568803	Uncharacterized conserved protein, AIM24 family	S - Function Unknown
COG2849	10.96765408	0.942777355	11.98577	1.46322	-2.458538259	0.019102047	Antitoxin component YwqK of the YwqJK toxin-antitoxin module	V - Defence Mechanisms
COG5277	587.2662992	92.25214966	467.9022	25.66921	-2.429454011	8.27104E-06	Actin-related protein	Z - Cytoskeleton

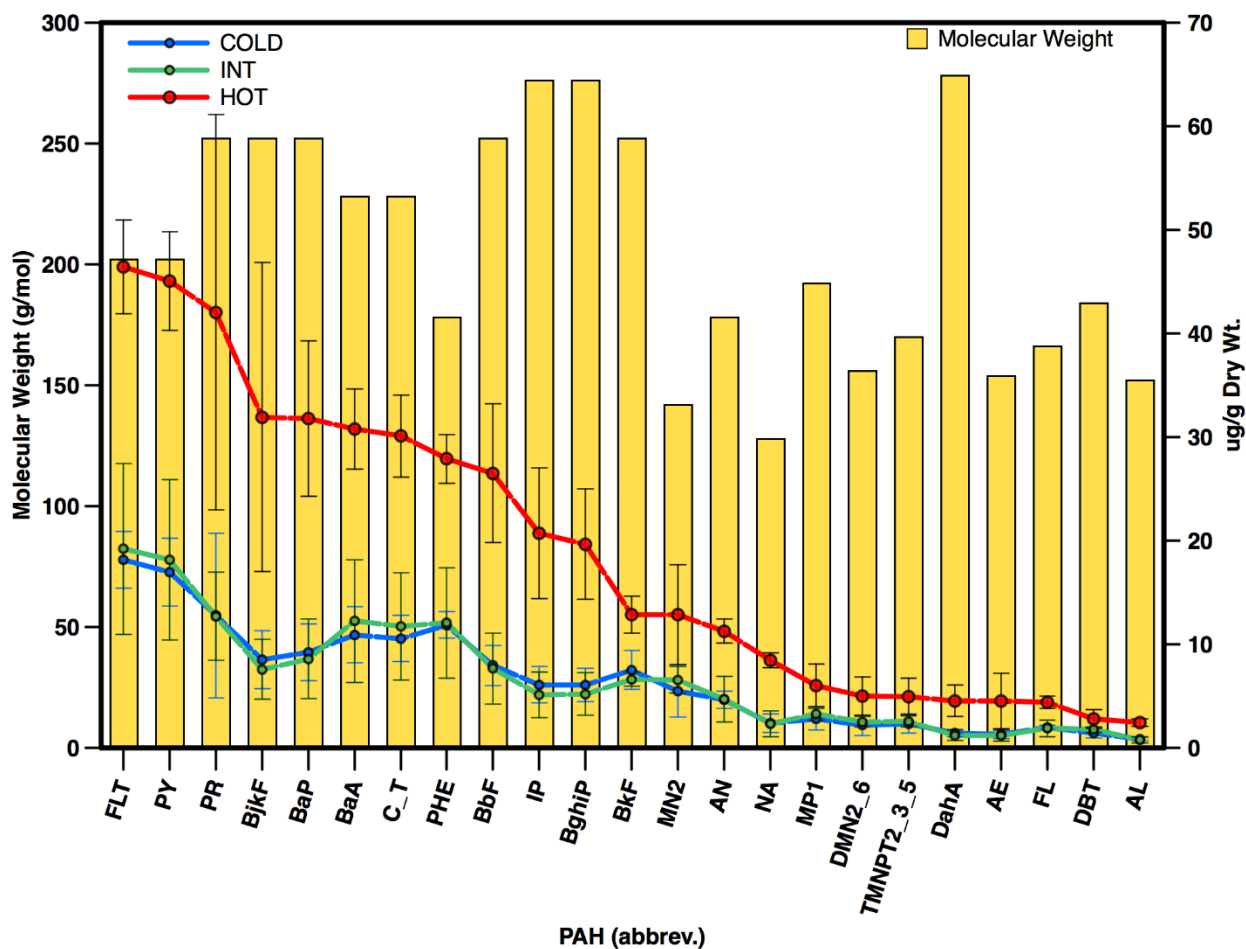


Figure S1: Interpolated weighted average concentrations ($\mu\text{g g}^{-1}$) of PAH's across COLD, HOT, and INT sediments of the Detroit River against molecular weight (g mol^{-1}). Error bars represent \pm standard deviation. AE: Acenaphthene, AL: Acenaphthylene, AN: Anthracene, BaA: Benz(a)anthracene, BaP: Benzo(a)pyrene, BbF: Benzo(b)fluoranthene, BghiP: Benzo(ghi)perylene, BjkF: Benzo(j,k)fluoranthene, BkF: Benzo(k)fluoranthene, C_T: Chrysene and Triphenylene, DahA: Dibenzo(a,h)anthracene, DBT: Dibenzothiophene, DMN2_6: 2,6-Dimethylnaphthalene, FL: Fluorene, FLT: Fluoroanthene, IP: Indeno(1,2,3-cd)pyrene; MN2: 2-Methylnaphthalene, MP1: 1-Methylphenanthrene, NA: Naphthalene, PHE: Phenanthrene, PR: Perylene PY: Pyrene, TMNPT2_3_5: 2,3,5-Trimethylnaphthalene

Appendix B (Chapter 3)

Table S1.

Detailed Watershed characteristics of Big Creek

	Big Creek (BC)
Location	42°12'18" N, 82°31'12" W
Gross Drainage Area (km²)	56.9
Köppen-Geiger Climate Classification	Dfb
Mean annual air temp (°C)	9
Annual Precipitation (mm)	686 - 849
Land Use	> 70% agriculture, < 10% forested
Soil Characteristics	Clay loam soils (Brookston Clay)
Agriculture Characteristics	Soybean, wheat, and corn
Livestock Density (animal units ha⁻¹)	0.26 (Nelligan et al., 2020)
Tile Drainage %	> 90% (Nelligan et al., 2020)
Average Slope (m km⁻¹)	0.39
Length of Study Reach (km)	0.7
Stream order of study reach	2 nd order: *several ephemeral agricultural ditches connect upstream of the study reach, increasing the hydrological connectivity of the reach during periods of high flow
Total length of watercourse (km)	25
Watercourse mouth	Southeast Lake St. Clair, Ontario, Canada

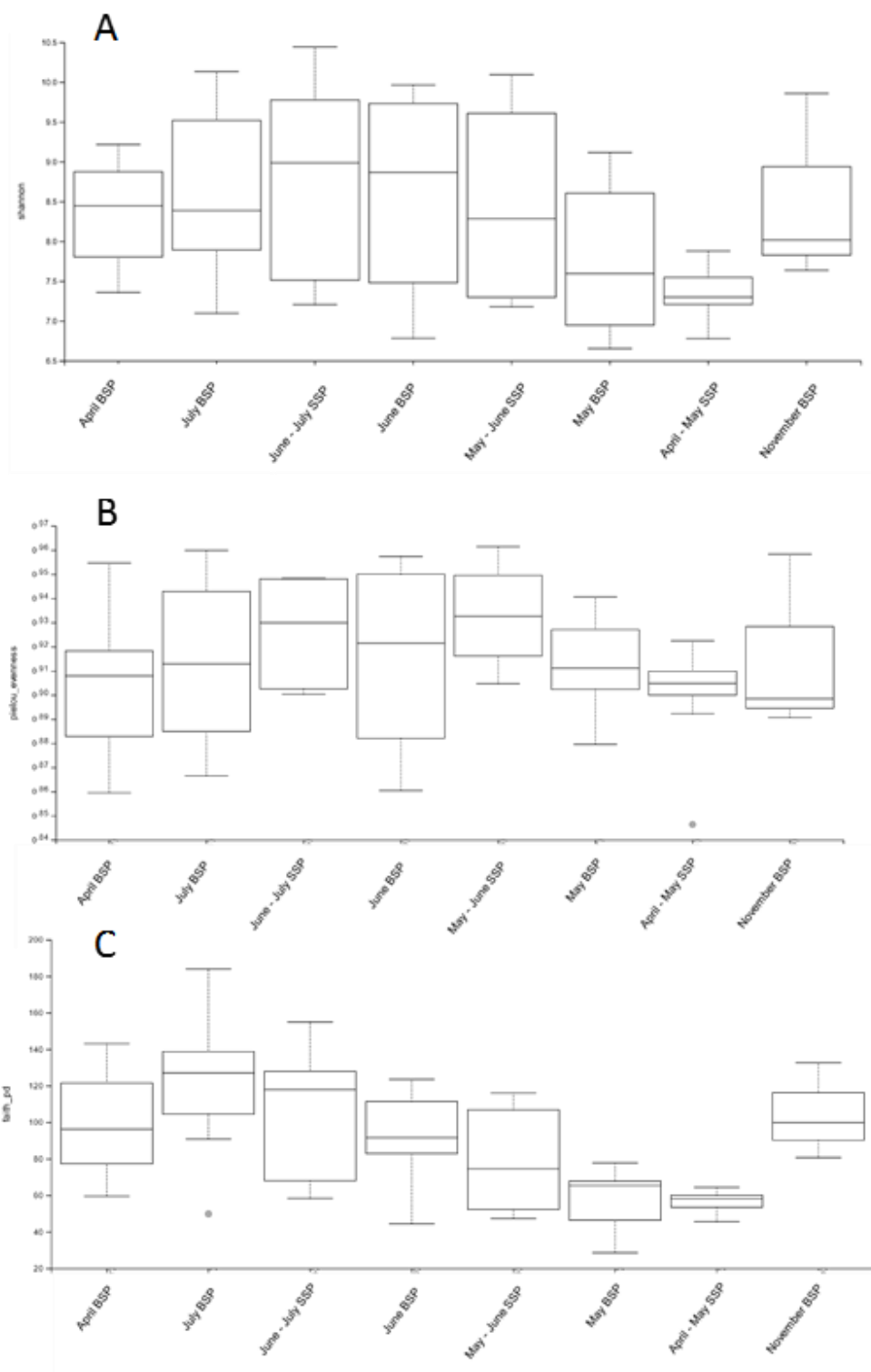


Figure S1. Alpha Diversity Box Plots for monthly Bed Sediment Phase (BSP) and Suspended Sediment Phase (SSP) microbial communities. A = Shannon, B = Evenness, C = Faith pd

Table S2. Alpha Diversity Pairwise Comparison Statistical Output. *Indicates significant comparison						
Group 1	Group 2	H	p-value	q-value	Index	Test
S1_AM_SSP_left (n=2)	S1_AM_SSP_right (n=2)	0.000	1.000	1.000	Shannon	Replicate_PT_Sampler
S3_AM_SSP_left (n=2)	S3_AM_SSP_right (n=2)	2.400	0.121	0.364	Shannon	Replicate_PT_Sampler
S1_AM_SSP_left (n=2)	S1_AM_SSP_right (n=2)	0.000	1.000	1.000	Eveness	Replicate_PT_Sampler
S3_AM_SSP_left (n=2)	S3_AM_SSP_right (n=2)	2.400	0.121	0.364	Eveness	Replicate_PT_Sampler
S1_AM_SSP_left (n=2)	S1_AM_SSP_right (n=2)	0.600	0.439	0.526	Faith_pd	Replicate_PT_Sampler
S3_AM_SSP_left (n=2)	S3_AM_SSP_right (n=2)	2.400	0.121	0.364	Faith_pd	Replicate_PT_Sampler
S1_SSP_JJ (n=3)	S3_SSP_JJ (n=2)	0.333	0.564	0.826	Shannon	Sub-site_PT_Sampler
S1_SSP_MJ (n=3)	S3_SSP_MJ (n=3)	0.429	0.513	0.826	Shannon	Sub-site_PT_Sampler
S1_SSP_AP (n=6)	S3_SSP_AP (n=5)	0.000	1.000	1.000	Shannon	Sub-site_PT_Sampler
S1_SSP_JJ (n=3)	S3_SSP_JJ (n=2)	0.333	0.564	0.826	Eveness	Sub-site_PT_Sampler
S1_SSP_MJ (n=3)	S3_SSP_MJ (n=3)	0.048	0.827	0.944	Eveness	Sub-site_PT_Sampler
S1_SSP_AP (n=6)	S3_SSP_AP (n=5)	0.033	0.855	0.944	Eveness	Sub-site_PT_Sampler
S1_SSP_JJ (n=3)	S3_SSP_JJ (n=2)	0.333	0.564	0.705	Faith_pd	Sub-site_PT_Sampler
S1_SSP_MJ (n=3)	S3_SSP_MJ (n=3)	2.333	0.127	0.271	Faith_pd	Sub-site_PT_Sampler
S1_SSP_AP (n=6)	S3_SSP_AP (n=5)	0.033	0.855	0.881	Faith_pd	Sub-site_PT_Sampler
S1_BSP_april (n=1)	S2_BSP_april (n=6)	0.250	0.617	0.929	Shannon	Sub-site_BSP
S1_BSP_april (n=1)	S3_BSP_april (n=5)	0.771	0.380	0.929	Shannon	Sub-site_BSP
S1_BSP_july (n=5)	S2_BSP_july (n=4)	1.500	0.221	0.929	Shannon	Sub-site_BSP
S1_BSP_july (n=5)	S3_BSP_july (n=2)	0.600	0.439	0.929	Shannon	Sub-site_BSP
S1_BSP_june (n=3)	S2_BSP_june (n=4)	0.000	1.000	1.000	Shannon	Sub-site_BSP
S1_BSP_june (n=3)	S3_BSP_june (n=3)	0.048	0.827	0.968	Shannon	Sub-site_BSP
S1_BSP_may (n=2)	S2_BSP_may (n=3)	0.333	0.564	0.929	Shannon	Sub-site_BSP
S1_BSP_may (n=2)	S3_BSP_may (n=2)	0.600	0.439	0.929	Shannon	Sub-site_BSP
S2_BSP_april (n=6)	S3_BSP_april (n=5)	0.300	0.584	0.929	Shannon	Sub-site_BSP
S2_BSP_july (n=4)	S3_BSP_july (n=2)	0.000	1.000	1.000	Shannon	Sub-site_BSP
S2_BSP_june (n=4)	S3_BSP_june (n=3)	0.500	0.480	0.929	Shannon	Sub-site_BSP

S2_BSP_may (n=3)	S3_BSP_may (n=2)	1.333	0.248	0.929	Shannon	Sub-site_BSP
S1_BSP_april (n=1)	S2_BSP_april (n=6)	0.250	0.617	0.972	Eveness	Sub-site_BSP
S1_BSP_april (n=1)	S3_BSP_april (n=5)	0.086	0.770	0.972	Eveness	Sub-site_BSP
S1_BSP_july (n=5)	S2_BSP_july (n=4)	0.540	0.462	0.972	Eveness	Sub-site_BSP
S1_BSP_july (n=5)	S3_BSP_july (n=2)	0.150	0.699	0.972	Eveness	Sub-site_BSP
S1_BSP_june (n=3)	S2_BSP_june (n=4)	0.125	0.724	0.972	Eveness	Sub-site_BSP
S1_BSP_june (n=3)	S3_BSP_june (n=3)	1.190	0.275	0.972	Eveness	Sub-site_BSP
S1_BSP_may (n=2)	S2_BSP_may (n=3)	3.000	0.083	0.972	Eveness	Sub-site_BSP
S1_BSP_may (n=2)	S3_BSP_may (n=2)	0.600	0.439	0.972	Eveness	Sub-site_BSP
S2_BSP_april (n=6)	S3_BSP_april (n=5)	0.133	0.715	0.972	Eveness	Sub-site_BSP
S2_BSP_july (n=4)	S3_BSP_july (n=2)	0.000	1.000	1.000	Eveness	Sub-site_BSP
S2_BSP_june (n=4)	S3_BSP_june (n=3)	1.125	0.289	0.972	Eveness	Sub-site_BSP
S2_BSP_may (n=3)	S3_BSP_may (n=2)	3.000	0.083	0.972	Eveness	Sub-site_BSP
S1_BSP_april (n=1)	S2_BSP_april (n=6)	2.250	0.134	0.289	Faith_pd	Sub-site_BSP
S1_BSP_april (n=1)	S3_BSP_april (n=5)	0.771	0.380	0.581	Faith_pd	Sub-site_BSP
S1_BSP_july (n=5)	S2_BSP_july (n=4)	2.940	0.086	0.250	Faith_pd	Sub-site_BSP
S1_BSP_july (n=5)	S3_BSP_july (n=2)	1.350	0.245	0.440	Faith_pd	Sub-site_BSP
S1_BSP_june (n=3)	S2_BSP_june (n=4)	0.500	0.480	0.634	Faith_pd	Sub-site_BSP
S1_BSP_june (n=3)	S3_BSP_june (n=3)	0.048	0.827	0.884	Faith_pd	Sub-site_BSP
S1_BSP_may (n=2)	S2_BSP_may (n=3)	0.000	1.000	1.000	Faith_pd	Sub-site_BSP
S1_BSP_may (n=2)	S3_BSP_may (n=2)	0.600	0.439	0.634	Faith_pd	Sub-site_BSP
S2_BSP_april (n=6)	S3_BSP_april (n=5)	0.833	0.361	0.575	Faith_pd	Sub-site_BSP
S2_BSP_july (n=4)	S3_BSP_july (n=2)	0.857	0.355	0.575	Faith_pd	Sub-site_BSP
S2_BSP_june (n=4)	S3_BSP_june (n=3)	0.500	0.480	0.634	Faith_pd	Sub-site_BSP
S2_BSP_may (n=3)	S3_BSP_may (n=2)	0.000	1.000	1.000	Faith_pd	Sub-site_BSP
april_BSP (n=12)	july_BSP (n=11)	0.545	0.460	0.848	Shannon	Monthly_BSP_SSP
april_BSP (n=12)	JJ_SSP (n=5)	0.400	0.527	0.848	Shannon	Monthly_BSP_SSP
april_BSP (n=12)	june_BSP (n=10)	0.526	0.468	0.848	Shannon	Monthly_BSP_SSP

april_BSP (n=12)	MJ_SSP (n=6)	0.009	0.925	0.990	Shannon	Monthly_BSP_SSP
april_BSP (n=12)	may_BSP (n=7)	1.207	0.272	0.692	Shannon	Monthly_BSP_SSP
april_BSP (n=12)	AM_SSP (n=11)	11.045	0.001	0.016*	Shannon	Monthly_BSP_SSP
april_BSP (n=12)	nov_BSP (n=3)	0.083	0.773	0.941	Shannon	Monthly_BSP_SSP
july_BSP (n=11)	JJ_SSP (n=5)	0.003	0.955	0.990	Shannon	Monthly_BSP_SSP
july_BSP (n=11)	june_BSP (n=10)	0.179	0.673	0.897	Shannon	Monthly_BSP_SSP
july_BSP (n=11)	MJ_SSP (n=6)	0.364	0.546	0.848	Shannon	Monthly_BSP_SSP
july_BSP (n=11)	may_BSP (n=7)	2.512	0.113	0.474	Shannon	Monthly_BSP_SSP
july_BSP (n=11)	AM_SSP (n=11)	10.565	0.001	0.016*	Shannon	Monthly_BSP_SSP
july_BSP (n=11)	nov_BSP (n=3)	0.297	0.586	0.848	Shannon	Monthly_BSP_SSP
JJ_SSP (n=5)	june_BSP (n=10)	0.060	0.806	0.941	Shannon	Monthly_BSP_SSP
JJ_SSP (n=5)	MJ_SSP (n=6)	0.300	0.584	0.848	Shannon	Monthly_BSP_SSP
JJ_SSP (n=5)	may_BSP (n=7)	1.484	0.223	0.692	Shannon	Monthly_BSP_SSP
JJ_SSP (n=5)	AM_SSP (n=11)	3.083	0.079	0.443	Shannon	Monthly_BSP_SSP
JJ_SSP (n=5)	nov_BSP (n=3)	0.022	0.881	0.987	Shannon	Monthly_BSP_SSP
june_BSP (n=10)	MJ_SSP (n=6)	0.106	0.745	0.941	Shannon	Monthly_BSP_SSP
june_BSP (n=10)	may_BSP (n=7)	2.438	0.118	0.474	Shannon	Monthly_BSP_SSP
june_BSP (n=10)	AM_SSP (n=11)	6.074	0.014	0.111	Shannon	Monthly_BSP_SSP
june_BSP (n=10)	nov_BSP (n=3)	0.000	1.000	1.000	Shannon	Monthly_BSP_SSP
MJ_SSP (n=6)	may_BSP (n=7)	1.306	0.253	0.692	Shannon	Monthly_BSP_SSP
MJ_SSP (n=6)	AM_SSP (n=11)	1.707	0.191	0.670	Shannon	Monthly_BSP_SSP
MJ_SSP (n=6)	nov_BSP (n=3)	0.267	0.606	0.848	Shannon	Monthly_BSP_SSP
may_BSP (n=7)	AM_SSP (n=11)	0.347	0.556	0.848	Shannon	Monthly_BSP_SSP
may_BSP (n=7)	nov_BSP (n=3)	1.052	0.305	0.712	Shannon	Monthly_BSP_SSP
AM_SSP (n=11)	nov_BSP (n=3)	5.824	0.016	0.111	Shannon	Monthly_BSP_SSP
april_BSP (n=12)	july_BSP (n=11)	0.852	0.356	0.858	Eveness	Monthly_BSP_SSP
april_BSP (n=12)	JJ_SSP (n=5)	1.344	0.246	0.858	Eveness	Monthly_BSP_SSP
april_BSP (n=12)	june_BSP (n=10)	0.352	0.553	0.858	Eveness	Monthly_BSP_SSP

april_BSP (n=12)	MJ_SSP (n=6)	4.246	0.039	0.551	Eveness	Monthly_BSP_SSP
april_BSP (n=12)	may_BSP (n=7)	0.579	0.447	0.858	Eveness	Monthly_BSP_SSP
april_BSP (n=12)	AM_SSP (n=11)	0.136	0.712	0.858	Eveness	Monthly_BSP_SSP
april_BSP (n=12)	nov_BSP (n=3)	0.083	0.773	0.866	Eveness	Monthly_BSP_SSP
july_BSP (n=11)	JJ_SSP (n=5)	0.542	0.462	0.858	Eveness	Monthly_BSP_SSP
july_BSP (n=11)	june_BSP (n=10)	0.179	0.673	0.858	Eveness	Monthly_BSP_SSP
july_BSP (n=11)	MJ_SSP (n=6)	1.222	0.269	0.858	Eveness	Monthly_BSP_SSP
july_BSP (n=11)	may_BSP (n=7)	0.002	0.964	1.000	Eveness	Monthly_BSP_SSP
july_BSP (n=11)	AM_SSP (n=11)	0.389	0.533	0.858	Eveness	Monthly_BSP_SSP
july_BSP (n=11)	nov_BSP (n=3)	0.006	0.938	1.000	Eveness	Monthly_BSP_SSP
JJ_SSP (n=5)	june_BSP (n=10)	0.000	1.000	1.000	Eveness	Monthly_BSP_SSP
JJ_SSP (n=5)	MJ_SSP (n=6)	0.300	0.584	0.858	Eveness	Monthly_BSP_SSP
JJ_SSP (n=5)	may_BSP (n=7)	1.114	0.291	0.858	Eveness	Monthly_BSP_SSP
JJ_SSP (n=5)	AM_SSP (n=11)	2.339	0.126	0.858	Eveness	Monthly_BSP_SSP
JJ_SSP (n=5)	nov_BSP (n=3)	0.556	0.456	0.858	Eveness	Monthly_BSP_SSP
june_BSP (n=10)	MJ_SSP (n=6)	0.953	0.329	0.858	Eveness	Monthly_BSP_SSP
june_BSP (n=10)	may_BSP (n=7)	0.152	0.696	0.858	Eveness	Monthly_BSP_SSP
june_BSP (n=10)	AM_SSP (n=11)	0.402	0.526	0.858	Eveness	Monthly_BSP_SSP
june_BSP (n=10)	nov_BSP (n=3)	0.114	0.735	0.858	Eveness	Monthly_BSP_SSP
MJ_SSP (n=6)	may_BSP (n=7)	2.041	0.153	0.858	Eveness	Monthly_BSP_SSP
MJ_SSP (n=6)	AM_SSP (n=11)	6.828	0.009	0.251	Eveness	Monthly_BSP_SSP
MJ_SSP (n=6)	nov_BSP (n=3)	1.067	0.302	0.858	Eveness	Monthly_BSP_SSP
may_BSP (n=7)	AM_SSP (n=11)	1.085	0.298	0.858	Eveness	Monthly_BSP_SSP
may_BSP (n=7)	nov_BSP (n=3)	0.117	0.732	0.858	Eveness	Monthly_BSP_SSP
AM_SSP (n=11)	nov_BSP (n=3)	0.152	0.697	0.858	Eveness	Monthly_BSP_SSP
april_BSP (n=12)	july_BSP (n=11)	2.367	0.124	0.248	Shannon	Monthly_BSP_SSP
april_BSP (n=12)	JJ_SSP (n=5)	0.011	0.916	0.916	Shannon	Monthly_BSP_SSP
april_BSP (n=12)	june_BSP (n=10)	0.109	0.742	0.831	Shannon	Monthly_BSP_SSP

april_BSP (n=12)	MJ_SSP (n=6)	1.719	0.190	0.332	Shannon	Monthly_BSP_SSP
april_BSP (n=12)	may_BSP (n=7)	8.257	0.004	0.022*	Shannon	Monthly_BSP_SSP
april_BSP (n=12)	AM_SSP (n=11)	15.034	0.000	0.003*	Shannon	Monthly_BSP_SSP
april_BSP (n=12)	nov_BSP (n=3)	0.021	0.885	0.916	Shannon	Monthly_BSP_SSP
july_BSP (n=11)	JJ_SSP (n=5)	0.260	0.610	0.743	Shannon	Monthly_BSP_SSP
july_BSP (n=11)	june_BSP (n=10)	5.078	0.024	0.068	Shannon	Monthly_BSP_SSP
july_BSP (n=11)	MJ_SSP (n=6)	4.455	0.035	0.089	Shannon	Monthly_BSP_SSP
july_BSP (n=11)	may_BSP (n=7)	9.763	0.002	0.014*	Shannon	Monthly_BSP_SSP
july_BSP (n=11)	AM_SSP (n=11)	10.996	0.001	0.013*	Shannon	Monthly_BSP_SSP
july_BSP (n=11)	nov_BSP (n=3)	1.752	0.186	0.332	Shannon	Monthly_BSP_SSP
JJ_SSP (n=5)	june_BSP (n=10)	0.540	0.462	0.681	Shannon	Monthly_BSP_SSP
JJ_SSP (n=5)	MJ_SSP (n=6)	2.700	0.100	0.216	Shannon	Monthly_BSP_SSP
JJ_SSP (n=5)	may_BSP (n=7)	3.488	0.062	0.144	Shannon	Monthly_BSP_SSP
JJ_SSP (n=5)	AM_SSP (n=11)	6.497	0.011	0.038*	Shannon	Monthly_BSP_SSP
JJ_SSP (n=5)	nov_BSP (n=3)	0.022	0.881	0.916	Shannon	Monthly_BSP_SSP
june_BSP (n=10)	MJ_SSP (n=6)	0.424	0.515	0.687	Shannon	Monthly_BSP_SSP
june_BSP (n=10)	may_BSP (n=7)	8.010	0.005	0.022*	Shannon	Monthly_BSP_SSP
june_BSP (n=10)	AM_SSP (n=11)	9.600	0.002	0.014*	Shannon	Monthly_BSP_SSP
june_BSP (n=10)	nov_BSP (n=3)	0.457	0.499	0.687	Shannon	Monthly_BSP_SSP
MJ_SSP (n=6)	may_BSP (n=7)	1.306	0.253	0.417	Shannon	Monthly_BSP_SSP
MJ_SSP (n=6)	AM_SSP (n=11)	0.162	0.688	0.802	Shannon	Monthly_BSP_SSP
MJ_SSP (n=6)	nov_BSP (n=3)	1.067	0.302	0.469	Shannon	Monthly_BSP_SSP
may_BSP (n=7)	AM_SSP (n=11)	0.347	0.556	0.708	Shannon	Monthly_BSP_SSP
may_BSP (n=7)	nov_BSP (n=3)	5.727	0.017	0.052	Shannon	Monthly_BSP_SSP
AM_SSP (n=11)	nov_BSP (n=3)	6.600	0.010	0.038*	Shannon	Monthly_BSP_SSP
BSP = Bed Sediment Phase						
SSP = Suspended Sediment Phase						
nov = November						
AM = April – May						

MJ = May – June

JJ = June - July

Table S3. Bray Curtis Pairwise Comparison Statistical Output. *Indicates significant comparison						
Group 1	Group 2	Sample size	<i>pseudo-F</i>	p-value	q-value	Test
S1_AM_SSP_left	S1_AM_SSP_right	4	0.931228	0.661	0.822	Replicate_PT_Sampler
S3_AM_SSP_left	S3_AM_SSP_right	4	1.08286	0.342	0.748	Replicate_PT_Sampler
S1_SSP_JJ	S3_SSP_JJ	5	1.128357	0.3	0.346	Sub-site_PT_Sampler
S1_SSP_MJ	S3_SSP_MJ	6	0.973133	0.505	0.505	Sub-site_PT_Sampler
S1_SSP_AM	S3_SSP_AM	11	0.996772	0.449	0.481	Sub-site_PT_Sampler
S1_BSP_april	S2_BSP_april	7	0.88117	0.706	0.737	Sub-site_BSP
S1_BSP_april	S2_BSP_april	6	0.925516	1	1	Sub-site_BSP
S1_BSP_july	S2_BSP_july	9	0.990275	0.432	0.489	Sub-site_BSP
S1_BSP_july	S3_BSP_july	7	0.909382	0.705	0.737	Sub-site_BSP
S1_BSP_june	S2_BSP_june	7	1.549007	0.057	0.195	Sub-site_BSP
S1_BSP_june	S3_BSP_june	6	1.164515	0.313	0.391	Sub-site_BSP
S1_BSP_may	S2_BSP_may	5	1.299222	0.307	0.391	Sub-site_BSP
S1_BSP_may	S3_BSP_may	4	1.586495	0.351	0.421	Sub-site_BSP
S2_BSP_april	S3_BSP_april	11	1.483597	0.023	0.151	Sub-site_BSP
S2_BSP_july	S3_BSP_july	6	1.046658	0.252	0.357	Sub-site_BSP
S2_BSP_june	S3_BSP_june	7	1.734004	0.029	0.151	Sub-site_BSP
S2_BSP_may	S3_BSP_may	5	2.135035	0.092	0.203	Sub-site_BSP
april_BSP	july_BSP	23	1.756677	0.001	0.003*	Monthly_BSP_SSP
april_BSP	JJ_SSP	17	2.635545	0.001	0.003*	Monthly_BSP_SSP
april_BSP	june_BSP	22	1.29154	0.045	0.047*	Monthly_BSP_SSP
april_BSP	MJ_SSP	18	2.516195	0.001	0.003*	Monthly_BSP_SSP
april_BSP	may_BSP	19	1.481626	0.024	0.027*	Monthly_BSP_SSP
april_BSP	AM_SSP	23	3.27475	0.001	0.003*	Monthly_BSP_SSP
april_BSP	nov_BSP	15	1.583026	0.006	0.008*	Monthly_BSP_SSP
july_BSP	JJ_SSP	16	2.105739	0.001	0.003*	Monthly_BSP_SSP
july_BSP	june_BSP	21	1.605971	0.005	0.007*	Monthly_BSP_SSP
july_BSP	MJ_SSP	17	2.270861	0.001	0.003*	Monthly_BSP_SSP
july_BSP	may_BSP	18	2.045583	0.002	0.003*	Monthly_BSP_SSP
july_BSP	AM_SSP	22	3.253662	0.001	0.003*	Monthly_BSP_SSP
july_BSP	nov_BSP	14	1.58675	0.002	0.003*	Monthly_BSP_SSP
JJ_SSP	june_BSP	15	2.439304	0.002	0.003*	Monthly_BSP_SSP
JJ_SSP	MJ_SSP	11	1.534152	0.004	0.006*	Monthly_BSP_SSP
JJ_SSP	may_BSP	12	2.568109	0.002	0.003*	Monthly_BSP_SSP
JJ_SSP	AM_SSP	16	2.56616	0.002	0.003*	Monthly_BSP_SSP
JJ_SSP	nov_BSP	8	1.642396	0.017	0.021*	Monthly_BSP_SSP
june_BSP	MJ_SSP	16	2.290524	0.001	0.003*	Monthly_BSP_SSP

june_BSP	may_BSP	17	1.181898	0.176	0.176	Monthly_BSP_SSP
june_BSP	AM_SSP	21	3.13699	0.001	0.003*	Monthly_BSP_SSP
june_BSP	nov_BSP	13	1.600757	0.018	0.021*	Monthly_BSP_SSP
MJ_SSP	may_BSP	13	2.256455	0.005	0.007*	Monthly_BSP_SSP
MJ_SSP	AM_SSP	17	1.961514	0.001	0.003*	Monthly_BSP_SSP
MJ_SSP	nov_BSP	9	1.525499	0.015	0.019*	Monthly_BSP_SSP
may_BSP	AM_SSP	18	2.670985	0.001	0.003*	Monthly_BSP_SSP
may_BSP	nov_BSP	10	1.591615	0.041	0.044*	Monthly_BSP_SSP
AM_SSP	nov_BSP	14	1.875819	0.002	0.003*	Monthly_BSP_SSP
BSP = Bed Sediment Phase SSP = Suspended Sediment Phase nov = November AM = April – May MJ = May – June JJ = June - July						

Additional Methods

Grab Sampling of Surface Water:

For each of triplicate surface water samples, a clean 250 mL HDPE, opaque, wide-mouth bottle was used for collection. With the collector facing upstream, the cap of the bottle was unscrewed in the field close to the water surface and the bottle lowered into the watercourse at a depth of about 10-20 cm from the surface. The bottle was rinsed three times with sample, being emptied downstream and filled again, taking care to not collect in an area that was disturbed by wading. If wading disturbed sediment, then the collector waited until the suspended sediment settled or was washed downstream. Bottles were filled completely to avoid any oxygen in headspace of the bottle and placed on ice until returning from the field. Samples were then either processed immediately or frozen at -20 degrees C, in which case approximately 5-10 mL were emptied from the bottle to avoid rupturing of the container during freezing.

Sterilization:

All consumable materials (bottles, buckets, containers) were either sterilized by the manufacturer and used new or sterilized beforehand in bleach or 70% ethanol.

Appendix C (Chapter 4)

Table S1

General watershed characteristics of Big Creek, Nissouri Creek, and Saugeen River

	Big Creek (BC)	Nissouri Creek (NC)	Saugeen River (SR)
Sampling Location	42°12'18" N, 82°31'12" W	43°07'48" N, 80°57'48" W	44° 11' 07" N, 80° 47' 14" W
Gross Drainage Area (km²)	56.9	29.1	329
Mean annual air temp (°C)	9	7.4	7.3
Annual Average Precipitation (mm)	686 - 849	946	946
Land Use	> 70% agriculture, < 10% forested	> 70% agriculture, < 10% forested	58% agriculture; 35% forested; 1.4% urban
Soil Characteristics	Clay loam soils (Brookston Clay)	Loam/silt loam soils (Guelph Loam)	Sandy, well- drained loam soils (Sargent Loam, Harriston Loam, Pike Lake Loam)
Agriculture Characteristics	Soybean, wheat, and corn	Pasture, corn, soybean, wheat, hay, beef, dairy, swine livestock	Pasture, corn, soybean, wheat, hay, beef, dairy, swine livestock
Average Slope (m km⁻¹)	0.39	0.92	7.13

Table S2

Significant Phylum and Genus Bioindicator Taxa Nissouri Creek Mid Spring 2019

Phyla		
Taxa	Adjusted p-value	LDA Score
Proteobacteria	0.000193	5.91
Actinobacteria	0.000337	5.59
Firmicutes	4.05E-05	4.67
Thaumarchaeota	0.000401	4.46
Genera		
Taxa	Adjusted p-value	LDA Score
<i>Dechloromonas</i>	5.01E-05	2.3
<i>Rhodoferax</i>	0.000148	2.26
<i>Thauera</i>	0.000193	1.99
<i>Unassigned</i>	0.00048	3.09
<i>Rhizobacter</i>	0.000538	2.08
<i>Candidatus Nitrosocosmicus</i>	0.000667	1.56
<i>Nocardioides</i>	0.000885	1.7
<i>Bacillus</i>	0.000986	1.62
<i>Polaromonas</i>	0.001698	2.21
<i>Aquabacterium</i>	0.001827	2.3
<i>Mycobacterium</i>	0.002009	1.58
<i>Gaiella</i>	0.00632	1.93
<i>Ilumatobacter</i>	0.015745	1.73
<i>Undibacterium</i>	0.061701	1.11
P-values represent adjusted False Detection Rates (FDR) as calculated via Linear discriminant analysis (LDA) Effect Size (LEfSe).		

Table S3: Site Statistics for Total Nitrogen (TN) and Total Phosphorus (TP) Concentrations and TN:TP ratios

Total Nitrogen (TN) Concentrations				
<u>Site</u>	<u>Data Set</u>	<u>Mean TN (mg L⁻¹)</u>	<u>Median TN (mg L⁻¹)</u>	<u>Standard Deviation (mg L⁻¹)</u>
Big creek	Current Study	1.6766444	0.9557	1.687836
Big creek	PWQMN	3.4522222	2.595	3.0076029
Nissouri	Current Study	2.736125	1.2055	3.5265564
Nissouri	PWQMN	7.3714516	6.565	3.4903914
Saugeen	Current Study	0.5786625	0.62285	0.1253462
Saugeen	PWQMN	0.8028	0.65	0.3681229
Total Phosphorus (TP) Concentrations				
<u>Site</u>	<u>Data Set</u>	<u>Mean TP (mg L⁻¹)</u>	<u>Median TP (mg L⁻¹)</u>	<u>Standard Deviation (mg L⁻¹)</u>
Big creek	Current Study	0.226	0.197	0.090052762
Big creek	PWQMN	0.163353	0.109	0.172409287
Nissouri	Current Study	0.0615	0.0605	0.002380476
Nissouri	PWQMN	0.06498984	0.031	0.103032011
Saugeen	Current Study	0.0095	0.009	0.005259911
Saugeen	PWQMN	0.008905813	0.007	0.007874002
TN:TP				
<u>Site</u>	<u>Data Set</u>	<u>Mean TN:TP</u>	<u>Median TN:TP</u>	<u>Standard Deviation</u>
Big creek	Current Study	20.41663	18.40163	11.48286
Big creek	PWQMN	66.68257	36.64314	57.95752
Nissouri	Current Study	195.1038	237.4486	166.952
Nissouri	PWQMN	510.7075	468.7108	351.9491
Saugeen	Current Study	129.0901	107.1656	41.45926
Saugeen	PWQMN	227.9876	195.8627	126.1765

Table S4: Wilcoxon rank sum test with continuity correction for TP and NO₃-N

Total Phosphorus (TP)	
BC_Current vs BC_PWQMN	W = 373, p-value = 0.06527
BC_Current vs NC_Current	W = 20, p-value = 0.01945*
BC_Current vs SR_Current	W = 20, p-value = 0.01945*
BC_PWQMN vs NC_PWQMN	W = 14992, p-value < 2.2e-16*
BC_PWQMN vs SR_PWQMN	W = 15896, p-value < 2.2e-16*
NO ₃ -N	
BC_Current vs NC_Current	W = 8, p-value = 0.2353
BC_Current vs SR_Current	W = 28, p-value = 0.02248*
NC_Current vs SR_Current	W = 24, p-value = 0.02157*
BC_PWQMN vs NC_PWQMN	W = 5876.5, p-value = 1.323e-06*
BC_PWQMN vs SR_PWQMN	W = 6285.5, p-value = 0.00219*
NC_PWQMN vs SR_PWQMN	W = 32464, p-value < 2.2e-16*

Table S5

Annual Mean SRP and EPC₀ Values for Big Creek, Nissouri Creek, and the Saugeen River

Site/Year	SRP (mg L ⁻¹)	EPC ₀ (mg L ⁻¹)	EPC ₀ -SRP % Difference
BC 2018	0.023	0.015	-35%
BC 2019	0.087	0.0096	-89%
BC 2020	0.065	0.0051	-92%
NC 2019	0.030	0.037	23%
NC 2020	0.095	0.015	-84%
SR 2019	0.0017	0.0024	43%
SR 2020	0.015	0.00079	-95%

SRP = Soluble Reactive Phosphorus

EPC₀ = Zero Equilibrium Phosphorus Concentration

BC = Big Creek

NC = Nissouri Creek

SR = Saugeen River

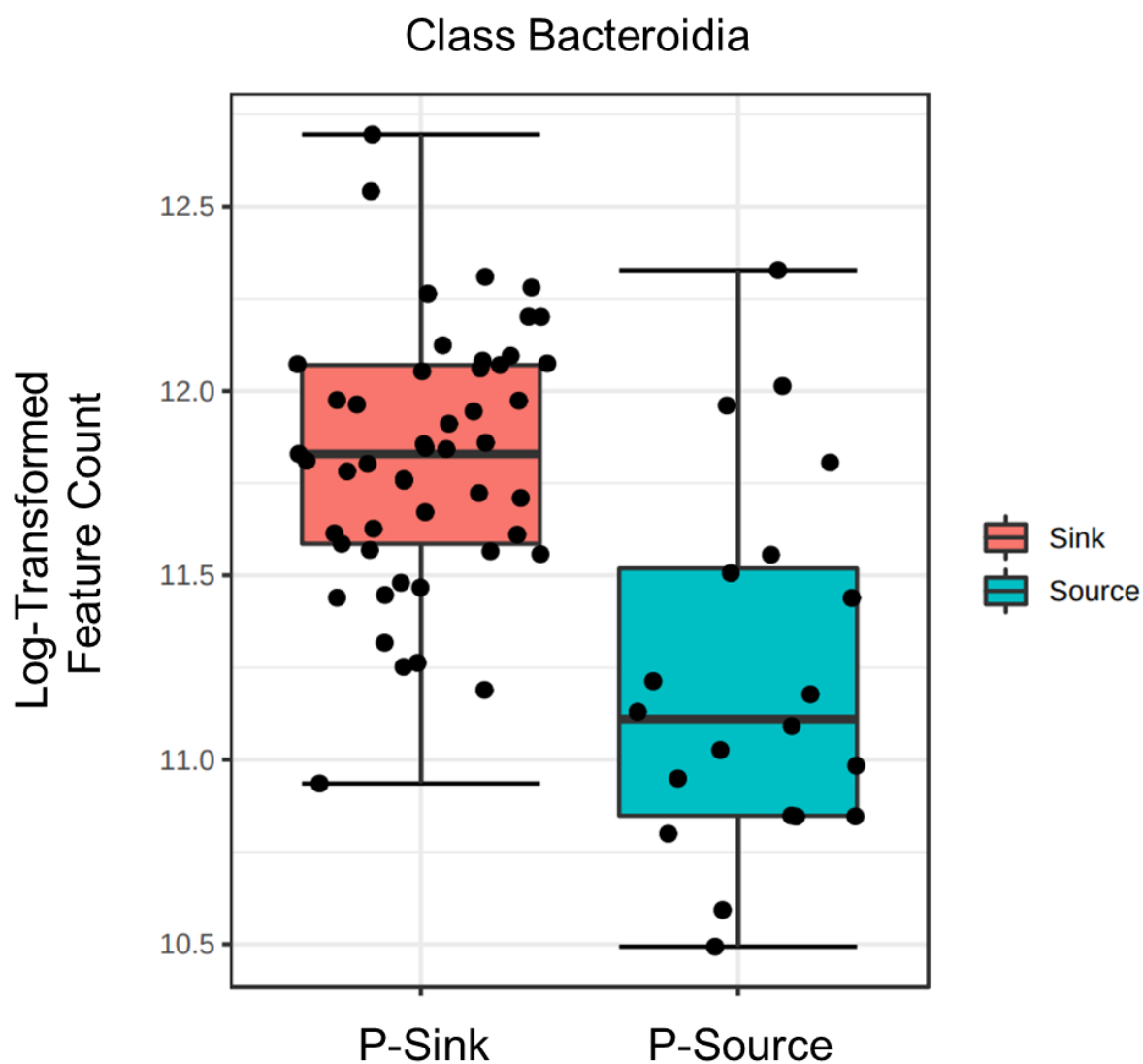


Figure S1: Log-transformed count comparison of Bacteroidia in phosphorus sink (P-sink) and phosphorus source (P-source) sediment across all study samples. Linear discriminant analysis Effect Size (LEfSe) False detection rate (FDR) adjusted p-value = 0.0010953.

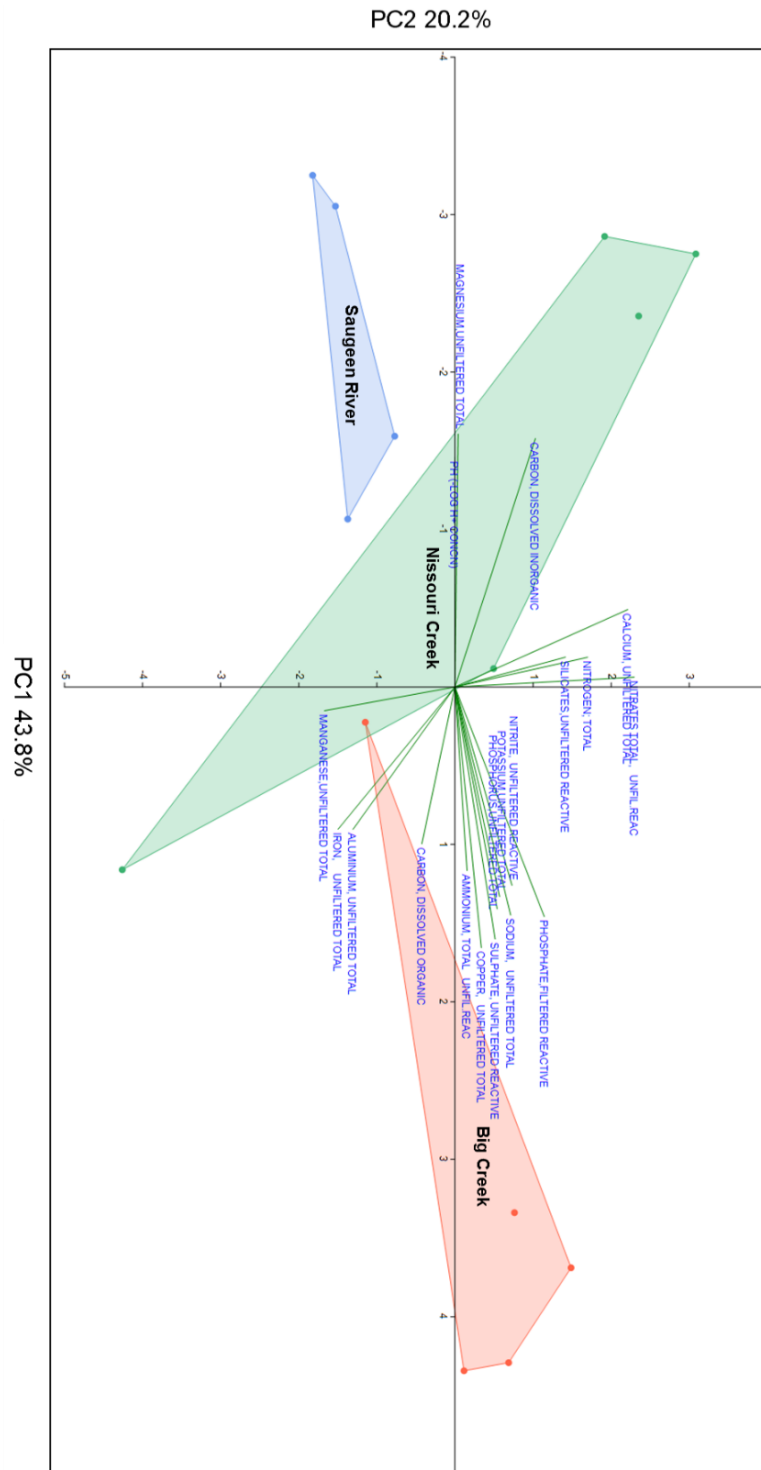


Figure S2: Principal Component Analysis (PCA) of surface water parameters for Big Creek, Nissouri Creek, and the Saugeen River 2019

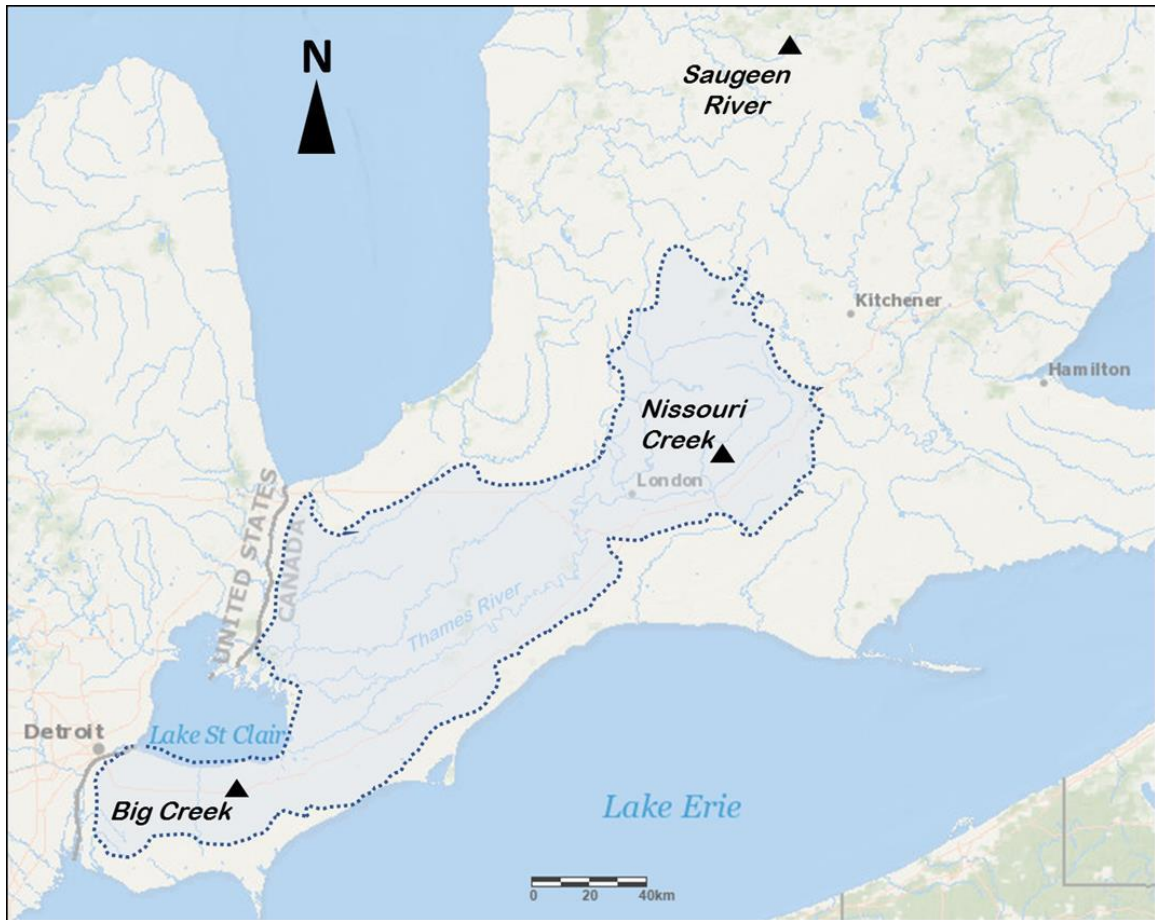


Figure S3: Site sampling locations in southwestern Ontario. Big Creek (BC) flows north into Lake St. Clair, Nissouri Creek flows south into the Middle Thames, and the Saugeen River flows West into the lower arm of Lake Huron. The dotted line region represents the Huron-Erie Corridor Watershed.

Appendix D (Chapter 5)

Table S1

Bed Sediment Metatranscriptomic Sample Details

Sample ID	Seq. Count	Location	Time Point	Coordinates
BCreek_EF_2_S30_R	13,878,212	Big Creek	Fall 2020	42.2036, -82.5196
BCreek_EF_1_S30_R	36,082,857	Big Creek	Fall 2020	42.2036, -82.5196
NCreek_1_O3_R	12,209,141	Nissouri Creek	Fall 2020	43.1302, -80.9628
NCreek_2_O3_R	12,066,537	Nissouri Creek	Fall 2020	43.1302, -80.9628
NCreek_1_O3_R	12,447,519	Nissouri Creek	Fall 2020	43.1302, -80.9628
SRiver_2_O3_R	15,936,264	Saugeen River	Fall 2020	44.1858, -80.7877
BCreek_EF_2_S30_R	17,145,852	Big Creek	Fall 2020	42.2036, -82.5196
SRiver_1_O3_R*	70,728,983	Saugeen River	Fall 2020	44.1858, -80.7877
NCreek_2_O3_R	16,206,728	Nissouri Creek	Fall 2020	43.1302, -80.9628
SRiver_2_O3_R	15,734,024	Saugeen River	Fall 2020	44.1858, -80.7877
NCreek_1_J31_R	18,995,421	Nissouri Creek	Summer 2020	43.1302, -80.9628
SRiver_2_A01_R	19,309,234	Saugeen River	Summer 2020	44.1858, -80.7877
Bcreek_AB1_J30_R	21,554,179	Big Creek	Summer 2020	42.2036, -82.5196
Bcreek_AB2_J30_R	18,735,457	Big Creek	Summer 2020	42.2036, -82.5196
NCreek_2_J31_R	17,892,806	Nissouri Creek	Summer 2020	43.1302, -80.9628
SRiver_1_A01_R	16,145,621	Saugeen River	Summer 2020	44.1858, -80.7877
Average Seq. Count = 20,941,802				

*Sample removed due to low protein-coding reads

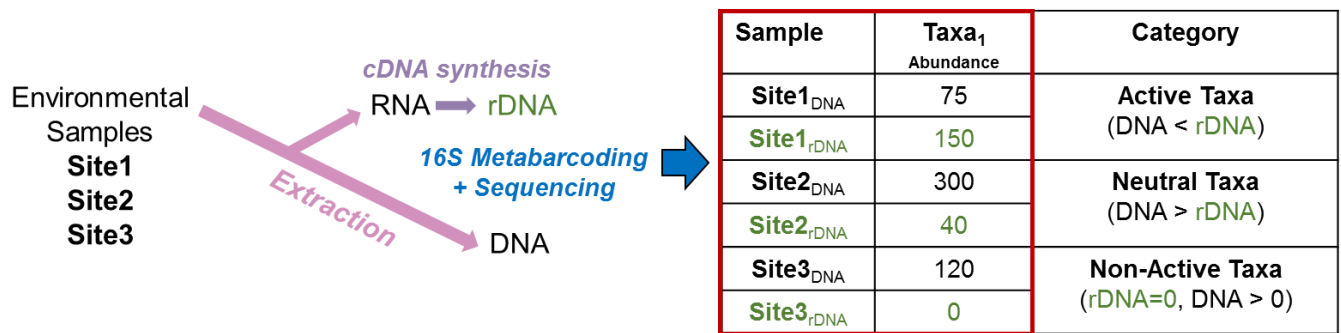


Figure S1: Simplified methodology flow chart of classifying Active, Neutral, and Non-Active taxonomic features across samples. Environmental samples are collected at specific sites and times and coextracted for total RNA and DNA. The RNA is converted into cDNA via reverse transcriptase. Samples undergo metabarcoding and sequencing targeting the 16S rRNA gene. After sequence processing and normalization, the result is a taxonomic feature table with samples as rows and taxonomic features as columns. The abundances of each taxon from DNA and RNA are then statistically compared through LEfSe differential analysis, demonstrated here by the hypothetical “Taxa1”. In this scenario, Taxa1 would be considered Active at Site1, Neutral at Site2, and Non-Active at Site3.

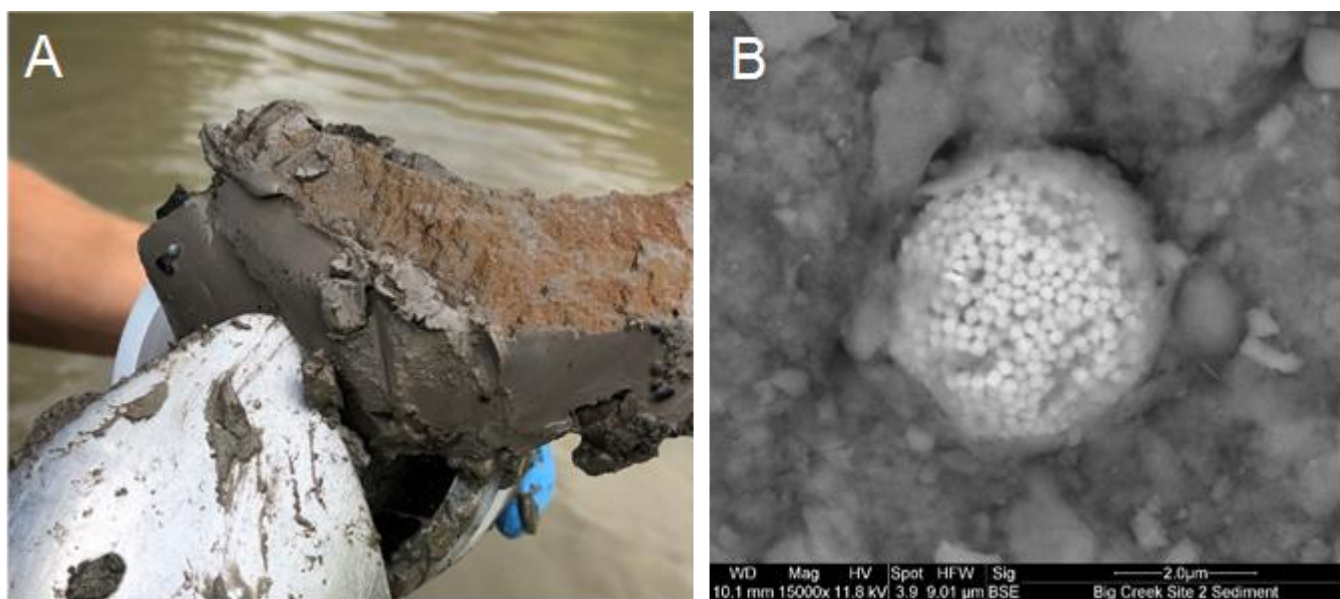


Figure S2: Evidence of Fe oxidation-reduction in Big Creek bed sediments. A) Surface sediment exhibiting Fe-oxidation colouration. B) Framboidal-like mineral phases in surface sediments suspected to be reduced FeS.

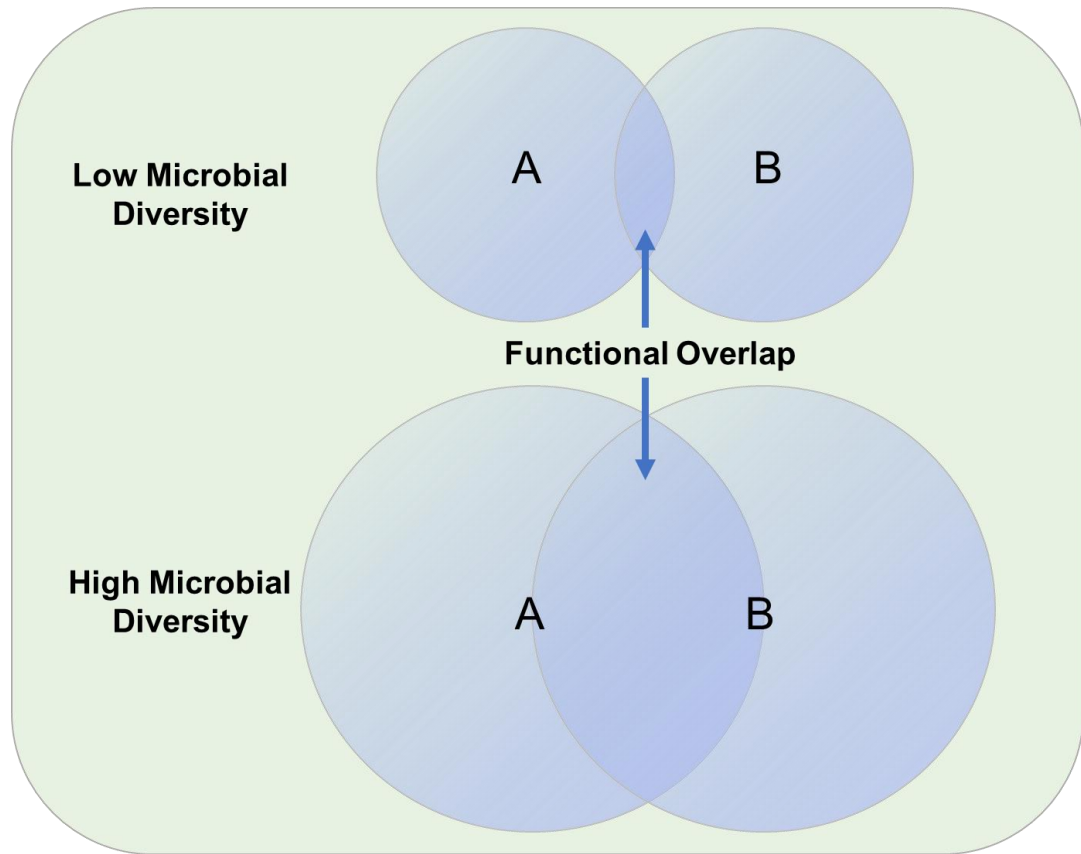


Figure S3: A theoretical conceptual diagram relating microbial community diversity to microbial functional potential in two groups (A and B). As diversity increases in one or both groups, represented by the size of the circle, there is a greater area of overlap in the two circles, representing the shared functional potential. In a low diversity scenario, the overlap is small, and it's less likely that a gene present in one group is represented in the other. In a high diversity scenario, the overlap is larger, and it's more likely that a gene will be shared between the two groups.

VITA AUCTORIS

Nicholas Falk was born in Windsor, Ontario. He attended Concord Public School followed by Riverside Secondary School from which he graduated in 2009. He obtained a B.Sc. (Honours) in Environmental Science followed by a M.Sc. from the University of Windsor. This thesis comprises his work towards a PhD degree at the University of Windsor's Great Lakes Institute for Environmental Research. Nicholas is a former member and lifelong supporter of the Windsor Lancers varsity Cross Country and Track and Field programs.